DYNAMIC ANALYSIS OF SHEAR WALLS AND DISCRETELY CONNECTED PANEL STRUCTURES USING A SUPER FINITE ELEMENT TECHNIQUE

Hans-Peter Huttelmaier

A Thesis

in

The Faculty

of

Engineering

Presented in Partial Fulfillment of the Requirements
for the degree of Doctor of Philosophy at
Concordia University
Montréal, Québec, Canada

November 1978

ABSTRACT

DYNAMIC ANALYSIS OF SHEAR WALLS AND DISCRETELY CONNECTED PANEL STRUCTURES USING A SUPER FINITE ELEMENT TECHNIQUE

Hans-Peter Huttelmaier, Ph.D.
Concordia University, 1978

The modularity employed by the building industry, apparent in the increased use of large-panel construction, invites the application of substructuring techniques in analysis and design. This results in an efficient and economical use of the finite element method.

The aim of this research is the development of a versatile substructuring technique for dynamic analysis, applicable to shear wall-type structures. Intended applications are precast panel structures and their seismic response.

First, the theoretical background for dynamic substructuring is reviewed. This is followed by the development of a substructuring scheme which is described as a multilevel super-finite element technique, based on a series of static condensations. The "panel element" thus derived consists of a rectangular substructure with interior nodes eliminated and flexible boundary node arrangement. Inertia

characteristics are represented by either a consistent or a lumped mass matrix. A substructure stress-displacement matrix allows full stress recovery. The present coded version for the panel element is attached to a multipurpose linear analysis program (SAP4) in the form of SUBROUTINE PANEL.

Applications in free vibration analysis and stress computation demonstrate the versatility of the scheme as well as a reduction in computational effort. Accuracy is tested with respect to mass representation. It is found that a homogeneous mass distribution may require a consistent substructure mass matrix; however, if concentrated masses exist (e.g., floor masses in multi-storey structures) a lumped mass representation may suffice.

The seismic behaviour of a 12-storey panel structure is investigated in a parametric study, representing an additional application of the substructure technique. A modal analysis was used for this purpose. Forces in vertical joints are transmitted through discrete connectors located at floor levels, whereas horizontal joints are assumed as rigid and continuous. Response is evaluated for structural discontinuities such as monolithic storeys and missing panels, with emphasis on connector forces. The investigation concludes with a comparison of dynamic analysis and static Code loading.

ACKNOWLEDGEMENTS

ACKNOWLEDGEMENTS

The author wishes to thank his supervisor, Professor O.A. Pekau for his guidance and advice during the development of this thesis.

Special thanks are extended to the software group at the Computer Centre of Concordia University, in particular to Steve Bush.

This work was supported by the National Research Council of Canada under Grant No. A8258.

TABLE OF CONTENTS

TABLE OF CONTENTS

PAGE

CHAPTER V SEISMIC BEHAVIOUR OF A 12-STOREY PRECAST PANEL STRUCTURE

LIST OF TABLES

LIST OF TABLES

LIST OF FIGURES

LIST OF FIGURES

CHAPTER I

INTRODUCTION

CHAPTER I

INTRODUCTION

1.1 GENERAL

Tall structures, in particular those represented by shear wall or coupled shear wall systems, have traditionally been analyzed using approximate methods. This implies uniform structural patterns not allowing irregularities in the stiffness or mass distribution along the height of the structure.

Modern digital computers and the advancement of the finite element method allow the analysis of complex civil engineering structures within high accuracy; this includes shear wall-type structures of arbitrary three-dimensional arrangement. Detailed information for structural response can be obtained, such as complete deformation shapes, or the stress concentrations around openings, for example.

However, the prohibitive computational costs for large-size structures urged the reorganization of solution schemes of the conventional finite element analysis, apparent through the appearance of substructuring techniques. Structures with many hundreds, or even thousands, of degrees of freedom, can thus be analyzed economically, particularly

when repetitive structural patterns are present, as occurs in many modern highrise structures.

Savings are particularly noticeable for dynamic analysis, since the solution of the dynamic equilibrium equations - in many cases identical to the solution of an eigenvalue problem - is particularly costly for large structural systems. Reduction of an equation set in dynamic analysis, i.e., "dynamic substructuring" requires, however, greater analytical effort than in the case of static analysis, the actual effort depending on the desired level of refinement in the representation of the mass. In some cases, crude lumping may result in good approximations of dynamic properties. In other cases a "consistent mass matrix" or even "component modes" may need to be applied in a substructuring technique in order to achieve satisfactory results.

Development of new analytical techniques - or adapting available ones to present needs - is a basic requirement in any technological process. The modularity applied by the modern building industry invites the use of substructuring techniques. Moreover, in the development of these techniques, consideration should be given to increased industrialization evident in the form of large-panel constructions, where continuous or discrete panel-to-panel connections may exist. Thus, a substructuring technique should possess the

versatility to be applicable not only to the more conventional "continuous" type of construction but also to precast panel structures where substructures may be employed to represent actual physical panels interconnected at selected points.

Finally, the need to include dynamic procedures in structural analysis programs, namely, to include appropriate mass representation in the substructuring technique, becomes increasingly apparent as building codes begin to treat the true dynamic nature of wind and earthquake loadings.

1.2 REVIEW OF PREVIOUS WORK

In a discussion of substructuring techniques one may consider static substructuring and dynamic substructuring as two different but interrelated developments. Previous work performed in static substructuring, also known as static condensation, will be presented first. An additional review of research applied to shear wall and panel structures is given in Section 5.1.

1.2.1 Static Substructuring

During the early development stages of finite element analysis, static condensation was applied for a single element to eliminate internal degrees of freedom. The use of complete polynomials to express displacement shapes, or in another

case,creation of quadrilateral elements assembled from triangular elements, result in internal nodes [1,2]. As a subsequent development, static condensation was applied to eliminate element degrees of freedom originated by incompatible modes [3]. In all the above cases more refined element behaviour is obtained without increasing the number of degrees of freedom.

The concept of eliminating selected degrees of freedom in a complete structural assembly became popular mainly for frame structures, where degrees of freedom of secondary importance were removed. Eliminated degrees of freedom relate mostly to small deformations (e.g., axial or rotational), or to points where there exist no applied external loads. Primarily work which may be summarized as "matrix structural analysis"[4,5,6] made use of this approach.

A further step in the development of static substructuring is characterized by the more systematic approach where internal degrees of freedom of individual structural components are eliminated; thus, the total structure is composed of substructures and is represented only by the nodal points at the substructure boundaries. These reduced subassemblies are also described as super finite elements or macro elements. Their use is particularly effective when repetitively applied. Some of the more recent work is mentioned below.

Egeland and Araldsen [7] described a general purpose program which allows generation of a super finite element library. This program was utilized to provide large savings in the analysis of ship hulls. A more systematic procedure with automatic partitioning of the structure into substructures performed according to available core memory, was designed by Utku [8]. This scheme allows efficient solution of large structures even on small size computers.

An efficient and refined special purpose program for linear analysis of complex reinforced concrete walls was developed by Peterson and Popov [9,10]. Rectangular substructures, defined by the user, may be divided into any finite element mesh; different material properties as well as openings can be included. Arbitrary loading and flexibility in desired displacement and stress output contribute to the versatility of this program.

1.2.2 Dynamic Substructuring

Most of the above work, although designed for static analysis, may be used for a dynamic analysis if appropriate lumped masses are introduced and if the solution of the equations is extended to a dynamic problem. This approach is used effectively for many practical engineering problems. However, adequate mass representation depends to a large

extent on the experience of the analyst.

Guyan [11] introduced a more refined mass formulation for the reduced subsystem, by subjecting the mass matrix to the same reduction constraints as the stiffness matrix. Thus, inertia characteristics of a substructure can be expressed by an "energy consistent", fully occupied mass matrix which results in an improved representation of the dynamic substructure properties. For an ideal situation, i.e., when complete and identical displacement shapes exist for the element stiffness and mass matrices, [12], upper bound solutions are obtained for the structural system, since the procedure is then equivalent to a Rayleigh-Ritz analysis [13].

Derivation of the consistent substructure mass matrix has been presented by many authors [6,7,15,23]. Applications have been reported by Egelund and Araldsen [7] who describe the use as well as the limitation of the consistent mass matrix, incorporated in a program using the super finite element technique. Goodno and Gere [14,15] investigated concrete shear cores using three-dimensional floor-to-floor subassemblies modelled by a consistent mass formulation. However, a lumped mass representation resulted in the same accuracy, with less computational effort.

The component mode synthesis can be considered as a separate development in dynamic substructuring. In this

scheme additional displacement shapes represented by normal modes of the constrained substructure are superimposed on the consistent formulation. The method was originated by Hurty [16,17] and later summarized by Hurty and Hou [18]. In more recent work, Holze and Boresi [19] applied the method to plate vibrations, with emphasis on numerical aspects. The component mode synthesis is rarely used for multistorey structures; however, Barber and Blotter [20] demonstrated economic application compared to standard dynamic analysis. Their investigation includes free vibration analysis of 4 and 6-storey structures divided into two components or substructures.

The close relationship between dynamic substructuring and the solution of the structural eigenvalue problem should be emphasized, since the reduction of the dynamic equilibrium equations to a more compact form is an intermediate step toward the solution of the eigenproblem. Moreover, regarding the subspace iteration technique, the two procedures are equivalent, since a similar mathematical formulation exists. The subspace iteration technique developed by Bathe and Wilson [21,22] is an efficient scheme for computation of the significant lowest eigenpair; thus, it can be described as concealed dynamic substructuring.

1.3 PRESENT STUDY

The purpose of this study is the development of a versatile and efficient substructuring procedure for rectangular structural patterns which includes a generation of mass properties. Thus, a more economical dynamic analysis than usually available from general purpose programs can be performed. The class of structures to be investigated includes shear wall type structures and, in particular, large-panel structures where discrete connections may exist. In future applications of the procedure it is expected to obtain further insight into the response characteristics of panelized structures subjected to dynamic excitation.

The general scope of this work involves the development of a computer subroutine attached as a substructure option to an efficient and widely used multipurpose program, rather than the creation of an independent program. The popular linear static and dynamic analysis program SAP4 [24] was chosen for this purpose.

The following Chapters describe the development of a super finite element technique and present applications which include a detailed parametric study of a large-panel structure subjected to earthquake excitation. The content of individual Chapters is outlined below.

In Chapter II, different methods for substructuring in dynamic analysis are reviewed. Mathematical formulations of the procedures are presented as congruence transformations based on a Rayleigh-Ritz analysis.

Chapter III describes the substructuring technique used in this study. It is formulated as a multilevel substructuring scheme for the creation of a rectangular "panel element". Stiffness and mass, as well as stress-displacement, matrices are derived. The major considerations focus on:

(1) Numerical procedures for the reduction algorithm, and

(2) Description of the multilevel growth scheme including the necessary input identifications.

The stress recovery procedure and the storage scheme for dynamic arrays are also discussed.

Chapter IV presents applications of the panel element in free vibration analysis, as well as a stress recovery using static analysis. Plate bending vibrations are investigated for different arrangements of panel elements, using consistent and lumped mass models. Shear wall problems demonstrate the influence of concentrated floor masses on the accuracy and the versatility with which the panel element is applied.

In Chapter V a large-panel precast structure consisting of 12 storeys is investigated for earthquake loading using elastic response spectrum analysis. Horizontal joints are assumed continuous, whereas discrete connectors exist in vertical joints at floor levels. Overall structural response with emphasis on connector forces is evaluated for

(1) Uniformly distributed stiffness and inertia properties, and

(2) Structural discontinuities over the height of the structure. This includes rigid or monolithic storeys, missing panels and non-uniform floor mass distribution.

The results obtained from a parametric investigation of this structure are summarized in Section 5.5.

Chapter VI contains a brief summary of this study, together with concluding remarks.

CHAPTER II

SOLUTION OF EQUILIBRIUM EQUATIONS IN DYNAMIC ANALYSIS USING SUBSTRUCTURING TECHNIQUES

CHAPTER II

SOLUTION OF EQUILIBRIUM EQUATIONS IN DYNAMIC ANALYSIS USING SUBSTRUCTURING TECHNIQUES

2.1 INTRODUCTION

In this Chapter, the theoretical aspects necessary for derivation of a reduced set of dynamic equilibrium equations are discussed. Several methods of substructuring applied for this purpose are summarized in the following Sections, namely static condensation, component mode synthesis and the super finite element technique, where the latter is a procedure based on static condensation. However, for a presentation of the general formulation, a summary of the Rayleigh-Ritz method is given first.

2.2 REDUCED EQUILIBRIUM EQUATIONS IN DYNAMIC ANALYSIS

In this Section the equilibrium equations for a discretized system and its equivalent reduced set are identified.

The governing matrix equation for a dynamic finite element system is expressed by [25],[26],[27]

$$[M]\{\ddot{u}\} + [C]\{\dot{u}\} + [K]\{u\} = \{P\} \qquad (2.1)$$

This equation states equilibrium of all forces at time t, with $\{u\}$,$\{\dot{u}\}$ and $\{\ddot{u}\}$ being the time-dependent state vectors expressing displacements, velocities and accelerations. Forces consist of inertia forces $\{F_I\} = [M]\{\ddot{u}\}$, viscous

damping forces $\{F_D\} = [C]\{\dot{u}\}$, elastic forces $\{F_E\} = [K]\{u\}$ and the time-dependent load vector $\{P\}$. Coefficient matrices $[M]$,$[C]$ and $[K]$ represent mass, damping and stiffness matrices respectively. If the coefficient matrices remain constant the problem is a linear one, and for its solution there exist basically two methods: direct integration and mode superposition. The latter is preceded by a solution of the eigenvalue problem.

The major concern in this work is the reduction of system equation (2.1) prior to its solution. This is generally achieved by creating subregions or substructures, and instead of working with the original finite element assembly, only those degrees of freedom representing boundaries of the subregions enter into the main equation.

A new set of equations which represents the reduced system is written as

$$[\bar{M}]\{\ddot{y}\} + [\bar{C}]\{\dot{y}\} + [\bar{K}]\{y\} = \{\bar{P}\} \qquad (2.2)$$

where

$$[\bar{M}] = [T]^T[M][T] \qquad (2.3a)$$

$$[\bar{C}] = [T]^T[C][T] \qquad (2.3b)$$

$$[\bar{K}] = [T]^T[K][T] \qquad (2.3c)$$

and

$$\{\bar{P}\} = [T]^T\{P\} \qquad (2.3d)$$

Transformation matrix [T], of order n by q, thus transforms the original equation set of order n by n into a new reduced set of order q by q. The nodal displacements {y} relating to the reduced set are then expressed by

$$\{u\} = [T]\{y\} \tag{2.4}$$

For a solution of the original system (Eq. (2.1)) by first solving the free vibration problem assuming harmonic time-varying displacements, one arrives at the eigenvalue problem of the original system:

$$[K]\{\phi\} - \omega^2[M]\{\phi\} = \{0\} \tag{2.5}$$

where

ω is the circular frequency

and

$\{\phi\}$ represents modal displacement shapes.

Subjecting the coefficient matrices [K] and [M] in Eq. (2.5) to the same constraints as applied in Eqs. (2.3a) and (2.3c) results in the reduced eigenvalue problem

$$[\bar{K}]\{a\} - \rho[\bar{M}]\{a\} = \{0\} \tag{2.6}$$

The new eigenpairs ρ_i and $\{a\}_i$ represent approximations to frequencies and mode shapes of the unreduced system. Approximated normalized modal displacements of eliminated degrees of freedom can be retrieved from Eq. (2.4) by inserting $\{a\}_i$ for back substitution.

The reduced eigenvalue problem as stated in Eq. (2.6) is the core equation in dynamic substructuring. The reduced equation set must result in good approximations of the first significant frequencies and mode shapes in order to consider a substructuring technique.

For the solution of a reduced system the following assumption is made: subregions stay linear during solution phase and constant damping exists within a subregion. In this study Rayleigh damping is assumed; damping is therefore excluded in the description and demonstration of reduction procedures.

The external force vector $\{P\}$ is not reduced if nodal forces are applied only at retained degrees of freedom. To retrieve eliminated displacements and hence stresses, after solution Eq. (2.4) can be applied. An alternative method, of retaining stresses more directly, will be presented in Chapter III.

Application of substructuring techniques, namely static condensation, component mode synthesis and the super finite element technique, all described in the following Sections, leads to a reduced set of equations, as presented by Eq. (2.2) or (2.6). The theoretical basis of these reduction procedures lies in a Rayleigh-Ritz analysis. A review of this method, therefore, is presented next.

2.3 REVIEW OF RAYLEIGH-RITZ ANALYSIS

The deformation-based finite element method, for static as well as for dynamic analysis, is basically recognized as a Rayleigh-Ritz (or Ritz) analysis [28,29]. This applies to a continuum which is reduced to a discrete system, as well as to a discrete system which is further reduced to fewer degrees of freedom. The second case applies to the procedures presented in the following Sections. The Rayleigh Ritz method is therefore discussed for a discrete dynamic system.

The unreduced generalized eigenvalue problem of order n is restated from Section 2.1:

$$[K]\{\phi\} - \omega^2[M]\{\phi\} = \{0\} \qquad (2.5)$$

In a Ritz analysis approximations are derived for the first p significant solutions ω_i and $\{\phi\}_i$, $i = 1,p$, by assuming basis vectors $\{\psi\}_i$, $i = 1,q$, where $p < q < n$.

The first p approximate solution shapes are then represented by linear combinations as

$$\{v\} = \sum_{i=1}^{q} c_i \{\psi\}_i \qquad (2.7)$$

where

c_i are the Ritz coordinates which determine the participation of a basis vector in a deformation shape.

A set of chosen basis vectors must approximate the least dominant subspace spanned by the exact solution vectors.

To arrive at the reduced eigenvalue problem, Rayleigh's quotient ρ is stated as

$$\rho(\phi) = \frac{\{\phi\}^T[K]\{\phi\}}{\{\phi\}^T[M]\{\phi\}} \qquad (2.8)$$

where $\rho(\phi)$ is the minimum over all possible vectors $\{\phi\}$ and represents an upper bound on frequencies [13,28,30]. Substituting the deformation shapes $\{v\}$ from Eq. (2.7) for $\{\phi\}$ in Eq. (2.8); leads to

$$\rho(v) = \frac{\sum_{i=1}^{q}\sum_{j=1}^{q} c_i c_j \bar{k}_{ij}}{\sum_{i=1}^{q}\sum_{j=1}^{q} c_i c_j \bar{m}_{ij}} \qquad (2.9)$$

with

$$\bar{k}_{ij} = \{\psi\}_i^T[K]\{\psi\}_j \qquad (2.10a)$$

and

$$\bar{m}_{ij} = \{\psi\}_i^T[M]\{\psi\}_j \qquad (2.10b)$$

Extremizing $\rho(v)$ with respect to the coefficients c_i yields

$$[\bar{K}]\{a\} - \rho[\bar{M}]\{a\} = \{0\} \qquad (2.6)$$

which is the reduced eigenvalue problem as stated in Section 2.1.

Coefficient matrices $[\bar{K}]$ and $[\bar{M}]$ consist of elements $\bar{k}_{ij}$ and $\bar{m}_{ij}$, respectively. The reduced system is of order q and is solved for q eigenpairs $\rho_i, \{a\}_i$, i = 1,q, where ρ_i represents an upper bound solution for frequencies, and vector $\{a\}_i$ represents the Ritz coordinates. The reduced matrices $[\bar{K}]$ and $[\bar{M}]$ can thus be derived in a congruence transformation from the unreduced matrices:

$$[\bar{K}] = [T]^T[K][T] \qquad (2.3c)$$

and

$$[\bar{M}] = [T]^T[M][T] \qquad (2.3a)$$

where

$$[T] = [\{\psi\}_1 \ \{\psi\}_2, \ \ldots, \ \{\psi\}_q] \qquad (2.11)$$

The transformation matrix [T] thus consists of the chosen basis vectors and is of order n by q.

Matrices $[\bar{K}]$ and $[\bar{M}]$ may be visualized as projected operators on q-dimensional space, represented by [T], or alternatively in a physical interpretation their elements may be seen as energy terms, expressed by Eq. (2.10). If transformation matrix [T] of Eq. (2.11) is also applied to damping matrix and load vector, the complete dynamic equilibrium equation is reduced, as expressed by Eq. (2.2).

Static condensation and component mode synthesis, discussed in the following Sections, are both Ritz transformations and differ only in the choice of basis vectors in matrix [T]. It should be mentioned that the subspace iteration technique [21,24] used for the solution of the generalized eigenvalue problem, consists of a sequence of Ritz transformations, applied in an iterative manner.

2.4 STATIC CONDENSATION

In order to derive Ritz transformation shapes used in static condensation, Eq. (2.5) which may in this case represent the full system or only a substructure is rewritten in partitioned form [31,32]:

$$\left(\begin{bmatrix}[K_{11}][K_{12}]\\ [K_{21}][K_{22}]\end{bmatrix} - \omega^2 \begin{bmatrix}[M_{11}][M_{12}]\\ [M_{21}][M_{22}]\end{bmatrix}\right)\begin{Bmatrix}\{x_1\}\\ \{x_2\}\end{Bmatrix} = \{0\} \quad (2.12)$$

This system of equations consists of two sets, unknown in displacement vectors $\{x_1\}$ and $\{x_2\}$, where $\{x_2\}$ defines displacements which are to be eliminated. Using the second equation set, subvector $\{x_2\}$ can be expressed in terms of subvector $\{x_1\}$ in the following manner:

$$\{x_2\} = -([K_{22}] - \omega^2[M_{22}])^{-1}([K_{21}] - \omega^2[M_{21}])\{x_1\}$$

or

$$\{x\} = \begin{Bmatrix}\{x_1\}\\ \{x_2\}\end{Bmatrix} = [T(\omega)]\{x_1\} \quad (2.13)$$

with

$$[T(\omega)] = \begin{bmatrix}[I]\\ -([K_{22}] - \omega^2[M_{22}])^{-1}([K_{21}] - \omega^2[M_{21}])\end{bmatrix} \quad (2.14)$$

Equation (2.13) is equivalent to Eq.(2.4); however, transformation matrix $[T]$ is expressed as a function of ω (Eq.(2.14)). Since frequency ω is not known prior to the solution, Eq.(2.14) can only be applied in an iterative fashion and is impractical for large systems [31]. A common convention in static condensation, therefore, is to

assume $\omega = 0$. This results in the simplified transformation matrix

$$[T(0)] = [T] = \begin{bmatrix} [I] \\ -[K_{22}]^{-1}[K_{21}] \end{bmatrix} \qquad (2.15)$$

Inertia forces inside subregions, discussed in more detail in Sections 2.5 and 2.6, are neglected in Eq. (2.15). In physical terms, transformation matrix [T] from Eq. (2.15) represents deformation shapes generated by unit displacements at the retained nodes when degrees of freedom to be eliminated are released.

Applying Eq. (2.15) to stiffness and mass matrices, according to Eqs. (2.3a) and (2.3c), results in the reduced stiffness matrix

$$[\bar{K}] = [K_{11}] - [K_{12}][K_{22}]^{-1}[K_{21}] \qquad (2.16)$$

and in the reduced mass matrix

$$[\bar{M}] = [M_{11}] - [M_{12}][K_{22}]^{-1}[K_{21}] - [K_{12}][K_{22}]^{-1}[M_{21}] + [K_{21}][K_{22}]^{-1}[M_{22}][K_{22}]^{-1}[K_{12}] \qquad (2.17)$$

This simultaneous reduction of stiffness and mass matrices was first derived by Guyan [11] and was subsequently described and applied by several authors as a technique for dynamic substructuring [6,7,15,23].

If a lumped mass model is used, i.e., $[M_{12}] = [M_{21}]^T = [0]$, Eq.(2.17) may be simplified to

$$[\bar{M}] = [M_{11}] + [K_{21}][K_{22}]^{-1}[M_{22}][K_{22}]^{-1}[K_{12}] \qquad (2.18)$$

The reduced mass matrix $[\bar{M}]$ in Eqs. (2.17) and (2.18) will always be consistent and full, where consistent is meant in the sense of energy consistent with stiffness matrix $[\bar{K}]$, since identical deformation shapes are used for reduction of both matrices. In mathematical terms the procedure is equivalent to a Gauss elimination on stiffness matrix $[K]$. Numerical aspects for efficient application of Eqs. (2.16) through (2.18) are discussed in Chapter III.

For many engineering applications it is common practice to assume masses of eliminated degrees of freedom as zero. The complete equation set (Eq.2.12)) is then written as:

$$\left(\begin{bmatrix} [K_{11}] & [K_{12}] \\ [K_{21}] & [K_{22}] \end{bmatrix} - \omega^2 \begin{bmatrix} [M] & [0] \\ [0] & [0] \end{bmatrix} \right) \begin{Bmatrix} \{x_1\} \\ \{x_2\} \end{Bmatrix} = \{0\} \qquad (2.19)$$

Applying the reduction leads to

$$([\bar{K}] - \omega^2[M])\ \{x_1\} = \{0\} \qquad (2.20)$$

where $[\bar{K}]$ is stated in Eq. (2.16) and $[M]$ represents diagonal mass terms associated with the retained degrees of

freedom. Assumption of zero masses at eliminated degrees of freedom is the only case where the reduced system leads to exactly the same results as the original system.

Internal inertia forces, related to eliminated degrees of freedom and neglected in Eq. (2.15), will be considered in the component mode synthesis, summarized in the following section.

2.5 COMPONENT MODE SYNTHESIS

The component mode synthesis [16,17,33], leads to an improved representation of mass characteristics of a substructure. A short summary of the method, mainly according to [34] is given below. Formulations presented for one component, use the following subscripts: B refers to retained boundary nodes, I represents eliminated interior nodes and N represents a transformation by normal modes.

The unreduced component matrices are partitioned according to boundary and interior degrees of freedom

$$[K] = \begin{bmatrix} [K_{BB}] & [K_{BI}] \\ [K_{IB}] & [K_{II}] \end{bmatrix} \qquad (2.21a)$$

and

$$[M] = \begin{bmatrix} [M_{BB}] & [M_{BI}] \\ [M_{IB}] & [M_{II}] \end{bmatrix} \tag{2.21b}$$

A transformation is then performed using Eqs.(2.3a) and (2.3c) with transformation matrix

$$[T'] = \begin{bmatrix} [I] & [0] \\ [T_S] & [T_N] \end{bmatrix} \tag{2.22}$$

Matrix $[T']$ is composed of submatrix

$$[T_I] = \begin{bmatrix} [I] \\ [T_S] \end{bmatrix} = \begin{bmatrix} [I] \\ -[K_{II}]^{-1}[K_{IB}] \end{bmatrix} \tag{2.23}$$

which corresponds to Eq. (2.15) and represents a static condensation, with $[T_S] = -[K_{II}]^{-1}[K_{IB}]$. The submatrix

$$[T_N] = [\{\phi_I\}_1, \{\phi_I\}_2, \ldots, \{\phi_I\}_p] \tag{2.24}$$

contains the first p normal modes, derived from the solution of the eigenvalue problem:

$$([K_{II}] - \omega^2[M_{II}])\{\phi_I\} = \{0\} \tag{2.25}$$

represented by the internal degrees of freedom.

Applying the congruence transformation to [K] and [M], using [T'] (and Eqs. 2.3a,c), leads to the reduced matrices

$$[\bar{K}] = \begin{bmatrix} [\bar{K}_{BB}] & [0] \\ [0] & [\bar{K}_{NN}] \end{bmatrix} \tag{2.26}$$

and

$$[\bar{M}] = \begin{bmatrix} [\bar{M}_{BB}] & [\bar{M}_{BN}] \\ [\bar{M}_{NB}] & [\bar{M}_{NN}] \end{bmatrix} \tag{2.27}$$

The submatrices in $[\bar{K}]$ are defined as follows:

$$[\bar{K}_{BB}] = [T_I]^T[K][T_I]$$

$$= [K_{BB}] - [K_{IB}][K_{II}]^{-1}[K_{BI}]$$

and

$$[\bar{K}_{NN}] = [T_N]^T[K_{II}][T_N]$$

Due to the special nature of [T'], the off-diagonal matrices in $[\bar{K}]$ are zero. Submatrices in $[\bar{M}]$ are:

$$[\bar{M}_{BB}] = [T_I]^T[M][T_I]$$

which, when expanded corresponds to Eq. (2.17), and

$$[\bar{M}_{BN}] = [\bar{M}_{NB}]^T = [T_S]^T[M_{II}][T_N] + [M_{BI}][T_N]$$

$$= -[K_{BI}][K_{II}]^{-1}[M_{II}][T_N] + [M_{BI}][T_N]$$

representing mixed modes.

If the mode shapes of the constrained component are orthonormalized with respect to $[M_{II}]$; i.e.,

$$\{\phi_I\}_i \, [M_{II}]\{\phi_I\}_j = \delta_{ij}$$

with

$$\delta_{ij} = \begin{cases} 0, & \text{for } i \neq j \\ 1, & \text{for } i = j \end{cases}$$

the reduced equations are simplified to

$$[\bar{K}] = \begin{bmatrix} [\bar{K}_{BB}] & & \\ & \omega_1^2 & \\ & & \omega_p^2 \end{bmatrix} \qquad (2.28a)$$

and

$$[\bar{M}] = \begin{bmatrix} [\bar{M}_{BB}] & [\bar{M}_{BN}] \\ [\bar{M}_{NB}] & [I] \end{bmatrix} \qquad (2.28b)$$

Component frequencies ω_1 to ω_p were derived from the internal eigenvalue problem (Eq.(2.25)). The fact that $[\bar{M}_{BN}] = [\bar{M}_{NB}]^T \neq [0]$, creates a "generalized inertia coupling"

[35] which leads to a higher occupancy in the mass matrix as compared to the stiffness matrix.

Matrices $[\bar{K}]$ and $[\bar{M}]$ are assembled into the system equation for solution. Internal degrees of freedom can be visualized as p internal nodal points with one degree of freedom each, representing generalized coordinates or amplitudes of the normal modes.

In summary, the component mode synthesis consists basically of a static condensation and additionally imposed generalized displacements represented by the p lowest normal modes of the constrained components. These additional degrees of freedom allow a good approximation of internal inertia forces. A component or a substructure can therefore be of any dimension, as long as all significant normal modes are included in the analysis. Selection of the p lowest modes, however, may involve difficulties [36]. It is also noted that during the solution of the eigenvalue problem of Eq. (2.25) all interior degrees of freedom need to be kept in core. Component mode synthesis, therefore, fails when advantage is taken of repetitive patterns inside the component, as is done in multilevel substructuring.

2.6 SUPER FINITE ELEMENT TECHNIQUE

The super finite element technique can be applied for static as well as for dynamic analysis. [7,15,28] In a static analysis this method may be regarded as straightforward, whereas in a dynamic analysis several considerations concerning internal inertia forces are necessary, partially discussed in Sections 2.3 and 2.4.

A super element is a multilevel substructure subjected to a series of static condensations. A first-level element, for example, is initially composed of basic elements (i.e., zero level elements) which were derived by assuming continuous displacement fields. The displacement fields of a first level element are then described by a linear combination of (discrete) nodal displacements at eliminated degrees of freedom originally introduced by zero level elements. First level degrees of freedom are now the basis for a second level element. The procedure is continued to any multilevel stage and can thus be described as a series of transformations from one set of variables to a reduced set of super variables [7]. In Fig. 2.1, typical examples for multilevel substructuring are given for one - and two - dimensional finite elements.

2.6.1 Reduction of Static Equilibrium Equations

Static condensation of stiffness matrix [K] applied in a multilevel scheme implies the creation of transformation matrix [T] (Eq. (2.15)) at each level. The series of transformations, beginning with zero level and ending with the $m^{\underline{th}}$ level equation may be summarized as

$$\begin{aligned} [K_0]\{X_0\} &= \{P_0\} \\ &\vdots \\ [\bar{K}_m]\{\bar{X}_m\} &= \{\bar{P}_m\} \end{aligned} \tag{2.29}$$

The procedure is initiated by a transformation from zero to first level equations; i.e.,

$$[\bar{K}_1] = [T_0]^T[K_0][T_0] \tag{2.30a}$$

$$\{\bar{P}_1\} = [T_0]^T\{P_0\} \tag{2.30b}$$

and

$$\{\bar{X}_1\} = [T_0]^T\{X_0\} \tag{2.30c}$$

It can be shown that the $m^{\underline{th}}$ level assembly furnishes exactly the same results as the fully assembled equation set. A formal mathematical proof is given in [7]. A short proof, which also provides insight into the numerical procedure, is given by the following reasoning: static condensation on stiffness matrix [K] is equivalent to a Gauss elimin-

ation; thus, elimination of the $s^{\underline{th}}$ equation has the following effect on the $j^{\underline{th}}$ element in the $i^{\underline{th}}$ equation:

$$\bar{k}_{ij} = k_{ij} - k_{sj}\, k_{is}/k_{ss}$$

and for the RHS

$$\bar{P}_i = P_i - P_s\, k_{is}/k_{ss}$$

It is important to realize that the sequence of eliminations is arbitrary in order. In the super finite element technique the sequence is chosen such that repeating blocks of identical equation formations are eliminated only once. Or in physical terms, constraints in equivalent subregions are released simultaneously.

2.6.2 Reduction of Dynamic Equilibrium Equations

A dynamic analysis using super finite elements can be considered as an extension of the static analysis since the mass matrix is reduced in a parallel fashion; i.e.,

$$[\bar{M}_1] = [T_0]^T[M_0][T_0] \qquad (2.31)$$

thus leading to an extension of equation set (2.30). A simultaneous elimination of internal inertia terms in repeating subregions, or equation blocks, takes place by imposing static deflection shapes as constraints. The $m^{\underline{th}}$

level matrices $[\bar{K}_m]$ and $[\bar{M}_m]$ representing stiffness and mass properties of a substructure are assembled into the overall system equation.

Whereas the reduced matrix $[\bar{K}_m]$ stores the exact stiffness properties, mass matrix $[\bar{M}_m]$, derived by energy consistent transformations, represents only approximations of the original inertia properties, unless reduced to massless degrees of freedom only (see Section 2.3). Thus, solutions are always approximate, however, they possess the favourable features of a Ritz solution, namely convergence to the lowest frequencies and mode shapes with a higher convergence rate for lower modes, as well as upper bound solutions if complete and consistent deformation shapes are used in the basic elements.

Internal forces are not known in advance as in a static analysis. Inertia forces which are activated by the natural frequencies of the structure are therefore not taken into account (only those created by static deformation-shapes). Magnitude of the inertia forces inside the sub-region or component, due to dynamic deformation $\{X\}$, is estimated by the product $\{X\}^T\{m\}$, [7]. Deformation vector $\{X\}$ can be expressed as a superposition of normal modes of the component. Vector $\{m\}$ represents internal nodal masses.

Large internal masses and/or large dynamic internal deformations, lead to large values of $\{X\}^T\{m\}$. Thus, errors are introduced into the analysis unless component modes are used. It is therefore vital to limit the size of the super-elements in regions of high mass concentration. Or more generally, the size of the super element should be such that the lowest natural frequencies of the constrained super-element are higher in magnitude than the highest significant natural frequencies of the total structure.

2.7 CONCLUDING REMARKS

Component mode synthesis and static condensation, both based on a Ritz analysis, are two different approaches in dynamic substructuring. It should be mentioned here that the component mode method is quite popular in aerospace work where, for example, one aeroplane wing is represented by one component and obviously normal component modes cannot be neglected in this case. On the other hand, in multi-storey structures - the field of interest in this study - one component such as a panel will not have a significant modal contribution to the total structure. This is one main reason why component modes are not taken into account in the present study. At the same time advantage can be taken of multilevel substructuring, since it is impractical to use multilevel substructuring and component modes in one proce-

dure (Section 2.4). The use of deformation shapes other than the static ones, for the reduction of the mass matrix, was studied but not applied in this work.

Multilevel substructuring is implemented in the next Chapter, in the derivation of a panel element. Emphasis is placed on numerical considerations and on an efficient growth scheme.

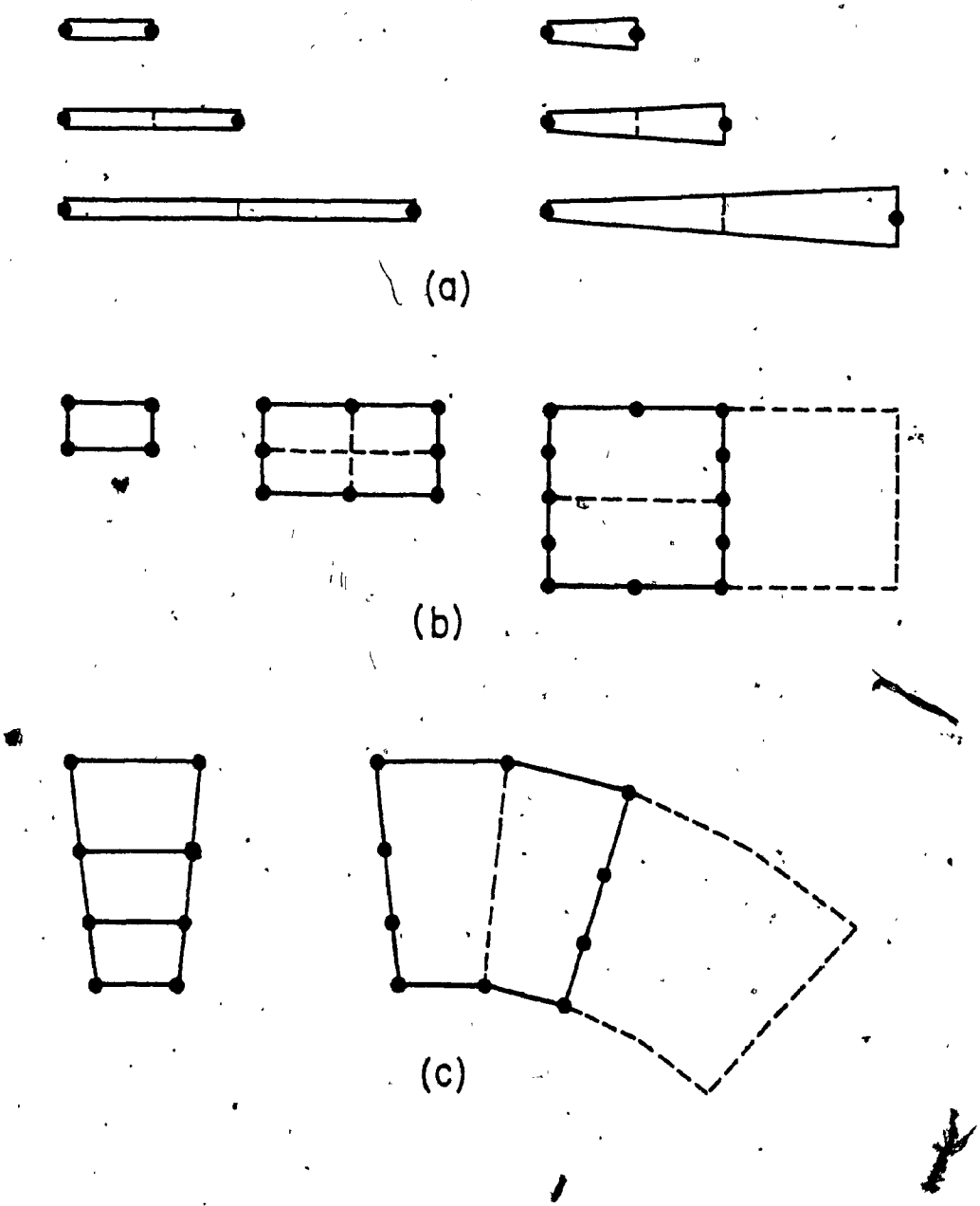

FIG. 2.1 TYPICAL EXAMPLES OF SUPER FINITE ELEMENTS
(a) LINE ELEMENTS, (b) RECTANGULAR ELEMENTS, AND (c) TRAPEZOIDAL ELEMENTS

CHAPTER III

DEVELOPMENT OF A PANEL SUPER ELEMENT

CHAPTER III

DEVELOPMENT OF A PANEL SUPER ELEMENT

3.1 INTRODUCTION

The objective of this Chapter is the derivation of a homogeneous rectangular super finite element which allows an efficient dynamic analysis of shear wall type or box-type multistorey structures. One super element could represent a substructure in a continuous model or an actual physical panel such as a prefabricated panel connected to a structural system in a discrete or continuous manner.

Following the concepts of the previous Chapter, one panel is considered as a substructure where all interior nodes are eliminated, leaving only boundary nodes. Considerations which result in the development of a fourth level super element, in the following called "panel super element" or simply "panel element", are listed below:

(1) Flexibility in boundary node arrangement is desired, mainly to avoid unnecessary boundary degrees of freedom in the system equation.

(2) Minimization of eliminated internal nodes and of storage requirements, achieved by multilevel substructuring.

(3) An efficient and simple reduction algorithm.

(4) The scheme should allow simple coding procedures as well as practical input.

In terms of computer program development, SUBROUTINE PANEL is created to furnish stiffness, mass and stress-displacement matrices for a panel element or a desired rectangular substructure. This Subroutine is meant to be attached to the element library of a multipurpose program. The present version of SUBROUTINE PANEL, listed in Appendix D, is compatible with SAP4 [24]. The latter is a structural analysis program for linear static and dynamic analysis. Corresponding input instructions for the panel element are included in Appendix C.

Major development steps necessary to establish the Subroutine are discussed in the following Sections. The presentation is best understood by considering one coupling step in a multilevel substructuring procedure, consisting of:

(a) creation of connectivity arrays,

(b) assembly into the higher level element, and

(c) reduction of the matrices to the chosen boundary nodes.

The manner in which connectivity arrays are created depends largely on the "growth pattern" of the super element. This aspect is discussed in Section 3.3, with emphasis on the pattern used in this development. For the assembly, reference is made to standard finite element texts since assembly is straightforward once the connectivity is known. In this study, major consideration is given to the reduction procedure. Whereas in the previous Chapter the theoretical background of a reduction, or static condensation, is formulated, the following Section discusses purely numerical aspects. Two reduction procedures are considered and presented in detail. An in-core solution during the reduction is chosen; thus an efficient storage scheme, discussed in Section 3.5, is an additional requirement in the overall performance of the Subroutine. A procedure for stress recovery adapted to the multilevel substructuring scheme is discussed separately in Section 3.4.

3.2 NUMERICAL CONSIDERATIONS FOR THE REDUCTION PROCEDURE

Since an in-core solution is applied, panel element matrices - namely, stiffness matrix [K], mass matrix [M] as well as stress-displacement matrix [S] - are stored and operated on simultaneously. Load vector {P} is not included in the procedure. Consequently, external loads

may be applied only at retained boundary nodes.

In the following discussion of numerical aspects, only matrices [K] and [M] are considered. The reduction procedure itself is presented for one typical transformation step from, level i to level (i+1). Thus, [K] and [M] are assumed to be full. It should be noted that, during the first reduction step, [K] could be banded whereas [M] could be either banded or diagonally lumped.

In order to demonstrate a typical transformation, matrices [K] and [M] (both of order n), representing an assembly from the $i^{\underline{th}}$ level, are partitioned as follows:

$$[K] = \begin{bmatrix} [K_{11}] & [K_{12}] \\ [K_{21}] & [K_{22}] \end{bmatrix} \tag{3.1a}$$

and

$$[M] = \begin{bmatrix} [M_{11}] & [M_{12}] \\ [M_{21}] & [M_{22}] \end{bmatrix} \tag{3.1b}$$

where subscripts 1 and 2 indicate degrees of freedom to be retained and to be eliminated, respectively. Applying a congruence transformation using matrix [T] from Eq.(2.15), of order n by (n-r), leads to reduced matrices $[\bar{K}]$ and $[\bar{M}]$ of Eqs.(2.16) and (2.17), representing level (i+1). The reduced system is then of order (n-r), where n is the order of the unreduced system, and r represents the

number of degrees of freedom to be eliminated.

A congruence transformation or a reduction procedure implies a numerical algorithm for the evaluation of Eqs.(2.16) and (2.17). In this study two algorithms are compared, which may be termed "block elimination", and "step elimination". In a block elimination a Cholesky decomposition is applied [19], whereas the step elimination is based on an algorithm presented by Wilson [37] and extended in this study to include mass effects.

3.2.1 Block Elimination

To demonstrate the operations necessary in this procedure, reduced stiffness and mass matrices are restated from Eqs. (2.16) and (2.17):

$$[\bar{K}] = [K_{11}] - [K_{12}][K_{22}]^{-1}[K_{21}] \qquad (2.16)$$

and

$$[\bar{M}] = [M_{11}] - [M_{12}][K_{22}]^{-1}[K_{21}] - [K_{12}][K_{22}]^{-1}[M_{21}] + [K_{21}][K_{22}]^{-1}[M_{22}][K_{22}]^{-1}[K_{12}] \qquad (2.17)$$

Evaluation of the two equations is initiated by Cholesky decomposition of submatrix $[K_{22}]$

$$[K_{22}] = [\tilde{L}][\tilde{L}]^T \qquad (3.2)$$

where it should be noted that the formulation $[\tilde{L}] = [L][D]^{\frac{1}{2}}$ with $[K_{22}] = [L][D][L]^T$ is slightly more efficient [4]. Matrices $[\tilde{L}]$ and $[L]$ are of a lower triangular form, whereas $[D]$ is diagonal.

Proceeding with a forward substitution

$$[\tilde{L}][R] = [K_{12}] \tag{3.3}$$

yields $[R]$, used for composition of the reduced stiffness matrix

$$[\bar{K}] = [K_{11}] - [R]^T[R] \tag{3.4}$$

which is equivalent to Eq.(2.16). To reduce the mass matrix, $[R]$ is applied in a backward substitution

$$[\tilde{L}]^T[Y] = [R] \tag{3.5}$$

where it can be shown that $[Y] = [K_{22}]^{-1}[K_{21}]$. The reduced mass matrix is then expressed as

$$[\bar{M}] = [M_{11}] - [M_{12}][Y] - [Y]^T([M_{21}] - [M_{22}][Y]) \tag{3.6}$$

a formulation which is equivalent to Eq. (2.17).

3.2.2 Step Elimination

In order to discuss this procedure, the partitioned matrices from Eq. (3.1) are rewritten as

$$[K] = \begin{bmatrix} [K_{11}] & \{g\} \\ \{g\}^T & k_{nn} \end{bmatrix} \tag{3.7a}$$

and

$$[M] = \begin{bmatrix} [M_{11}] & \{h\} \\ \{h\}^T & m_{nn} \end{bmatrix} \tag{3.7b}$$

where $\{g\}$ and $\{h\}$ are vectors of order (n-1) by 1, corresponding to submatrices $[K_{12}]$ and $[M_{12}]$ of Eq.(3.1). Transformation matrix $[T]$ from Eq. (2.15) is now of order n by (n-1) and is expressed as

$$[T] = \begin{bmatrix} [I] \\ -\dfrac{\{g\}^T}{k_{nn}} \end{bmatrix} \tag{3.8}$$

Equations (3.7a) and (3.7b) are thus transformed into

$$[\bar{K}] = [K_{11}] - \frac{1}{k_{nn}} \{g\}\{g\}^T \tag{3.9}$$

and

$$[\bar{M}] = [M_{11}] - \frac{1}{k_{nn}} \{h\}\{g\}^T - \frac{1}{k_{nn}} \{g\}\{h\}^T +$$

$$+ \frac{m_{nn}}{k_{nn}} \{g\}\{g\}^T \qquad (3.10)$$

reducing [K] and [M] by rank one. Applying this step r times leads to the reduced system which is of order (n-r). A prerequisite for this procedure is a numbering scheme which assigns the highest numbers to the degrees of freedom to be eliminated.

This stepwise elimination procedure is applied in an elegant algorithm, described by Wilson [37] for the reduction of stiffness matrix, stress-displacement matrix and force vector. For this study the mass matrix as expressed by Eq.(3.10) is incorporated into the algorithm. A formulation similar to Eqs. (3.9) and (3.10) was presented by Irons [38] using energy expressions which lead to development of the frontal solution method [39] for reducing the stiffness matrix.

In order to assess block elimination and step elimination in an appropriate manner, a comparison of the two algorithms is included in Section 3.2.3.

3.2.3 Comparison of the Two Procedures

To compare two numerical procedures effectively, it is best to perform an operation count and compute storage requirements [40]. This is demonstrated in Appendix A, while in this Section only the results are discussed. The basic assumption under which the two methods are compared is that both matrices [K] and [M] are full and are reduced simultaneously.

In the operation count, only higher terms of the number of multiplications and divisions are retained according to generally accepted conventions. In Appendix A the following expressions are derived for operation counts:

$$OB = \frac{3}{2} n^2 r - nr^2 - \frac{1}{3} r^3 \qquad (3.11)$$

and

$$OS = 2n^2 r - 2nr^2 + \frac{2}{3} r^3 \qquad (3.12)$$

where OB and OS are the number of operations for block elimination and step elimination, respectively, and n and r denote total and reduced number of degrees of freedom (see Section 3.2). For comparison, it is convenient to divide both equations by n^3 and to use the substitution: $z = r/n$, where $z < 1$.

Then,

$$\overline{OB} = OB/n^3 = \frac{3}{2} z - z^2 - \frac{1}{3} z^3 \qquad (3.13)$$

and

$$\overline{OS} = OS/n^3 = 2z - 2z^2 + \frac{2}{3} z^3 \qquad (3.14)$$

Evaluation of these equations for z leads to ratios $\overline{OB}/\overline{OS}$ as a useful criteria for comparison. Variation of z results in the following $\overline{OB}/\overline{OS}$ ratios:

z	$\overline{OB}/\overline{OS}$
0.1	0.77
0.2	0.79
0.3	0.80
0.4	0.80
0.5	0.79
0.6	0.75
0.7	0.69
0.8	0.59
0.9	0.45

This shows that for most practical cases, i.e., for $z = r/n = 0.1$ to 0.7, a block elimination executes only 70 to 80 percent as many operations as are performed in a step elimination.

Considering storage requirements, the following approximate expressions are derived in Appendix A:

$$\text{Block elimination} : n^2 + (n-r)r$$

$$\text{Step elimination} : n^2$$

The above comparison shows that step elimination is less favorable according to an operation count, but more favorable with regard to storage requirements. Since an in-core reduction scheme is chosen, the storage requirement is considered of higher priority. In addition, for most of the applications in this study the reduction process for a substructure requires only a fraction of the computing time consumed during the solution of the system equations. Thus, application of block elimination would lead to only negligible savings. A step elimination is therefore used in the multilevel reduction scheme. It should be emphasized that a step elimination algorithm is conveniently attached to a computer program, assuming degrees of freedom are labelled as discussed in Section 3.2.2.

A flow chart of the algorithm is attached in Appendix B. Reduction of the stress-displacement matrix, also included in the flow chart, is discussed in Section 3.4. A FORTRAN listing of the step elimination is included in Appendix D (see SUBROUTINE STAR). It is noted that matrices

are stored as one-dimensional arrays, which requires that stiffness and mass matrices be stored in Mode 1, shown in Fig. 3.1(a).

3.3 THE MULTILEVEL GROWTH SCHEME

3.3.1 General Scheme

The general concept of the super finite element technique or multilevel substructuring is discussed in Chapter II, and examples are presented in Fig. 2.1.

Rectangular structural components allow the application of multilevel schemes (Fig. 2.1(b)); however, the growth should be directed so as to allow arbitrary aspect ratios and reasonable flexibility for the retained boundary nodes. Important additional requirements to influence selection of a growth scheme are listed in Section 3.1.

Rectangular growth patterns are possible in two fashions:

(1) Using double progression, and

(2) Using single progression, as demonstrated in Table 3.1.

Inspection of the patterns shows that a double progression results in fewer eliminations. However, it is also apparent that a variation of aspect ratio is more difficult and, additionally, more complicated coding procedures are to be expected compared to a single progression.

Thus, a single progression scheme was chosen for the formation of a panel element. In the multilevel scheme described in the following Section, levels from zero to four are included, leading to a doubly symmetric substructure or panel element.

3.3.2 Description of the Suggested Scheme

The applied growth scheme demonstrated in Fig. 3.2 follows the principle of single progression. Hence, the dimension in the horizontal direction (x-direction) remains constant, whereas expansion takes place in the vertical direction (in negative y-direction). The stepwise growth pattern leading to a fourth level panel element can be visualized in three stages:

(1) Creation of the basic 4-node element (zero level).

(2) Creation of separate super element formations as shown in Fig. 3.2(a), namely end element, and level one and level two elements. These super elements can assume any of the formations demonstrated in Table 3.1 for single progression. Sequence of creation is indicated in Fig. 3.2(a) by the "growth direction".

(3) Coupling of the created super elements, which leads to level three (Fig. 3.2(b)) or to level four (Fig. 3.2(c)) in an additional symmetric coupling.

Levels from zero to four are presented below, referring to Figs. 3.3 through 3.7 and to Tables 3.2 and 3.3. The presentation discusses the different possibilities for boundary node arrangements and demonstrates type identifications necessary for input.

3.3.2.1 Level zero

The basic finite element is created. Any type of 4-node, preferably rectangular, finite element is acceptable. Length A and height B for the element, indicated in Fig. 3.3(a), are determined by panel dimensions and by the desired mesh size. Stiffness and mass properties of the 4-node element determine the properties of the panel element.

It should be noted that element mass matrix may be consistent or of a semi-definite nature (diagonal with possible zero terms along the diagonal, see Chapter IV). Considerations necessary for the basic stress-displacement matrix are discussed in Section 3.4.

The sequence of nodal numbering for the 4-node basic element is counter-clockwise, starting with the node on the lower left-hand corner, as shown in Fig. 3.3(a). This numbering convention remains the same for all higher level elements. Figures 3.2(b) and 3.2(c) show the numbering of degrees of freedom for the membrane element and the plate bending element used in this study.

3.3.2.2 Level one

Two types of super elements are created, start element and end element. Both are assembled in a horizontal manner from the basic 4-node finite element as shown in Table 3.2. The panel dimension as well as mesh size in horizontal direction (x-direction), both defined at this level, are expressed by XL, and by NHN the number of horizontal nodal points, respectively (see Table 3.2 and Appendix C).

The start element is basically supplied for the creation of level two elements. For dimensions in vertical direction two possibilities are indicated in Table 3.2, namely B1 or B2, thus allowing a certain flexibility for boundary node arrangement along the vertical side of the

panel element. Three-digit type identification numbers are used for input, i.e., (100)* and (200) when B1 or B2 are applied, respectively. After assembly, start elements are directly carried into level two, or through tape writing into level three.

An end element defines the boundary node arrangement along the upper horizontal side. Six different types (symmetric) are included in the present version of the program, identified by one-digit numbers, ranging from (1) to (6) (see Table 3.2). It is noted that end elements are always of height B1. The matrices for an end element are written on tape, retrieved either in level three or level four.

3.3.2.3 Level two

A single progression using start elements from level one is generated in this level. Two options for level two elements are possible, as apparent from Table 3.3:

(1) boundary nodes on vertical sides are retained, or

(2) boundary nodes on vertical sides are eliminated.

---

* Input identification or the type of super elements is within brackets in Figures, Tables and in the text.

In addition, a level two element may be composed of B1 or B2 start elements.

For input identification the 3-digit number from level one is applied, with the first digit indicating if B1 or B2 is used. The boundary node option is determined by specifying the number of coupling steps with the second or third digit as follows: for eliminated boundary nodes the second location is used (e.g., type (120)) and for retained boundary nodes the third location is used (e.g., type (102)).

For retained boundary nodes at vertical edges, the generation of connectivity arrays can be based on the following observation: the number of boundary nodes increases by $2(2^{NSP}-1)$, where NSP gives the number of coupling steps.

Generated level two elements are stored on tape in order to be coupled in level three. Or, alternatively, level two elements are used directly as output elements, or substructures.

3.3.2.4 Level three

Level three is identified by a coupling procedure of level one and level two elements, both retrieved from tape. Each coupling step leaves the two possibilities:

(1) Boundary nodes are eliminated (NCOPL = 1), or

(2) Boundary nodes are retained (NCOPL = 2).

Coupling may be demonstrated by the following two examples.

Example 1

Three elements of level one and two, i.e., types (2), (100) and (210), as shown in Fig.3.4(a) are to be coupled. Two coupling steps are necessary, chosen as NCOPL(1) = 1, and NCOPL(2) = 2, thus leaving one boundary node in each of the vertical sides. The new level three element shown in Fig. 3.4(b) may be written in short form as (2,100,210/1,2).

Example 2

For the panel element shown in Fig. 3.5, all boundary nodes on the vertical sides are retained. The type of the coupled element is identified as (3,201/2).

A level-three element may be written on tape to be used in level-four, or it could be used for output.

3.3.2.5 Level four

In this level a symmetric coupling is provided for a level-three element or for an end element. A symmetric coupling can be achieved by a rotation about the x-axis, or by an in-plane rotation about the z'-axis, as demonstrated in Fig. 3.6(a). The in-plane rotation was chosen for this procedure.

The two coupling options - namely, boundary nodes, are to be retained or eliminated - are in level four determined by NCOP4 = 1 and NCOP4 = 2, respectively. In Fig.3.6 symmetric coupling is demonstrated for a level three element of type (2,110/1). Figures 3.6(b) and 3.6(c) show corresponding level four elements, types (2,110/1,1) and (2,110/1,2), respectively. It is noted that the short form of level three is extended by the value for NCOP4.

An example which demonstrates the connectivity arrays necessary for a symmetric coupling is given by Fig.3.7 and Table 3.4. Connectivity arrays are listed for a membrane case (ND = 2) and for a bending case (ND = 3) (see Table 3.4). Numbering conventions follow those established in level zero (Fig.3.3).

3.4 STRESS RECOVERY

In this work a procedure for stress recovery is used, following the multilevel scheme of Section 3.3.2. Thus, a reduced stress-displacement matrix is created, which relates internal stresses to the remaining boundary degrees of freedom. Whereas assembly and reduction of stiffness and mass matrix take place in a closely related manner, separate considerations are necessary for the stress-displacement matrix. A reduction of the stress-displacement matrix is usually performed in finite element analysis when internal nodes in a basic element are eliminated (see also [37]). The same concept is, in the following, adapted to the super finite element technique.

An alternate procedure, normally applied in substructuring, is the complete retrieval of internal displacements and, consequently, any desired stress recovery is possible [7]. In a multilevel scheme this would necessitate a series of back substitutions using Eq. (2.30c). As a result complicated coding procedures are to be expected. For the stress recovery described below a back substitution is therefore not applied. This results, however, in the limitation that displacement output is only available for the retained super nodes. This restriction should be acceptable for most practical applications.

The theoretical aspects which follow are an extension of the concepts presented in Section 2.5, as expressed by Eqs. (2.29) through (2.31).

On element level (level zero) the relationship between stresses and displacements can be stated as

$$\{\sigma\} = [S]\{u\}$$

where $\{\sigma\}$ is the stress vector, $\{u\}$ represents the nodal displacement and $[S]$ is the stress-displacement matrix of order NS by ND, with NS the number of stress components and ND the number of degrees of freedom. The stress-displacement matrix is reassembled and transformed through several levels in an analog manner as demonstrated in Eqs. (2.29) and (2.30) for stiffness and mass matrix, i.e.,

$$\begin{aligned} [\bar{S}_1] &= [S_0][T_0] \\ &\vdots \\ [\bar{S}_m] &= [\bar{S}_{m-1}][\bar{T}_{m-1}] \end{aligned} \tag{3.15}$$

The final stress vector for the subregion, $[\sigma_m]$, is then expressed as

$$[\sigma_m] = [\bar{S}_m]\{\bar{x}_m\} \tag{3.16}$$

where

$\{\bar{x}_m\}$ are displacements of the super nodes.

Equation (3.15) represents a series of coordinate transformations; stresses from Eq. (3.16) are therefore exact to machine precision compared to those which are derived from an equivalent fully assembled finite element model.

To conform the reduction of the stress-displacement matrix with the step elimination algorithm from Section 3.2.2, matrix $[S]$ is stored according to the scheme of Fig.3.8 and is then partitioned as follows

$$[S] = [[S_1]\{w\}] \tag{3.17}$$

where

$\{w\}$ represents the last column and

$[S_1]$ represents the remaining submatrix of $[S]$.

Applying now the transformation using $[T]$ from Eq. (3.8) results in the reduced stress-displacement matrix

$$[\bar{S}] = [S_1] - \frac{1}{k_{nn}} \{g\}\{w\}^T \tag{3.18}$$

which is compatible with stiffness and mass matrices from Eqs. (3.9) and (3.10). The algorithm requires the eliminated degrees of freedom to be labelled with the highest

numbers in the numbering sequence (see also Section 3.2.2).

The incorporation of Eq. (3.18) into the reduction algorithm is demonstrated by the flow-chart of Appendix B and by SUBROUTINE STAR in Appendix D.

The stress-displacement matrix of the $m^{\underline{th}}$ level, $[\overline{S}_m]$, is produced in an accumulative way during several reduction steps (see Equation Set (3.15)). Thus, if matrix $[S_0]$ for the basic zero level element represents NS stress components, matrix $[\overline{S}_m]$ for the panel element represents NS*M stress components, where M is the number of basic elements of which the panel element is composed. Locations of stress points, specified in the basic element, determine therefore the distribution of stress points over the whole panel element, as demonstrated in the example of Fig. 3.8. For an assumed situation of plane stress with NS = 3 (i.e., $\sigma_x, \sigma_y, \sigma_{xy}$) and two degrees of freedom per node, the order for the stress-displacement matrix in the example presented would be of 24 by 20.

The above example indicates that stress-displacement matrices can be of a large order. On the other hand, the nature of the accumulative procedure does not allow a more selective stress computation which would result in lower order matrices. Core storage is therefore more likely to be exceeded when a stress computation is included in the analysis.

3.5 STORAGE SCHEME

An in-core solution requires that stiffness, mass and stress-displacement matrices as well as those matrices from the previous level used for assembly be kept in high speed storage simultaneously. Computation of starting locations and length of the dynamic arrays, as well as total storage requirement, is therefore necessary at the beginning of the procedure.

The scheme outlined in Table 3.5 indicates 3 in-core storage phases:

(1) Storage of elements from level zero to level two,

(2) storage of level-three elements, and

(3) storage of level-four elements.

Tape storage is used to transfer the arrays from one storage phase to another. The scheme in Table 3.5 gives starting locations for stiffness matrices only (L0 to L5); mass and stress-displacement matrices are stored in a parallel manner, as apparent from the general arrangement.

During all stages the matrices are stored as one-dimensional arrays, stiffness and mass matrices in Mode 1 during reduction phase and in Mode 2 during output phase

(Fig.3.1), stress-displacement matrices are stored according to Fig. 3.9.

3.6 DISCUSSION AND CONCLUDING REMARKS

A rectangular substructure or panel element is derived where internal nodes are eliminated and which allows flexibility in locations of nodes along the boundaries. A multilevel scheme is developed and a reduction procedure is used which operates efficiently for the scheme presented. The panel element is created in stages from level zero to level four and may be either symmetric (level three) or doubly symmetric (level two and four), as demonstrated in Figs. 3.4 through 3.7 and Table 3.3. Stress recovery is consistent with the multilevel scheme and allows a complete stress computation within the substructure.

Applications in Chapter IV demonstrate the efficient use of the panel element as well as its limitations, in vibration analysis of structures. Examples are also presented for static analysis and stress recovery.

The scheme presented in this Chapter may be considered as the necessary basic development. Extensions to the present version, which may lead to a more general panel element, are possible with little effort.

Suggested additions for the start element (level one) are the following:

(1) An irregular pattern for the start element allows different spacing of vertical grid lines.

(2) Allowance of different material properties in the start element could simulate ribs or openings.

(3) Creation of more than two possible start elements (i.e., introduction of height B3 and B4).

More variations for boundary node arrangement could be achieved by:

(1) More arbitrary selection for retained nodes in the end element.

(2) Option of retaining boundary nodes only on one vertical side.

Rotations of the element as a rigid body are independent of the above-mentioned developments and may be included through:

(1) In-plane rotations

(2) Out-of-plane rotations, thus allowing a three-dimensional analysis

(3) Mirror image.

TABLE 3.1 GROWTH PATTERNS

DOUBLE PROGRESSION		SINGLE PROGRESSION
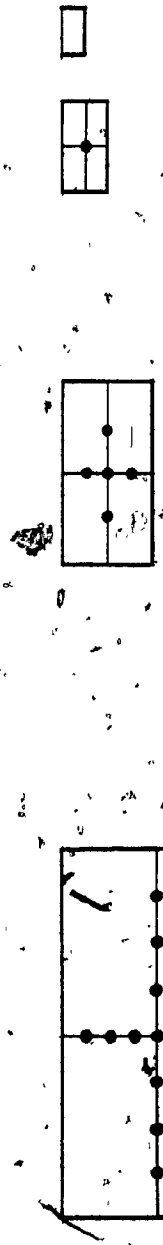	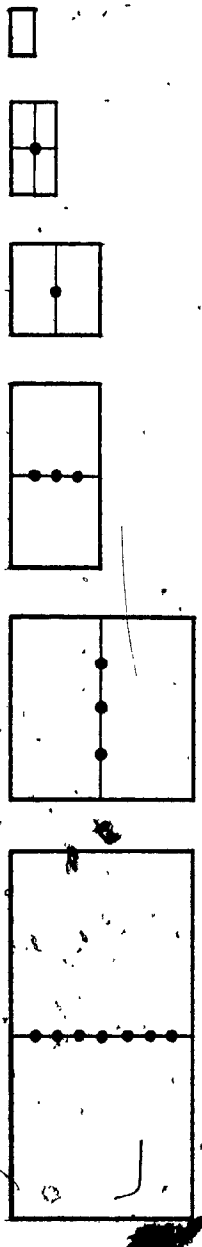	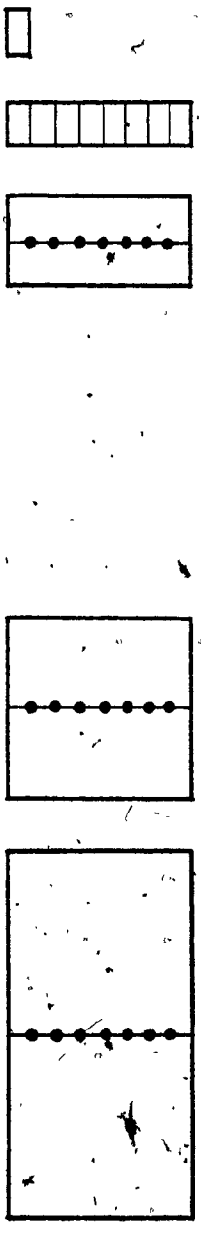
19 Eliminations in 3 Stages	15 Eliminations in 5 Stages	21 Eliminations in 4 Stages

NOTE: Boundary Nodes are not shown.

TABLE 3.2 LEVEL ONE ELEMENTS

IDENTIFICATION (FOR NHN = 5)		TYPE
START ELEMENTS	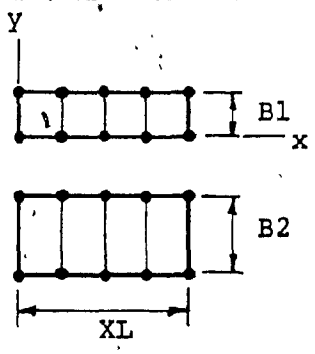	(100) (200)
END ELEMENTS	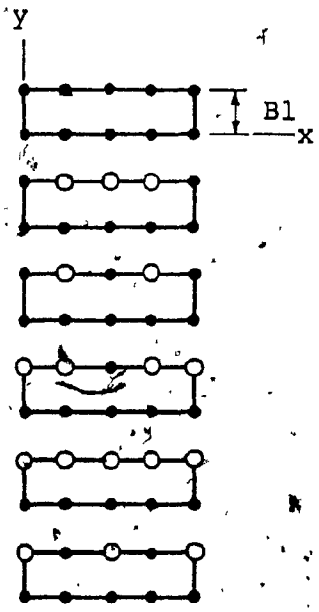	(1) or (100) (2) (3) (4) (5) (6)

● Retained Nodes ○ Eliminated Nodes

NOTES TO END ELEMENTS:

TYPE (3): Corner and midside nodes are retained (NHN $\geq$ 5)
TYPE (4): Midside node is retained (NHN $\geq$ 3)
TYPE (6): Nodes next to corner nodes are retained (NHN $\geq$ 5)

TABLE 3.3 LEVEL TWO ELEMENTS

IDENTIFICATION (FOR NHN = 5)	TYPE		REMARKS
	USING B1	USING B2	
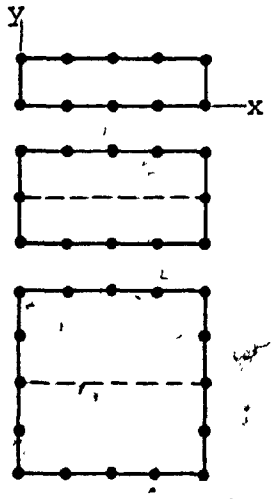 etc.	(100) (101) (102)	(200) (201) (202)	vertical boundary nodes are retained
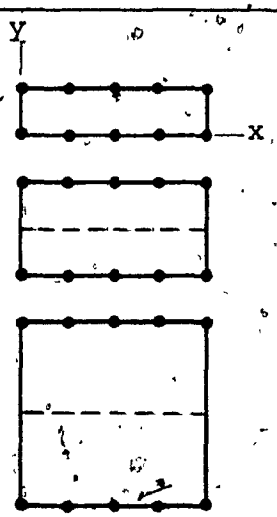 etc.	(100) (110) (120)	(200) (210) (220)	vertical boundary nodes are eliminated

• Retained nodes
Eliminated nodes are not shown

TABLE 3.4 COUPLING IN LEVEL FOUR (EXAMPLE 2)
NUMBERING OF DEGREES OF FREEDOM

Number of Degrees of Freedom	ND = 2		ND = 3	
	Element (1)	Element (2)	Element (1)	Element (2)
1	11	-5	16	7
2	12	-6	17	-8
3	15	-13	18	-9
4	16	-14	22	19
5	13	-15	23	-20
6	14	-16	24	-21
7	5	-11	19	22
8	6	-12	20	-23
9	7	-1	21	-24
10	8	-2	7	16
11	9	-3	8	-17
12	10	-4	9	-18
13			10	1
14			11	-2
15			12	-3
16			13	4
17			14	-5
18			15	-6

TABLE 3.5 DYNAMIC STORAGE ARRAYS FOR MATRICES

GENERAL ARRANGEMENT FOR ARRAYS	LOCATIONS DURING LEVEL ZERO TO LEVEL TWO	LOCATIONS DURING LEVEL THREE	LOCATIONS DURING LEVEL FOUR

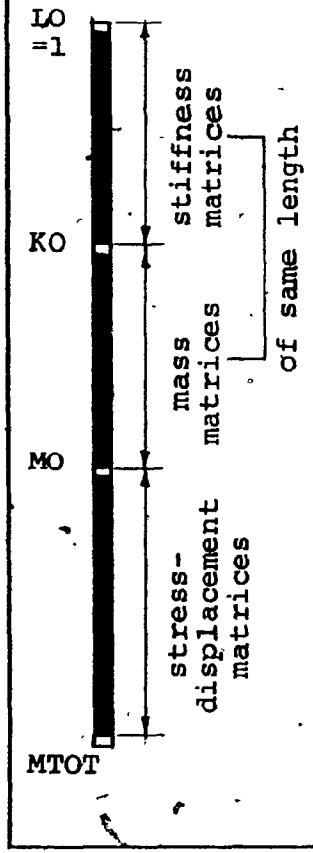

Level	Remarks
LO	
zero	for B1
L1	
zero	for B2
L2	
one	start element for B1
L3	
one	start element for B2
L4	
two	second last coupling step
L5	
one and two	end element last step
KO	

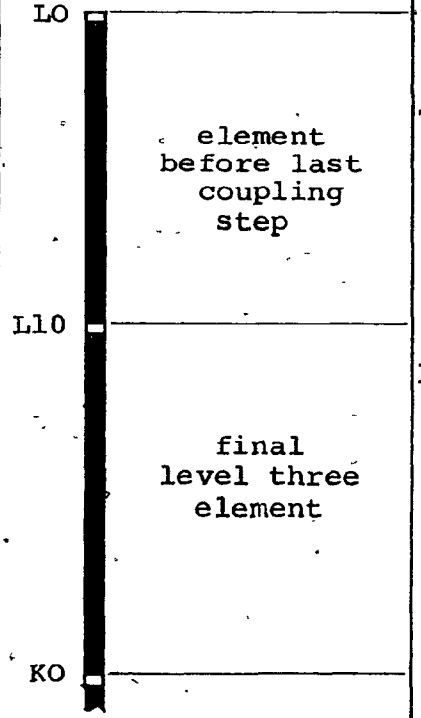

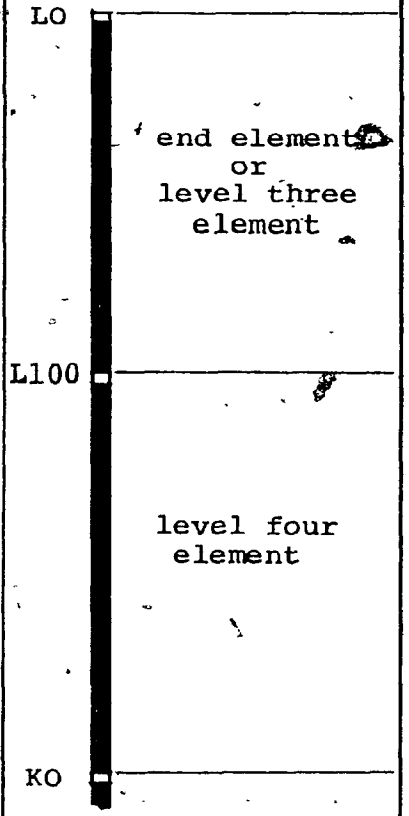

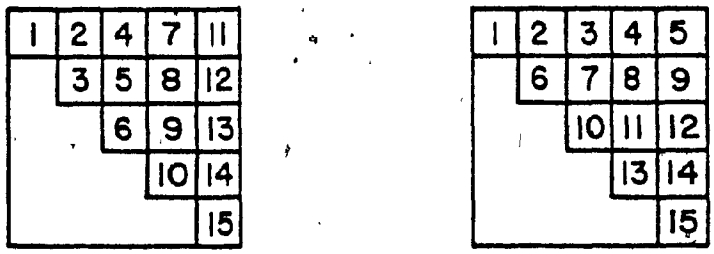

FIG. 3.1 STORAGE SCHEMES FOR STIFFNESS AND MASS MATRIX

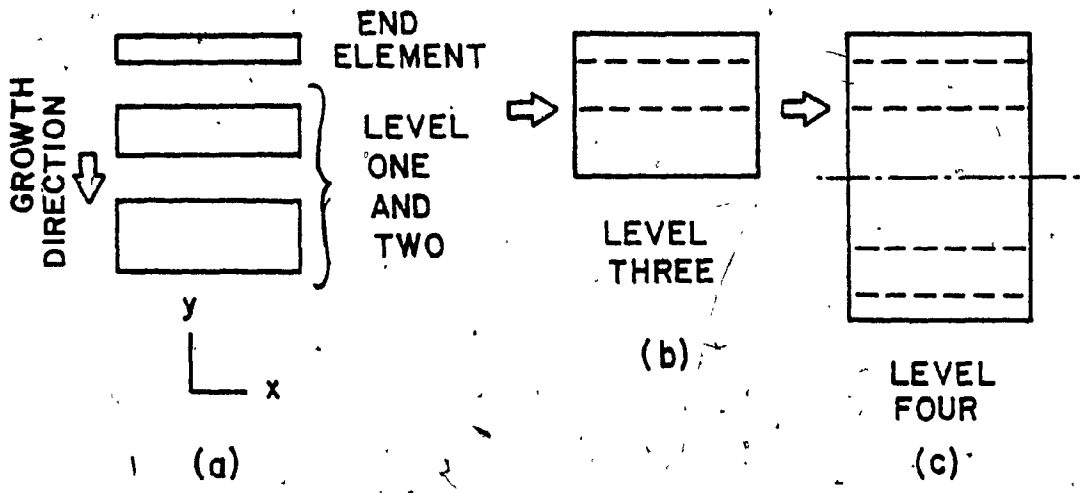

FIG. 3.2 GROWTH SCHEME OF THE LEVEL-FOUR PANEL ELEMENT

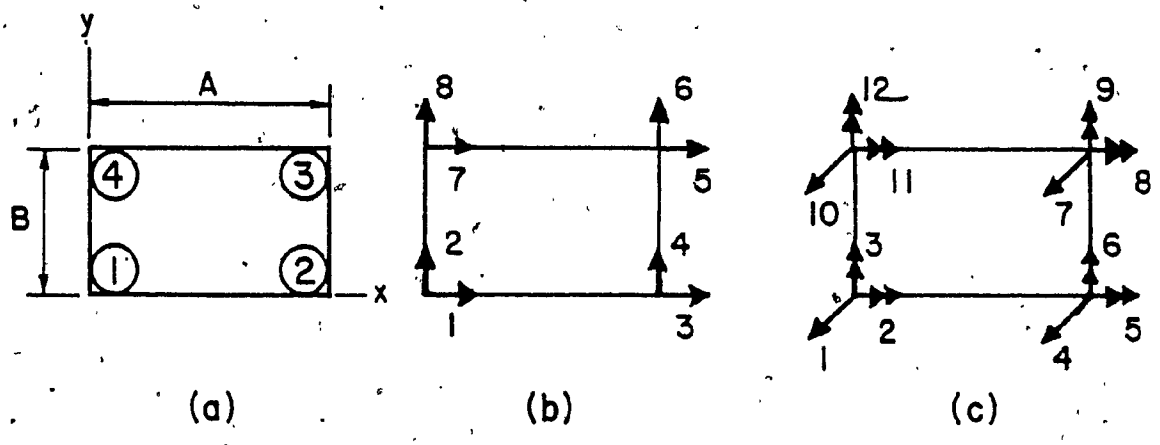

FIG. 3.3 NUMBERING OF 4-NODE ELEMENTS; (a) NODAL NUMBERING, (b) DEGREES OF FREEDOM FOR PLANE STRESS, AND (c) DEGREES OF FREEDOM FOR PLATE BENDING

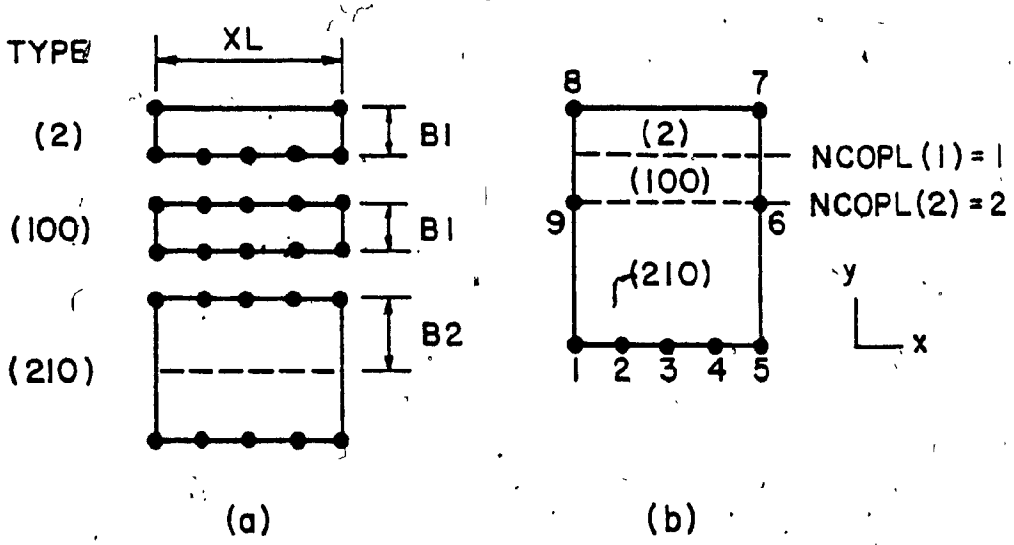

FIG. 3.4 COUPLING IN LEVEL THREE (EXAMPLE 1); (a) LEVEL ONE AND LEVEL TWO ELEMENTS, AND (b) LEVEL THREE ELEMENTS

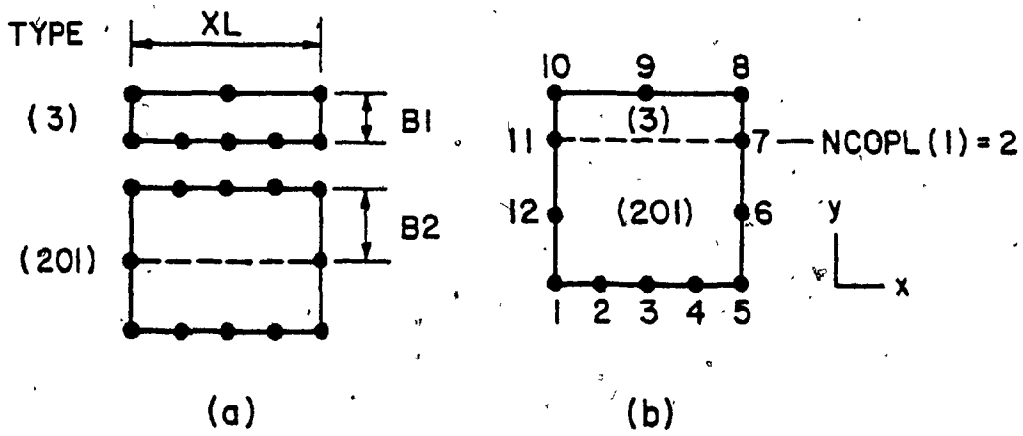

FIG. 3.5 COUPLING IN LEVEL THREE (EXAMPLE 2); (a) LEVEL ONE AND LEVEL TWO ELEMENTS, AND (b) LEVEL THREE ELEMENT

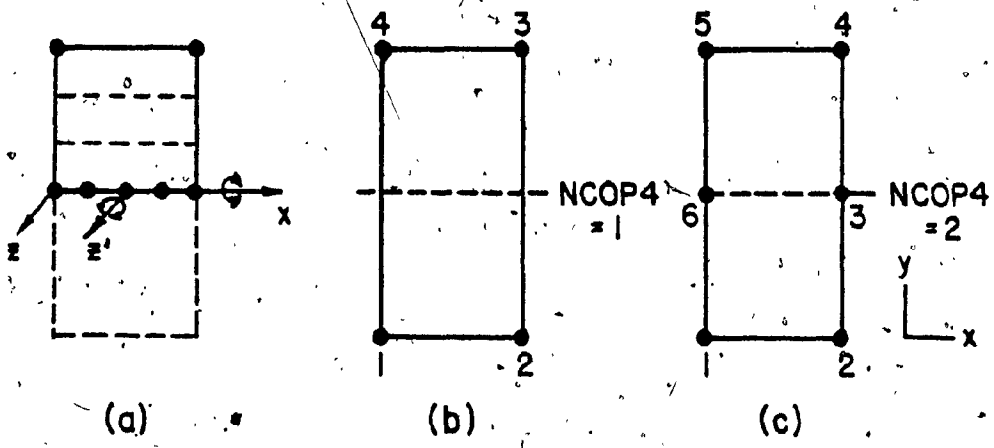

FIG.3.6 COUPLING IN LEVEL FOUR (EXAMPLE 1)

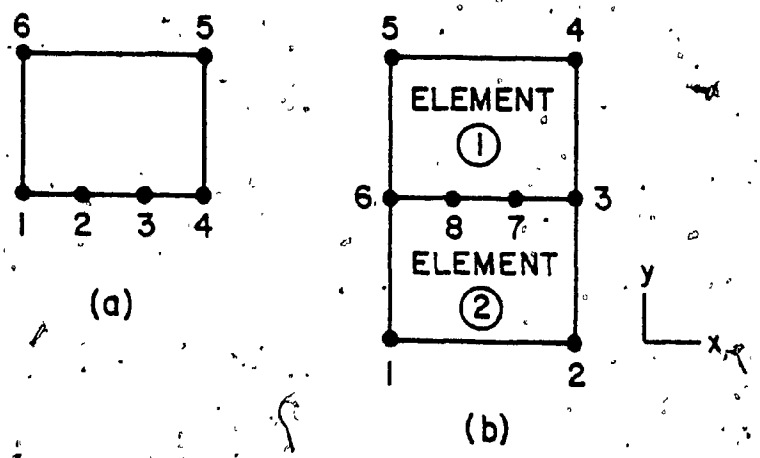

FIG. 3.7 COUPLING IN LEVEL FOUR (EXAMPLE 2); (a) NODAL NUMBERING FOR LEVEL THREE ELEMENT, AND (b) NODAL NUMBERING FOR LEVEL FOUR ELEMENT BEFORE REDUCTION OF INTERNAL NODES

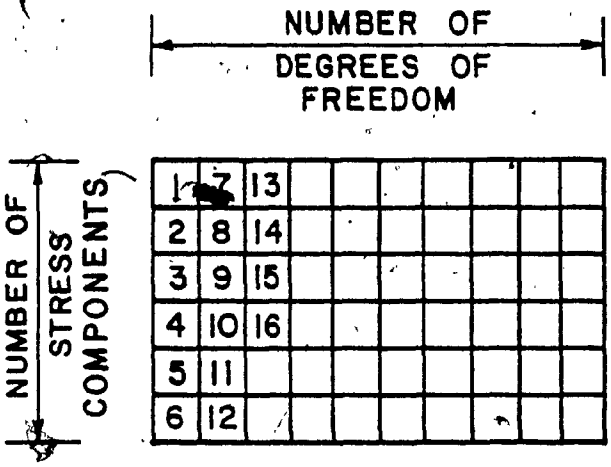

FIG. 3.8 STORAGE SCHEME FOR STRESS-DISPLACEMENT MATRIX

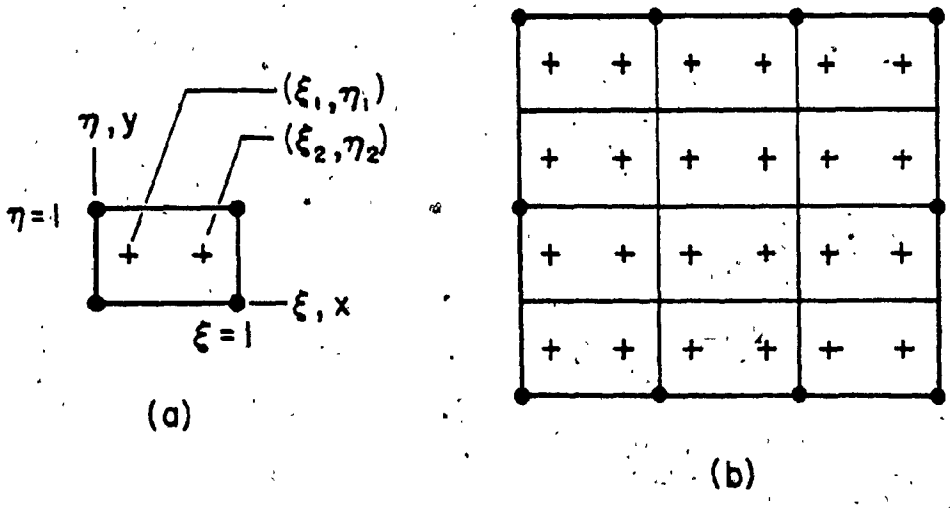

FIG. 3.9 EXAMPLE FOR STRESS POINT LOCATIONS; (a) BASIC 4-NODE ELEMENT, AND (b) PANEL ELEMENT

CHAPTER IV

APPLICATIONS USING PANEL ELEMENTS

CHAPTER IV

APPLICATIONS USING PANEL ELEMENTS

4.1 INTRODUCTION

In this Chapter, the panel element described previously and represented by SUBROUTINE PANEL in Appendix D is applied as a substructure option in conjunction with the general purpose program SAP4. For the examples to be presented, full displacement continuity along boundaries between substructures is assumed.

Emphasis is placed on structures subjected to membrane action, which includes free vibrations of shear walls. Static loading is also considered, primarily to demonstrate stress recovery. Solutions of membrane problems are compared to the solutions where a fully assembled finite element model is used.

To demonstrate accuracy and limitations of substructuring techniques in out of plane bending problems, cases of plate bending vibration are studied. Results are compared with analytic solutions.

An important aspect in dynamic analysis of structures is the representation of mass or inertia characteristics. In the previous Chapter mass matrices were assumed to be

consistent and full. However, in practical applications it may be more desirable to employ a lumped mass model in order to reduce computational effort, particularly for large systems. It has been observed that, for many situations in structural engineering, the lumped mass model results in solutions of sufficient accuracy [26]. A lumped mass option is therefore introduced for the panel element.

Mass lumping is conveniently achieved by distributing the total mass of the substructure along the diagonal of the mass matrix according to the diagonal terms of the consistent mass matrix. This procedure is applied easily when only translational degrees of freedom exist, as in plane stress elements or, more generally in all isoparametric finite elements. However, difficulties arise when rotational degrees of freedom are introduced, as may occur in plate bending. The latter is discussed in Section 4.2.

The predominant influence of mass concentration at floor levels in multi-storey structures may override the refined mass representation of an individual panel substructure. This situation is discussed for a plane stress shear wall model in Section 4.3.

For the solution of the free vibration problem the available eigenvalue routines from SAP4 were applied when lumped mass models were used. For consistent mass representa-

tion an in-core solver based on subspace iteration [21] was employed.

4.2 PLATE BENDING VIBRATIONS

In this Section free out of plane vibrations are studied for a single panel substructure which may be considered as one structural element. Since only the lowest modes of an individual panel are likely to contribute to overall structural response, only the first 4 modes are examined. The primary point of interest may be formulated thus: to what degree of accuracy can boundary nodes represent the dynamic properties of a substructure?

The following cases are studied using a non-conforming plate bending element [6]:

(1) Cantilever plate - investigated for accuracy of frequencies and mode shapes when consistent and lumped mass models are used.

(2) Square free-free plate - studied for accuracy of frequencies when consistent and lumped mass models are used.

(3) Cantilever plate - where internal degrees of freedom are introduced by employing panel assemblies.

4.2.1 Single Panel Element as Cantilever Plate

Dimensions, boundary node arrangement and mesh size of the panel element investigated are shown in Fig.4.1(a). Plate thickness is assumed as 0.1 in. (2.54 mm) and material properties are: Young's modulus = 3.0×10^4 ksi (2.07×10^5 MN/m^2), Poisson's ratio = 0.3 and mass density = 0.733×10^{-6} $kips\text{-}sec^2/in^4$ (0.00785 kg/cm^3). Results, expressed in terms of the four lowest natural frequencies with corresponding mode shapes, are compared to analytic solutions published by Barton [41]. The latter are based on 18-term Rayleigh-Ritz expansions and agree well with experimental results. Influence of the following parameters on accuracy for the free vibration problem are investigated:

(1) Consistent and lumped mass models using different strategies for lumping of rotary terms.

(2) Influence of variations in boundary nodes and mesh size.

At the basic element level (zero level) the mass matrix can be introduced either as consistent or as diagonally lumped. The final panel mass matrix is in both cases consistent, and in both cases the computational effort is practically the same. A study of plate bending vibrations showed that it is more desirable to start with a consistent mass matrix, for the following reasons: First, a noticeable improvement in accuracy

is achieved, assuming a consistent mass matrix is also used for the solution of the eigenvalue problem. Secondly, for some deformation shapes applied during elimination, a lumped mass matrix at the basic element level leads to zero rows and columns in the consistent mass matrix of the panel element, thus resulting in numerical instabilities.

The lumping procedure for the consistent mass matrix of the panel element was established from the following considerations. Hinton et al [42] derived expressions of lumped mass terms for certain isoparametric elements, an approach equivalent to scaling the diagonal terms according to the consistent mass matrix when the total element mass is preserved. This method, which may be termed "consistent lumping", is applied in this study for the derivation of a lumped mass matrix for the panel element substructure. Figure 4.2 demonstrates lumping of the translational degrees of freedom for the panel element of Fig. 4.1(a), assuming total panel mass of unity. It is shown that consistent lumping (Fig.4.2(a)) results in mass terms that are similar to those for lumping according to assumed tributary areas (Fig.4.2(b)).

For the lumping of rotary terms four possibilities were considered:

Case A:

Zero rotary terms are assumed.

Case B:

The rotary moment of inertia is taken over the thickness of the plate, for unit length, and is then multiplied by the total panel area. This quantity is distributed along the diagonal according to consistent lumping.

Case C:

Rotary inertia terms are used directly from the diagonal of the consistent mass matrix.

Case D:

The mass moment of inertia about the center of gravity of the panel is distributed according to consistent lumping.

In Table 4.1 frequencies, derived from both consistent as well as lumped models, are compared with values available in [41] using the following expression:

$$\varepsilon_F = \frac{\omega_E - \omega_A}{\omega_E} \times 100 \qquad (4.1)$$

where

ω_E and ω_A are frequencies obtained from [41] and from the present study, respectively.

The Table demonstrates good agreement for the consistent model, whereas the use of a lumped model results in large differences for all cases. It is apparent that Cases A to C are very close, thus, the influence of rotary terms lumped according to Cases B and C are of no practical significance. Case D, on the other hand leads to an over-estimation of rotary inertia terms. Therefore, rotary inertia is not included in further investigations (i.e., Case A is used).

Shapes of the four lowest modes are compared in Table 4.2 for consistent and lumped (Case A) models, when maximum amplitudes are normalized to one. Figure 4.3 shows the normalized mode shapes for the symmetric half-plate. As a measure of accuracy the length of the residual ε_s (i.e., Euklidean norm) is used, expressed as:

$$\varepsilon_s = \left\| \{\phi_E\} - \{\phi_A\} \right\|_2 \qquad (4.2)$$

where

$\{\phi_E\}$ and $\{\phi_A\}$ represent mode shapes from [41] and from this study, respectively.

Table 4.3 contains the corresponding ε_s values for the consistent and the lumped mass models.

A decrease in the number of boundary nodes, as well as different mesh sizes, compared to the panel element of Fig. 4.1(a), is represented by two cases in Table 4.4. As apparent from the values for ε_F and ε_s, frequencies and mode shapes are not significantly affected by these changes (compared to Tables 4.1 and 4.3).

4.2.2 Single Panel Element as Free-Free Plate

The plate with free-free boundary conditions presented in Fig. 4.1(b) is investigated for frequency accuracy. Plate thickness and material properties have the same values as used in Section 4.2.1.

A free-free body requires the application of eigenvalue shifting [28] in order to eliminate rigid body modes:

$$([K] - \alpha[M])\{\phi\} - \mu[M]\{\phi\} = \{0\} \qquad (4.3)$$

The natural frequencies of the plate are then expressed as $\omega_i^2 = \mu_i - \alpha$. For shift value α an approximation of the lowest frequency was used.

Differences in frequencies ε_F (see Eq. (4.1)) using [43], are presented in Table 4.5. The values of ε_F

are in the range of those for the cantilever plate, Table 4.1. A decrease in accuracy for the consistent model in the third mode is due to the particular nature of the third modal configuration, where the maximum amplitude occurs at the center of the plate.

4.2.3 Assembly of Panel Elements as Cantilever Plate

The investigations of the previous Sections have demonstrated that the use of lumped mass models in plate bending problems results in poor approximations of dynamic properties. To improve accuracy, a panel substructure may be composed of an assembly of panel elements, thereby increasing the number of degrees of freedom and at the same time introducing internal nodes.

The cantilever plate of Fig. 4.1(a) (see Section 4.2.1) is chosen for this study. Table 4.6 demonstrates the assemblies of two, four and eight-panel elements. Differences for frequencies as well as mode shapes, compared to [41], are presented for the consistent and the lumped mass model. As expected, improvements are achieved for both mass models with increasing number and distribution of nodal points over the plate. However, the Table demonstrates also that it is difficult to achieve accurate results in plate bending vibrations when lumped mass models are used. Thus, a consistent mass

model should be applied for substructures whenever plate bending contributes significantly to the overall structural response, and when a distributed inertia characteristic exists.

4.3 STRUCTURAL PROBLEMS IN MEMBRANE ACTION

In this Section applications in the field of structural engineering are presented. Dynamic properties of the total structure are studied, rather than for the substructure only. A single panel element may represent an actual panel or a substructure, where full continuity along the boundaries between substructures is assumed.

In the following examples plane stress elements are used which include incompatible modes, unless mentioned otherwise. The mass matrix at zero element level is represented by a lumped model. For the panel element the mass matrix is derived by consistent lumping as described in Section 4.2.

The applications to follow concentrate primarily on shear wall structures and are:

(1) Free vibration analysis of a single bay shear wall where floor mass intensity is varied.

(2) Free vibration analysis of a coupled shear wall.

(3) Stress recovery, demonstrated for static analysis of a coupled shear wall and a beam bending problem.

4.3.1 Single Bay Shear Wall With Varied Floor Mass Intensity

The 5-storey shear wall shown in Fig. 4.4 is analyzed using the three different panel elements labelled Model A, B and C. Solutions derived for these models are compared to the full finite element assembly of Fig. 4.4(a). The models are studied for homogeneously distributed mass, as well as for mass concentrated at floor levels. Material properties are as follows: Young's modulus = 5.76×10^5 kips/ft^2 (2.76×10^4 MN/m^2), Poisson's ratio = 0.20 and mass density = 0.00482 kips - sec^2/ft^4 (0.0025 kg/cm^3). The wall thickness is assumed as 0.667 ft (0.203 m).

Differences in the periods of vibration with respect to the full finite element model, presented for the first 12 modes, are expressed as

$$\varepsilon_p = \frac{T_E - T_A}{T_A} \times 100 \quad , \qquad (4.4)$$

with T_E and T_A representing the periods of the full model and of the models using panel elements, respectively. Values for ε_p, derived for homogeneous mass distribution, are shown in Table 4.7. Differences become quite large for higher modes, increasing from Model A to C. Thus, a lumped mass representa-

tion for panel elements may not result in satisfactory solutions for the homogeneous shear wall. Improvement in accuracy could be achieved using a consistent mass model.

Introduction of a concentrated mass at floor levels, however, results in a more realistic situation for practical applications. Figure 4.5 presents differences in frequencies, ε_p, for the first 12 modes as a function of floor level mass intensity. Floor mass intensity, or "concentrated mass intensity", is expressed in terms of multiples of the total homogeneous shear wall mass, equally distributed over storey degrees of freedom. It is noted that for a concentrated mass intensity of 10 all periods up to the twelfth mode are approximated within or very close to one per cent, relative to those of the full finite element model. It was also observed that vertical extensional modes (e.g., modes 3 and 6) experience a higher rate of convergence.

Table 4.8 compares the mode shapes of Models A, B and C to those of the full model, for a concentrated mass intensity of 10. The mode shapes are represented by the displacements of five characteristic nodes (left side node at each floor level). Equation (4.2) is applied to derive the length of the residual ε_s, with $\{\phi_E\}$ and $\{\phi_A\}$ representing mode shapes of the full model and the model using panel elements, respectively. The magnitudes of ε_s demonstrate good approximations for all 12 modes.

The preceding observations indicate that degrees of freedom representing concentrated masses may become predominant in the system equation, thus resulting in close agreement of the lowest eigenpairs for the shear wall models of Fig. 4.4. For concentrated mass intensity less than 1.0, however, good agreement is achieved only for some of the lowest modes. Additionally, the curves in Fig. 4.5 may become discontinuous for higher modes (see for example the dotted lines for modes 9 and 10). This characteristic is due to changes in the sequence of modal configurations.

The application of substructuring techniques does not necessarily lead to savings in execution time, since a large bandwidth may be introduced into the system equation. In addition matrices tend to lose their sparsity due to high connectivity of substructure degrees of freedom. Thus, more iteration steps are necessary (although with fewer degrees of freedom) when subspace iteration is applied for the solution of the eigenvalue problem.

In the preceding examples, approximate execution times expressed as percentages of the full model time were:

(a) Model A - 100 per cent

(b) Model B - 50 per cent

(c) Model C - 30 per cent.

Therefore, it can be concluded that no savings in computing time can be expected when all boundary nodes of the substructure are retained. However, if some of the boundary nodes are eliminated, considerable savings can be achieved.

The results presented and evaluated in this Section can give representative guidelines for possible savings in computing time, but even more so for the range of accuracy when similar shear wall examples are analyzed using substructuring techniques. For cases with approximately the same number of degrees of freedom, adequately distributed and with concentrated mass intensity of magnitude 10 or higher, satisfactory accuracy should be obtained. If the number of degrees of freedom is increased (i.e., increase in number of storeys or bays), similar accuracy can be expected for lower concentrated mass intensity.

4.3.2 Free Vibration of a Coupled Shear Wall

Figure 4.6 shows a coupled shear wall, represented by a full finite element model and by the corresponding model using panel elements. The following properties are assumed: $E = 5.76 \times 10^5$ kips/ft^2 (2.76×10^4 MN/m^2), $\nu = 0.20$, $\rho = 0.00482$ kips-sec^2/ft^4 (0.0025 kg/cm^3), and wall thickness = 1 ft (0.305 m).

The modularity of this structure allows the use of panel elements in an effective way. Figure 4.6(b) shows that three different types of panel elements are created, leading to fairly even distribution of nodal points. Thus, good approximation to the full model can be expected, even for low concentrated mass intensity. It is noted that additional nodes are introduced at the two piers and in connecting beams, to improve mass representation.

In Table 4.9 the first 12 periods for the 2 models are compared. Values for ε_p, derived from Eq. (4.4), indicate only small differences between the periods of the two models when mass distribution is homogeneous. Accuracy, however, is still noticeably improved when concentrated floor masses are introduced. For this example, only the weight of floor slabs is considered (slab thickness = 7 in. (0.178 m), span = 24 ft (7.36 m)), leading to a concentrated mass intensity of 3.2.

Execution time for the model using the panel element representation was 85 to 90 per cent that of the full finite element model. The real advantage for using panel elements in this case, however, was demonstrated by a simple and short formulation of the input data.

4.3.3 Static Analysis of a Coupled Shear Wall

A coupled shear wall, similar to the one discussed in the previous Section, is taken from [44]. The full model, as applied in [44], and its panel representation are shown in Figs. 4.7(a) and 4.7(b), respectively. Material properties are: $E = 4.0 \times 10^6$ psi (2.76×10^4 MN/m^2), and $\nu = 0.4$. Wall thickness is assumed as 1 ft (0.305 m). Lateral loading is indicated in Fig. 4.7(a) and corresponds to [44]. For this analysis plane stress elements, without incompatible modes, are used.

Distribution of nodal points is not important in a static analysis. Thus, when applying panel elements, only those nodes are retained which are needed for connectivity and symmetry, together with nodes where displacement output is desired. Figure 4.7(b) demonstrates the use of four different panel elements.

Lateral displacements of the left wall are plotted in Fig. 4.8. Results obtained using panel elements are identical to [44]. A stress recovery is performed for the lower left pier. Corresponding to Fig. 3.9(a), two stress points are introduced for the basic element: $\xi_1 = 0.25$, $\eta_1 = 0.5$ and $\xi_2 = 0.75$, $\eta_2 = 0.5$. This arrangement gives full information for normal stress σ_y in the y-direction, inside the basic

4-node element. Figure 4.9 shows the isobars of σ_y. These are in good agreement with [44].

4.3.4 Stress Recovery for Cantilever Beam

A cantilever beam represented by one panel element (Type (140)) and the corresponding full model are shown in Figs. 4.10(b) and 4.10(a), respectively. Material properties are: $E = 3.0 \times 10^4$ ksi (2.07×10^5 MN/m^2) and $\nu = 0.3$. Beam width is assumed as 0.5 in. (1.27 cm). The total load of 1 kip(4.45 kN) is applied at nodal points according to a parabolic distribution.

This example demonstrates stress recovery within the substructure. Two stress points are selected in the same manner as in Section 4.3.3; thus, full information is available for normal stresses σ_y and shear stresses σ_{xy}, along $\eta = 0.5$ in each basic element. Magnitudes of σ_y and σ_{xy} are plotted for several sections along the y-axis, as shown in Fig. 4.11. These stresses were compared with an analysis using the full model and one stress point per basic element. The results obtained agreed to machine precision.

4.4 SUMMARY

The panel element derived in Chapter III and attached to the element library of SAP4 was, in the previous Chapter, applied as an effective substructure option. Accuracy achieved and effectiveness with respect to execution time, as well as general applicability, were discussed for examples in plate bending vibrations, plane stress vibrations and in stress recovery. The observations noted are summarized below:

(a) Free vibration analyses for a cantilever plate and a free-free plate, both consisting of a single panel element (Fig. 4.1), were compared to analytic solutions. Studies of mass representation resulted in the following conclusions:

(i) A consistent mass model leads to good approximations of frequencies and associated mode shapes (Fig. 4.3 and Tables 4.1 through 4.6).

(ii) Lumped mass models derived by "consistent lumping" (see Section 4.2.1) did not result in satisfactory solutions (Tables 4.1 and 4.4 through 4.5). Different strategies for lumping of rotational degrees of freedom indicated that inclusion of lumped rotary inertia terms

is not necessary. Improvement can be achieved by introducing internal nodes using panel assemblies (Table 4.6).

(b) For free vibration of a one-bay shear wall (Fig.4.4) and a coupled shear wall (Fig. 4.6), comparison with the equivalent full finite element model provided the following conclusions:

(i) A lumped mass representation for panel element substructures leads to accurate results, provided (1) nodal points are adequately distributed, or (2) concentrated masses are introduced which are of predominant influence relative to panel masses (Fig.4.5).

(ii) Execution time can be significantly reduced when panel elements are applied (Models B and C of Fig. 4.4). However, if all boundary nodes are retained, no savings can be expected (Model A in Fig.4.4).

(iii) Use of panel elements as a substructure option results in significant savings in data preparation.

(c) A static analysis of a coupled shear wall (Fig.4.7) and a cantilever beam (Fig.4.10) demonstrated the

effectiveness of the stress recovery scheme (Figs. 4.9 and 4.11).

TABLE 4.1 COMPARISON OF FREQUENCIES - CANTILEVER PLATE

Mode	Frequencies (cps)		ε_F				
	Ref. [44]	Consistent Mass	Consistent Mass	Lumped Mass CASE A	CASE B	CASE C	CASE D
1	840	838	0.20	7.7	7.8	9.0	58.0
2	3613	3614	-0.03	34.0	34.0	34.0	62.0
3	5350	5350	-2.3	19.5	20.0	21.0	65.0
4	11930	11930	-1.2	36.6	37.0	38.0	62.0

TABLE 4.2. COMPARISON OF NORMALIZED MODE SHAPES - CANTILEVER PLATE

Mode	Node No.	Ref. [41]	Consistent Mass	Lumped Mass CASE A
1	1	0.089	0.087	0.084
	2	0.328	0.327	0.321
	3	0.651	0.649	0.644
	4	0.997	0.997	0.997
	5	0.998	0.999	0.999
	6	1.0	1.0	1.0
2	1	0.234	0.245	0.264
	2	0.609	0.600	0.639
	3	0.845	0.864	0.889
	4	1.0	1.0	1.0
	5	0.504	0.505	0.505
	6	0.0	0.0	0.0
3	1	0.432	0.439	0.502
	2	0.758	0.803	1.0
	3	0.192	0.247	0.490
	4	-0.952	-0.935	-0.771
	5	-0.972	-0.982	-0.875
	6	-1.0	-1.0	-0.917
4	1	0.592	0.580	0.477
	2	0.681	0.715	0.532
	3	-0.133	-0.113	-0.278
	4	-1.0	-1.0	-1.0
	5	-0.530	-0.540	-0.539
	6	0.0	0.0	0.0

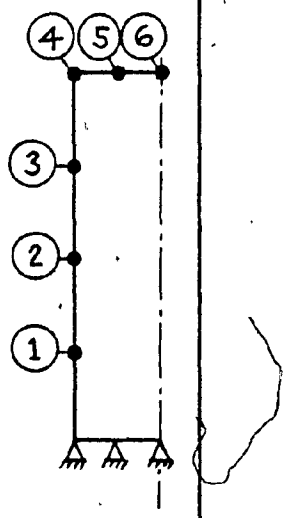

NODE NUMBERING

TABLE 4.3 MODE SHAPES COMPARED TO REF. [41] - CANTILEVER PLATE

Mode	ε_s	
	Consis-tent Mass	Lumped Mass CASE A
1	0.001	0.005
2	0.011	0.026
3	0.018	0.234
4	0.025	0.158

TABLE 4.4 FREQUENCIES AND MODE SHAPES COMPARED TO REF. [41] - CANTILEVER PLATE AND DIFFERENT PANEL ELEMENTS

Panel Element Type	Mode	Consistent Mass		Lumped Mass CASE A	
		ε_F	ε_s	ε_F	ε_s
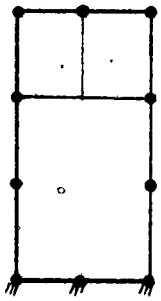 (100,101/2)	1	0.10	0.002	7.5	0.007
	2	-0.30	0.003	35.0	0.018
	3	-2.8	0.022	19.6	0.239
	4	-0.40	0.020	39.7	0.126
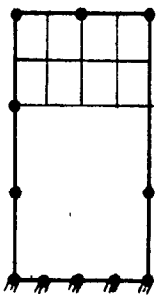 (3,100,110, 110/1,2,2)	1	0.20	0.001	8.1	0.006
	2	-0.20	0.004	35.2	0.027
	3	-2.8	0.018	21.7	0.222
	4	-2.7	0.022	38.3	0.147

TABLE 4.5 COMPARISON OF FREQUENCIES - FREE-FREE PLATE

Mode	Frequencies (cps)		ε_F	
	Ref. [43]	Consis-tent Mass	Consis-tent Mass	Lumped Mass (CASE A)
1_d	3257	3302	-1.4	23.1
2	4738	4807	-1.4	38.0
3	5900	6642	-9.1	11.0
4	8500	8585	-1.0	38.0

TABLE 4.6 FREQUENCIES AND MODE SHAPES COMPARED TO REF. [41] - CANTILEVER PLATE AS PANEL ASSEMBLIES

Panel Element Type	Mode	Consistent Mass		Lumped Mass CASE A	
		ε_F	ε_s	ε_F	ε_s
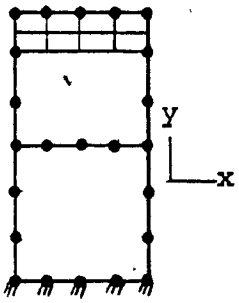 2 x (1,101/1,1)	1	0.3	0.0008	5.4	0.005
	2	0.1	0.005	23.4	0.003
	3	-0.5	0.010	18.2	0.018
	4	-0.2	0.024	25.0	0.039
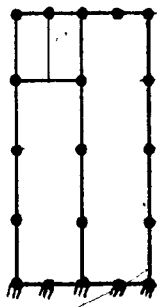 2 x (102)	1	0.1	0.001	3.6	0.004
	2	-0.03	0.011	15.6	0.012
	3	-0.7	0.011	10.8	0.116
	4	-0.4	0.021	20.0	0.041

TABLE 4.6 (continued)

Panel Element Type	Mode	Consistent Mass		Lumped Mass CASE A	
		ε_F	ε_s	ε_F	ε_s
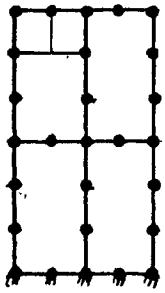 4 x (1,101/2,2)	1	0.2	0.001	2.1	0.002
	2	0.08	0.004	14.1	0.003
	3	-0.4	0.011	7.7	0.063
	4	0.05	0.022	15.6	0.035
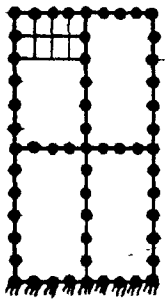 4 x (1,101/2,2)	1	0.3	0.001	2.3	0.002
	2	0.2	0.011	14.9	0.012
	3	0.0	0.008	6.5	0.054
	4	0.1	0.023	15.7	0.053
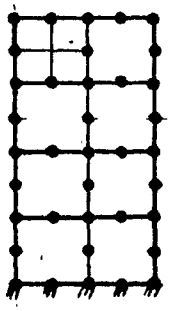 8 x (101)	1	0.2	0.001	1.5	0.002
	2	0.1	0.011	10.4	0.011
	3	-0.3	0.011	4.8	0.039
	4	0.2	0.021	9.1	0.026

TABLE 4.7 NATURAL PERIODS COMPARED TO FULL FINITE ELEMENT MODEL - HOMOGENEOUS SINGLE BAY SHEAR WALL

Mode	Period (sec)	ε_p		
	FULL MODEL	MODEL A	MODEL B	MODEL C
1	0.1455	1.1	1.2	1.6
2	0.0268	3.8	3.8	5.0
3	0.0183	0.2	0.3	0.4
4	0.0111	5.8	6.1	8.1
5	0.0067	8.3	9.1	12.9
6	0.0061	2.1	2.5	3.4
7	0.0047	11.9	13.7	20.6
8	0.0037	5.8	7.0	10.8
9	0.0036	0.7	0.3	8.9
10	0.0030	10.8	17.3	11.9
11	0.0028	15.3	17.7	14.7
12	0.0027	17.3	18.6	16.7

TABLE 4.8 MODE SHAPES COMPARED TO FULL FINITE ELEMENT MODEL - SINGLE BAY SHEAR WALL WITH CONCENTRATED FLOOR MASSES

Mode	ε_s		
	MODEL A	MODEL B	MODEL C
1	0.0001	0.0001	0.0002
2	0.0025	0.0029	0.0043
3	0.0005	0.0004	0.0003
4	0.0042	0.0049	0.0072
5	0.0047	0.0060	0.0096
6	0.0100	0.0083	0.0097
7	0.0059	0.0087	0.0150
8	0.0072	0.0047	0.0059
9	0.0084	0.0038	0.0046
10	0.0690	0.0770	0.0640
11	0.0640	0.0770	0.0790
12	0.0062	0.0160	0.0670

TABLE 4.9 NATURAL PERIODS COMPARED TO FULL FINITE ELEMENT MODEL - COUPLED SHEAR WALL

	Mode	Period (sec)		ε_p
		FULL MODEL	USING PANEL ELEMENTS	
Homogeneous Wall	1	0.1895	0.1902	0.50
	2	0.0420	0.0414	1.50
	3	0.0330	0.0329	0.40
	4	0.0314	0.0312	0.84
	5	0.0186	0.0185	1.50
	6	0.0185	0.0181	2.10
	7	0.0174	0.0175	0.56
	8	0.0150	0.0149	0.65
	9	0.0138	0.0136	0.88
	10	0.0130	0.0127	2.20
	11	0.0128	0.0124	2.90
	12	0.0127	0.0123	3.10
Including Floor Masses	1	0.4390	0.4386	0.09
	2	0.0932	0.0935	0.28
	3	0.0734	0.0734	0.14
	4	0.0691	0.0692	0.20
	5	0.0430	0.0430	0.17
	6	0.0400	0.0400	0.08
	7	0.0389	0.0391	0.66
	8	0.0363	0.0364	0.25
	9	0.0340	0.0342	0.44
	10	0.0332	0.0334	0.53
	11	0.0330	0.0332	0.56
	12	0.0329	0.0331	0.59

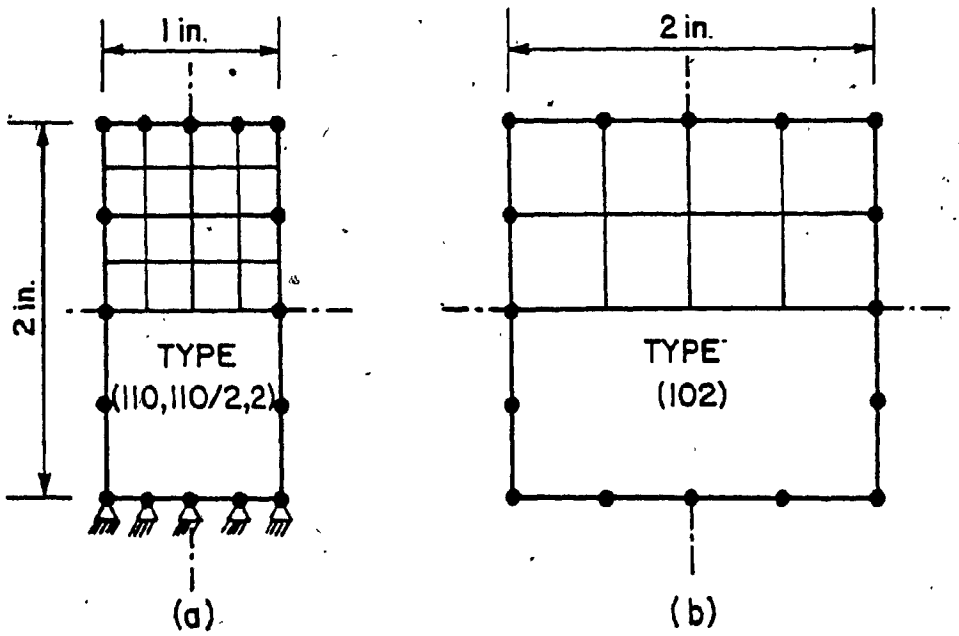

FIG. 4.1 PANEL ELEMENT MODELS FOR FREE VIBRATION IN PLATE BENDING; (a) CANTILEVER PLATE, AND (b) FREE-FREE PLATE

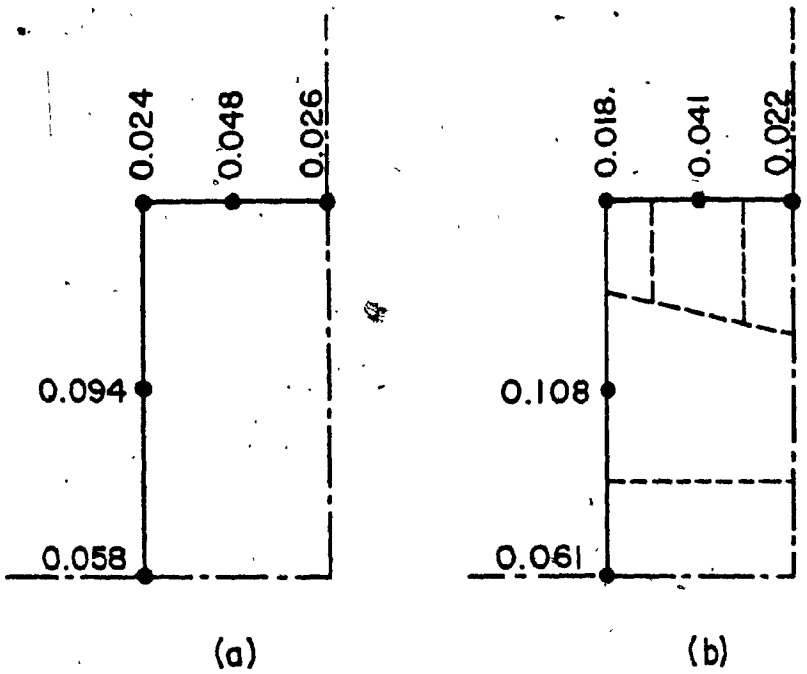

FIG. 4.2 LUMPING OF PANEL MASS IN LATERAL DIRECTION; (a) CONSISTENT LUMPING, AND (b) LUMPING BY TRIBUTARY AREAS

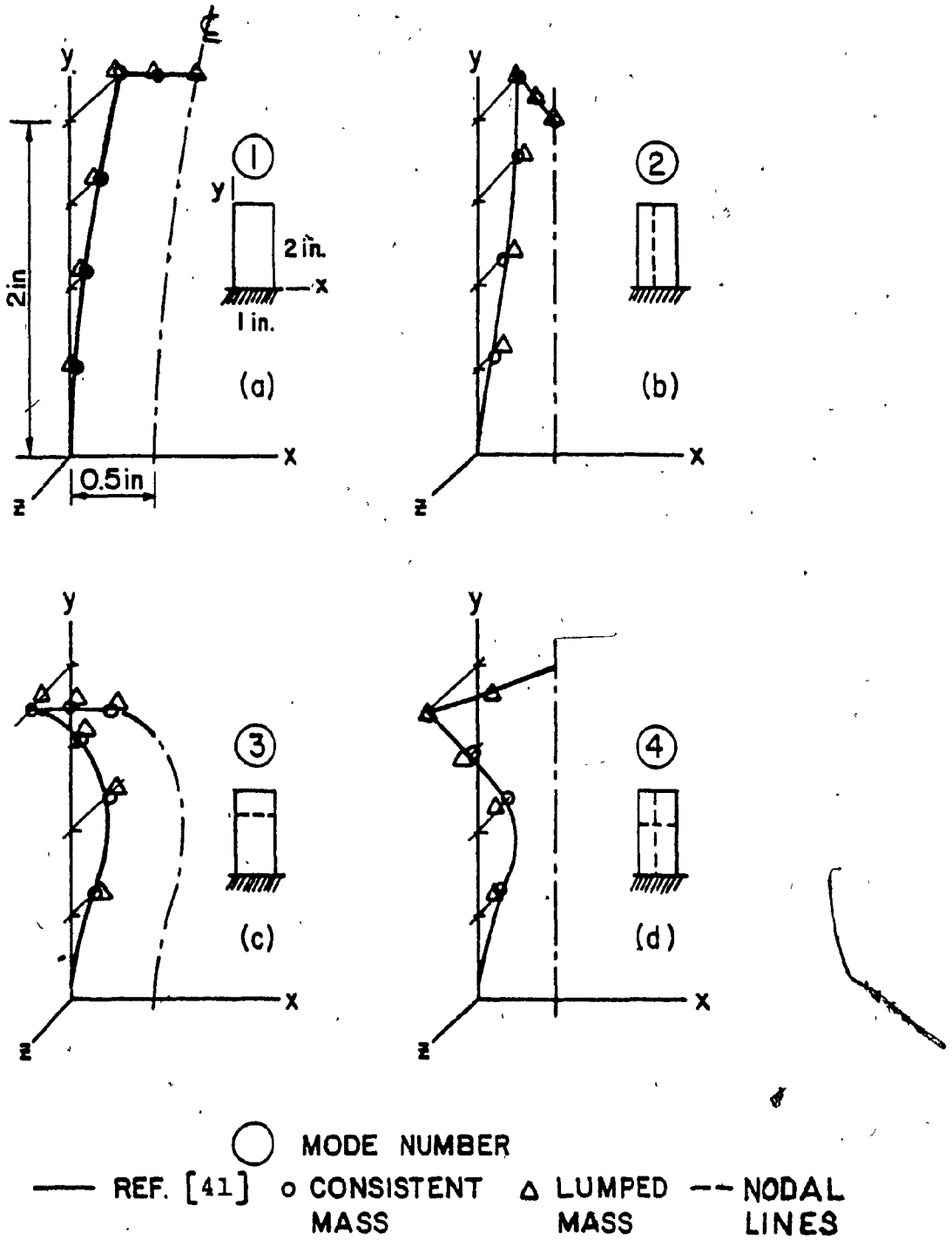

FIG. 4.3 COMPARISON OF MODE SHAPES FOR CANTILEVER PLATE

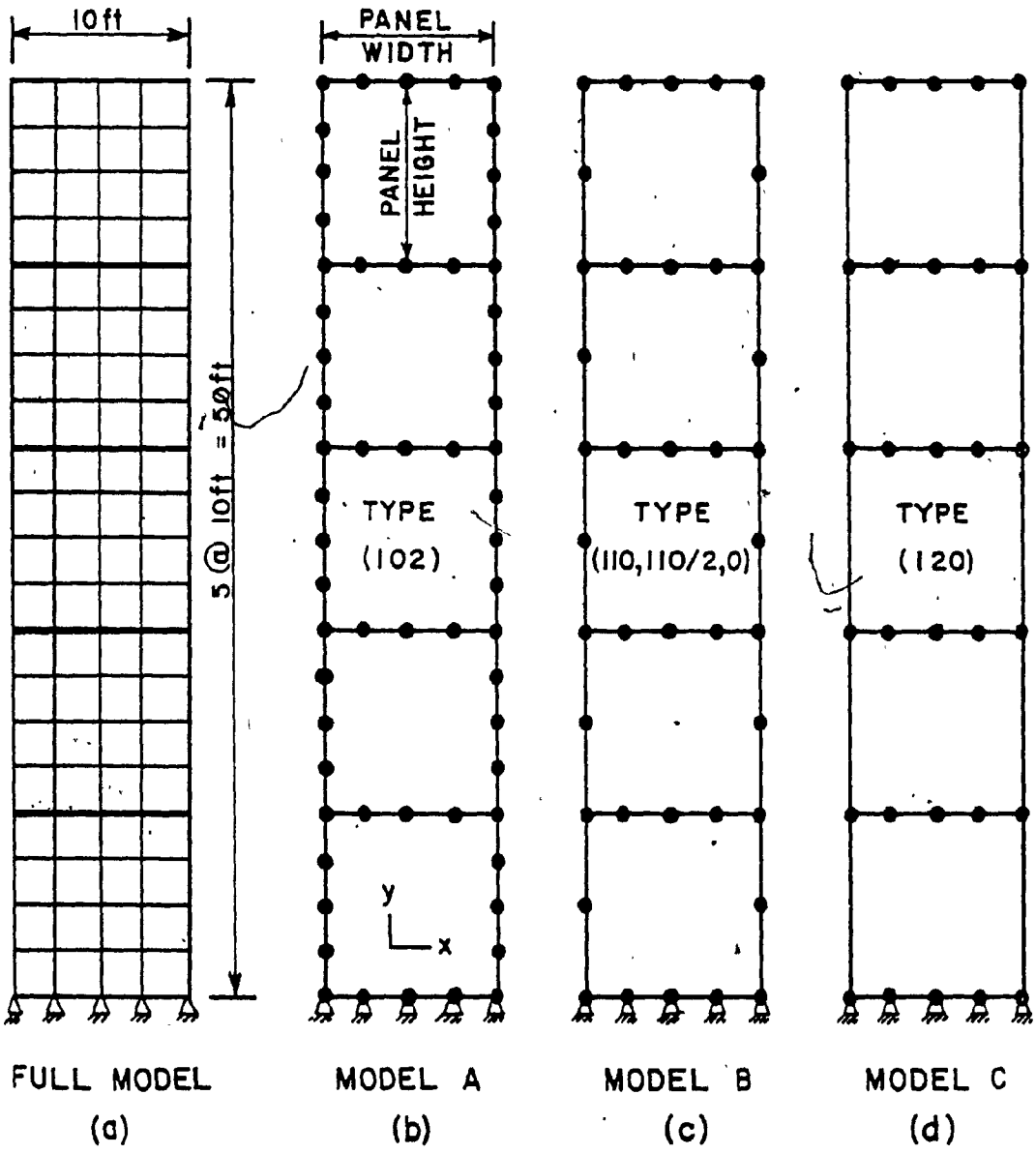

FIG. 4.4 SINGLE BAY SHEAR WALL; (a) FULL FINITE ELEMENT MODEL, AND (b) - (d) USING PANEL ELEMENTS (1 ft = 0.305 m)

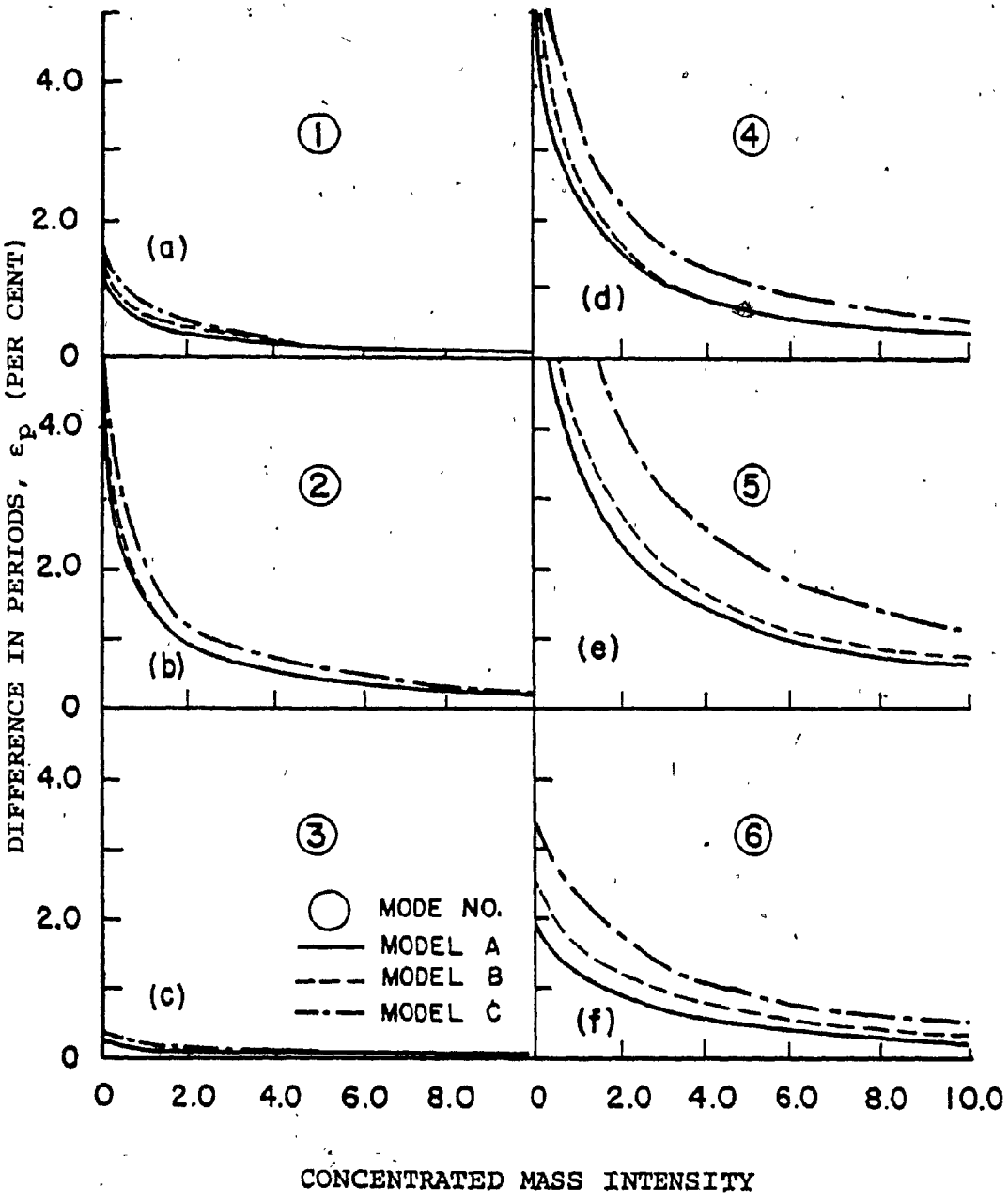

FIG. 4.5 EFFECT OF FLOOR MASS INTENSITY ON DIFFERENCE IN NATURAL PERIODS COMPARED TO THE FULL FINITE ELEMENT MODEL

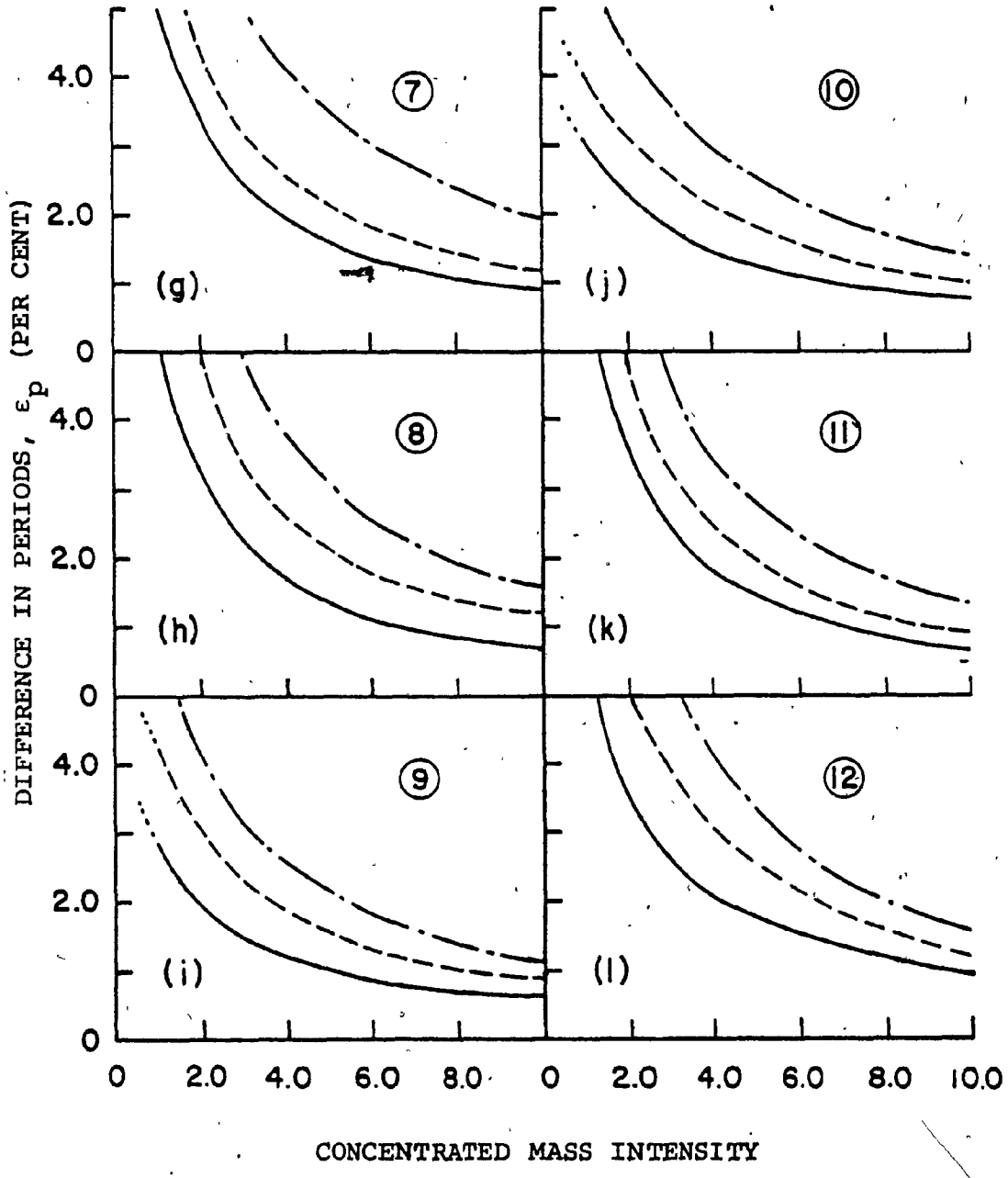

FIGURE 4.5 (continued)

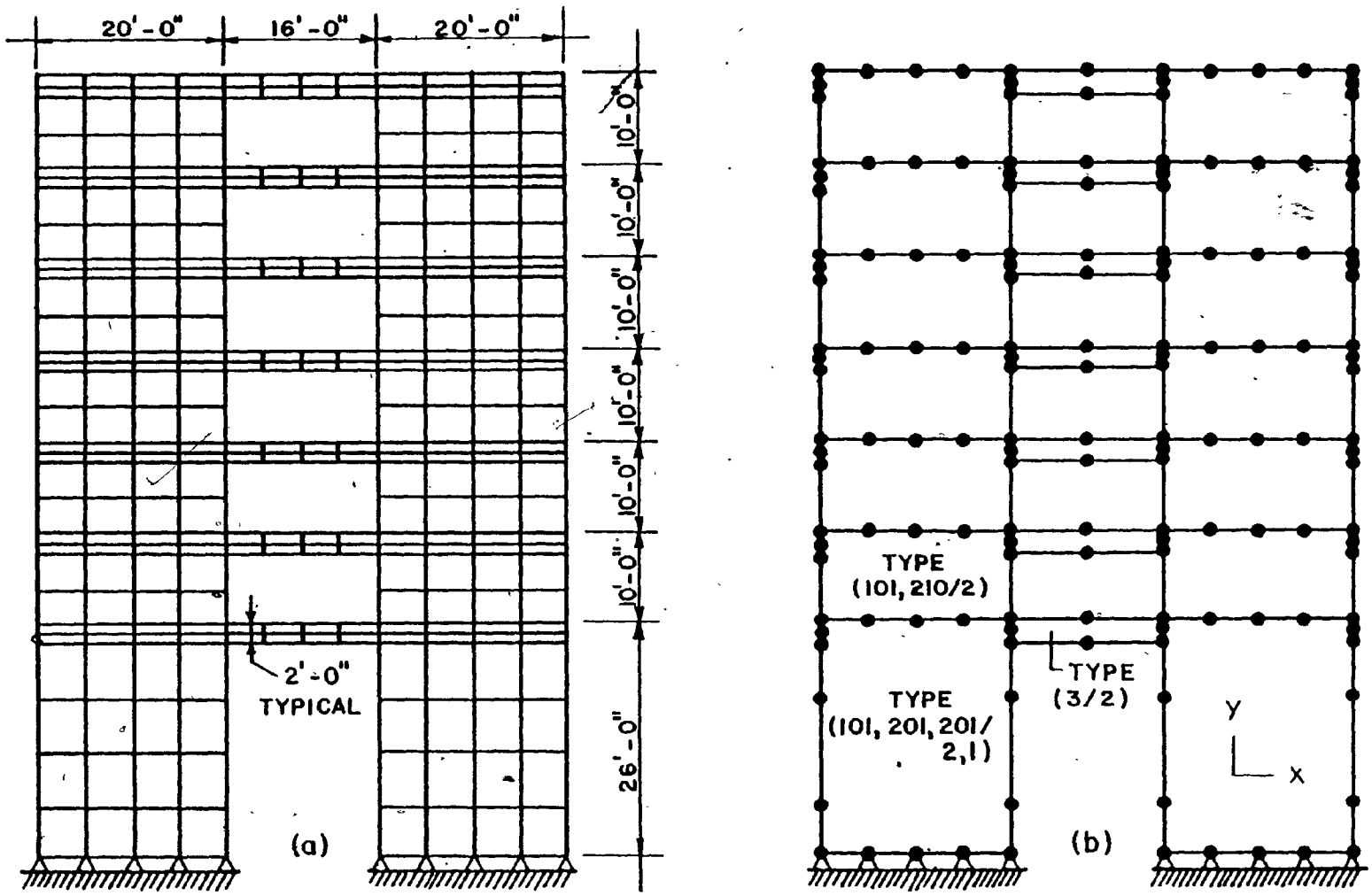

FIG. 4.6 COUPLED SHEAR WALL FOR DYNAMIC ANALYSIS; (a) FULL FINITE ELEMENT MODEL, AND (b) PANEL SUBSTRUCTURE REPRESENTATION (1 ft = 0.305 m)

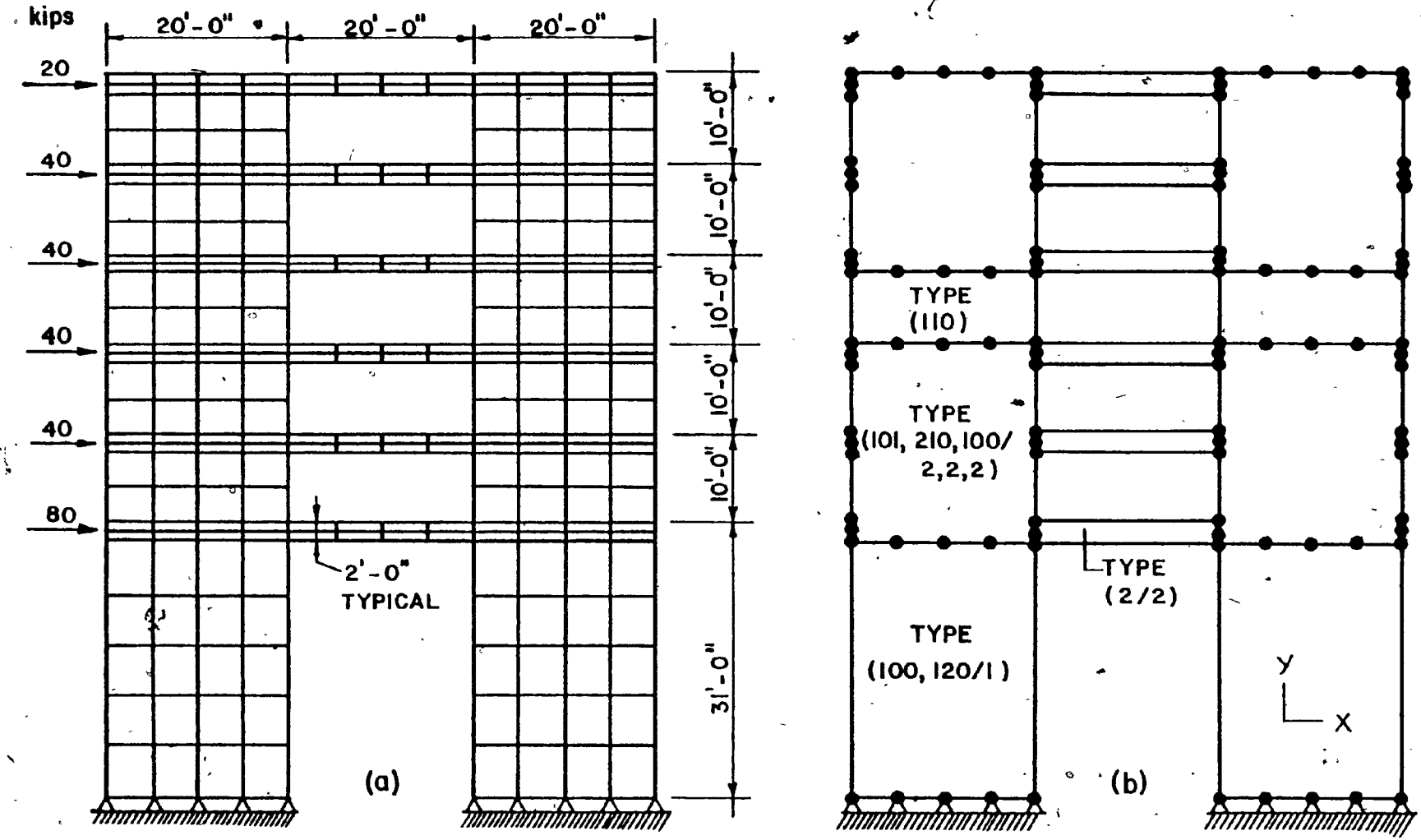

FIG. 4.7 COUPLED SHEAR WALL FOR STATIC ANALYSIS; (a) FULL FINITE ELEMENT MODEL (FROM [44]), AND (b) PANEL SUBSTRUCTURE REPRESENTATION (1 ft = 0.305 m)

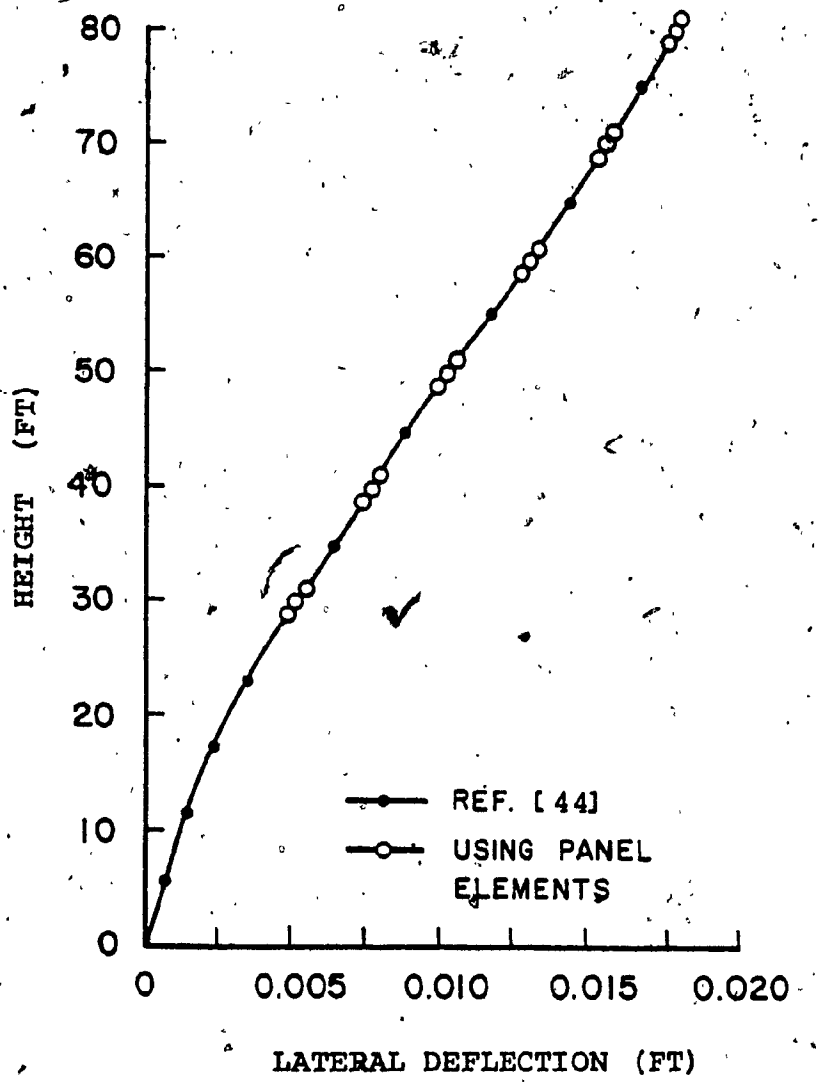

FIG. 4.8 LATERAL DEFLECTION UNDER STATIC LOADING; LEFT WALL (1 ft = 0.305 m)

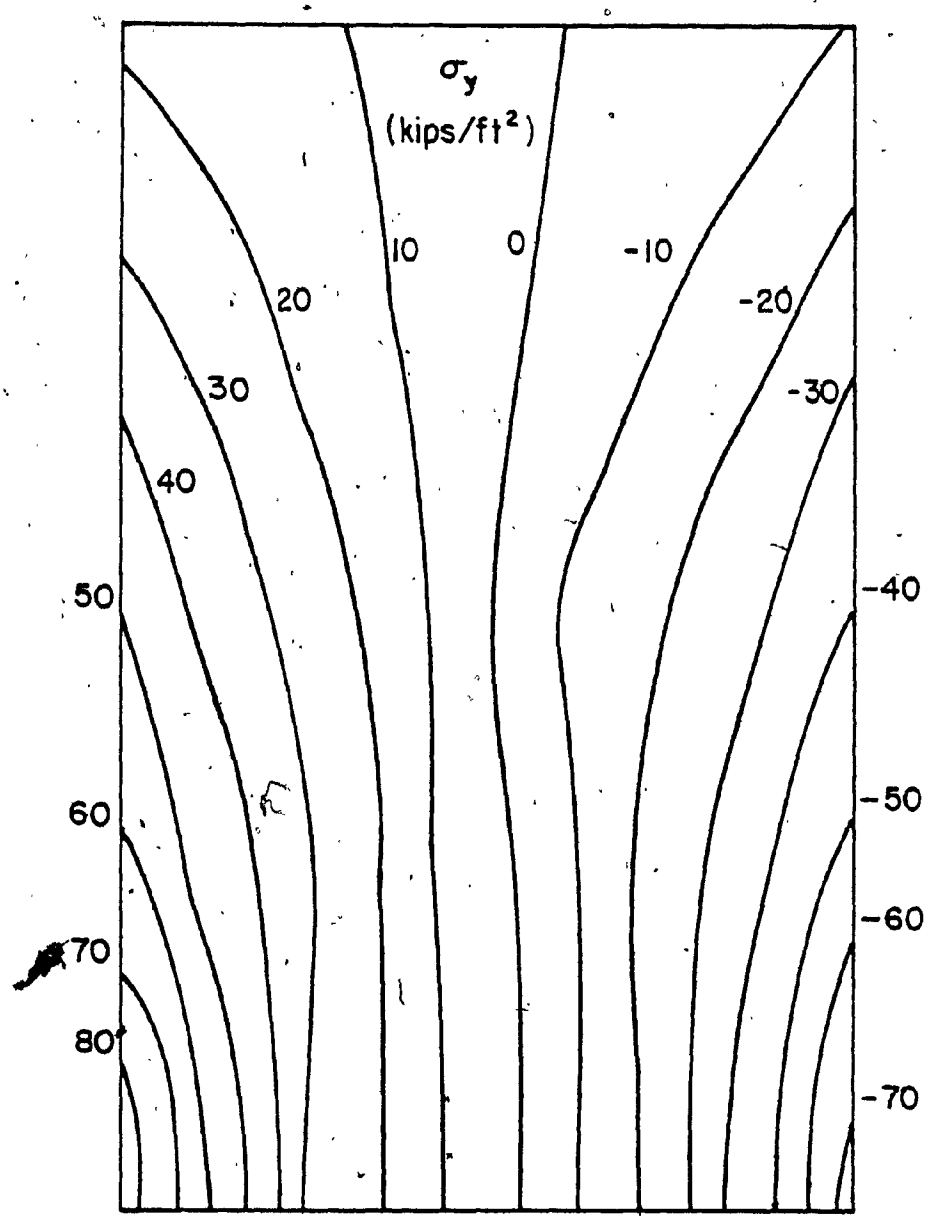

FIG. 4.9 ISOBARS OF σ_y STRESSES DUE TO STATIC LOADING IN LOWER LEFT PIER
(1 kip/ft^2 = 47.9 kN/m^2)

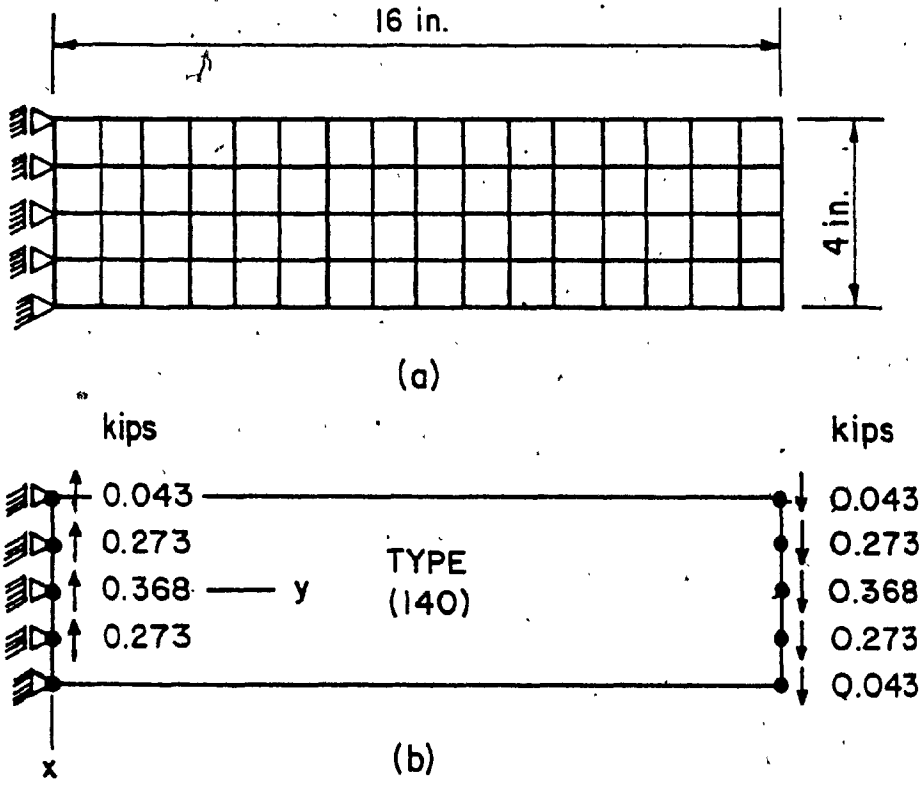

FIG. 4.10 CANTILEVER BEAM UNDER STATIC LOADING; (a) FULL FINITE ELEMENT MODEL, AND (b) PANEL SUBSTRUCTURE (1 in = 2.54 cm, 1 kip = 4.45 kN)

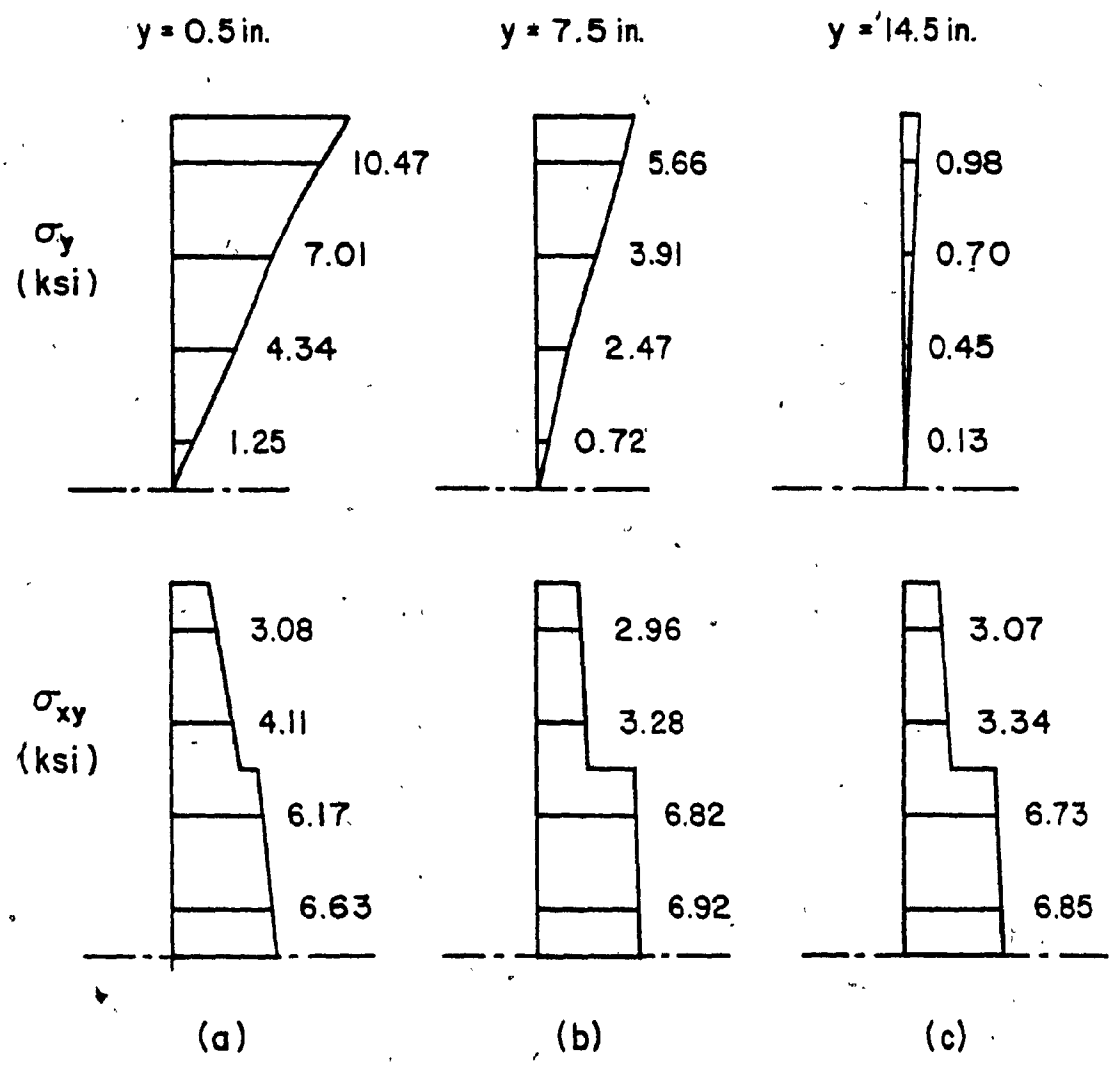

FIG. 4.11 NORMAL STRESS σ_y AND SHEAR STRESS σ_{xy} AT DIFFERENT CROSS SECTIONS OF CANTILEVER BEAM (1 in = 2.54 cm, 1 ksi = 6.9 MN/m^2)

CHAPTER V

SEISMIC BEHAVIOUR OF A 12-STOREY PRECAST PANEL SHEAR WALL

CHAPTER V

SEISMIC BEHAVIOUR OF A 12-STOREY PRECAST PANEL SHEAR WALL

5.1 INTRODUCTION

In the first part of this study, a panel element was developed using a super finite element technique. Special considerations which are necessary in dynamic substructuring, such as mass representation and adequate distribution of degrees of freedom over the structure, were discussed in detail. Illustrative examples were presented, for plate bending and shear wall problems, representing applications of panel elements as a substructure option for cases where full continuity exists at the interface of substructures.

The real potential of panel elements in the field of structural engineering lies, however, in applications for prefabricated structures or, more precisely, for large-panel structures. Here, panel elements represent prefabricated concrete panels or panels manufactured of other materials, such as corrugated steel. The resulting analysis becomes particularly efficient when panels are connected only at discrete points since a large number of boundary nodes can be eliminated; band width of system matrices, normally increased when applying substructuring techniques, is then significantly decreased.

Precast panel structures are generally visualized as three-dimensional panel assemblies where the main difference from conventional construction lies in the existence of connections at joints between panels, introducing discontinuities into the otherwise monolithic structure. Vertical in-plane panel walls maintain their function as shear walls to resist lateral loads; joint discontinuities along vertical or horizontal lines, however, introduce new aspects into shear wall design and analysis.

If full continuity at horizontal joints exists because of governing vertical loads - a commonly used assumption - individual "panel-columns" act as "elementary cantilevers" interconnected at their vertical interfaces. Alternatively, the shear wall as a whole may be described as a "complex cantilever" and belongs to the category of coupled shear walls.

The literature for precast panel structures involves the area of construction with large prefabricates in a more general sense, which includes also behaviour and design of joints and connections across joints. From the analytical viewpoint, and considering lateral load resistance, it encompasses the field of shear wall design with particular emphasis on coupled shear walls.

Lewicki [45], followed by others [46,47], reviewed procedures for design as well as analysis of fully-panelized and semi-panelized (i.e., with cast-in-place floors) systems. Vertical continuous shear joints attracted most of the attention in the area of connections in panel structures and were studied and reviewed by Lewicki and Pauw [48], as well as by Cholewicki [49] and Olesen [50]. Shemie [51,52] investigated the strength and slip behaviour of discrete connectors for a particular prefabricated system.

The coupled shear wall problem has been solved mostly for uniform cantilevers by assuming a continuous shear and moment resisting lamina, using differential equations or energy methods. Originally proposed by Rosman [53], numerous investigations have been reported for static loading, while more recent developments have concentrated on dynamic analysis [54,55,56,57]. Paulay [58] presented a comprehensive work on shear wall as well as coupled shear wall design for seismic loading. In a recent study by MacLeod [59] an extensive literature review is given on coupled shear wall analysis.

Analytical work on shear walls, with particular attention to panel structures, was performed by Stafford-Smith and Lau [60] who investigated static stability in panel assemblies including three-dimensional cases. Burnett and Rajendra [61] investigated a panelized wall system coupl-

ed by floor slabs and subjected to lateral static loading. Different degrees of fixity in the wall-to-floor connections were assumed with vertical joints either rigid or fully plastic.

Failure sequences were studied by Stafford-Smith and Rahman [62] in order to establish a collapse limit state for precast panel structures, using the finite element method and assuming strength models for joints. Pollner et al [63] analyzed large-panel shear walls with full fixity in horizontal joints, assuming non-linear vertical joint, and lintel beam, characteristics and applying stepwise lateral static loading; a matrix formulation was used in the analysis. A linear dynamic analysis of large precast panel buildings with panels represented by substructures was performed by Frank et al [64]. Horizontal joints, modeled by anisotropic finite elements, were the major parameter in this study.

The present study examines the dynamic behaviour of a large-panel shear wall using response spectrum analysis to account for seismic loading. Horizontal joints are assumed to be rigid (i.e., elementary cantilevers exist) and discrete connectors are located along the vertical joints at floor levels. Elastic behaviour is assumed throughout the structure. The panel structure itself consists of 12 storeys and 3 bays, where panels extend over one storey and one bay. The substructuring technique presented in Chapters III and IV is applied for efficient panel modelling.

The first part of the investigation deals with variations in structural response due to connector shear stiffness, where magnitude changes from rigid to fully flexible while full rigidity in the axial direction is assumed. The effect of non-uniform distribution of connector shear stiffness along the height of the structure is examined; this includes the introduction of monolithic storeys.

In the second part of this investigation the effect of horizontal discontinuities is studied, created by a missing panel or by non-uniform floor mass distribution. Assessment of the importance of connector axial stiffness and a comparison of dynamic analysis to a code static loading concludes the investigation.

Response characteristics are evaluated for overall structural behaviour. However, emphasis is placed on forces incurred in connectors since connections represent the major problem in the design of precast panel structures.

5.2 COMPONENTS OF PANEL STRUCTURES

5.2.1 Overall Structural Functioning

A precast panel structure must fulfill the same structural functions in terms of vertical and horizontal loading as does a conventional fully monolithic structure. Principal differences lie in the more industrialized fabri-

cation and erection procedures, which leads immediately to the problem of joints and connections. The main elements in a panel structure are therefore the panels and the connections or joints between panels. Force transmission across joints can take place in a continuous fashion or through discrete connectors.

An additional consideration, common to conventional monolithic structures as well as to panelized systems but not included in this study, is the interaction between vertical walls and the horizontal slab - or horizontal floor panels - where the slab introduces gravity loads to the walls and performs also the important function of a stiff diaphragm distributing lateral loads to individual resisting walls. The latter are represented in this case by vertical panel assemblies functioning as shear walls.

Stability concepts in panelized systems are generally of a more complex nature than encountered for monolithic structures. Local failure of one panel, e.g., due to failure of connectors at the joints, may lead to partial or overall collapse of the structure, commonly known as progressive collapse.

5.2.2 Panels

In a panel shear wall a single panel or several panels, could be used to extend over the wall width; in the case of a single panel no vertical joints exist. In height, a panel extends normally over one or two storeys. Panel thickness can vary according to building height. Very often, however, panel dimensions are governed by practical considerations such as transportation, for example.

Forces in wall panels are mainly due to membrane action. The magnitude and nature of membrane forces depend largely on the location of the panel in the shear wall and on the type of connections introducing these forces. Special provisions (e.g., in reinforcement) may be necessary when force concentrations exist. Ribs, particularly along panel edges, may improve panel performance and overall strength, as well as the detailing of the connections.

5.2.3 Joints

Properties of the connections across joints influence significantly the overall rigidity of concrete panel structures, for lateral as well as vertical loading. Connection properties affecting response are mainly the shear and axial stiffness. If non-linear effects are taken into account, ductility as expressed by the force-displacement characteristics

becomes important also. Connections can be classified as vertical joints, functioning predominantly as "shear joints", and as horizontal joints, which are predominantly "compression joints", although tension or shear may become critical in particular cases. Depending upon actual details, different connections may be either of the (1) continuous, or (2) discrete type.

In continuous vertical connections, shear stiffness as well as shear strength depend on the degree of reinforcement and the type of joint (e.g., keyed joints) [48,50]. In the axial direction incompressibility is usually assumed. Horizontal, continuously reinforced joints result normally in monolithic behaviour. This leads to the concept of elementary cantilevers in the analysis of panelized structures [46,50].

For discrete connectors, shear and axial stiffnesses are lumped at a point. Large force concentrations can occur with discrete connectors, resulting in localized strength and ductility requirements. Discrete connectors in a vertical joint, subjected mainly to shear forces, could consist of concrete components such as floor slabs or short shear beams, or they could be represented by mechanical connectors. If a mechanical device is applied, not more than two connectors should be used per side, as close as possible to the panel corners, principally for practical reasons [51]. In analysis, this arrangement allows lumping of connectors

from adjacent storeys into one connector at the floor level, provided rigid horizontal joints exist.

Horizontal joints with discrete connectors are generally "drypacked" and a rigid continuity may be preserved due to vertical compressive forces and also to the accompanying frictional resistance (i.e., elementary cantilevers can be assumed in analysis). A drypacked joint should be investigated for tension under lateral loading, since discrete connectors have to accommodate the tension forces. In a tension zone continuity does not exist and non-linear characteristics are introduced into the structure and its analysis.

5.3 DESCRIPTION OF STRUCTURE AND ANALYTIC CONSIDERATIONS

5.3.1 Geometric and Material Properties

The structure selected for study consists of the 12-storey 3-bay concrete panel shear wall shown in Fig.5.1. All panels are one storey in height (i.e., 10 ft (3.05 m)), panel width is 12 ft (3.66 m) and panel thickness is 8 inches (0.203 m). Assumed values for material properties, specified in terms of Young's modulus, Poisson's ratio and mass density, are, respectively: $E = 4{,}000$ kips/in^2.(2.76×10^7 kN/ m^2), $\nu = 0.17$ and $\rho = 0.00482$ kips-sec^2/ft^4 (0.0025 kg/cm^3). Floor masses are based on a 25 ft (7.63 m) width

of tributary floor area. An allowance for a 7-inch (0.178 m) concrete slab, partitions and exterior walls leads to a uniformly distributed dead load of 3.7 kips per ft-width of the wall (54 kN/m) applied at each floor level.* Assumed characteristics and properties for connectors are discussed in Section 5.3.2.

5.3.2 Connector Model and Connector Stiffnesses

The mathematical model of a connector can be described by an idealized two-node spring element with 4 degrees of freedom and zero dimensions in space, as shown in Fig.5.2. The connector element stiffness matrix is then formulated simply as

$$[K]_c = \begin{bmatrix} k_a & 0 & -k_a & 0 \\ 0 & k_v & 0 & -k_v \\ -k_a & 0 & k_a & 0 \\ 0 & -k_v & 0 & k_v \end{bmatrix} \qquad (5.1)$$

where k_a and k_v are connector axial and shear stiffness, respectively. This connector element is also described in the literature as the "bond element" [64].

---

* For simplicity and to allow for possible roof loads (e.g., mechanical equipment) all storeys, including the roof have a lumped mass corresponding to 36x3.7=133.2 kips (593.0 kN).

Computer analysis showed that values of shear stiffness k_v must be varied by an order of magnitude to effect significant changes in response. Analysis also showed that, for the present structure, a value of $k_v = 10^7$ kips/ft (14.6×10^7 kN/in) results in fully rigid conditions. This means that $k_v = 10^7$ kips/ft yields the same results as for a rigid model (i.e., full continuity at connector locations), disregarding minor numerical differences. There was also no noticeable change in the rate of convergence during a subspace iteration for solution of the eigenvalue problem.

It is therefore possible to perform an analysis with values for k_v ranging from 10^7 kips/ft (14.6×10^7 kN/m) to zero and model the given structure with panel-to-panel connection from full fixity at the connecting points to full flexibility between the individual cantilevers. Since the axial stiffness in vertical joints is generally of much less importance than the shear stiffness, k_a was assumed as fully rigid, i.e., $k_a = 10^7$ kips/ft (14.6×10^7 kN/m) in all of the following analyses.

To relate connector stiffness to practical values, two interpretations are possible. First, in relation to a mathematical panel model, Fig. 5.4 shows a half-panel with fixed conditions on one side and possible vertical displacements on the other. A distributed force results in a "panel

stiffness" of k = 1.25 x 10^5 kips/ft (18.2 x 10^5 kN/m). Another, more practical, approach consists of distributing the concentrated stiffness of the panel connector and computing an equivalent distributed stiffness per unit area of the joint which can be compared to values reported in the literature [48,50] for continuous connections. Table 5.1 shows the relation between panel, distributed joint, and discrete connector stiffnesses.

5.3.3 Summary of Assumptions

Dimensions and material properties of the investigated panel shear wall (see Fig. 5.1) were discussed in Section 5.3.1. The panel mathematical model used in the analysis is derived by applying the substructuring technique described in Chapters III and IV. Connector model and possible connector stiffnesses are presented in Section 5.3.2.

The physical assumptions related to structural behaviour and the approximations made for the finite element analysis are summarized below:

(1) Each wall, or panel column, acts as an elementary cantilever since full continuity is assumed along horizontal joints. Connections across the vertical joints between individual cantilevers exist only at floor levels, thus leading to a

coupled shear wall effect.

(2) Panel walls are represented by panels extending over one bay and one storey. The finite element models of panels are shown in Fig. 5.3. Interior nodes are eliminated, whereas vertical boundary nodes may be eliminated or may remain if full continuity is desired (see Sections 5.4.1 and 5.4.2). For the basic four-node element at zero level, plane stress and incompatible displacement modes are assumed. Linear elastic behaviour exists in panel walls.

(3) Nodal points, with 2 degrees of freedom per node, exist only at connection points between panels or between panels and connectors. At the same time, nodal points are located where high mass concentrations occur, i.e., at floor levels.

(4) A lumped mass representation is used, expressed by the retained degrees of freedom. Panel masses are defined by the panel lumped mass matrix (see Sections 4.1 and 4.3), whereas floor masses are inserted separately at each floor level.

(5) The assumed mass lumping, together with the selected number of degrees of freedom, results in solutions of the reduced eigenvalue problem sufficiently

accurate for practical purposes, compared to the full finite element model (see Section 4.3.1).

(6) Connection between cantilever walls is maintained by discrete connectors located at floor levels and acting as vertical and horizontal springs (Fig. 5.2(a)). Thus, transmission of shear and axial forces is ensured, while moments are not transmitted by connectors. In the axial direction connectors are assumed to be incompressible (i.e., $k_a = 10^7$ kips/ft (14.6×10^7 kN/m)) throughout the investigation. Shear stiffness, however, is varied from rigid to fully flexible (i.e., from $k_v = 10^7$ kips/ft (14.6×10^7 kN/m) to $k_v = 0$). Elastic connector behaviour is assumed.

(7) Response of the structure due to earthquake excitation is predicted by the response spectrum analysis summarized in Section 5.3.4.

5.3.4 Response Spectrum Analysis

All matrices in this Section represent the reduced system. Nevertheless, notations normally assigned to the full finite element model are used, e.g., [K] instead of $[\overline{K}]$ (see Chapter II). For analytical modelling of the panel

structure the reduced system stiffness matrix [K] is assembled from panel and connector elements, whereas the reduced diagonal lumped mass matrix [M] receives contributions directly from floor masses in addition to the panel mass.

Solution of the eigenvalue problem (see Eq. (2.5) or (2.6)) results in frequencies ω and mode shapes $\{\phi\}$, where it is noted that the shapes are expressed by nodal horizontal and vertical displacements in x- and y-directions, respectively. This results in two different types of mode shapes, some predominantly lateral and others predominantly extensional.

Since response is evaluated for lateral ground excitation, the $i^{\underline{th}}$ modal participation factor γ_i is evaluated for inertia forces acting in x-direction only:

$$\gamma_i = \{\phi\}_i^T [M] \{I_x\} \tag{5.2}$$

where

$\{I_x\}$ is a vector selecting masses only in the x-direction with elements either zero or unity.

It is noted that the $i^{\underline{th}}$ mode shape $\{\phi\}_i$ is orthonormalized with respect to mass matrix [M]:

$$\{\phi\}_i^T [\tilde{M}] \{\phi\}_i = 1 \tag{5.3}$$

For known spectral intensity, response is expressed by the following well known relationships [27]. Relative nodal displacements $\{u\}_i$ for the $i^{\underline{th}}$ mode are

$$\{u\}_i = \{\phi\}_i \gamma_i S_d \tag{5.4}$$

where

S_d represents the spectral displacement as a function of natural periods of vibration.

The $i^{\underline{th}}$ modal elastic force vector $\{P\}_i$ is conveniently expressed in terms of inertia forces:

$$\{P\}_i = [\tilde{M}] \{\phi\}_i \gamma_i S_a \tag{5.5}$$

where

S_a is the spectral acceleration with

$$S_a = \omega^2 S_d \tag{5.6}$$

Modal storey shears at any level are obtained by summation of the elastic forces in x-direction from Eq. (5.5). The modal base shear V_i is then expressed as

$$V_i = [1] \{P\}_{ix} \tag{5.7}$$

where

[1] is a row vector of ones

$\{P\}_{ix}$ contains the lateral components (in x-direction) of $\{P\}_i$

Modal base overturning moment M_i is also derived from Eq. (5.5) as

$$M_i = [x]\{P\}_{ix} \tag{5.8}$$

where

[x] is a row vector with elements x_j representing the height of mass j above the ground.

Modal forces in connectors are computed using the displacement response from Eq. (5.4). Axial and shear forces, F_a and F_v respectively, for the $i^{\underline{th}}$ mode are then computed as

$$\begin{Bmatrix} F_a \\ F_v \end{Bmatrix}_i = [S]\{u\}_i \tag{5.9}$$

where stress-displacement matrix [S] is derived from connector stiffness matrix $[K]_c$ of Eq. (5.1).

Total response is obtained by combining the first N modal response values in a probabilistic fashion using root-sum-of-squares (RSS). Displacement envelope {u}, which refers in this Chapter to lateral displacements along the outside of Wall 1 (Fig. 5.1), is derived from modal values as

$$u_\ell = \sqrt{u_{\ell_1}^2 + u_{\ell_2}^2 + \ldots + u_{\ell N}^2} \qquad (5.10)$$

where

u_ℓ signifies the ℓ^{th} element in vector $\{u\}$.

The maximum lateral top displacement D is then expressed as

$$D = u_L \qquad (5.11)$$

with L representing the lateral degree of freedom on top of the structure, located on the outside of Wall 1.

Relative vertical joint displacement δ in a connector can be formulated as

$$\delta = \sqrt{(u_{r_1}-u_{s_1})^2+(u_{r_2}-u_{s_2})^2+\ldots+(u_{rN}-u_{sN})^2} \qquad (5.12)$$

where

r and s signify the vertical degrees of freedom at nodes i and j (Fig.5.2(b)) for the connector under consideration.

The total response for the elastic force vector {P} is then expressed in terms of the $\ell^{\underline{th}}$ element P_ℓ as

$$P_\ell = \sqrt{P^2_{\ell_1}+P^2_{\ell_2}+\ldots+P^2_{\ell N}} \qquad (5.13)$$

Horizontal storey shears are derived in a similar manner to that for the modal storey shears. Response for total base shear and overturning moment are expressed as

$$V = \sqrt{V^2_1+V^2_2+\ldots+V^2_N} \qquad (5.14)$$

and

$$M = \sqrt{M^2_1+M^2_2+\ldots+M^2_N} \qquad (5.15)$$

Connector axial and shear forces, formulated as RSS values, are then written as

$$F_a = \sqrt{F^2_{a_1}+F^2_{a_2}+\ldots+F^2_{aN}} \qquad (5.16)$$

and

$$F_v = \sqrt{F^2_{v_1}+F^2_{v_2}+\ldots+F^2_{vN}} \qquad (5.17)$$

The dynamic response data reported in this study employs the first 12 modes, i.e., N = 12. It was found that approximately 6 to 8 out of the 12 modes are predominently lateral, thus contributing to lateral response. The alternating predominently vertical extensional modes were in some cases recognized to appear in as early as the third location

of the modal order.

Modal seismic response values are computed by employing an average spectrum based on the El Centro earthquake of 1940, N-S component, and 5 per cent damping, as given in [66]. All response computations are for this acceleration spectrum normalized to 1 g[1] peak acceleration. Figure 5.5 shows the El Centro response spectrum as well as that suggested by the 1977 National Building Code of Canada [67] (NBCC-1977), both normalized with respect to peak acceleration.[2] The NBCC-1977 spectrum is used in Section 5.4.6 where a comparison of dynamic and code static analyses is presented.

5.4 PARAMETRIC INVESTIGATION OF SEISMIC BEHAVIOUR

In the following investigation of seismic behaviour, based on the preceding mathematical representation and response spectrum analysis, overall response of the panel structure is examined with particular emphasis on forces generated in connectors. The analysis was implemented using SAP4 in modified form. The latter involves the introduction of the panel element substructuring, as well as the connector element and computation of the seismic response parameters from Eqs. (5.12) through (5.17). The scheme of the parametric

[1] g = gravitational constant

[2] Acceleration response according to NBCC-1977 for 5 per cent damping may be expressed as $S_a = 0.433\ T^{-1}$, where $S_a \leq 1.0$ when normalized to peak response.

investigation is intended to evaluate the importance of various parameters on expected earthquake behaviour.

The effect of vertical connector shear stiffness is studied for two situations:

(1) Uniform distribution of connector shear stiffness, and

(2) Non-uniform shear stiffness distribution over the height of the structure, concentrating on structures with monolithic storeys.

The following cases are studied when constant uniformly distributed connector shear stiffness is assumed:

(1) Structures with missing panels,

(2) Asymmetric distribution of floor mass, and

(3) Connectors with varying axial stiffness.

The monolithic shear wall is used as a convenient reference for evaluation of response. The panel element of Fig. 5.3(a) models monolithic behaviour. Use of the panel element of Fig. 5.3(b), with arrangement shown in Fig.5.3(d) and employing connector stiffness $k_v = 10^7$ kips/ft (14.6×10^7 kN/m), results, however, in differences noticeable only for higher modes, while basic response parameters remain

practically unchanged. Thus, connectors with stiffness of 10^7 kips/ft (14.6×10^7 kN/m) result in a rigidly connected structure and approximate closely monolithic behaviour. It should be noted that the panel element of Fig. 5.3(b) allows free displacements along the vertical sides, while full continuity is maintained for the element of Fig. 5.3(a). The panel element from Fig. 5.3(c) used in the arrangement of Fig. 5.3(e) is applied to model monolithic storeys (Section 5.4.2.2).

Table 5.2 shows the dynamic properties and maximum response values for the monolithic or homogeneous shear wall, denoted by subscript M and based on the El Centro spectrum of Fig. 5.5 normalized to 1 g. Results, presented and discussed in the following Subsections, are normalized to the corresponding values in Table 5.2.

5.4.1 Effect of Uniform Connector Shear Stiffness

With the magnitude of connector shear stiffness, uniformly distributed along the height of the structure, as the only parameter subjected to variation, the following dynamic properties and seismic response are evaluated for the panel structure when connector shear stiffness k_v varies from rigid (i.e., $k_v = 10^7$ kips/ft (14.6×10^7 kN/m)) to zero:

(1) Natural periods and modal participation factors for the four lowest lateral modes.

(2) Base shear, base overturning moment, top displacement and connector maximum relative displacement.

(3) Envelopes of maximum horizontal storey shears and maximum lateral displacement over the height of the structure.

(4) Shear and axial forces in connectors - their magnitude and distribution over the height of the structure.

(5) Magnitude and distribution of stresses in horizontal joints at different floor levels.

5.4.1.1 Overall Structural Response

In Fig. 5.6 lateral natural periods T and corresponding modal participation factors γ are plotted for the four lowest lateral modes as functions of connector stiffness k_v, normalized, respectively, to T_M and γ_M from Table 5.2.

The diagrams show the transition from a monolithic shear wall to three individual cantilevers as connector stiffness k_v decreases. Stiffness smaller than 10^2 kips/ft (14.6×10^2 kN/m) leads to the situation of free vibrating cantilevers linked only by axially stiff springs. Natural periods for the three linked cantilevers with zero shear

coupling are identical to those of a single cantilever.*

Noticeable changes in modal participation factors, for modal order as well as magnitude, within the transition $k_v = 10^6$ to 10^2 kips/ft (14.6×10^6 to 14.6×10^2 kN/m) indicate the different nature of the mode shapes caused by shear coupling (Fig. 5.6(b)).

Total response, based on the first twelve modes and using RSS modal summation, is presented in Figs. 5.7 through 5.12. Figures 5.7(a), 5.7(b) and 5.8(a) show the influence of connector stiffness k_v on base shear V, base overturning moment M and top displacement D, respectively. All values are normalized as indicated.

Figure 5.8(b) shows a diagram for connector relative displacement δ at top and mid-height of the structure, normalized to δ_s, the maximum relative displacement for independent cantilevers (Table 5.2). It should be noted that all response data are influenced by the form of the acceleration response spectrum, particularly since the structure (with $T_M = 0.55$ sec) falls into the short period range.

---

* This fact was verified by a separate analysis for one cantilever 12 ft (3.66 m) wide and 120 ft (36.6 m) high.

The diagrams of Fig. 5.7 indicate that base shear and base overturning moment decrease by 35 and 50 per cent, respectively, as connector stiffness decreases from rigid ($k_v = 10^7$ kips/ft (14.6×10^7 kN/m)) to zero. Assuming a panel structure with relatively soft shear connectors, e.g., k_v between 10^4 and 10^3 kips/ft (14.6×10^4 and 14.6×10^3 kN/m) corresponding decreases are still in the magnitude of 20 per cent and 30 per cent. Similarly, Fig. 5.8(a) shows that top deflection is nearly four times as large for zero connector shear stiffness compared to fully monolithic behaviour. For stiffnesses between 10^4 and 10^3 kips/ft, increases are still as large as 80 per cent. Connector relative displacements, zero for a monolithic wall, indicate similar increases shown in Fig. 5.8(b).

Horizontal storey shears, normalized with respect to V_M, are shown in Fig. 5.9(a). Differences in distribution along structure height, demonstrated in Fig. 5.9(b), are more evident for normalization with respect to corresponding base shears. It is apparent that changes in storey shear distribution are noticeable only in the upper part of the structure, provided soft shear connectors are used.

Envelopes of maximum lateral displacements for different connector shear stiffness are presented in Fig.5.10, with normalization to top deflection D_M of the monolithic wall in Fig. 5.10(a), and to corresponding top deflection D

in Fig. 5.10(b). As for horizontal storey shears, Fig.5.10(b) shows no significant changes for deflection distributions along the height for varying stiffness k_v. This fact is attributable to the assumption of continuous elementary cantilevers.

On the basis of the above observations, it may be concluded that the distribution of overall structural response parameters - namely storey shears and lateral deflections - is little affected by variation of magnitude of shear stiffness in the vertical joints, provided the panel structure consists of elementary cantilevers.

5.4.1.2 Forces in Connectors

Magnitude and distribution of connector forces are of particular interest in a panel structure. Figure 5.11 shows the effect of connector shear stiffness k_v on connector shear force F_v and on axial force F_a. Shear forces are normalized to F_R from Table 5.2, the maximum connector shear force in the structure with rigid connectors (i.e., $k_v = 10^7$ kips/ft (14.6×10^7 kN/m)), which occurs at the second floor level.

Figure 5.11(a) shows that maximum connector shear force decreases rapidly for decreasing shear stiffness and assumes zero values as k_v approaches zero. However, locations of maximum values shift; this results in more uniform distribution of connector forces for small values of k_v. It

is noted that stiffnesses of magnitude $k_v = 10^4$ and 10^3 kips/ft (14.6×10^4 and 14.6×10^3 kN/m) lead to decreases in connector maximum shear force of as much as 40 per cent and 80 per cent, respectively, compared to a structure with rigid connectors.

Connector axial force F_a is shown in Fig. 5.11(b), expressed as the ratio of corresponding shear force F_v. The magnitude of the axial force is seen to be generally small relative to the shear force. The ratio increases significantly only at the top and bottom of the structure, where corresponding shear forces are small.

It can therefore be concluded that axial connector forces in vertical joints of a panel structure are generally of minor importance if uniform cantilevers exist. Thus, shear force is the major design criterion unless soft connectors are used. Use of the latter, however, implies large deflections (Fig. 5.10).

5.4.1.3 Stresses in Horizontal Joints

The valid use of the concept of elementary cantilevers, where horizontal panel connections are continuous and rigid, requires that seismic forces do not cause excessive opening or slippage in horizontal joints. Hence, the behaviour remains basically elastic. This implies that (1) the seismic axial tension does not exceed the existing axial gravity stress, and

(2) the seismic shear forces do not exceed the frictional joint forces due to gravity. For the second case a coefficient of friction of $\mu = 0.3$ was chosen which represents a conservative value for the present investigation [47]. To examine the above conditions according to the loadings of this study, stresses on horizontal joints are computed at different floor levels. These stresses are obtained in analysis by inserting fully rigid connector elements at nodal points along the horizontal joints.

In Fig. 5.12 distribution of normal force is examined at the base of the structure and at floor levels 3,6 and 9, for various values of connector shear stiffness k_v. The magnitude of these stresses corresponds to 1 g maximum acceleration for the El Centro spectrum. It is noticed that the maximum stress is not affected significantly by different values of shear stiffness. As expected, the stress distribution changes from the rigid case to independent panel-column resistance as connector shear stiffness varies from 10^7 to 10^2 kips/ft (14.6×10^7 to 14.6×10^2 kN/m).

The maximum normal forces, as well as maximum shear forces for different seismic intensities, are compared to dead load forces in Table 5.3. The Table compares, for each floor level, two situations for seismic loading. Case 1 is computed for a peak spectral acceleration of 0.12 g whereas Case 2 is due to 0.24 g, corresponding to magnitudes suggested in NBCC-1977 for Zones II and III, respectively, when 5 per

cent damping exists.*

The comparison demonstrates that, for Case 1, seismic stresses in horizontal joints remain always smaller than the corresponding dead load stresses. For Case 2, however, it is observed that seismic axial tension exceeds gravity axial tension at the lowest three to four floor levels for $k_v \geq 10^4$ kips/ft (14.6×10^4 kN/m), and at the lowest nine floor levels for $k_v \leq 10^2$ kips/ft (14.6×10^2 kN/m). Also, seismic shear stresses exceed dead load stresses only in the upper two to three storeys and only if $k_v \geq 10^4$ kips/ft (14.6×10^4 kN/m).

Thus, the assumption of elementary cantilevers is valid for the present 12-storey structure for seismic intensity up to Zone II. In areas of seismic intensity corresponding to Zone III, the assumption may be maintained provided horizontal joints are designed for adequate transmission of tensile as well as shear forces.

5.4.1.4 Final Remarks

The preceding results show the transition from rigidly coupled shear walls to independent cantilevers - for all response parameters involved - when vertical shear stiffness is varied from rigid to fully flexible. Figures 5.6 through 5.8 show that

---

* Peak spectral accelerations 0.12 g and 0.24 g, correspond to the ground accelerations of 0.04 g and 0.08 g, respectively.

a noticeable loss in stiffness of the structure as a whole does not occur unless vertical connector shear stiffness k_v decreases below values between 10^6 and 10^5 kips/ft (14.6×10^6 and 14.6×10^5 kN/m).

This was observed also by Lewicki and Pauw [48] for continuous joints between concrete panels, where a decrease in stiffness from fully rigid to approximately 25 kips/in.^{3} (1821.0 kN/cm^3), (corresponding to lumped connector stiffness $k_v = 2.82 \times 10^5$ kips/ft (41.2×10^5 kN/m)) produced a decrease in rigidity of the total structure of about 5 per cent. Further decrease in connector shear stiffness, however, results in a significant loss in structural rigidity, as evident in Figs. 5.6, 5.7 and 5.8.

The 12-storey building of this study falls into the short period range, which means an increase in period of vibration - caused by softening of connector stiffness - leads to substantially reduced force attraction, in terms of base shear and overturning moment (Fig. 5.7). A designer can take advantage of this fact by using soft connectors if large deflections, particularly in the joints, can be accommodated. For severe earthquakes the structural damage can then deliberately be attracted to the vertical joints, allowing the panels themselves to remain elastic.

5.4.2 Effect of Irregular Distribution of Connector Shear Stiffness, Including Monolithic Storeys

The effect on structural response of the magnitude of connector shear stiffness in vertical joints, when uniformly distributed, was examined in Section 5.4.1. Variation in the distribution of shear stiffness along the height of the structure may be contemplated in practical applications. This aspect is now studied as a separate parameter. The effect of monolithic or rigid storeys on structural response is considered to be of particular interest; typical example for structures with monolithic storeys are shown in Fig. 5.13.

In this Section, the following variations and discontinuities in shear stiffness distribution are investigated:

(1) Non-uniform distribution of shear stiffness over the height of the structure,

(2) Structures with a monolithic top storey, as shown in Fig. 5.13(a), and

(3) Structures with a monolithic storey at top and at mid-height as shown in Fig. 5.13(b).

The introduction of a transition in stiffness reduces connector peak forces and is investigated for:

(1) Structures with monolithic top storey (Fig. 5.13(a)), and

(2) Structures with monolithic mid-height storey (Fig. 5.13(c)).

5.4.2.1 Non-Uniform Distribution of Connector Stiffness

The effect of different non-uniform distributions of connector stiffness k_v on connector forces F_v is studied in Fig. 5.14. Situations are examined where k_v varies in a linear or a stepwise manner along the height of the structure. Linear refers, in this case, to the distribution of exponent n, where $k_v = 10^n$ kips/ft (14.6×10^n kN/m). From bottom to top of the structure, stiffness k_v increases (Fig.5.14(b) or decreases (Fig. 5.14(a)) over the range from 10^6 to 10^2 kips/ft (14.6×10^6 to 14.6×10^2 kN/m).

For convenience, change of stiffness may be expressed in terms of "stiffness multiple" $m = k_i/k_{i+1}$ or k_{i+1}/k_i with m always greater than 1; k_i and k_{i+1} are connector stiffnesses at floor levels i and (i+1), respectively. Stiffness changes in Fig. 5.14 are of magnitude m = 10 for stepwise variation every third floor, and m = 2.31 for linear variation at every floor. For the latter stiffness exponent n changes by 0.364 at each floor level.

Figure 5.14 shows that connector forces differ significantly for linear and stepwise variations of connector shear stiffness k_v. It is observed that peak force characteristics are replaced by smooth distributions as the rate of change in stiffness k_v, over the height of the structure is decreased. Thus, it can be concluded that shear connector forces in vertical joints are sensitive to shear stiffness distribution. It is demonstrated that change of stiffness given by multiple $m \approx 2$ produces smooth shear force distributions, whereas $m \approx 10$ leads to the development of high peak forces. Other properties and response parameters, not shown here, do not differ appreciably for linear or stepwise distribution.

5.4.2.2 Monolithic Storeys

Rigid zones, or regions of high stiffness, are generally visualized as being undesirable. Experience of structural damage during earthquakes indicates that large forces are attracted to areas of stiffness concentration. On the other hand, in panelized buildings with discrete connectors it may be advantageous to introduce fully monolithic storeys for reasons of stability. This is particularly true for highrise buildings. Introduction of rigid storeys in the panel structure considered in this study may also be understood as the stiffening of a coupled shear wall, since elementary cantilevers are assumed.

In monolithic storeys no shear deformation takes place at the vertical joint lines. For the analytical representation full panel continuity is therefore required, obtained by the panel arrangement shown in Fig. 5.3(e). The latter is assembled from the panel elements of Fig. 5.3(c). A comparison of the panel arrangement of Fig. 5.3(e) with that of Fig. 5.3(d), however, indicates negligible differences in computed response when $k_v = 10^7$ kips/ft (14.6×10^7 kN/m). Hence, the rigidly connected panel arrangement of Fig. 5.3(d) is used to approximate monolithic behaviour, since it allows forces transmitted through rigid storeys to be expressed in terms of connector forces.

Results which demonstrate the influence of monolithic storeys on fundamental period T, as well as seismic response parameters V, M and D, are presented in Figs. 5.15 through 5.17. Corresponding curves for the uniform structure without monolithic storeys were discussed separately in Section 4.1 (Figs. 5.6 through 5.8). Using the example of a structure with shear stiffness $k_v = 10^3$ kips/ft (14.6×10^3 kN/m) allows the following quantitative evaluation of the effect of introducing the monolithic storeys:

(1) Stiffness gain of the total structure is measured directly by decrease in fundamental period. Figure 5.15 shows that reduction of T, compared to the

uniform structure, are (a) 20 per cent when a monolithic top storey is introduced, and (b) 45 per cent when monolithic top and mid-height storeys are introduced.

(2) Higher force attraction, however, is reflected in Figure 5.16 by increases in base shear V in the order of (a) 15 per cent, and (b) 35 per cent, and by corresponding increases in overturning moment M, of (a) 30 per cent, and (b) 55 per cent, when rigid top and rigid top and mid-height storeys are introduced respectively.

(3) Corresponding decreases for top deflection D, shown in Fig. 5.17, are (a) 30 per cent, and (b) 80 per cent.

The influence of monolithic storeys on envelopes of maximum lateral displacements are shown in Fig. 5.18(a) for shear stiffness $k_v = 10^4$ kips/ft (14.6×10^4 kN/m) and in Fig. 5.18(b) for shear stiffness $k_v = 10^3$ kips/ft (14.6×10^3 kN/m). Differences from the uniform structure become pronounced only for structures with soft shear connectors (i.e., $k_v \leq 10^3$ kips/ft (14.6×10^3 kN/m)). Normalized distribution curves of maximum horizontal storey shears, on the other hand, were found to differ little from those of a uniform structure.

5.4.2.3 Connector Forces in Structures With Monolithic Storeys

Figure 5.19 shows the effect of rigid storeys on connector shear force distribution, when connector stiffness in the non-rigid zones is varied from $k_v = 10^7$ to 10^2 kips/ft (14.6×10^7 to 14.6×10^2 kN/m).

If a monolithic storey exists only at top, Fig.5.19(a) shows that forces in the lower half of the structure differ little from those for the corresponding uniform structure. However, as expected, a large peak shear force develops in the rigid storey(for the cases presented $10 \leq m \leq 10^5$). A "peak force ratio" may conveniently be introduced to define the ratio between peak force in the rigid storey and the maximum connector shear force in the non-rigid zone. For example, the curves of Fig. 5.19(a) yield peak force ratios of 1.7 and 13.5 for connector shear stiffness $k_v = 10^4$ and 10^3 kips/ft (14.6×10^4 and 14.6×10^3 kN/m), respectively. Ratios increase significantly as k_v decreases.

The structures with monolithic top and mid-height storeys, presented in Fig. 5.19(b), show the predominant influence of a rigid storey at mid-height on the shear force distribution. High peak force ratios of 4.8 and 41.0, for $k_v = 10^4$ and 10^3 kips/ft (14.6×10^4 and 14.6×10^3 kN/m) respectively, lead to the conclusion that a structure with soft connectors relies almost entirely on the strength of a

few monolithic storeys. This is also apparent from the large stiffness increase due to introduction of rigid storeys observed in Figs. 5.15 through 5.17. Importance of axial connector forces, not presented here, remains similar to that for structures with uniform shear stiffness distribution, (see Section 5.4.1).

From the preceding observations, it can be concluded that the introduction of rigid or monolithic storeys increases significantly the stiffness of the structure as a whole. This leads to increased seismic base shear and base overturning moment, and to a corresponding decrease in top deflection (Figs. 5.15 through 5.17). A particular characteristic is the appearance of high peak shear forces, at locations of rigid storeys, of increasing intensity for decreasing connector shear stiffness (Fig. 5.19).

5.4.2.4 Transition in Stiffness

In Figure 5.14 it was demonstrated that irregular peak forces disappear as the rate of change in stiffness k_v decreases. Thus to avoid the large force concentrations of Fig. 5.19 stiffness transitions extending over several storeys are introduced.

For the study which follows connector shear stiffness k_v in the non-rigid zones is assumed as 10^4 kips/ft (14.6×10^4 kN/m). The transition therefore, must accommo-

date a change in stiffness from 10^4 kips/ft to fully rigid conditions (i.e., $k_v = 10^7$ kips/ft (14.6×10^7 kN/m)). For the present panel wall, transitions are considered for two cases: a structure with rigid top storey and one with rigid mid-height storey.

The procedure for selecting an appropriate transition is purely trial and error. The stiffness transitions indicated in Tables 5.4 and 5.5 are expressed in terms of exponent n and stiffness multiple m. A transition extends over either three or four storeys and is "linear" or "smooth". Linear implies a storey-to-storey change in n (as in Fig. 5.14); smooth denotes a more gradual change in connector stiffness k_v as expressed by both n as well as m.

The case of a structure with monolithic top storey is demonstrated in Fig. 5.20. The diagrams show that a linear transition is significantly less effective in reducing force concentration compared to one that is smooth. The latter is seen to lead to decrease of peak force and a more uniform distribution. For a smooth transition over four storeys, peak force decreases by approximately 33 per cent (Fig. 5.20(b)). These curves demonstrate also that a stiffness transition tends to draw peak forces in the direction where maximum shear force would occur in a structure with uniform shear stiffness distribution (see Fig. 5.11(a)).

A structure with monolithic storey at mid-height and smooth stiffness transitions above and below is presented in Fig. 5.21. Peak force is decreased by approximately 30 per cent; however, no major difference is noticed between the transitions over three or four storeys.

The above two examples demonstrate the possibility of avoiding, or at least controlling, peak forces due to the presence of rigid storeys by introducing stiffness transitions. To bridge effectively large stiffness differences the transition should be of the smooth type, beginning slowly (m = 1.5 to m = 2) after which a high stiffness can be approached rapidly as apparent from Figs. 5.20 and 5.21 together with Table 5.5.

5.4.3 Effect of Missing Panels

Structural discontinuities produced by soft zones where local concentration of flexibility occurs may be introduced into the panelized system by missing panels. Local panel failure during an earthquake could be the cause or, alternatively, architectural requirements at the design stage may dictate such openings. Consequently, the magnitude as well as the nature of force concentrations associated with missing panels requires study.

Considering the structural model of Fig. 5.1, situations are studied where panels are missing in (1) interior

wall 2, and (2) exterior wall 3 between floor levels 2-3, 6-7 and 10-11. Figures 5.22 and 5.23 show the resulting structures. For this study nearly rigid shear connectors were chosen using $k_v = 10^5$ kips/ft (14.6×10^5 kN/m). It is assumed that connectors at locations where panels are missing maintain full shear and axial stiffness, i.e., $k_v = 10^6$ kips/ft (14.6×10^5 kN/m) and $k_a = 10^7$ kips/ft (14.6×10^7 kN/m). If half stiffnesses are used for these connectors, (i.e., if stiffness multiple $m = 2$ exists), the resulting effect on force distribution is not significant.

The influence of missing panels on fundamental period and on top deflection is summarized in Table 5.6. The data indicate that missing interior panels have little effect on overall structural response, whereas missing exterior panels result in significant softening. For example fundamental period and top deflection both increase by approximately 50 per cent when a panel is removed in wall 3 at level 2-3.

Horizontal storey shears for missing exterior panels, normalized to monolithic base shear V_M, are shown in Fig. 5.24. Except for decreased magnitude, distribution along the height is not particularly sensitive to the introduction of a wall opening. Envelopes of maximum lateral displacements are shown in Fig. 5.25(a) for missing interior panels and in Fig. 5.25(b) for missing exterior panels. Only the latter indicates significant differences compared to the uniform structure.

5.4.3.1 Connector Forces

Figures 5.26 through 5.28 show connector force distributions when panels are missing in the interior bay (Wall 2). It is observed that the discontinuity effect is confined mainly to the vicinity of the opening, with only small increases in shear forces F_v (a maximum of 15 per cent when a panel is removed at level 2-3, Fig. 5.26(a)).

However, a large increase in axial force F_a in the connectors immediately adjacent to the missing panel is to be expected since a concentration of normal stress trajectories takes place next to the opening. Figures 5.26(b), 5.27(b) and 5.28(b) demonstrate this increase which can amount to as much as 20 times the corresponding values for the uniform structure. This maximum occurs when a panel is removed at level 2-3 (Fig. 5.26(b)). The magnitude of peak axial force decreases for panels missing at higher levels (Figs. 5.27(b) and 5.28(b)). The curves for axial-to-shear force ratios indicate similar localized effects, as shown by Figs. 5.26(c), 5.27(c) and 5.28(c).

A large increase in axial force F_a in the connectors immediately adjacent to the missing panel is the most important result, as seen in Figs. 5.26(b), 5.27(b), and 5.28(b). Axial forces increase to as much as 20 times the correspond-

ing values for the uniform structure. This maximum occurs when a panel is removed at level 2-3 (Fig. 5.26(b)). The magnitude of peak axial force decreases for panels missing at higher levels (Figs. 5.27(b) and 5.28(b)). The curves for axial-to-shear force ratios indicate similar localized effects, as shown by Figs. 5.26(c), 5.27(c) and 5.28(c).

Thus, it may be concluded that the redistribution of internal forces, accomplished by large increases of axial connector forces, allows a structure with missing interior panels to maintain the overall response characteristics of the full structure without openings (see Table 5.6, Wall 2).

Figures 5.29 through 5.31 present connector force distributions for panels missing in the exterior bay (Wall 3). Force concentrations are not as localized as for missing centre panels. Also, peak forces tend to assume much larger values. Shear force F_v increases by as much as 50 to 150 per cent compared to the uniform structure, depending on the floor level where panels are missing (Figs. 5.29(a) through 5.31(a)). Axial forces F_a experience extremely large increases, not only immediately adjacent to the missing panel but also well beyond. Peak axial forces reach values up to 40 times those for the corresponding uniform structure (Figs. 5.29(b) through 5.31(b)).

5.4.3.2 Final Remarks

Shear, rather than axial, forces usually govern the design for connectors in vertical joints of panelized structures. Introduction of perforations due to missing panels, however, results in high axial forces. The diagrams in Figs.5.26(c) through 5.31(c) demonstrate that the ratios between axial and shear force can assume values approaching 2 for certain cases. Connector design must therefore incorporate both shear and axial forces.

The preceding observations indicate that a panel missing in an outer bay results in a major reduction in panel wall overall rigidity, while the corresponding effect from an interior bay is small. It is realized that the softening of one panel shear wall leads, in a complete structure, to a force redistribution to other lateral resisting walls. A three-dimensional analysis is to be carried out in this case.

5.4.4 Asymmetric Floor Mass Distribution

For a panel structure, it is generally assumed that elementary cantilevers possess identical dynamic properties. This assumption is not valid when, for example, non-uniform floor mass distribution exists. To study the effect of the latter, a situation is assumed where 50 per cent of the total

floor mass is assigned to Wall 3, while Walls 1 and 2 carry 25 per cent each. Three cases of uniform connector shear stiffness are considered: $k_v = 10^7$ (14.6×10^7), 10^4(14.6×10^4) and 10^2(14.6×10^2) kips/ft (kN/m).

For all three of the above cases, no appreciable difference is evident for nearly all response values including connector shear forces, compared to the structure with uniform floor mass distribution. Changes reflecting non-uniformly distributed mass occur only in connector axial forces, as apparent from Fig. 5.32 where axial-to-shear force ratios are shown for $k_v = 10^7$(14.6×10^7) and 10^4 kips/ft(14.6×10^4 kN/m). These ratios indicate a noticeable increase in connector axial force of Joint 2 (Fig.5.1), adjacent to the higher intensity of floor mass. Axial forces in Joint 1, on the other hand, differ little from those for uniform floor mass distribution.

Thus, changes in axial forces, though generally small in magnitude, allow the panel structure to maintain its response characteristics completely when non-uniform floor mass distribution exists.

The discussions of this Section, as well as those of Section 5.4.3, lead to the conclusion that discontinuities in the horizontal direction within the structure, such as

non-uniform floor mass distribution or a missing panel, result in a redistribution of internal forces, apparent mainly through axial force increase. Thus, the structure as a whole preserves its dynamic properties and response characteristics close to, or in some cases completely identical with, those of the uniform structure (except for panels missing in Wall 3).

5.4.5 Connector Axial Stiffness

In the design of vertical joints and connectors for precast panel shear walls one generally assumes that in the axial direction sufficient strength and adequate stiffness exist. In results previously discussed in this study axial connections, even when fully rigid, do not attract axial forces of significant magnitude (Fig.5.11(b)), except under special conditions, such as with missing panels, for example. The question then arises: what is the required order of magnitude for axial stiffness sufficient to maintain the same structural response as for axially rigid connectors?

Figure 5.33 shows the influence of connector axial stiffness on fundamental period, when shear stiffness is kept constant at $k_v = 10^7$ and 10^4 kips/ft(14.6×10^7 and 14.6×10^4 kN/m). A transition to independent cantilevers, similar to shear stiffness variation of Fig. 5.6(a), is observed. However, in the present case of varying axial stiffness structural softening begins at much lower stiffness,

i.e.,

$$k_a \approx 10^2 \text{ kips/ft } (14.6 \times 10^2 \text{ kN/m})$$

Also, significant changes in modal configurations take place (not presented here), as is apparent from the reordering of modal participation factors as axial stiffness decreases below 10^2 kips/ft (14.6×10^2 kN/m). This is attributable to shear coupling which continues to exist even when k_a approaches zero.

Distribution of connector shear and axial forces are shown in Fig. 5.34, where shear stiffness is kept constant at $k_v = 10^4$ kips/ft (14.6×10^4 kN/m). The curves of Fig. 5.34(a) demonstrate that no significant change in shear force becomes apparent with variation of axial stiffness k_a. Axial forces, however, are more sensitive to change in connector stiffness k_a, although remaining small in magnitude. Irregular peaks in axial force distribution, at top and bottom of the structure, tend to disappear and smooth distributions develop, decreasing in magnitude from top to bottom, as axial connectors become very flexible (Fig. 5.34(b)).

It appears, therefore, that changes in structural response of only minimal significance occur when axial stiffness varies from fully rigid to very soft, i.e., from 10^7 to 10^2 kips/ft (14.6×10^7 to 14.6×10^2 kN/m). Assuming that adequate axial stiffness is provided (i.e., $k_a > 10^2$ kips/ft

(14.6×10^2 kN/m)), use, in analysis, of axially rigid connectors is justified.

In spite of the constraints imposed by shear coupling, the structure reaches the same fundamental period as independent cantilevers (Fig. 5.33). This result is due to particular kinematic conditions which exist when connector axial stiffness is nearly absent. Large axial displacements allow corresponding vertical displacements and an uncoupled first bending mode can develop. Corresponding shear forces computed from stiffness values satisfy merely numerical conditions and have no practical implications. For periods higher than the fundamental, however, the change in direction of mode shape curvature prevents large axial displacements; hence, shear coupling is activated. Figure 5.33 shows the corresponding increase in the values of the higher periods.

Axial strength as well as axial stiffness for connections across joints are little discussed in the literature on panel structures. Considering the above discussion, further experimental data, particularly for discrete connectors, are necessary to establish a practical range for axial stiffness.

5.4.6 Comparison With Code Static Loading

For economical design of structures, acceptance of non-linear deformation under severe seismic loading is re-

quired. Thus, aseismic codes [67] allow plastic deformation by specifying lateral static loads which result in corresponding computed response only a fraction of that derived in an elastic dynamic analysis. Ductility requirements are consequently established to guarantee structural functioning when plastic deformation takes place. Overall plastic behaviour is often expressed by horizontal storey shear ratios (i.e., dynamic storey shear/design static storey shear) [27,68], representing an estimated average ductility factor, which in this study is referred to as the "force reduction factor".

Panel structures with rigid horizontal joints experience yielding predominantly in the vertical joints, i.e., of vertical shear connectors. However, if flexible shear connectors exist, shear forces and hence the energy absorbed in connectors assume small values, i.e., zero values for the extreme case of independent cantilever action. In such cases panels or the connections across horizontal joints, are expected to participate increasingly in plastic deformation. As shear connector stiffness decreases in magnitude, emphasis on ductility requirements may thus shift from the vertical joints to the panel walls.

In this Section a code equivalent static analysis is compared to a linear dynamic analysis, according to NBCC-1977 specifications, in deriving force reduction factors. The following response parameters are studied:

(1) Base shear intensity with variation of connector shear stiffness,

(2) Horizontal storey shear distribution for a rigid panel shear wall ($k_v = 10^7$ kips/ft (14.6×10^7 kN/m)) and for independently acting cantilevers ($k_v = 0$),

(3) Maximum connector shear force for varying connector shear stiffness, and

(4) Distribution of connector shear force along the height of the structure.

Base shear V, from dynamic analysis, is shown in Fig. 5.35(a) as a function of shear stiffness k_v. The dynamic base shear is based on the NBCC-1977 spectrum from Fig. 5.5, assuming a ground acceleration of 0.08g which results in 0.24 g peak spectral acceleration when 5 per cent damping exists. Computed values for total base shear are 268 kips and 133 kips for the monolithic shear wall and for independent cantilever action, respectively; intermediate values represent the characteristic transition (see Fig. 5.7(a)).

Code [67] static base shear, also shown in Fig. 5.35(a), is obtained from the expression

$$V = ASKW$$

where

A represents ground acceleration

S is a seismic response factor

K denotes the structural system, and

W is the total weight of the structure.

Importance and foundation factors, also specified in the code, have here been taken as equal to unity. Assumed values are: A = 0.08g and W = 2030 kips. Value K is taken as 1.0 since continuity does not exist in vertical joints and also to account for a more ductile system (for precast concrete construction with spliced reinforcement the code recommends K=1.3). Seismic response factor, specified as $S = 0.5/\sqrt[3]{T}$ with fundamental period $T = 0.05\ H/\sqrt{D}$ (H = building height, D = building width), has values 0.50 and 0.41 for the monolithic wall and independent cantilevers, respectively. Corresponding base shears are V = 81.0 kips and V = 65.0 kips. The transition between these two values is not available from the code and interpolation following the dynamic analysis curve is employed, which leads to the static curve presented in Fig. 5.35(a).

To express possible plastic action, force reduction factor μ_v may be introduced as the ratio of dynamic to static horizontal storey shear. From the two curves for base shear of Fig. 5.35(a), this factor assumes values ranging from 2.0 to 3.3, as depicted by the curve of Fig. 5.35(b).

Distributions of horizontal storey shears corresponding to $k_v = 10^7$ kips/ft(14.6×10^7 kN/m), (i.e., monolithic shear wall) and to $k_v = 0$ (i.e., independent cantilever

action) are compared in Fig. 5.36, both for dynamic analysis, and for static loading. The code static loading is triangular, with a top force $F_t = 0.004(H/D_s)^2$, (D_s = dimension of the lateral force-resisting system in a direction parallel to the applied forces). For the present case F_t is 4.4 per cent of the base shear. The static and dynamic storey shear distributions result in force reduction factor μ_v varying along the building height. Values ranging from 1.3 to 3.3 are listed in Table 5.7.

Maximum connector shear force, max F_v is plotted in Fig. 5.37(a) as a function of shear stiffness k_v. Static connector shear forces are computed from a static analysis (i.e., using code triangular loading with top force) for magnitudes of base shear given by the static curve of Fig. 5.35(a). The curve for the force reduction factor for maximum connector shear force, defined as

$$\mu_c = \max F_v(\text{Dynamic})/\max F_v(\text{Static})$$

is shown in Fig.5.37(b). For small values of stiffness k_v, μ_c has little meaning since shear forces approach zero (shown as dashed line). The corresponding curve for base shear, also shown in Fig. 37(b), indicates that a redistribution of ductility demand from connectors to walls is expected to take place as shear connectors become increasingly more flexible.

Distributions of connector shear force over the height of the structure are compared in Fig. 5.38 for dynamic analysis and code static loading, with static base shears normalized to corresponding dynamic base shears. Close agreement exists for all cases of connector shear stiffness. Agreement, similar to that indicated in Fig. 5.38, was also observed for non-uniform shear stiffness distributions (not presented).

From the preceding comparison of dynamic and static seismic analyses for the 12-storey panel structure, it may be concluded that force reduction factors (i.e., ductility requirements) fall into the range from 1.3 to 3.3, depending on floor level and on connector stiffness k_v, (Fig. 5.35 and Table 5.7). Plastic deformation is expected to take place mainly in the vertical joints, but it may be transferred to the panel walls themselves when connector shear stiffness is small.

5.4.7 Extension to Non Linear Analysis

The preceding linear dynamic analysis of a panel structure which includes structural discontinuities such as non uniform stiffness distribution and missing panels, is directly applicable only for elastic response. If non linear behaviour is introduced, where local plastification leads to force redistributions, the preceding results can be employed to identify zones of increased ductility and

strength demands, as well as zones where progressive yielding is to be expected. Thus, initial assumptions for a non linear analysis can be deduced.

To initiate a non linear analysis of large panel structures a thorough study of the actual physical behaviour is necessary. A short summary thereof follows mainly References [71,72]. Generally one assumes that the non linearities are restricted to the planes of weakness represented by vertical and horizontal joints [73]. As for vertical joints, knowledge of realistic stress displacement relationships for shear and axial action as well as their coupling effect can be sufficient. However, stiffness degradation due to repeated loading may also need to be considered.

In horizontal joints two types of movements predominate: (1) rocking or tilting, and (2) slippage in the joint. The first movement is created by alternating normal tensile forces causing separation or opening at the edges of the horizontal joints. The second movement is caused by horizontal shear forces which overcome the gravitational friction. The coupling of rocking and slippage results in a concentration of shear as well as compressive forces. Of the two actions, slippage gains major importance with respect to energy dissipation.

Finite element procedures to model these rather complex joint characteristics are also suggested in References [71,72]. Four different element types are described: (1) spring connector element for vertical joints, (2) four-node horizontal connection element, and (3), (4) horizontal gap and stop elements. The latter two are to model opening of joints and limited slip due to dowel action, respectively. Since the panels themselves remain elastic they may be represented by substructures; thus, the super finite element technique of the present study may be implemented effectively.

For the solution of the incremental, non linear dynamic equilibrium equation,

$$[M]\,\Delta\ddot{x} + [C_t]\,\Delta\dot{x} + [K_t]\,\Delta x = \Delta P \qquad (5.18)$$

a step by step integration has to be applied. The incremental values $\Delta\ddot{x}, \Delta\dot{x}, \Delta x$ and ΔP represent acceleration, velocity, displcaement and applied force, respectively; $[C_t]$ and $[K_t]$ are tangent damping and stiffness matrices; [M] is the mass matrix. Many procedures have been applied for solution of the equilibrium equation [74,75] which are either explicit [76] or implicit schemes [69]. The two schemes differ in using the equilibrium conditions at the beginning, or at the end of the time step, respectively. The time step to be chosen depends largely on the highest significant frequency. For large panel structures an explicit scheme can be used

effectively [71]; particularly, since repetitive element groups are present and provided mass as well as damping matrices can be applied in diagonal form [28].

5.5 SUMMARY OF RESULTS

A 12-storey 3-bay precast panel structure has been analyzed for lateral seismic loading using response spectrum analysis and the finite element method. Rigid horizontal joints were assumed; at vertical joints flexible connectors are located at floor levels. Assumptions made in the application of the substructuring technique for panel modelling were summarized in Section 5.3.3. Connector model and range of possible connector stiffness were discussed in Section 5.3.2. The results were primarily expressed in terms of

(1) Overall structural response, and

(2) Distribution and magnitude of connector forces in vertical joints.

The conclusions from the parametric study in Section 5.4 are summarized below. Although the conclusions are directly applicable only to the 12-storey structure considered, it is believed, that additional studies would indicate a wider application of the results.

(A) The effect on structural response of the magnitude of connector shear stiffness k_v, uniformly distributed along the height of the structure, is summarized as follows:-

(1) Values for dynamic properties and maximum response - for natural period T, modal participation factors γ, base shear V, base overturning moment M and lateral top defection D - pass through a transition as vertical connector shear stiffness is varied from rigid ($k_v = 10^7$ kips/ft (14.6×10^7 kN/m)) to fully flexible ($k_v = 0$). Values correspond to those of a monolithic wall and of individual cantilevers for rigid and for fully flexible shear connectors, respectively (Figs.5.6 through 5.8).

(2) The normalized distribution of maximum response - horizontal storey shear and maximum lateral deflections - along the height of the structure are not significantly affected by change in shear stiffness k_v (Figs.5.9(b) and 5.10(b)).

(3) Shear forces in vertical connectors change significantly, in magnitude as well as in distribution along the height, as shear stiffness k_v

is varied (Fig. 5.11(a)). Axial forces, however, are of considerably less importance, since they remain small in magnitude (Fig. 5.11(b)).

(4) Horizontal joints, assumed as fully continuous in this study, are subjected to net tensile forces in the first three to four storeys in areas of Zone III seismicity (Table 5.3.)

(B) For structures with monolithic storeys the following observations were noted:

(1) Overall structural stiffness increases significantly when rigid storeys are introduced. These changes are apparent from (a) decreases in fundamental period T, and (b) decreases in top deflection D; however, larger forces are attracted, reflected by (c) increases in base shear V and base overturning moment M (Figs. 5.15 through 5.17).

(2) Shear force distribution in vertical joints is sensitive to the rate of change in connector shear stiffness k_v along the height of the structure (Fig. 5.14). Introduction of monolithic storeys results in large shear force concentra-

tions at the monolithic level, with magnitude depending on connector shear stiffness k_v in the non-rigid zone (Fig. 5.19).

(3) Stiffness transitions, introduced to control connector peak shear forces, need to be of a "smooth" type (Table 5.4) in order to be effective (Figs.5.20 and 5.21).

(C) Panels missing at different storey levels in Walls 2 and 3 (Figs. 5.22 and 5.23) affect structural response as follows:

(1) Removal of an interior panel (in Wall 2) does not alter structural overall behaviour significantly (Table 5.6 and Fig. 5.25(a)); the accompanying local redistribution of internal forces is characterized by large increases of connector axial forces (Figs. 5.26 (b) through 5.28 (b)).

(2) For missing exterior panels (in Wall 3) extensive change in structural response is encountered (Table 5.5 and Fig. 5.25(b)). Large increases in maximum values and significant redistributions take place for shear and axial forces in vertical connectors (Figs. 5.26 through 5.31).

(D) Asymmetric floor mass distribution, simulating non-identical dynamic properties of the elementary cantilevers results only in a redistribution in connector axial forces (Fig. 5.32); other response parameters remain unchanged.

(E) Variation of connector axial stiffness shows that the magnitude of this parameter is of little importance to structural response, unless relatively small values are involved, i.e., $k_a < 10^2$ kips/ft (14.6×10^2 kN/m), (Figs.5.33 and 5.34).

(F) A comparison of elastic dynamic analysis with response to code static loading, using NBCC-1977 results in the following observations:

(1) Force reduction factor μ_v, derived from a comparison of static and dynamic storey shears, ranges from 1.3 to 3.3, decreasing with height along the structure and with connector shear stiffness k_v (Table 5.7 and Fig. 5.35(b), respectively).

(2) Force reduction factor μ_c, derived from static and dynamic connector shear forces, ranges from 3.3 to approximately 1 and indicates a transfer of ductility requirement from vertical joints to walls in the panel structure, as connector shear stiffness k_v decreases to small values (Fig.5.37(b)).

(3) The distribution of connector shear forces along the height of the structure obtained from code static loading agrees closely with that from dynamic analysis.

TABLE 5.1 COMPARISON OF CONNECTOR SHEAR STIFFNESS DEFINITION

CONNECTOR STIFFNESS, kips/ft	EQUIVALENT DISTRIBUTED JOINT STIFFNESS, kips/in^3	$\frac{\text{CONNECTOR STIFFNESS}}{\text{PANEL STIFFNESS}}$
10^7	868.0	80.0
10^6	86.8	8.0
10^5	8.68	0.8
10^4	0.868	0.08

Note: 1 kip/ft = 14.6 kN/m
1 kip/in^3 = 2.72 x 10^5 kN/m

TABLE 5.2 ABSOLUTE RESPONSE VALUES

VALUES FOR MONOLITHIC WALL		
Lateral Mode No.	Lateral Natural Periods, T_M (sec)	Lateral Modal Participation Factors γ_M
1 (1)*	0.546	6.33
2 (2)	0.112	3.72
3 (4)	0.0497	2.11
4 (6)	0.0315	1.44

Base shear:	V_M = 798.6 kips
Base overturning moment:	M_M = 6.55 x 10^6 kips-ft
Top deflection:	D_M = 0.193 ft

VALUES FOR WALL WITH RIGID CONNECTORS

Maximum connector shear force:	F_R = 283.4 kips

VALUES FOR SINGLE WALLS

Relative joint displacement:	δ_s = 0.103 ft at top
	δ_s = 0.077 ft at mid-height

All response values are for 1 g peak acceleration (El Centro spectrum.

* Numbering in brackets corresponds to the actual modal order.

Note: 1 kip = 4.45 kN; 1kip-ft = 1.36 kN m; 1 ft = 0.305 m

Table 5.3 FORCES IN HORIZONTAL JOINTS DUE TO VERTICAL DEAD LOAD AND LATERAL SEISMIC LOAD FOR DIFFERENT CONNECTOR SHEAR STIFFNESS, $k_v = 10^n$ kips/ft.

	Floor Level	Maximum Forces from Seismic Loads, Kips/ft						Forces from Dead Load kips/ft
		n = 7		n = 4		n = 2		
		CASE 1	CASE 2	CASE 1	CASE 2	CASE 1	CASE 2	
NORMAL FORCES	11	1.8	3.5	1.1	2.1	1.8	3.5	4.7
	10	2.3	4.5	1.8	3.6	4.7	9.3	9.4
	9	4.3	8.6	3.5	7.0	8.0	16.0	14.1
	8	6.8	13.5	5.6	11.2	11.0	22.0	18.8
	7	8.8	17.6	8.1	16.2	13.9	27.8	23.5
	6	12.5	25.0	10.9	21.7	16.6	33.2	28.2
	5	15.7	31.4	13.9	27.8	19.3	38.5	32.9
	4	19.1	38.1	17.3	34.6	22.5	45.0	37.6
	3	22.6	45.1	21.4	42.7	25.5	51.0	42.3
	2	26.3	52.6	26.3	52.6	30.2	60.3	47.0
	1	30.6	61.1	32.5	65.0	35.3	70.5	51.7
	0	40.5	81.0	42.5	85.0	41.3	82.5	56.4
SHEAR FORCES FOR $\mu = 0.3$	11	1.1	2.1	1.2	2.3	0.6	1.1	1.4
	10	1.6	3.2	1.7	3.3	0.8	1.5	2.8
	9	2.3	4.5	2.0	3.9	1.0	1.9	4.2
	8	2.6	5.2	2.2	4.4	1.0	1.9	5.6
	7	3.0	6.0	2.5	5.0	1.0	1.9	7.0
	6	3.4	6.7	2.7	5.4	1.1	2.1	8.4
	5	3.7	7.4	2.9	5.8	1.2	2.4	9.8
	4	3.9	7.7	3.1	6.2	1.4	2.8	11.3
	3	4.1	8.1	3.2	6.3	1.6	3.2	12.7
	2	4.3	8.5	3.3	6.5	1.8	3.6	14.1
	1	4.5	9.0	3.3	6.5	2.0	3.9	15.5
	0	5.6	11.1	3.6	7.2	2.6	5.2	16.9

NOTE: 1 kip/ft = 14.6 kN/m

TABLE 5.4 LINEAR STIFFNESS TRANSITIONS

Transition Over 3-Storeys		Transition Over 4-Storeys	
Exponent n	Multiples m	Exponent n	Multiples m
7.00	5.62	7.00	3.98
6.25	5.62	6.40	3.98
5.50	5.62	5.80	3.98
4.75	5.62	5.20	3.98
4.00		4.60	3.98
		4.00	

TABLE 5.5 SMOOTH STIFFNESS TRANSITIONS

Transition Over 3-Storeys		Transition Over 4 Storeys	
Exponent n	Multiples m	Exponent n	Multiples m
7.00	39.8	7.00	25.1
5.40	6.31	5.60	6.31
4.60	2.51	4.80	2.51
4.20	1.58	4.40	1.58
4.00		4.20	1.58
		4.00	

TABLE 5.6 RATIOS FOR FUNDAMENTAL PERIOD AND TOP DEFLECTION FOR STRUCTURE WITH PANELS MISSING AT DIFFERENT FLOOR LEVELS

Floor Level	WALL (2)		WALL (3)	
	Period Ratio T/T_5	Top Deflection Ratio D/D_5	Period Ratio T/T_5	Top Deflection Ratio D/D_5
10-11	1.00	1.00	1.00	1.02
6-7	1.01	1.02	1.11	1.17
2-3	1.02	1.03	1.47	1.58

T_5 = 0.580 sec; Fundamental period for uniform stiffness distribution with $k_v = 10^5$ kips/ft.

D_5 = 0.213 ft; Top deflection for uniform stiffness distribution with $k_v = 10^5$ kips/ft and 1 g peak acceleration (El Centro spectrum).

Note: 1 ft = 0.305 m 1 kip/ft = 14.6 kN/m

TABLE 5.7 FORCE REDUCTION FACTORS μ_v ALONG STRUCTURE HEIGHT

Storey Level	Force Reduction Factor μ_v	
	Monolithic Shear Wall	Single Shear Walls
12	2.2	1.4
11	2.5	1.4
10	2.6	1.3
9	2.6	1.3
8	2.7	1.3
7	2.8	1.5
6	2.8	1.6
5	2.9	1.8
4	3.1	1.9
3	3.1	2.0
2	3.2	2.0
1	3.3	2.0

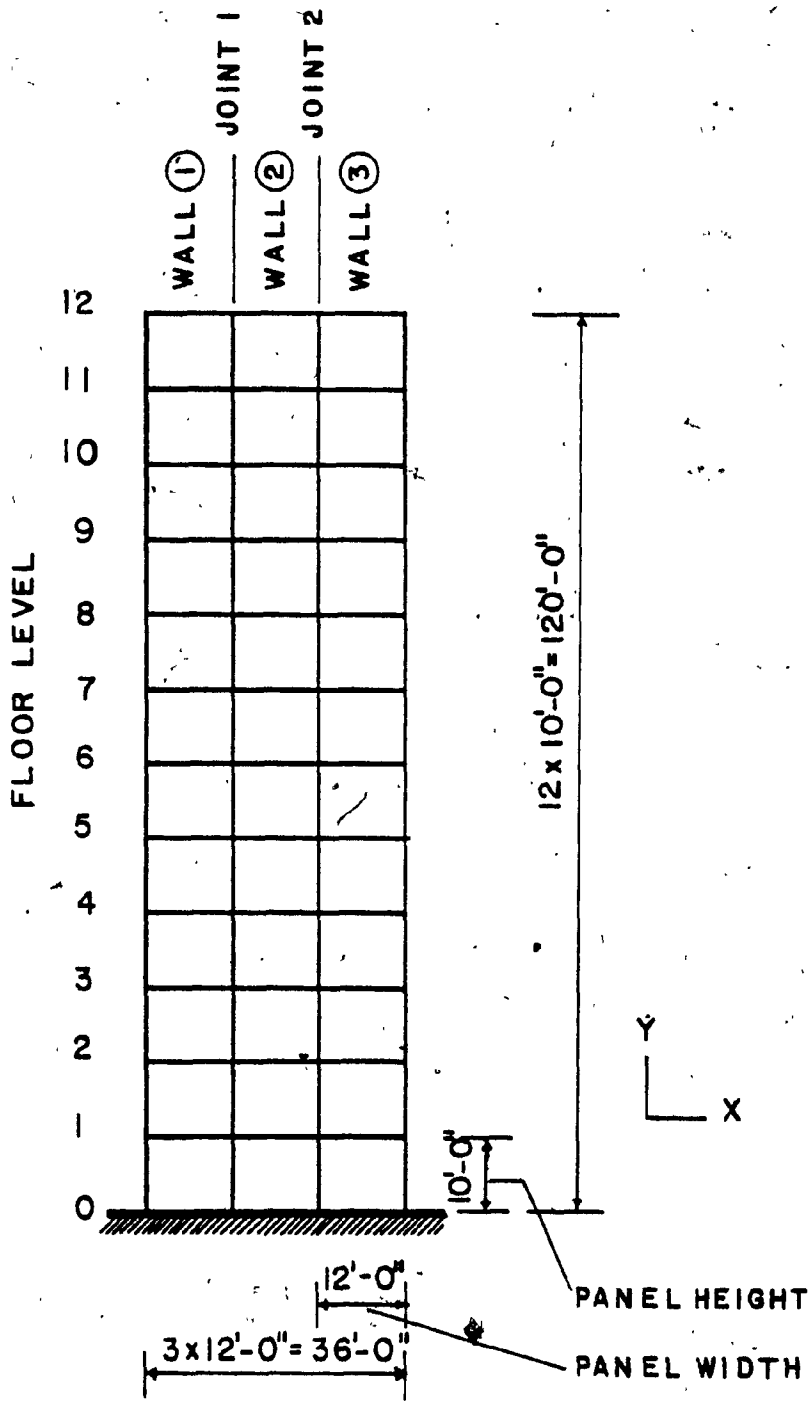

FIG. 5.1 ELEVATION OF PANEL STRUCTURE

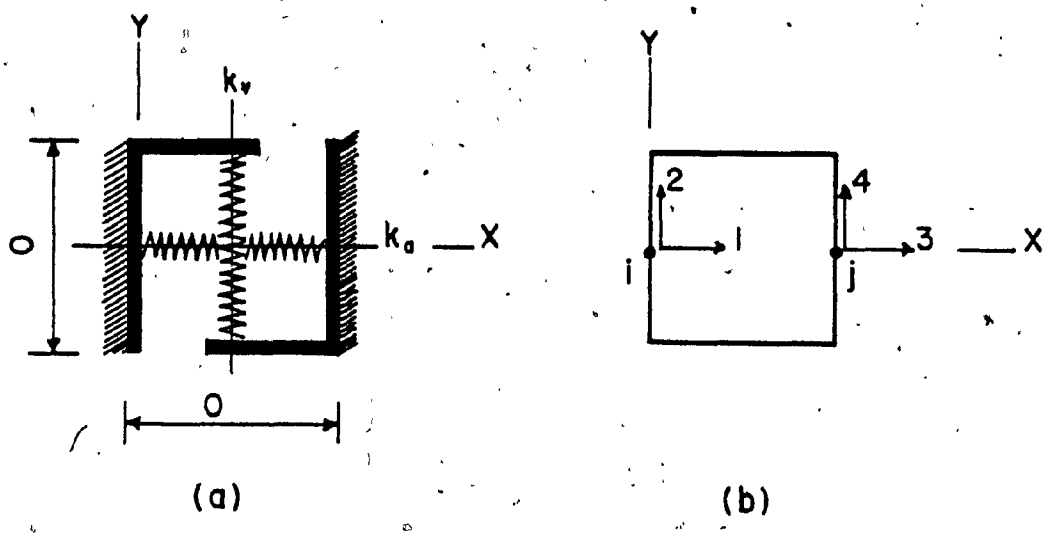

FIG. 5.2 CONNECTOR ELEMENT: (a) IDEALIZATION, AND (b) DEGREES OF FREEDOM

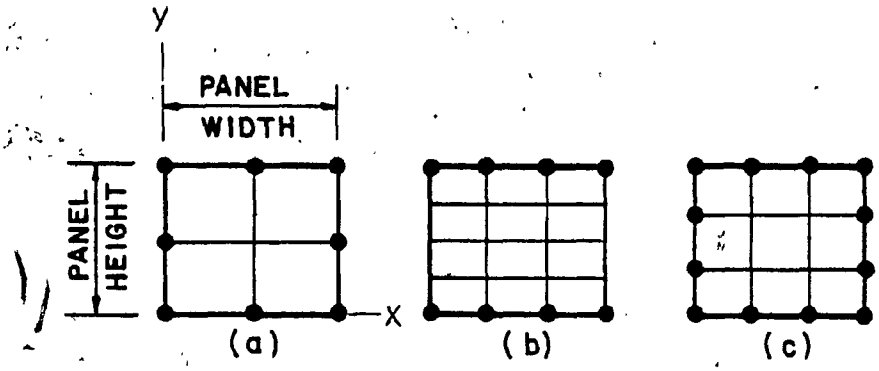

PANEL ELEMENTS

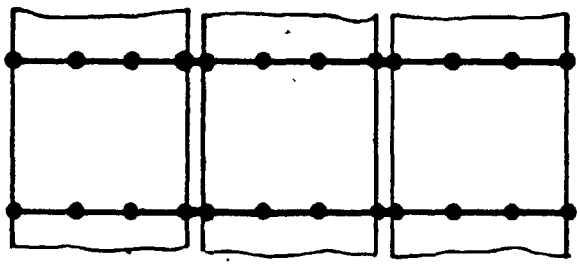

(d) STOREY WITH CONNECTORS

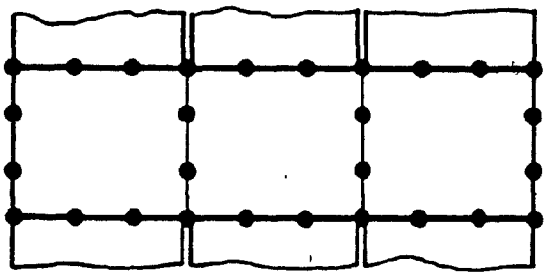

(e) MONOLITHIC STOREY

FIG. 5.3 PANEL ELEMENTS AND STOREY ARRANGEMENTS ((a) TYPE(101); (b) TYPE(120); (c) TYPE(101,100/2))

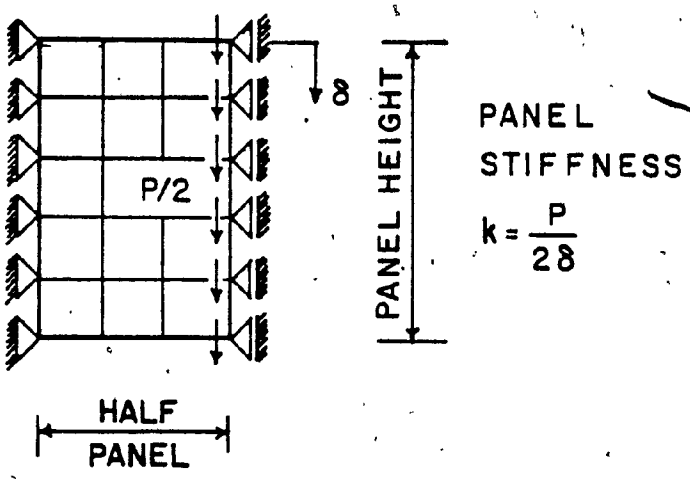

FIG. 5.4 DEFINITION OF PANEL STIFFNESS

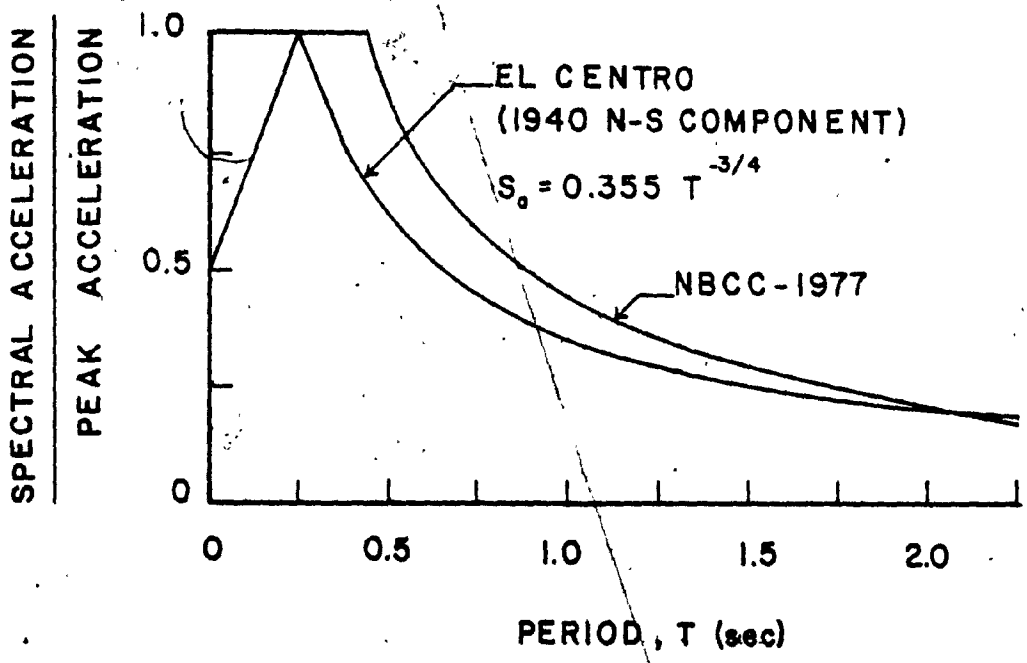

FIG. 5.5 ACCELERATION RESPONSE SPECTRA FOR 5 PER CENT DAMPING

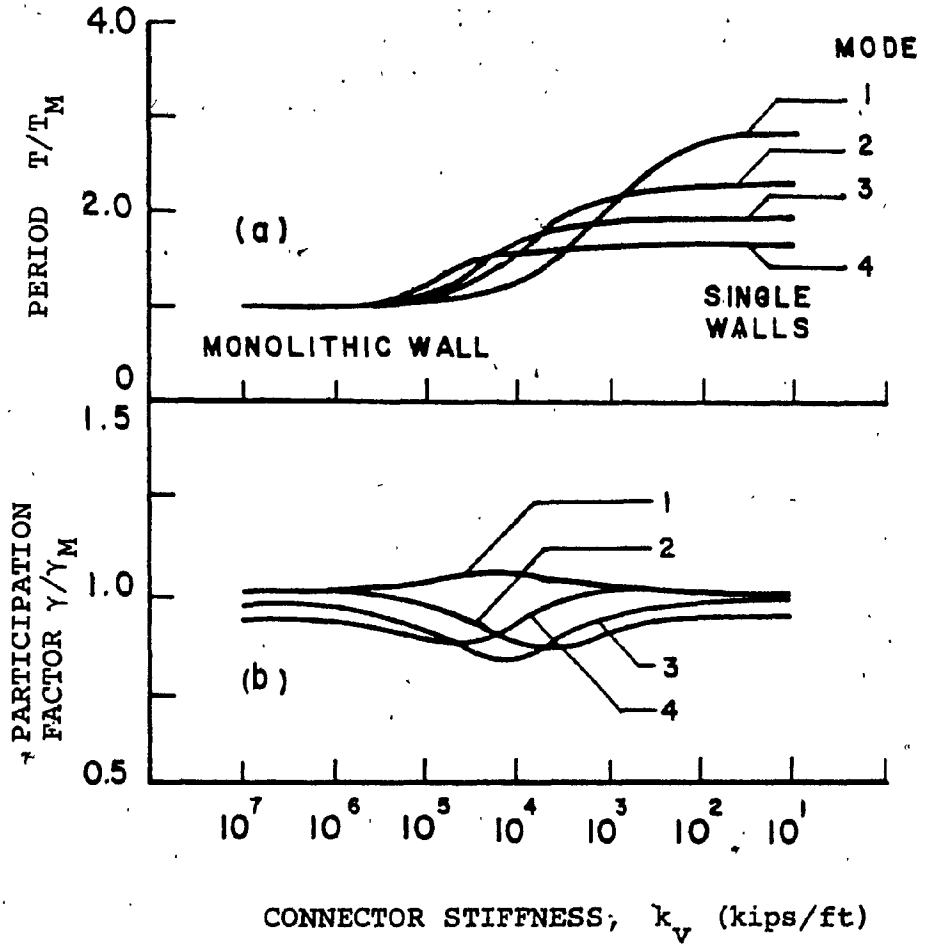

FIG. 5.6 NORMALIZED NATURAL PERIODS AND MODAL PARTICIPATION FACTORS AS FUNCTIONS OF CONNECTOR SHEAR STIFFNESS

(1 kip/ft = 14.6 kN/m)

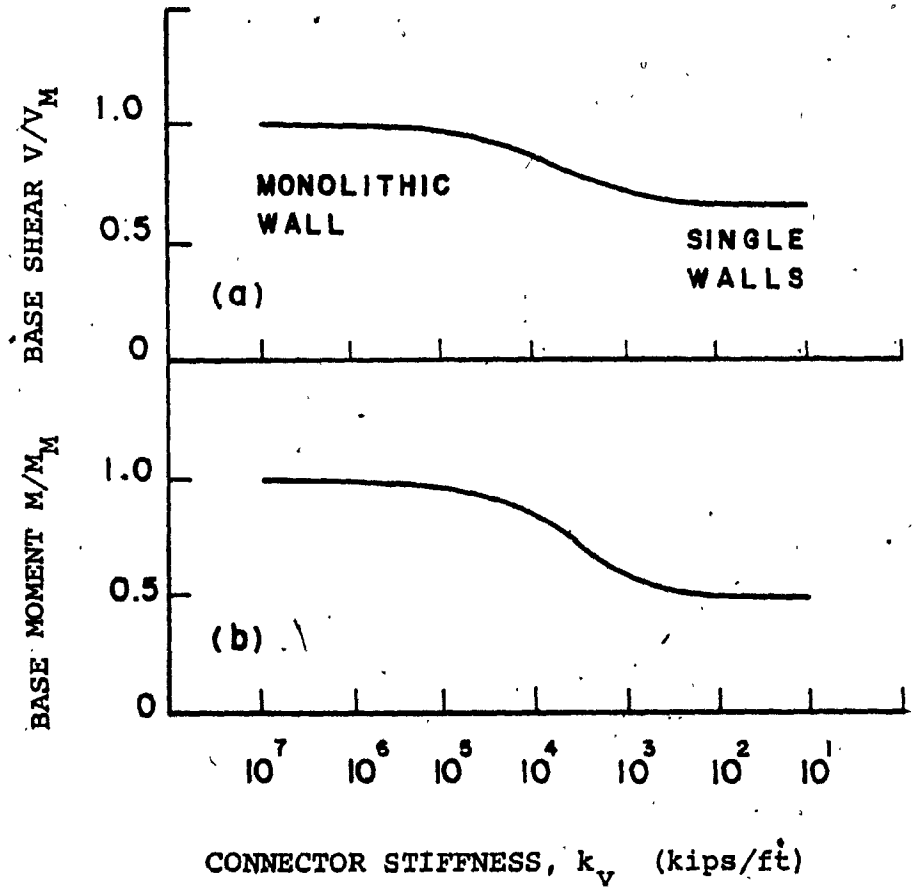

FIG. 5.7 NORMALIZED BASE SHEAR AND OVERTURNING MOMENT AS FUNCTIONS OF CONNECTOR SHEAR STIFFNESS (1 kip/ft = 14.6 kN/m)

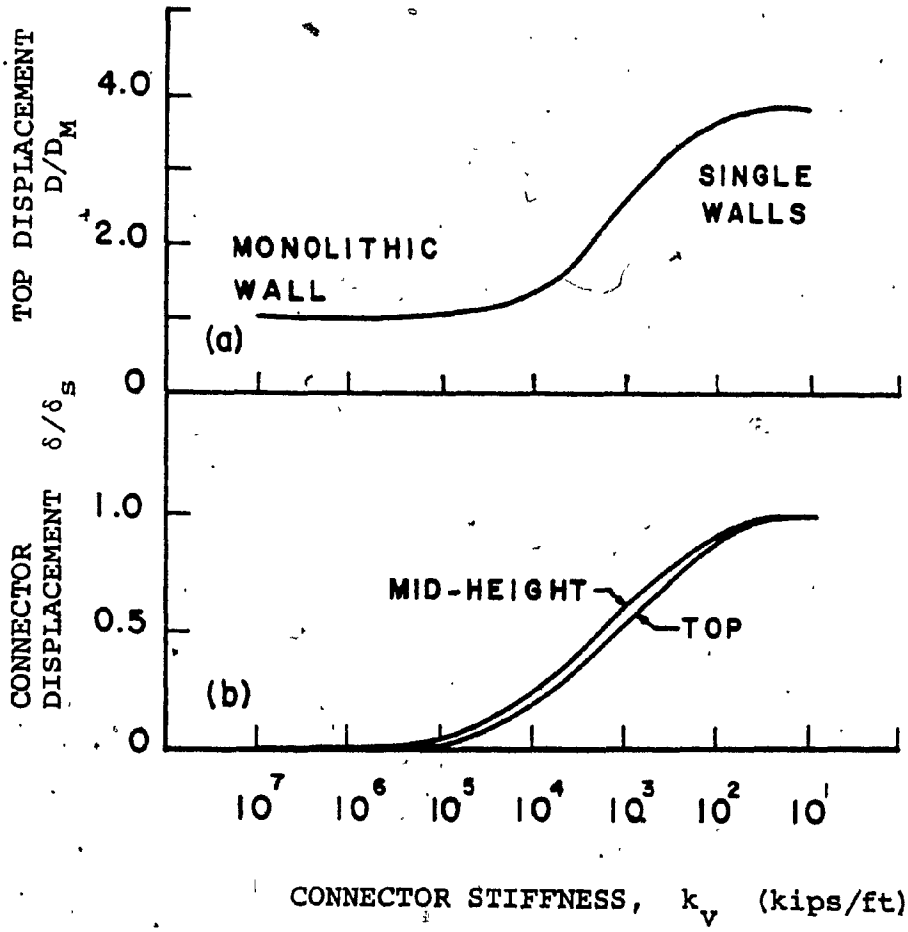

FIG. 5.8 NORMALIZED TOP AND CONNECTOR VERTICAL DISPLACEMENTS AS FUNCTIONS OF CONNECTOR SHEAR STIFFNESS (1 kip/ft = 14.6 kN/m)

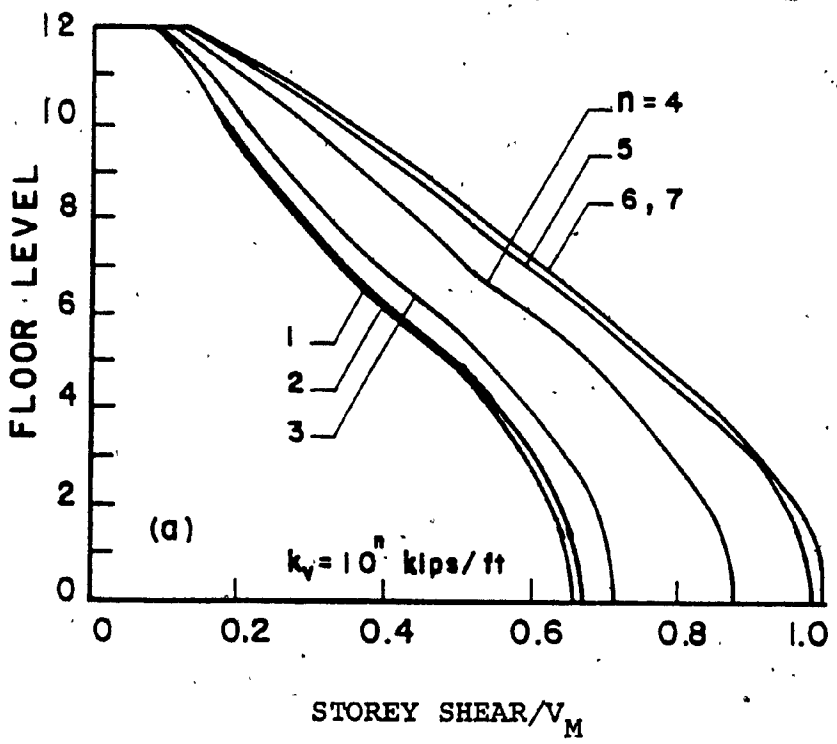

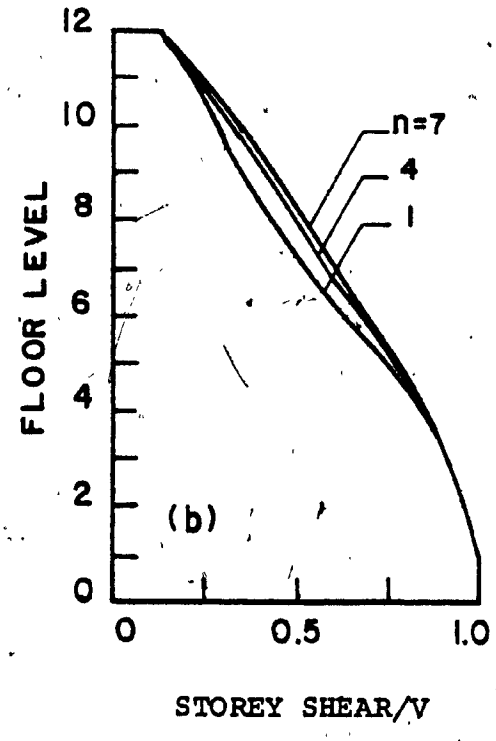

FIG. 5.9 DISTRIBUTION OF HORIZONTAL STOREY SHEARS FOR DIFFERENT CONNECTOR STIFFNESS k_v NORMALIZED TO; (a) BASE SHEAR OF MONOLITHIC WALL, AND (b) ACTUAL BASE SHEAR (1 kip/ft = 14.6 kN/m)

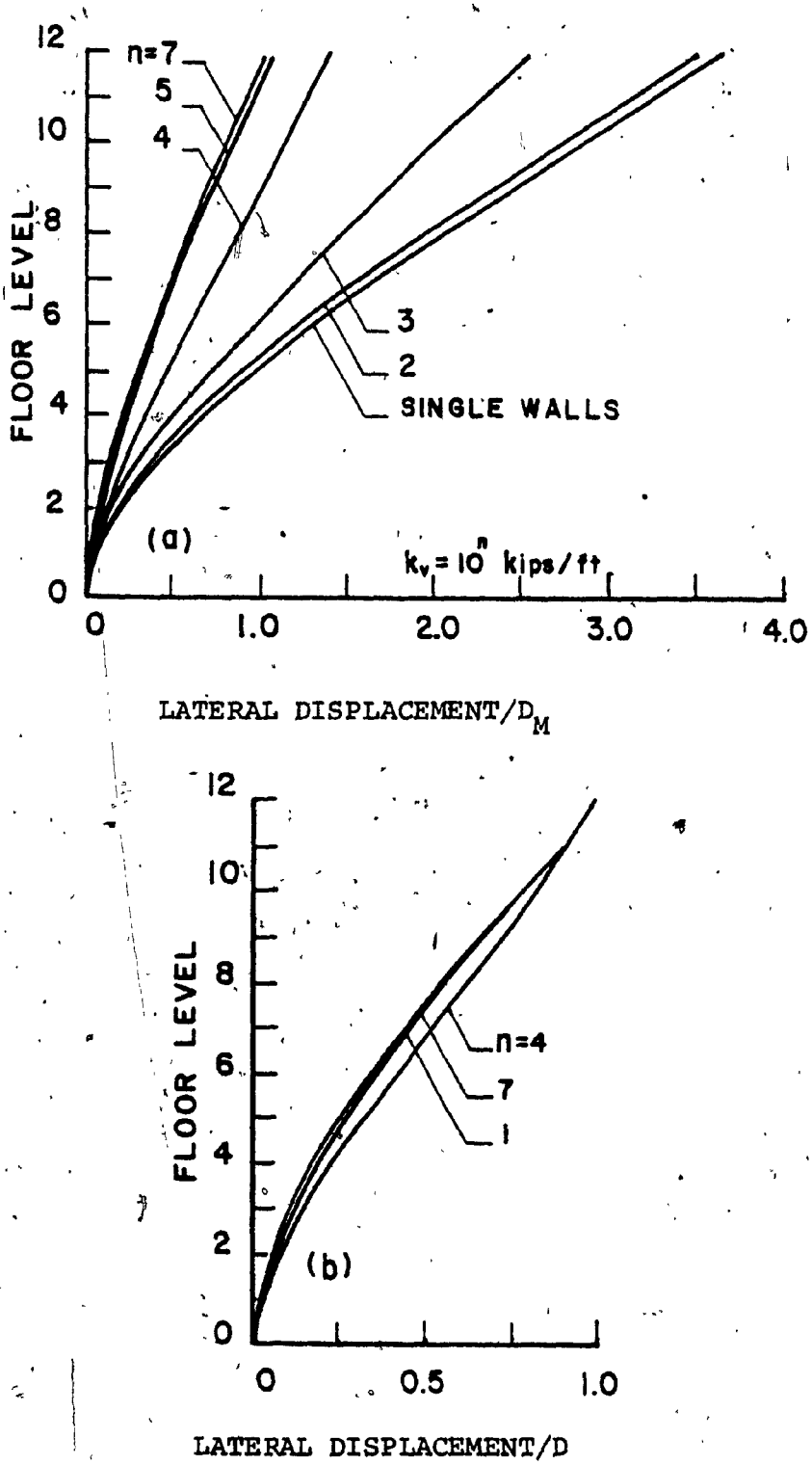

FIG. 5.10 ENVELOPES OF LATERAL DISPLACEMENTS FOR DIFFERENT CONNECTOR STIFFNESSES k_v NORMALIZED TO; (a) TOP DISPLACEMENT OF MONOLITHIC WALL, AND (b) ACTUAL TOP DISPLACEMENT (1 kip/ft = 14.6 kN/m)

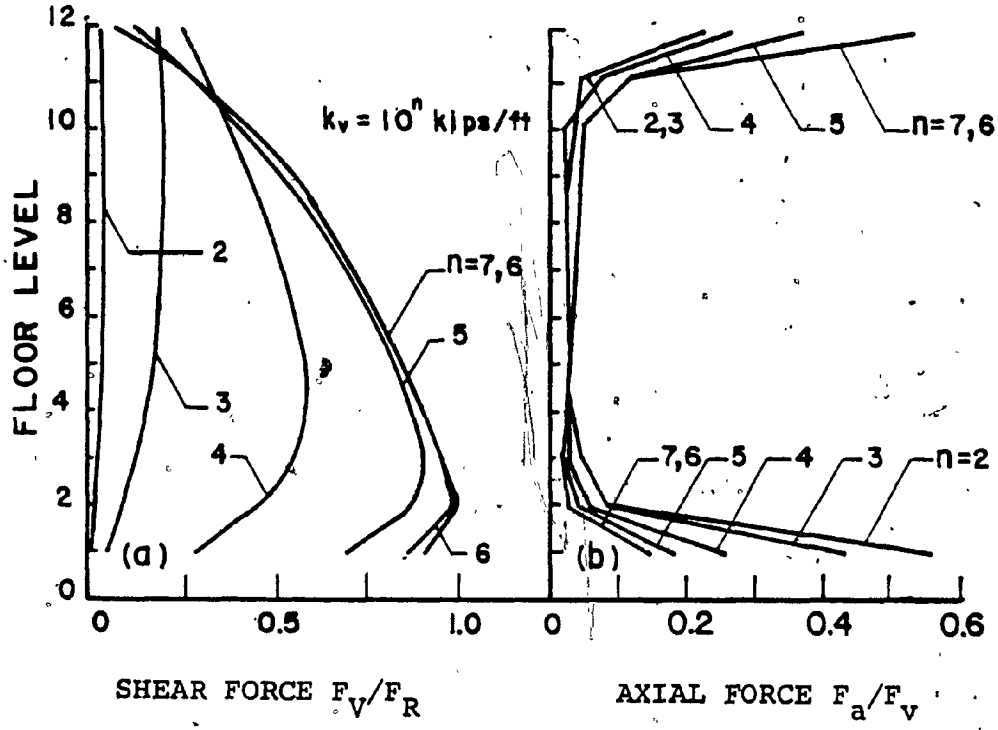

FIG. 5.11 NORMALIZED CONNECTOR SHEAR FORCES AND AXIAL-TO-SHEAR FORCE RATIOS FOR DIFFERENT STIFFNESS k_v
(1 kip/ft = 14.6 kN/m)

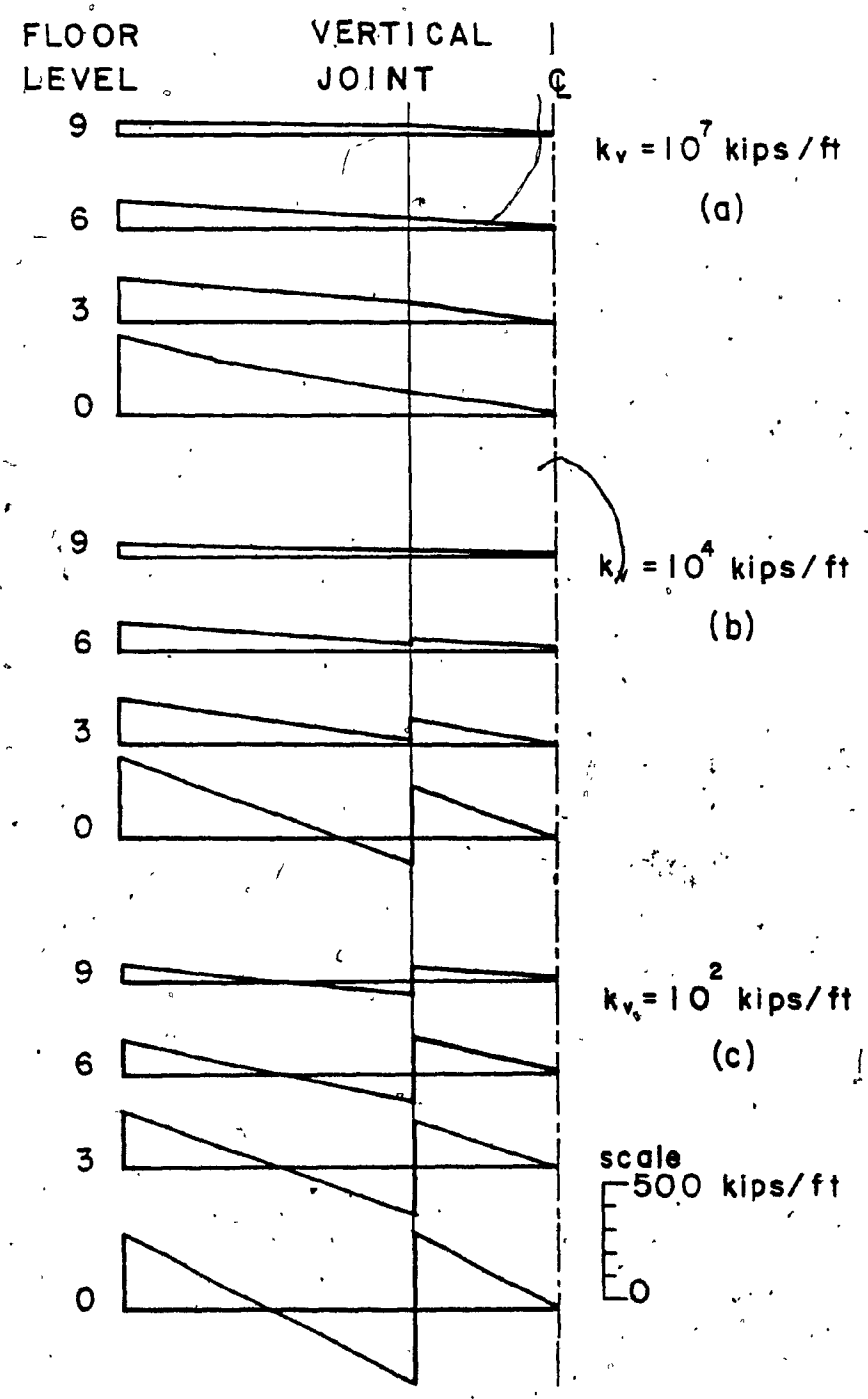

FIG. 5.12 NORMAL FORCES IN HORIZONTAL JOINTS FOR 1 g PEAK ACCELERATION (El Centro Spectrum) AND DIFFERENT CONNECTOR SHEAR STIFFNESS k_v (1 kip/ft = 14.6 kN/m)

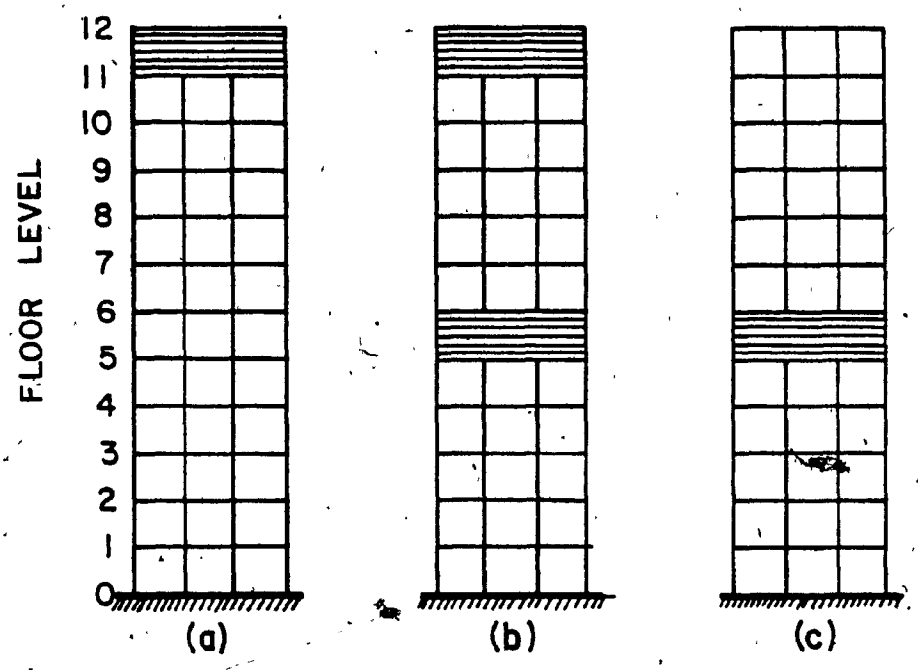

FIG. 5.13 STRUCTURES WITH MONOLITHIC STOREYS:

(a) MONOLITHIC TOP STOREY
(b) MONOLITHIC TOP AND MID-HEIGHT STOREY, AND
(c) MONOLITHIC MID-HEIGHT STOREY

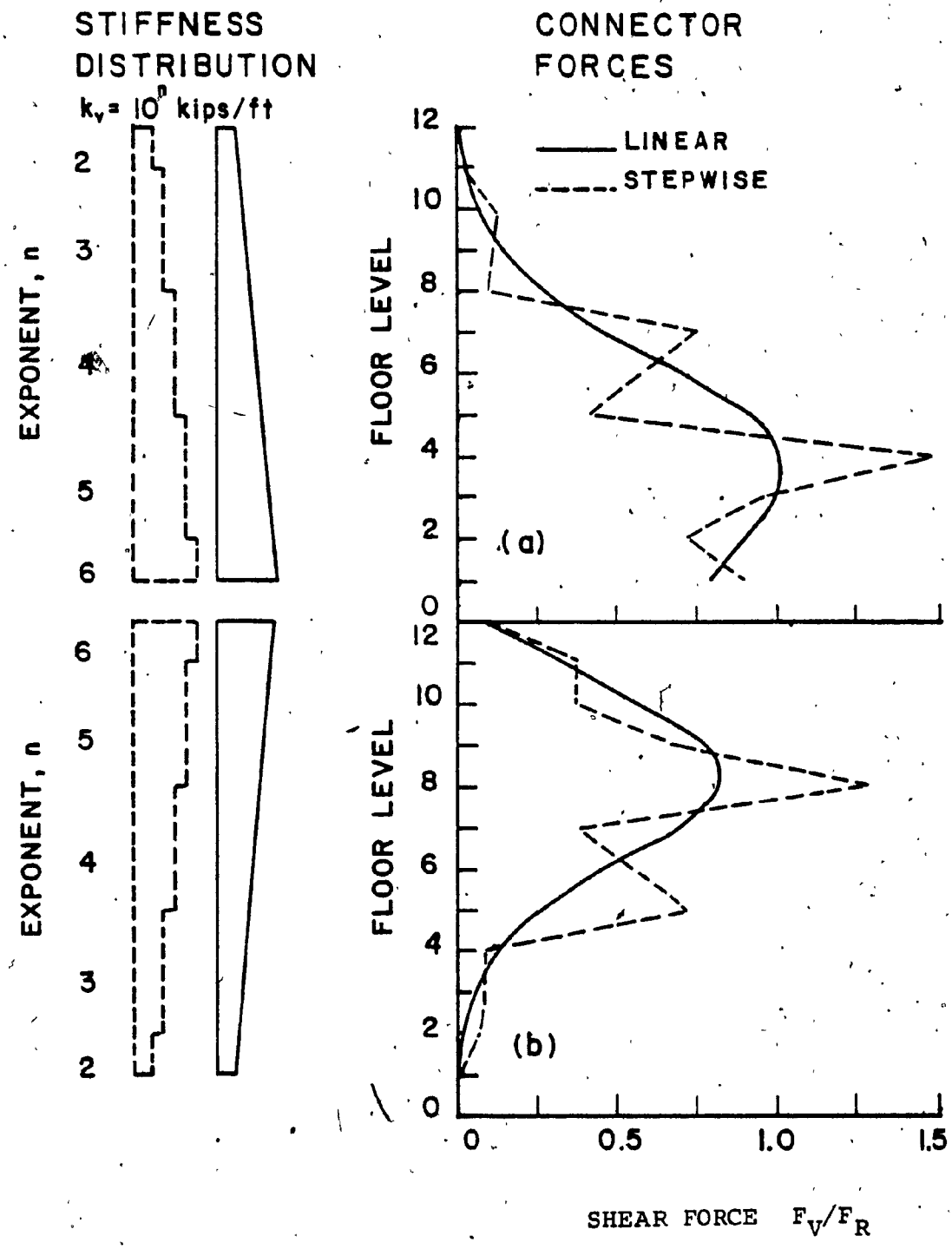

FIG. 5.14 EFFECT OF DISTRIBUTION OF CONNECTOR STIFFNESS k_v ON NORMALIZED CONNECTOR SHEAR FORCES
(1 kip/ft = 14.6 kN/m)

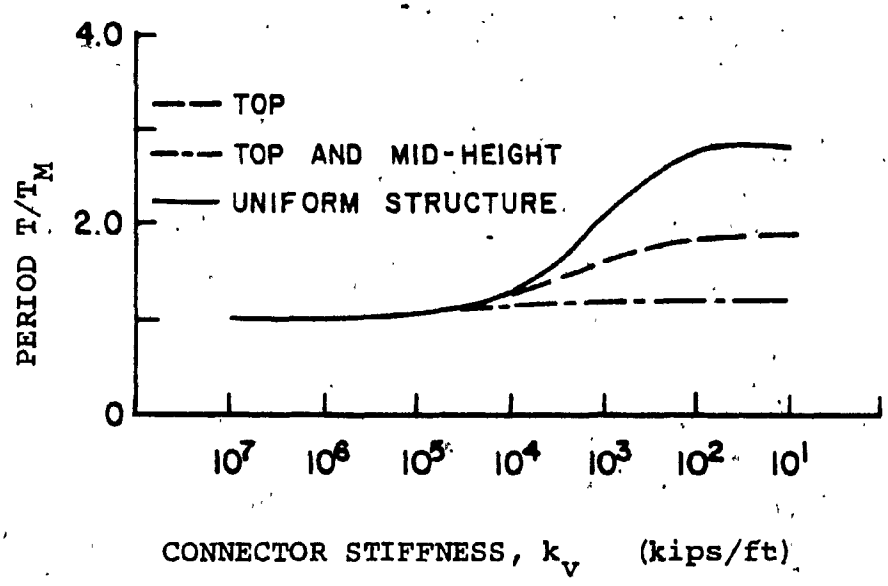

FIG. 5.15 EFFECT OF MONOLITHIC STOREYS AT TOP AND MID-HEIGHT ON NORMALIZED FUNDAMENTAL PERIOD (1 kip/ft = 14.6 kN/m)

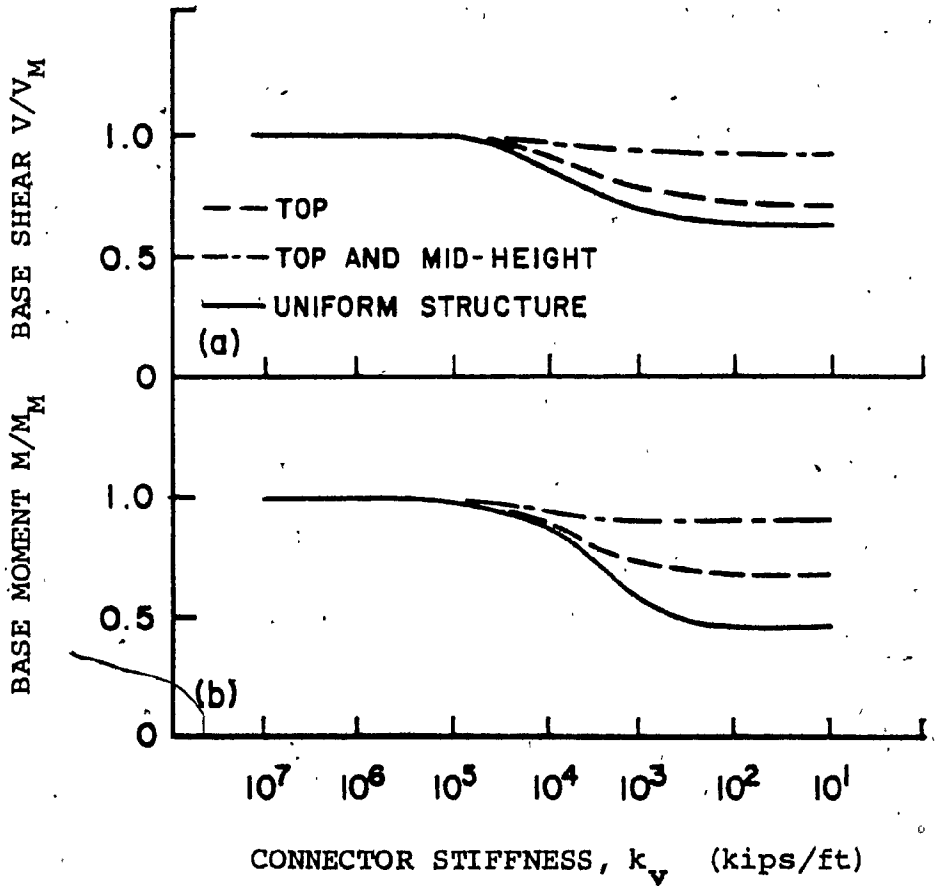

FIG. 5.16 EFFECT OF MONOLITHIC STOREYS AT TOP AND MID-HEIGHT ON NORMALIZED BASE SHEAR AND OVERTURNING MOMENT (1 kip/ft = 14.6 kN/m)

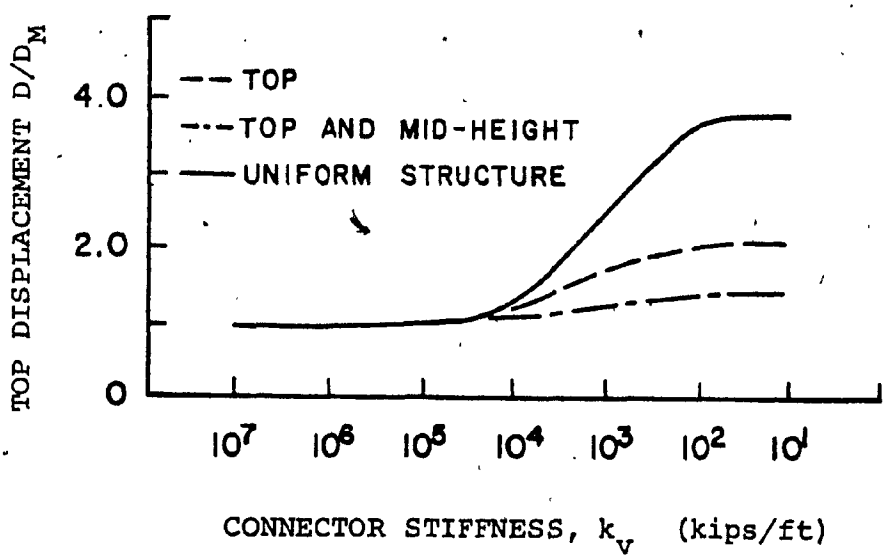

FIG. 5.17 EFFECT OF MONOLITHIC STOREYS AT TOP AND AT TOP AND MID-HEIGHT ON NORMALIZED TOP DEFLECTION (1 kip/ft = 14.6 kN/m)

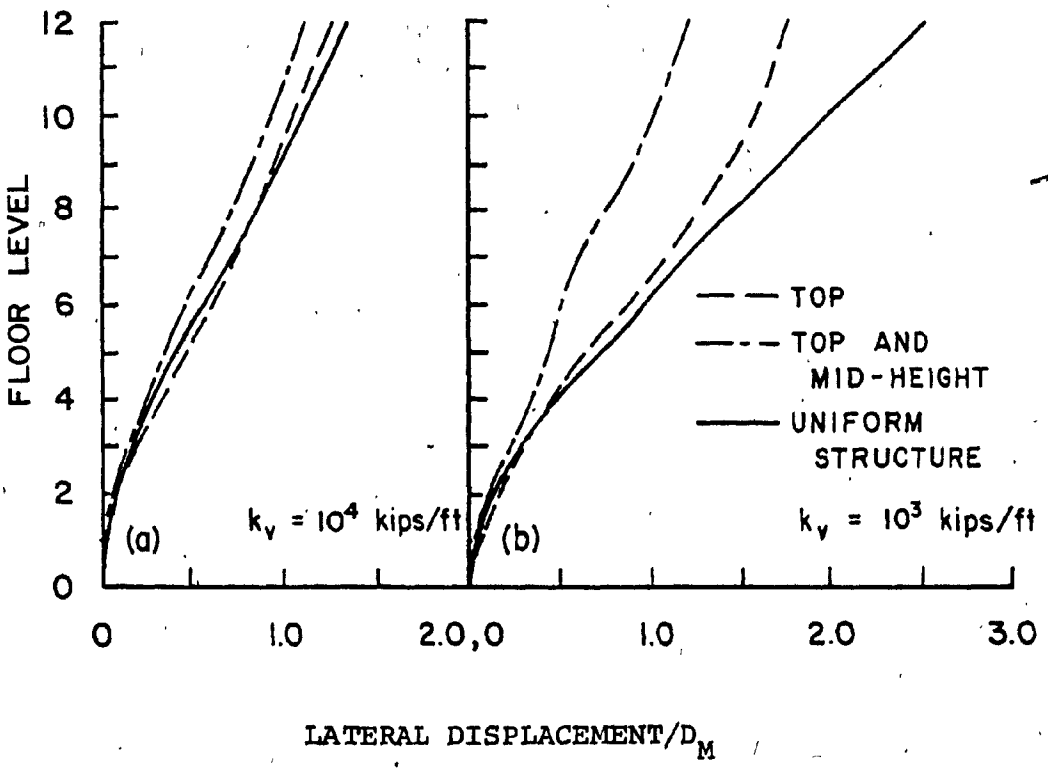

FIG. 5.18 EFFECT OF MONOLITHIC STOREYS AT TOP AND AT TOP AND MID-HEIGHT ON DEFLECTION ENVELOPES (1 kip/ft = 14.6 kN/m)

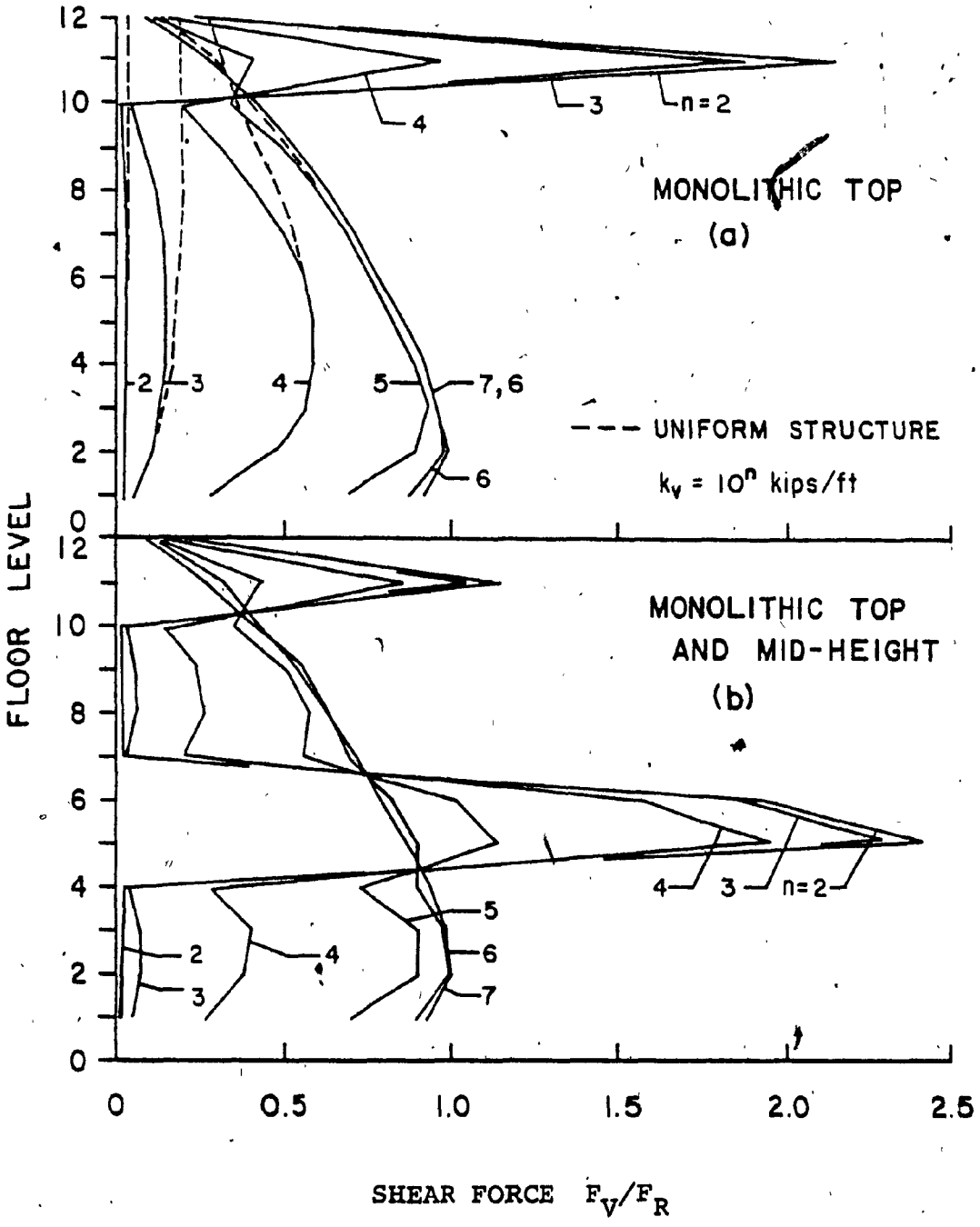

FIG. 5.19 NORMALIZED CONNECTOR SHEAR FORCES IN STRUCTURES WITH MONOLITHIC STOREYS FOR DIFFERENT CONNECTOR STIFFNESS k_v (1 kip/ft = 14.6 kN/m)

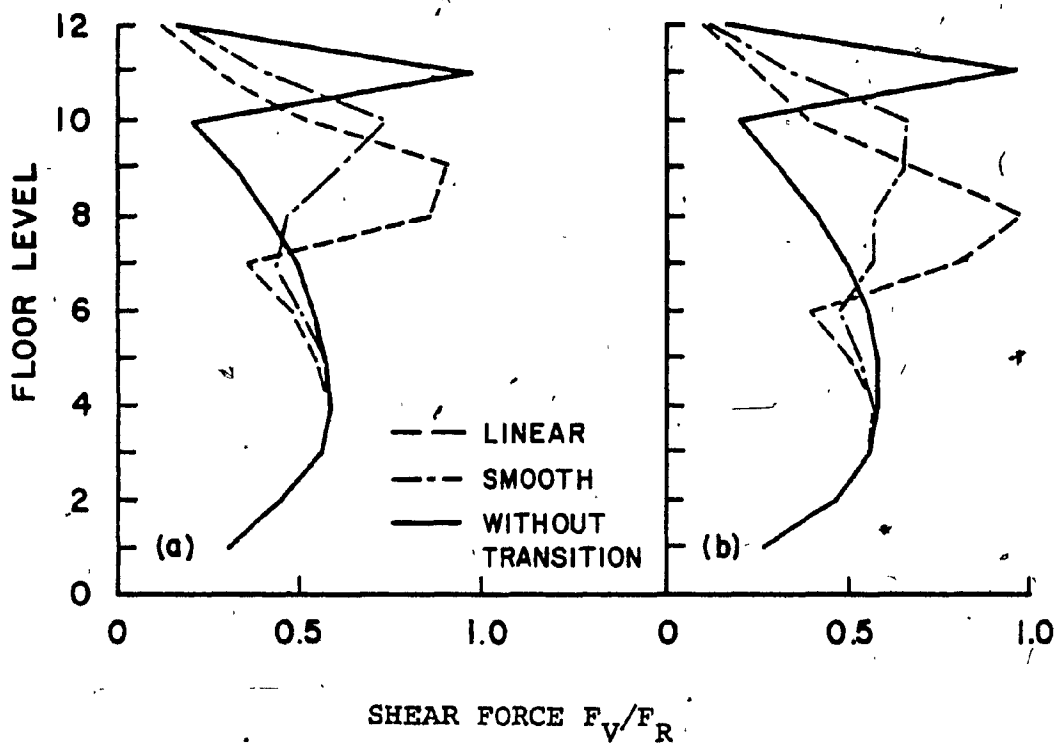

FIG. 5.20 COMPARISON OF LINEAR AND SMOOTH STIFFNESS TRANSITIONS FOR NORMALIZED CONNECTOR SHEAR FORCES IN STRUCTURES WITH MONOLITHIC TOP STOREY; (a) TRANSITION OVER 3 STOREYS, AND (b) TRANSITION OVER 4 STOREYS ($k_v = 10^4$ kips/ft (14.6×10^4 kN/m))

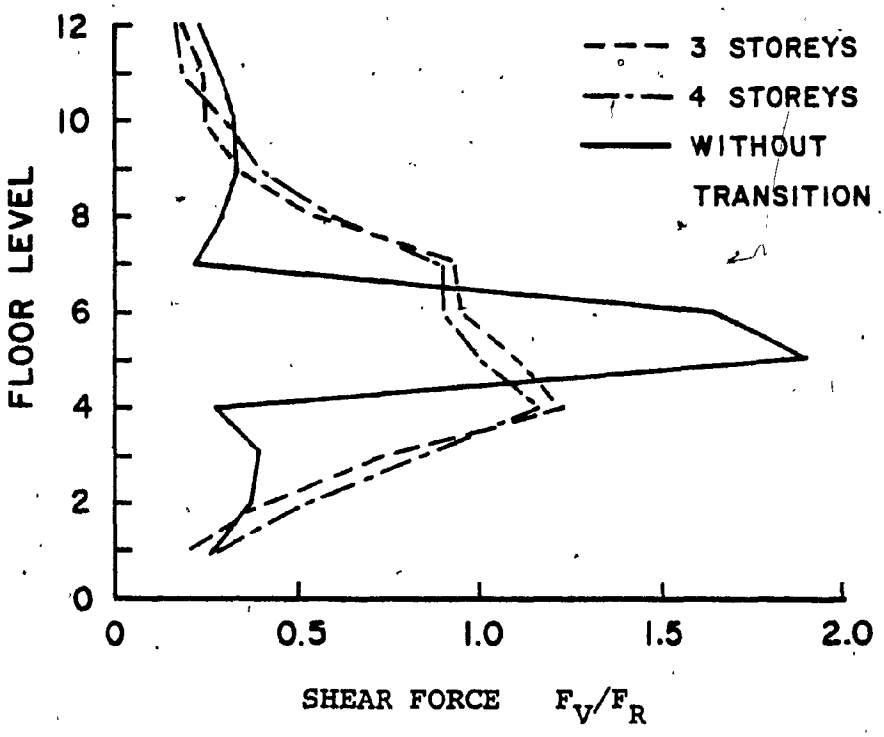

FIG. 5.21 EFFECT OF LENGTH OF SMOOTH STIFFNESS TRANSITION ON NORMALIZED CONNECTOR SHEAR FORCES IN STRUCTURE WITH MONOLITHIC MID-HEIGHT STOREY (k_v = 10^4 kips/ft (14.6×10^4 kN/m))

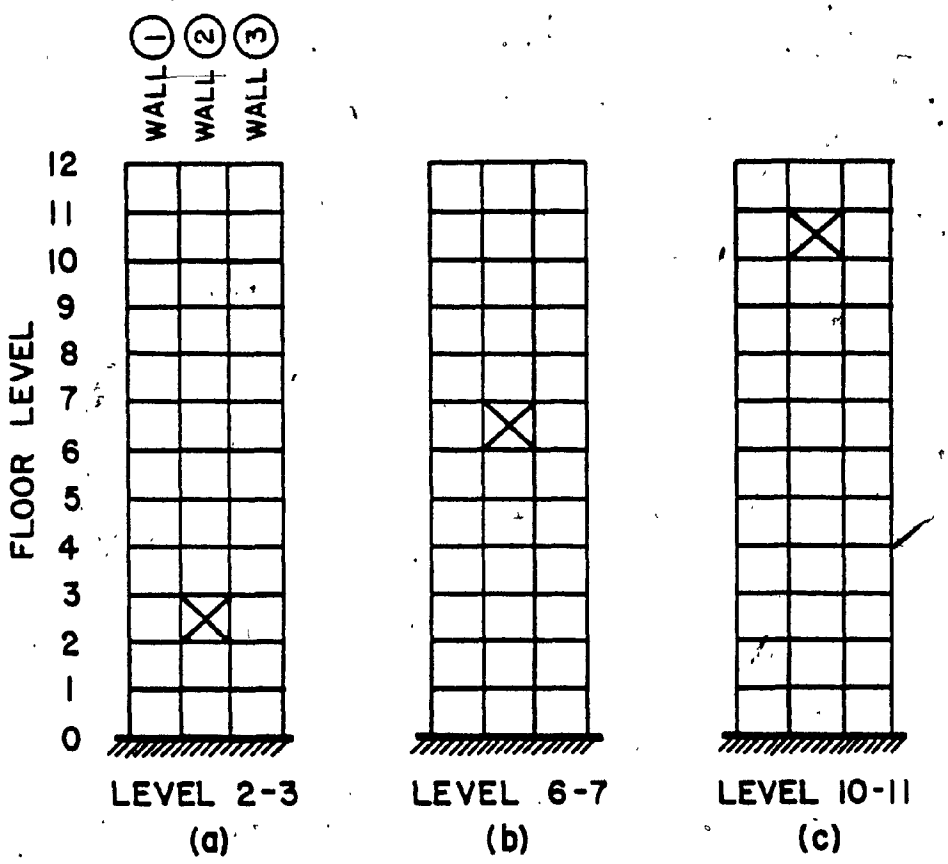

FIG. 5.22 STRUCTURES WITH A PANEL MISSING AT DIFFERENT LEVELS IN WALL 2

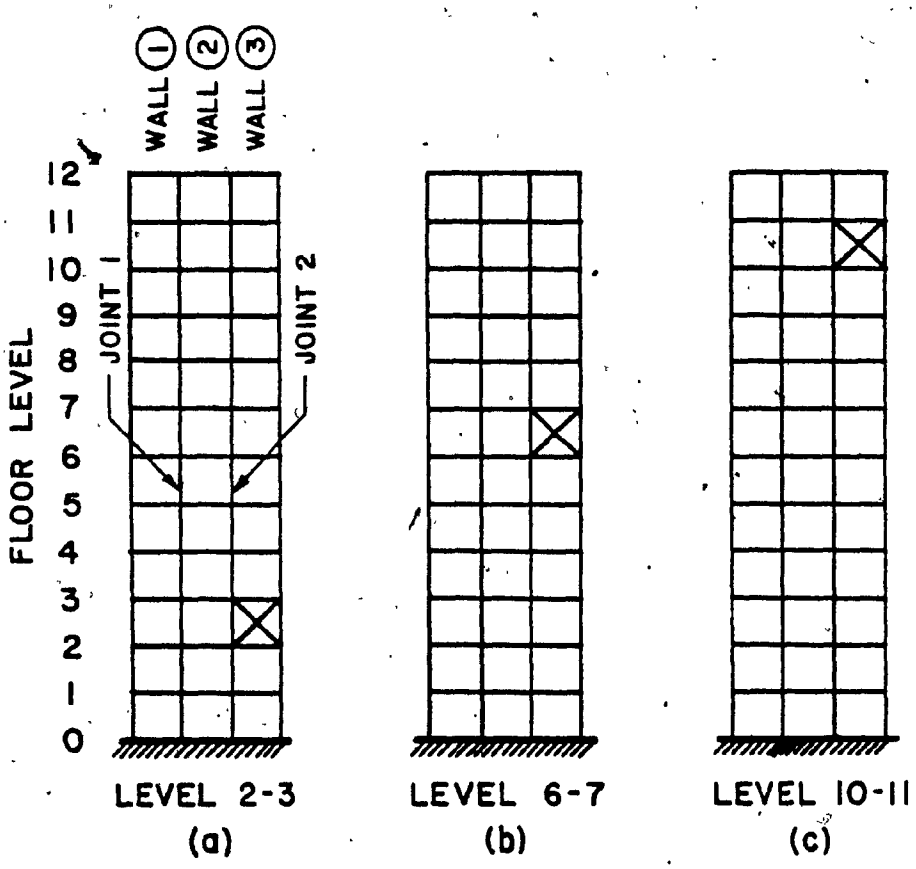

FIG. 5.23 STRUCTURES WITH A PANEL MISSING AT DIFFERENT LEVELS IN WALL 3

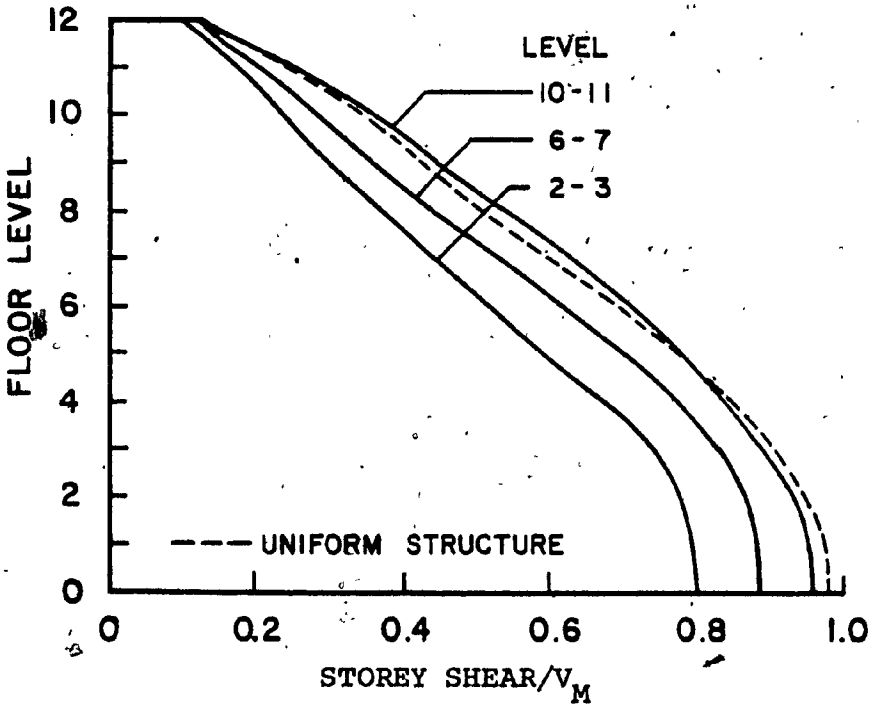

FIG. 5.24 EFFECT OF THE LEVEL OF PANELS MISSING IN WALL 3 ON NORMALIZED HORIZONTAL STOREY SHEARS (k_v = 10^5 kips/ft (14.6 x 10^5 kN/m))

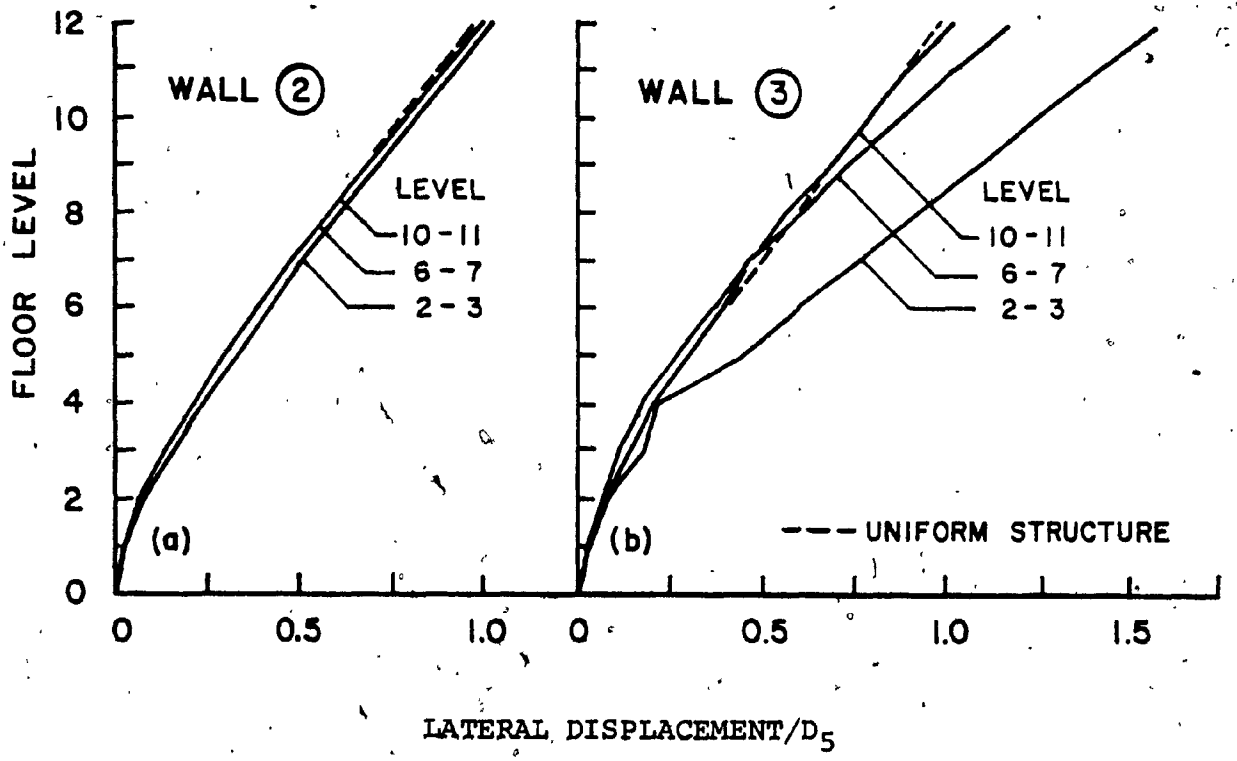

FIG. 5.25 EFFECT OF THE LEVEL OF MISSING PANELS ON NORMALIZED LATERAL DISPLACEMENTS (k_v = 10^5 kips/ft(14.6 x 10^5 kN/m))

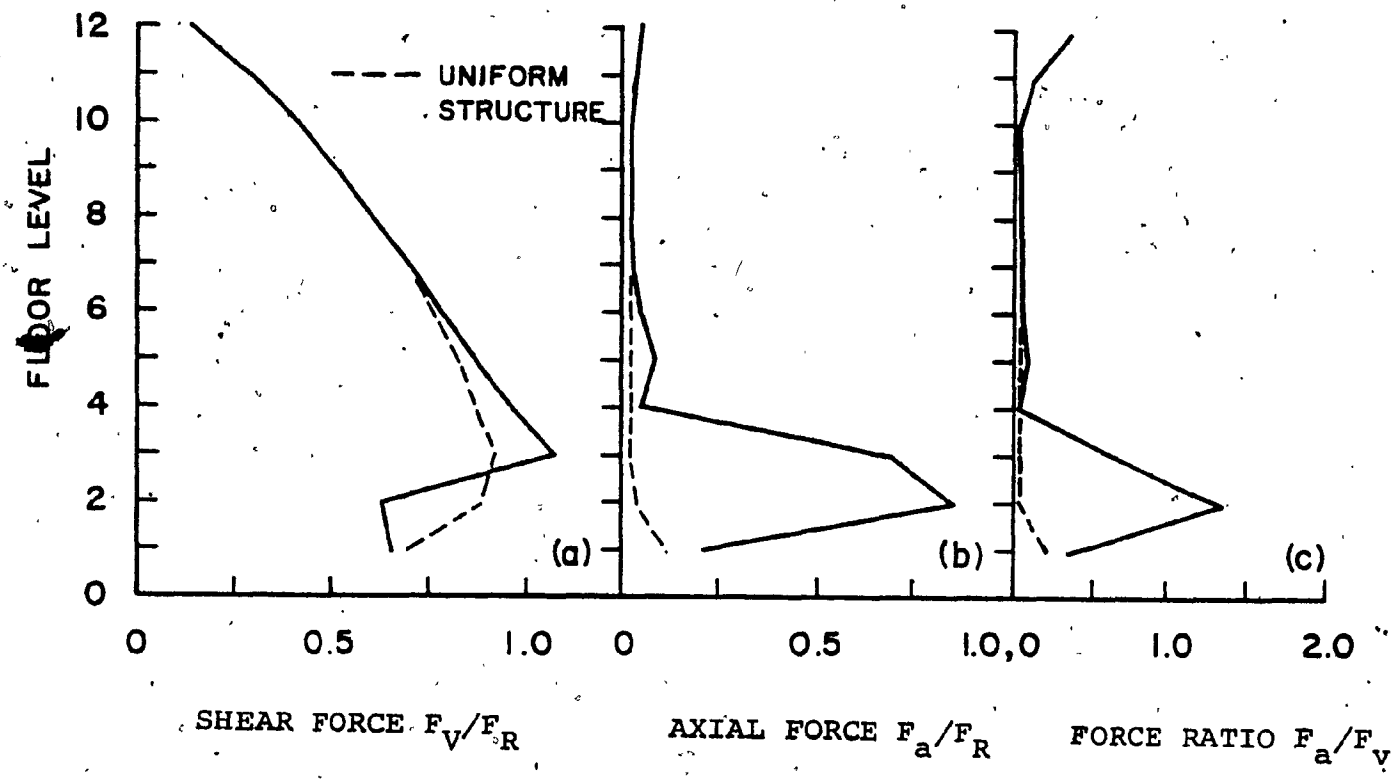

FIG. 5.26 EFFECT OF A PANEL MISSING AT LEVEL 2-3 IN WALL 2 ON NORMALIZED CONNECTOR FORCES (k_v = 10^5 kips/ft(14.6 x 10^5 kN/m))

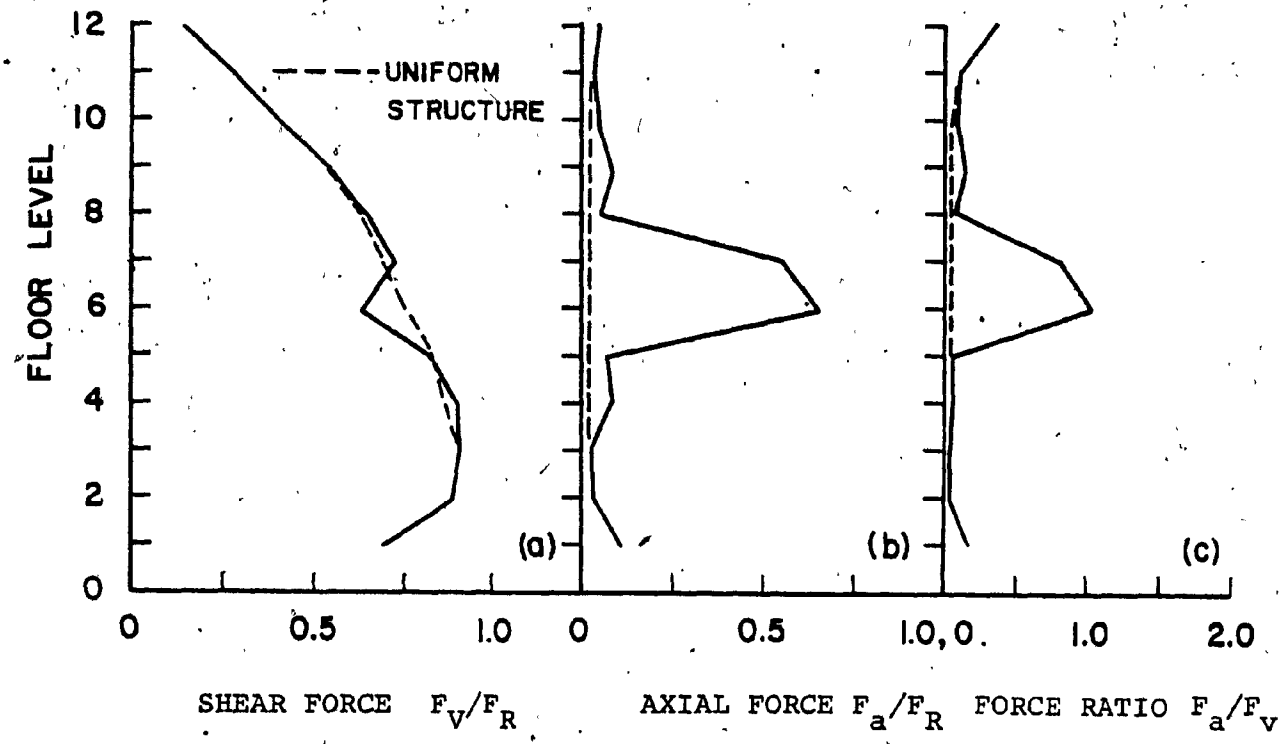

FIG. 5.27 EFFECT OF A PANEL MISSING AT LEVEL 6-7 IN WALL 2 ON NORMALIZED CONNECTOR FORCES (k_v = 10^5 kips/ft (14.6×10^5 kN/m))

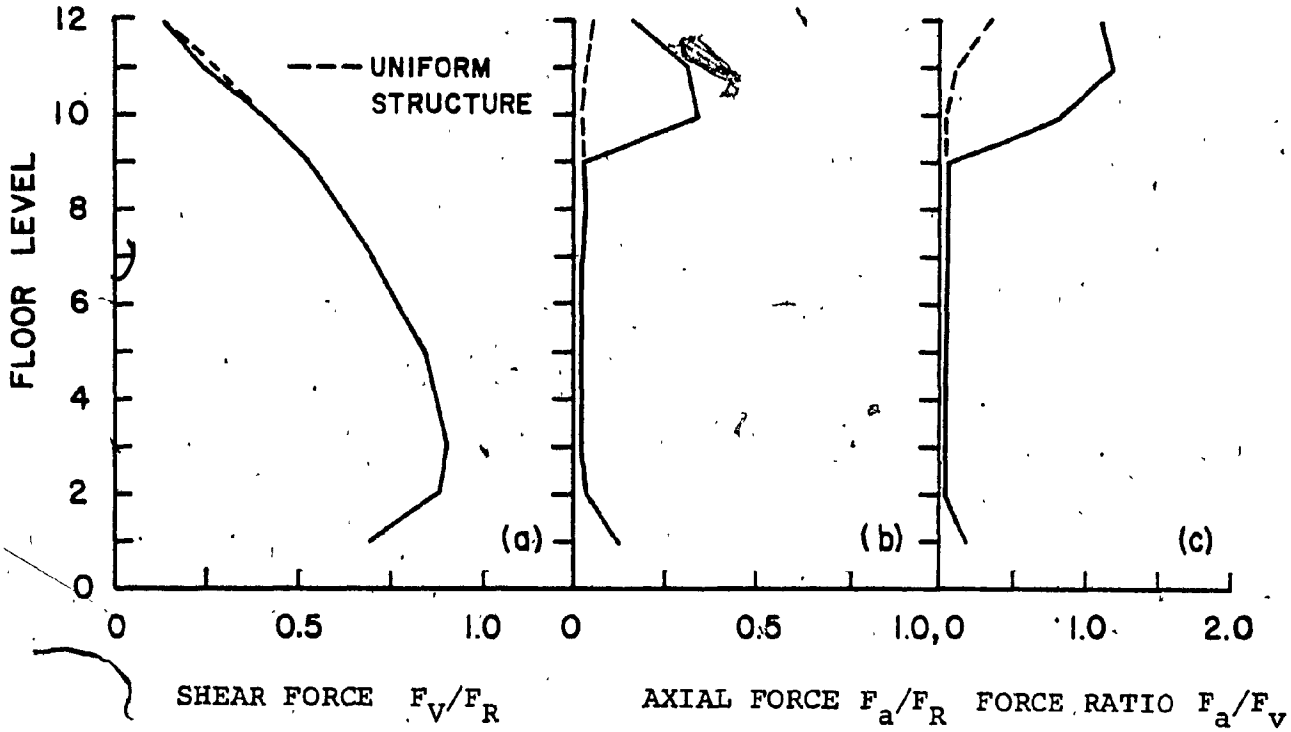

FIG. 5.28 EFFECT OF A PANEL MISSING AT LEVEL 10-11 IN WALL 2 ON NORMALIZED CONNECTOR FORCES (k_v = 10^5 kips/ft (14.6 x 10^5 kN/m))

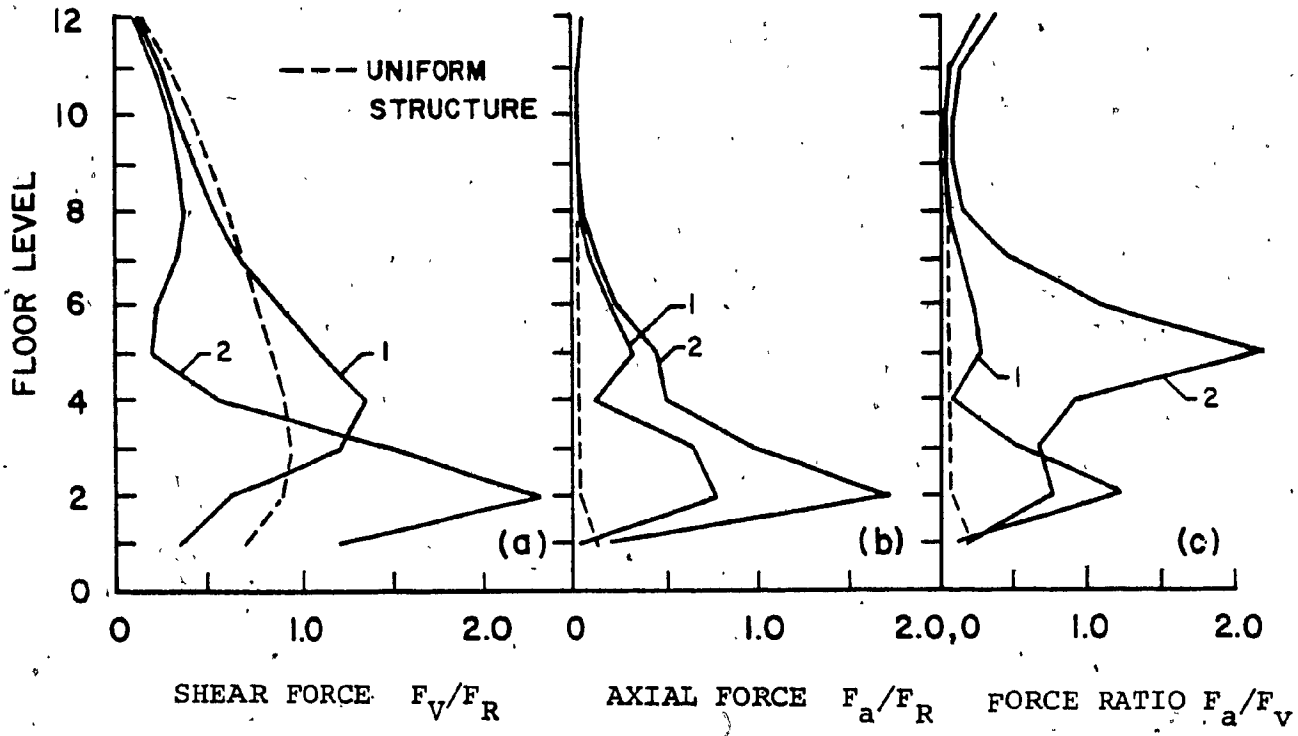

FIG. 5.29 EFFECT OF A PANEL MISSING AT LEVEL 2-3 IN WALL 3 ON NORMALIZED CONNECTOR FORCES ($k_v = 10^5$ kips/ft (14.6×10^5 kN/m))

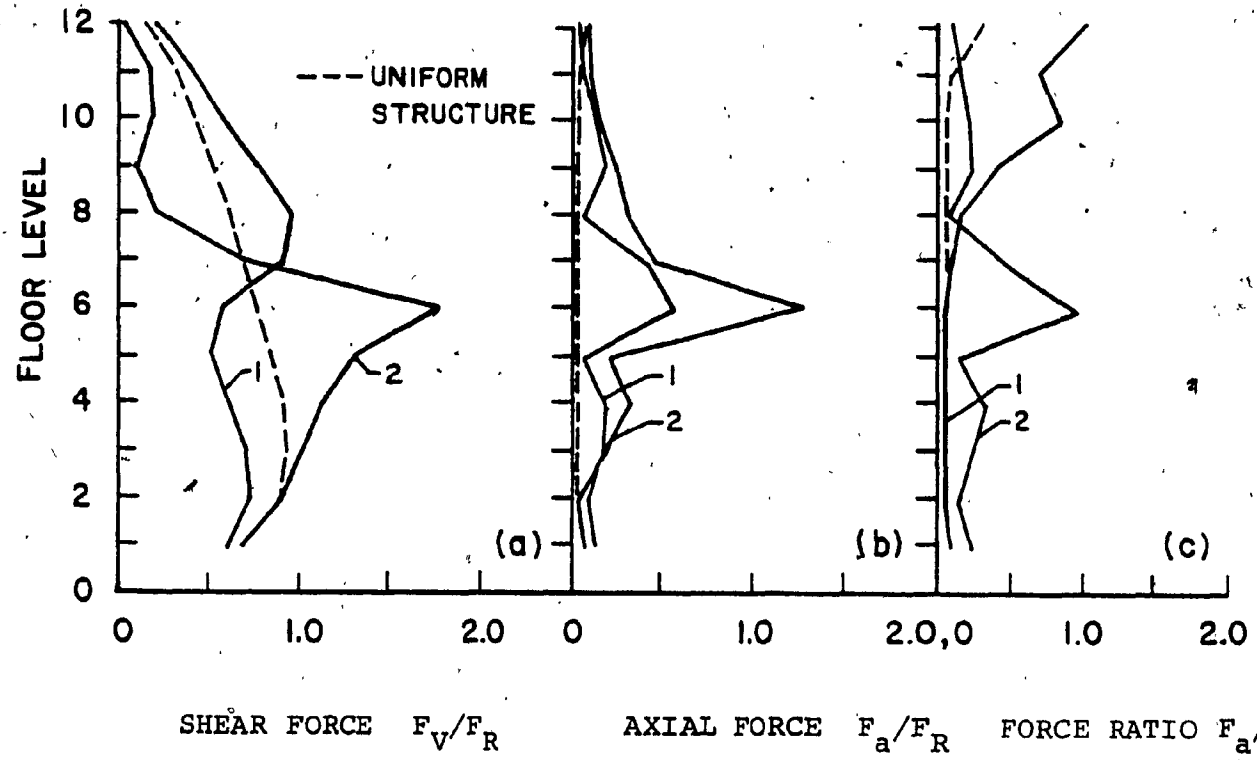

FIG. 5.30 EFFECT OF A PANEL MISSING AT LEVEL 6-7 IN WALL 3 ON NORMALIZED CONNECTOR FORCES (k_v = 10^5 kips/ft (14.6×10^5 kN/m))

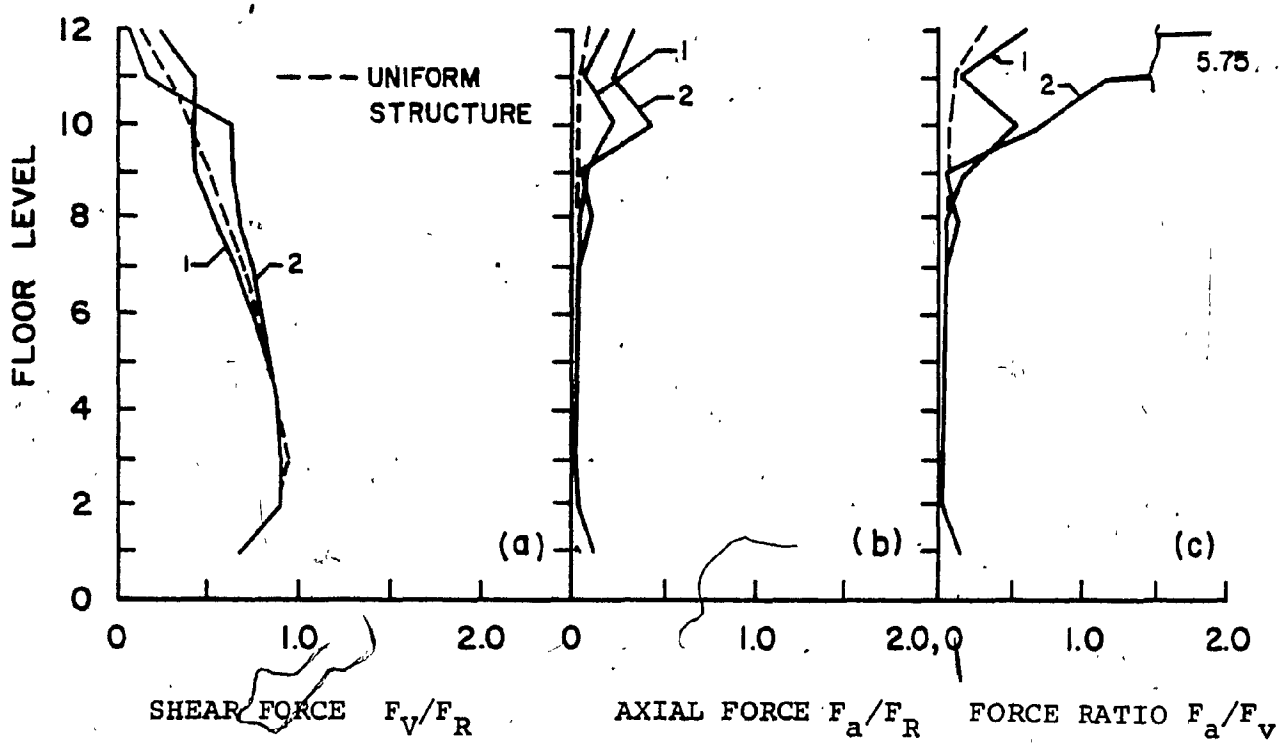

FIG. 5.31 EFFECT OF A PANEL MISSING AT LEVEL 10-11 IN WALL 3 ON NORMALIZED CONNECTOR FORCES ($k_v = 10^5$ kips/ft (14.6×10^5 kN/m))

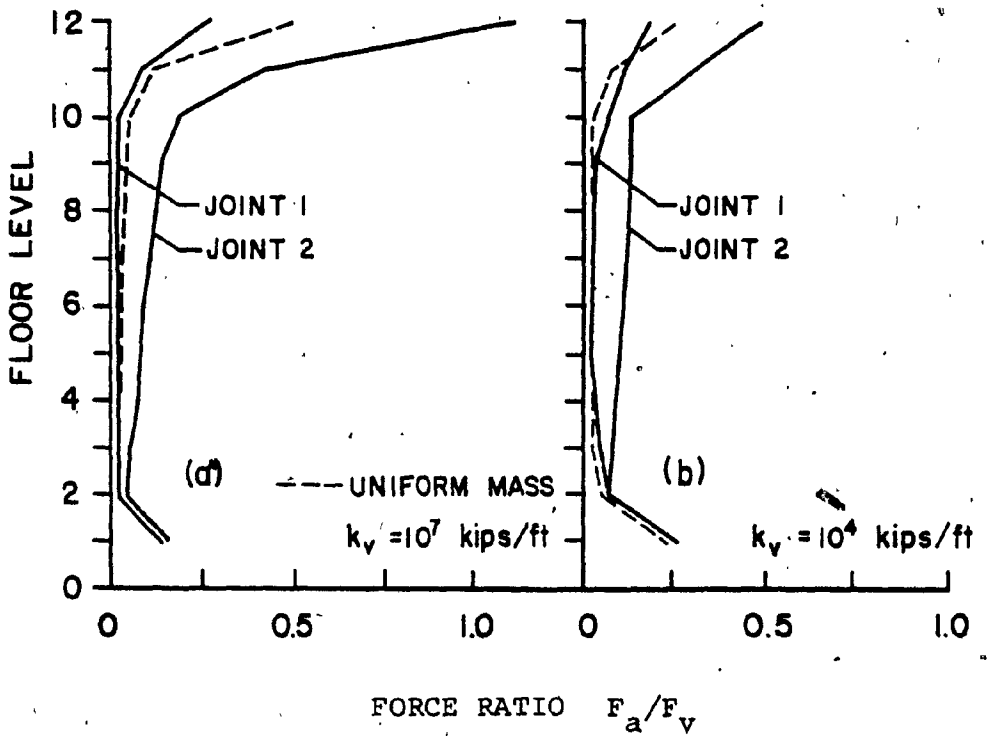

FIG. 5.32 EFFECT OF ASYMMETRIC FLOOR MASS DISTRIBUTION ON CONNECTOR AXIAL TO SHEAR FORCE RATIOS
(1 kip/ft = 14.6 kN/m)

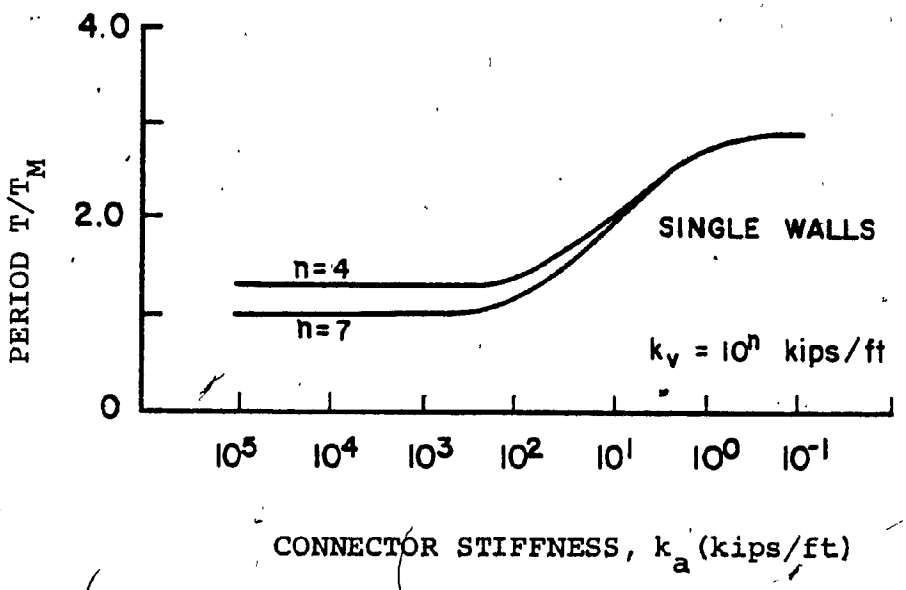

FIG. 5.33 INFLUENCE OF CONNECTOR AXIAL STIFFNESS k_a ON NORMALIZED FUNDAMENTAL PERIOD
(1 kip/ft = 14.6 kN/m)

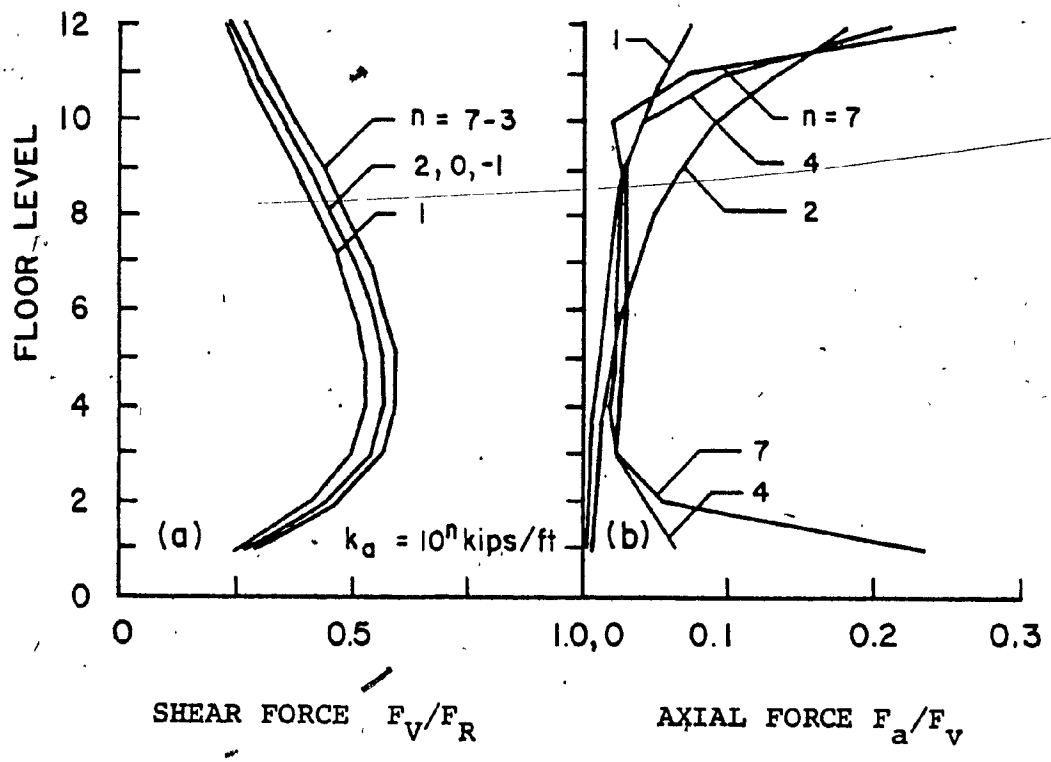

FIG. 5.34 INFLUENCE OF CONNECTOR AXIAL STIFFNESS k_a ON NORMALIZED CONNECTOR SHEAR FORCES AND AXIAL-TO-SHEAR FORCE RATIOS ($k_v = 10^4$ kips/ft (14.6 x 10^4 kN/m))

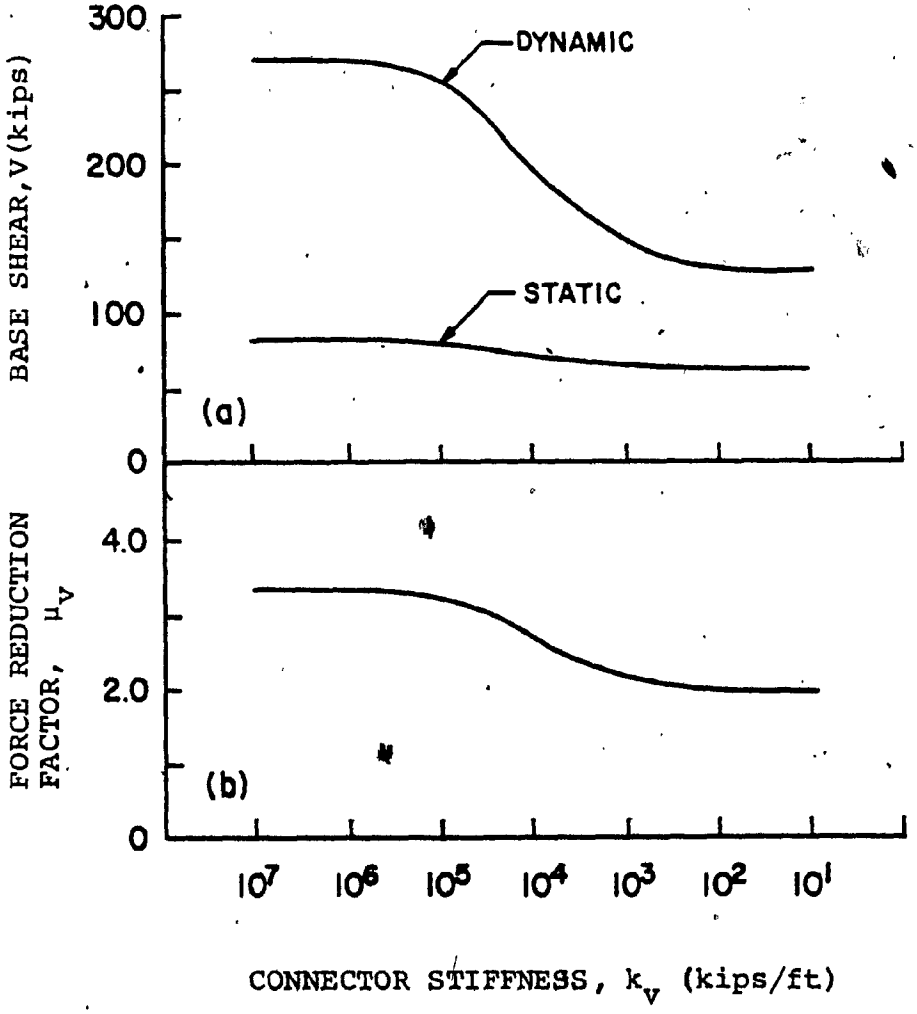

FIG. 5.35 COMPARISON OF BASE SHEARS FOR STATIC AND DYNAMIC ANALYSES (NBCC-1977) AND FORCE REDUCTION FACTOR μ_v (1 kips/ft = 14.6 kN/m, 1 kip = 4.45 kN)

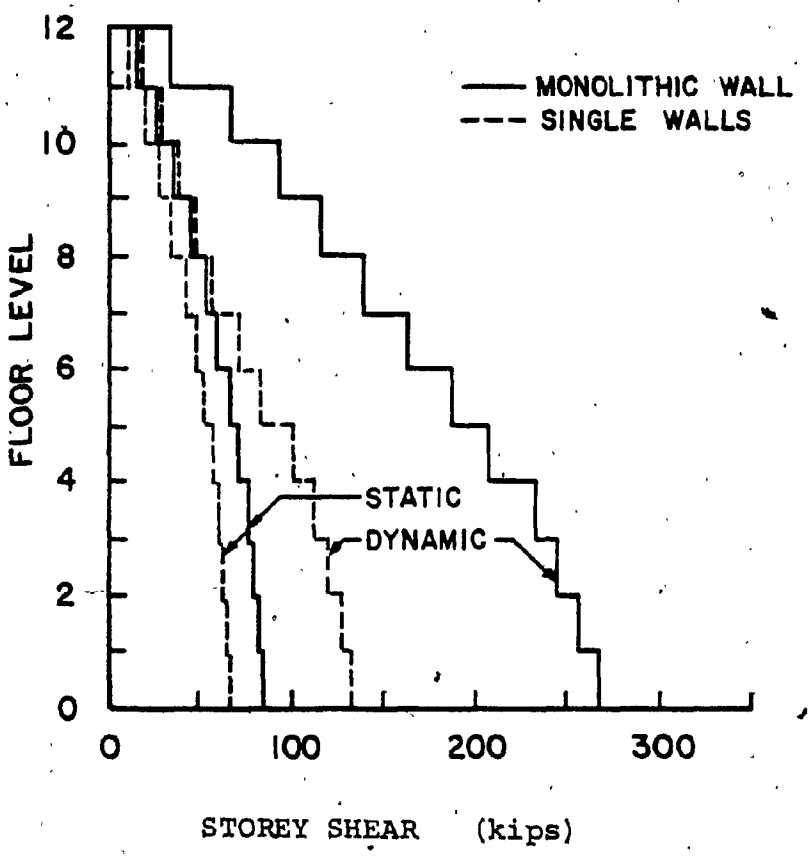

FIG. 5.36 COMPARISON OF HORIZONTAL STOREY SHEARS FOR STATIC AND DYNAMIC ANALYSES (NBCC-1977), (1 kip = 4.45 kN)

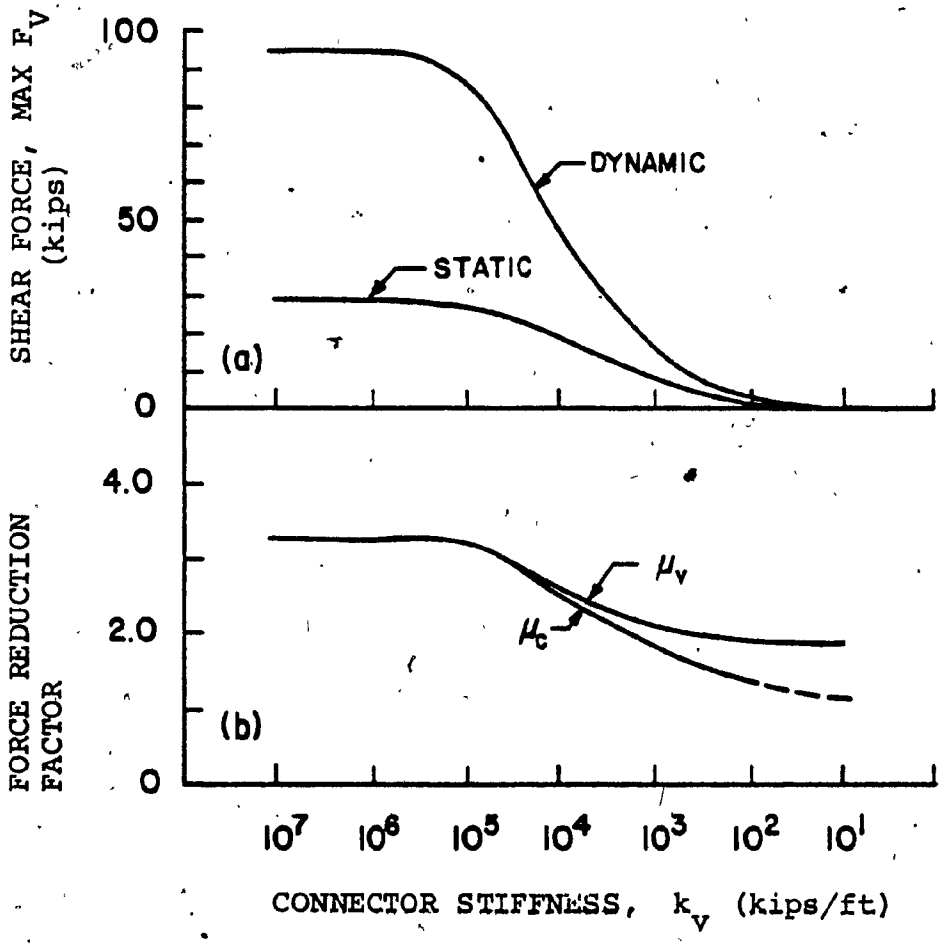

FIG. 5.37 COMPARISON OF MAXIMUM CONNECTOR SHEAR FORCES FOR STATIC AND DYNAMIC ANALYSES (NBCC-1977) AND ASSOCIATED FORCE REDUCTION FACTORS (1 kip/ft = 14.6 kN/m, 1 kip = 4.45 kN)

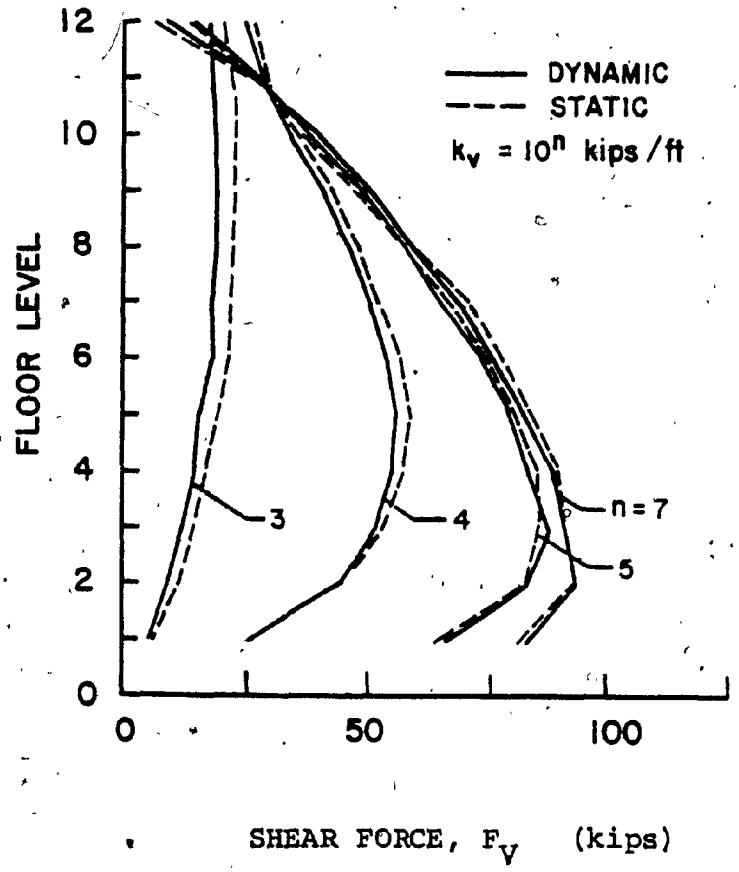

FIG. 5.38 COMPARISON OF CONNECTOR SHEAR FORCE DISTRIBUTIONS FOR DYNAMIC AND NORMALIZED STATIC ANALYSES (1 kip = 4.45 kN)

CHAPTER VI

SUMMARY AND CONCLUDING REMARKS

CHAPTER VI

SUMMARY AND CONCLUDING REMARKS

A substructuring technique based on the finite element method has been developed. This technique results in the creation of a rectangular panel element which may be applied efficiently in linear dynamic analysis, particularly for structural shear wall problems involving large-panel construction. The procedure is formulated in terms of a computer subroutine and the present version may be directly attached to SAP4 [24] as a substructure option.

A review of general theory and various methods applied in dynamic substructuring forms the basis for the present development. The procedure of this study utilizes multilevel substructuring and employs a sequence of static condensations leaving only chosen boundary nodes. Suitable numerical algorithms are investigated and a growth scheme is developed which allows versatile boundary node arrangement as well as simple input instructions. Possible extensions and refinement for the scheme are also discussed. The following panel element matrices, relating to retained boundary nodes can be created:

(1) stiffness matrix ,

(2) mass matrix, which may be consistent or, optionally, diagonally lumped and generated through consistent lumping,

(3) stress-displacement matrix which relates boundary degrees of freedom to evenly distributed stress points inside the substructure, thus allowing full stress recovery.

Several applications demonstrate the efficient and versatile applicability of the panel element and indicate also expected savings in computing time. The main focus, however, is on solution accuracy for different characteristics and corresponding representation of mass. For plate bending vibrations it is shown that homogeneous inertia properties must be expressed by a consistent substructure mass matrix, in order to model accurately the dynamic properties. However, if concentrated masses are present, a lumped substructure mass matrix is found to provide sufficiently accurate results. This situation is investigated for a 5-storey shear wall where floor mass intensity is varied. Full stress recovery within the substructure (for static loading) is also presented.

The parametric investigation of a 12-storey precast panel structure with discrete connectors along the vertical joints presents an additional and detailed application. Response spectrum analyses for seismic loading, following a parametric scheme, are carried out. Uniform as well as changing stiffness properties along the height are considered and response is evaluated primarily in terms of connector forces. Results which demonstrate the expected magnitudes of response as functions of connector properties, together with estimated ductility requirements, are summarized in Section 5.5. The necessity of a non linear analysis in further investigations as well as the required basic steps is outlined in Section 5.4.7.

For future studies it is recommended to include slip in connections as well as closing and opening of joints in the non linear joint behaviour. It is also suggested to extend the analysis to include different horizontal joint characteristics.

Other aspects concerning layout or geometry of the structure should be considered; namely, introduction of panel heights over two or more storeys, as well as variation of connector locations.

Whereas the present study is limited to a single

12-storey panel wall, future studies should include linked wall assemblies [70], where several panel walls are separated by openings and linked by beams or floor slabs. In addition, structural models should be extended to buildings of 20 and possibly more storeys.

REFERENCES

REFERENCES

[1] Zienkiewicz, O.C., The Finite Element Method in Engineering Science, McGraw-Hill, London, 1971.

[2] Gallagher, R.H., Finite Element Analysis Fundamentals, Prentice-Hall, Inc., Englewood Cliffs, New Jersey, 1975.

[3] Strang, G. and Fix, G.J., An Analysis of the Finite Element Method, Prentice-Hall, Inc., Englewood Cliffs, New Jersey, 1973.

[4] Rubinstein, M.F., Matrix Computer Analysis of Structures, Prentice-Hall, Inc., Englewood Cliffs, New Jersey, 1966.

[5] Jenkins, W.M., Matrix and Digital Computer Methods in Structural Analysis, McGraw-Hill, London, 1969.

[6] Przemieniecki, J.S., Theory of Matrix Structural Analysis, McGraw-Hill Book Company, New York, 1968.

[7] Egeland, O., and Araldsen, P.O., "SESAM-69 A General Purpose Finite Element Method Program", Computers and Structures, Vol.4, No.1, Jan. 1974, pp.41-68.

[8] Utku, S., "Systematic Substructuring", Journal of the Structural Division, ASCE, Vol.101, No. ST4, Proc. Paper 11244, April 1975, pp.717-730.

[9] Petersson, H., and Popov, E.P., "Substructuring and Equation System Solutions in Finite Element Analysis", International Journal of Computers and Structures, Vol.7, No.2, 1977, pp.197-206.

[10] Le, D.Q., Petersson, H. and Popov, E.P., "SUBWALL - A Special Purpose Finite Element Computer Program for Practical Elastic Analysis and Design of Structural Walls With Substructure Option", Report UCB/EERC-77/09, College of Engineering, University of California, Berkeley, Mar. 1977.

[11] Guyan, R.J., "Reduction of Stiffness and Mass Matrices", Journal of the American Institute of Aeronautics and Astronautics, Vol.3, No.2, Feb.1965, p.380.

[12] Archer, J.S., "Consistent Mass Matrix for Distributed Systems," Journal of the Structural Division, ASCE, Vol.3, No.ST4, Proc. Paper 3591, Aug.1963, pp.161-178.

[13] Dym, C.L., Shames, I.H., Solid Mechanics: A Variational Approach, McGraw-Hill Book Company, New York,N.Y., 1973.

[14] Goodno, B.J., "Dynamic Analysis of Suspended-Floor Highrise Buildings Using Super-Elements," Ph.D.Thesis. Presented to Stanford University, Stanford, California, 1974.

[15] Goodno, B.J., Gere, J.M., "Analysis of Shear Cores Using Superelements". Journal of the Structural Division, ASCE, Vol.102, No.ST1, Proc.Paper 11837, Jan. 1976, pp.267-283.

[16] Hurty, W.C., "Vibrations of Structural Systems By Component Mode Synthesis," Journal of the Mechanical Division, ASCE, Vol.86, No.EM4, Proc.Paper 2572, Aug.1960, pp.51-69.

[17] Hurty, W.C., "Dynamic Analysis of Structural Systems Using Component Modes," Journal of the American Institute of Aeronautics and Astronautics, Vol.3, No.4, April 1965, pp.678-685.

[18] Hou, S., "Review of Modal Synthesis Techniques and a New Approach," Shock and Vibration Bulletin, Vol.40, No.4, 1969.

[19] Holze, G.H., and Boresi, A.P., "Free Vibration Analysis Using Substructuring". Journal of the Structural Division, ASCE, Vol. 101, ST12, Proc.Paper 11788, Dec.1975, pp.2627-2639.

[20] Barber, R.B., and Blotter, P.T., "Component Mode Analysis of Frames With Shear Walls". International Journal of Computers and Structures, Vol.6, Nos.4/5, 1976, pp.397-403.

[21] Bathe, K.J., "Solution Methods of Large Generalized Eigenvalue Problems in Structural Engineering," Report UC SESM 71-20, Civil Engg., Dept., University of California, Berkeley, Nov.1971.

[22] Bathe, K.J. and Wilson, E.L., "Large Eigenvalue Problems in Dynamic Analysis", Journal of the Mechanical Division, ASCE, Vol.98, No.EM6, Proc. Paper 9433, Dec. 1972, pp.1471-1485.

[23] Warburton,G.B., The Dynamical Behaviour of Structures, Pergamon Press, Oxford, 1976.

[24] Bathe,K.J., Wilson, E.L., and Peterson,F.E., "SAPIV-A Structural Analysis Program For Static and Dynamic Response of Linear Systems," Report No.EERC 73-11, University of California, Berkeley, California. (Revised April 1974).

[25] Clough, R.W., Analysis of Structural Vibrations and Dynamic Response. Recent Advances in Matrix Methods of Structural Analysis and Design. (R.H. Gallagher, Y. Yamada, and J.T.Oden, eds.) University of Alabama Press, Huntsville, Alabama, 1971.

[26] Clough, R.W. and Bathe, K.J., Finite Element Analysis of Dynamic Response, Advances in Computational Methods in Structural Mechanics and Design, (Oden,J.T., Clough, R.W., and Yamamato, Y., eds.), University of Alabama Press, Huntsville, Alabama, 1972.

[27] Clough, R.W., and Penzien, J., Dynamics of Structures, McGraw-Hill Book Company, New York, N.Y. 1975.

[28] Bathe, K.J., Wilson,E.L., Numerical Methods in Finite Element Analysis, Prentice-Hall, Inc., N.J., 1976.

[29] Martin,H.C., and Carey, G.F., Introduction to Finite Element Analysis, McGraw-Hill Book Company, New York, N.Y., 1973.

[30] Hildebrand, F.B., Methods of Applied Mathematics, Prentice-Hall, Inc., N.J., Second Edition, 1965.

[31] Kidder, R.L., "Reduction of Structural Frequency Equations," Journal of the American Institute of Aeronautics and Astronautics, Vol.11,No.6, June 1973, p.892.

[32] Gawronski, W., "Free Vibration Analysis Using Substructuring, by Holze, G.H. and Boresi, A.P.," Discussion, Journal of the Structural Division, ASCE, Vol.102, No. ST11, Proc. Paper 12510, Nov.1976, p.2247.

[33] Hurty, W.C., "Introduction to Modal Synthesis Techniques," Synthesis of Vibrating Systems, The Winter Annual Meeting of the ASME, Washington,D.C., Nov.1971, pp.1-13.

[34] Craig, R., and Bampton, M., "Coupling of Substructures for Dynamic Analysis," Journal of the American Institute of Aeronautics and Astronautics, Vol.6, No.7, July 1968, pp.1313-1319.

[35] Benfield, W.A., and Hruda, R.F., "Vibration Analysis of Structures by Component Mode Substitution", Journal of the American Institute of Aeronautics and Astronautics, Vol.9,No.7, July 1971, pp.1255-1261.

[36] Johnson, E.S., and Hurty, W.C., "Convergence in Modal Synthesis," Journal of the Mechanical Division, ASCE, Vol. 98, No.EM5, Proc.Paper 9281, Oct.1972,pp.1105-1114.

[37] Wilson,E.L., "The Static Condensation Algorithm," International Journal for Numerical Methods in Engineering, Vol.8, No.1, 1974, pp.199-203.

[38] Irons, B.M., "Structural Eigenvalue Problems: Elimination of Unwanted Variables," Journal of the American Institute of Aeronautics and Astronautics, Vol.3, No.5, May 1965, pp.961-962.

[39] Irons, B.M., "A Frontal Solution Program for Finite Element Analysis," International Journal for Numerical Methods in Engineering, Vol.2, No.1, 1970, pp.5-32.

[40] Wilkinson, J.H., The Algebraic Eigenvalue Problem, Oxford Univ. Press, 1965.

[41] Barton, M.V., "Vibration of Rectangular and Skew Cantilever Plates," Journal of Applied Mechanics, Vol.18, June 1951, pp.129-134.

[42] Hinton, E., Rock,T., and Zienkiewicz, O.C., "A Note on Mass Lumping and Related Processes in the Finite Element Method," International Journal of Earthquake Engineering and Structural Dynamics, Vol.4, No.3, Jan.-Mar.1976, pp.245-249.

[43] Leissa, A.W., "Vibration of Plates," NASA Report, SP-160, Washington, D.C., 1969.

[44] Girijavallabhan, C.V., "Analysis of Shear Walls With Openings," Journal of the Structural Division, ASCE, Vol.95, No.ST10, Proc.Paper 6824, Oct.1969,pp.2093-2103.

[45] Lewicki, B., Building With Large Prefabricates, Elsevier Publishing Company, New York, N.Y., 1966.

[46] "Recommandations internationales unifiées pour le calcul et l'exécution des constructions en panneaux assemblés de grand format." C.E.B.Information Bulletin No.60, Paris, France, (Cement and Concrete Association - Translation No.137), April 1967.

[47] Hartland, R.A., Design of Precast Concrete, John Wiley and Sons, New York, N.Y., 1975.

[48] Lewicki, B., and Pauw, A., "Joints, Precast Panel Buildings," TC 21, SOA 2, Proceedings of the International Conference on Planning and Design of Tall Buildings, Lehigh Univ., Bethlehem, Pa., Vol.3, Aug.1972, pp.171-189.

[49] Cholewicki, A., "Loadbearing Capacity and Deformability of Vertical Joints in Structural Walls of Large Panel Buildings," International Journal of Building Science, Vol.6, No.4, 1971, pp.163-184.

[50] Olesen, S.O., "Effects of Vertical Keyed Shear Joints on the Design of Reinforced Concrete Shear Walls," American Concrete Institute, Publication SP-48, Industrialization in Concrete Building Construction, 1975, pp.85-110.

[51] Shemie, M., "Mechanical Joints in System Buildings Using Large Concrete Panels," M.Eng.thesis submitted to Sir George Williams University, Montreal, March, 1971.

[52] Shemie, M., "Bolted Connections in Large Panel System Buildings," Journal of the Prestressed Concrete Institute, Vol.18, No.1, Jan./Feb.1973, pp.27-33.

[53] Rosman, R., "Approximate Analysis of Shear Walls Subject to Lateral Loadings," Journal of the American Concrete Institute, Vol.61,No.6, June 1964, pp.717-733.

[54] Tso, W.K., and Chan, H.B., "Dynamic Analysis of Plane Coupled Shear Walls," Journal of the Engineering Mechanics Division,ASCE,Vol.97, No.EM1, Proc.Paper 7899, Feb.1971, pp.33-48.

[55] Tso, W.K., and Biswas, J.K., "An Approximate Seismic Analysis of Coupled Shear Walls," International Journal of Building Science, Vol.7, 1972, pp.249-256.

[56] Jennings, P.C., and Skattum,K.S., "Dynamic Properties of Planar, Coupled Shear Walls," International Journal of Earthquake Engineering and Structural Dynamics, Vol.1,No.4,Apr-June 1973,pp.387-405.

[57] Tso,W.K., and Rutenberg, A., "Seismic Spectral Response Analysis of Coupled Shear Walls," Journal of the Structural Division, ASCE, Vol.103,No.ST1, Proc. Paper 12671, Jan.1977, pp.181-197.

[58] Paulay, T., "Design Aspects of Shear Walls for Seismic Areas," Canadian Journal of Civil Engineering, Vol.2,No.3, Sept.1975, pp.321-344.

[59] MacLeod, I.A., "Structural Analysis of Wall Systems," The Structural Engineer, Vol.55, No.11, Nov.1977, pp.487-495.

[60] Stafford-Smith, B., and Lau, P.C.M., "A Method of Assessing the Static Stability of Panel Type Buildings," Proceedings of the Institution of Civil Engineers, Vol.53, Paper 7507, June 1972, pp.77-86.

[61] Burnett, E.F.P., and Rejendra, R.C.S., "Influence of Joints in Panelized Structural Systems," Journal of the Structural Division, ASCE, Vol.98, No.ST9, Proc. Paper 9207,Sept.1972,pp.1943-1955.

[62] Stafford-Smith, B., and Rahman, K.J.K., "A Theoretical Study of the Sequence of Failures on Precast Panel Walls," Proceedings of the Institution of Civil Engineers, Vol.55, Paper 7620, Sept.1973,pp.581-592.

[63] Pollner, E., Tso, W.K., and Heidelbrecht, A.C., "Analysis of Shear Walls in Large-Panel Construction," Canadian Journal of Civil Engineering, Vol.2, No.3, Sept.1975, pp.357-367.

[64] Frank, A. R., Becker, J. M., Biggs, J. M., "Dynamic Modeling of Large Precast Panel Buildings Using Finite Elements with Substructuring". Seismic Resistance of Precast Concrete Panel Buildings, Report No. 2. Publication No. R76-36, Department of Civil Engineering, MIT, Cambridge, Massachusetts, Aug. 1976.

[74] Stanley, P., Computing Developments in Experimental and Numerical Stress Analysis, Applied Science Publishers, London, 1976.

[75] Tillerson, J.R., Stricklin, J.A., and Haisler, W.E., "Numerical Methods for the Solution of Nonlinear Problems in Structural Analysis," Numerical Solution of Nonlinear Structural Problems, The Winter Annual Meeting of the ASME, Detroit, Michigan, Nov. 1973.

[76] Kanaan, A.E., and Powell, G.H., "DRAIN-2D, A General Purpose Computer Program For Dynamic Analysis of Inelastic Plane Structures." Report No. EERC 73-6 and EERC 73-22, Univ. of California, Berkeley, Ca., April 1973.

NOTATION

NOTATION

All symbols are defined in the text. In addition, those used most frequently are listed below, which may include alternative definitions for the same symbol. Notation which relates to input parameters for the computer program are defined in Appendix C.

$\{a\}$	eigenvector in Ritz solution
$[C]$	damping matrix
$[\bar{C}]$	reduced damping matrix
c_i	Ritz coordinates
D	top deflection (RSS)
D_M	top deflection (RSS) for monolithic shear wall
E	modulus of elasticity
F_a	connector axial force (RSS)
F_{ai}	connector axial force for $i^{\underline{th}}$ mode
F_v	connector shear force (RSS)
F_{vi}	connector shear force for $i^{\underline{th}}$ mode
F_R	maximum connector shear force (RSS) for rigid connectors
$\{g\}$	subvector in $[K]$
$\{h\}$	subvector in $[M]$
$[I]$	unity matrix
i	index
j	index

$[K]$	stiffness matrix
$[K_{IJ}]$	submatrix of $[K]$
$[K_o]$	stiffness matrix at zero level
$[\bar{K}]$	reduced stiffness matrix
$[\bar{K}_{IJ}]$	submatrix of $[\bar{K}]$
$[K_i]$	$i^{\underline{th}}$ reduced stiffness matrix
$[K]_c$	connector stiffness matrix
k_{ij}	element of $[K]$
$\bar{k}_{ij}$	element of $[\bar{K}]$
k_a	connector axial stiffness
k_v	connector shear stiffness
$[\tilde{L}]$	Cholesky decomposition of $[K]$
$[M]$	mass matrix
$[M]$	diagonal mass matrix
$[M_{IJ}]$	submatrix of $[M]$
$[M_o]$	mass matrix at zero level
$[\bar{M}]$	reduced mass mass matrix
$[\bar{M}_{IJ}]$	submatrix of $[\bar{M}]$
$[\bar{M}_i]$	$i^{\underline{th}}$ reduced mass matrix
M	base overturning moment (RSS); subscript for monolithic shear wall
M_M	base overturning moment (RSS) for monolithic shear wall
M_i	base overturning moment for $i^{\underline{th}}$ mode
m	stiffness multiple
m_{ij}	element in $[M]$

$\bar{m}_{ij}$	element in $[\bar{M}]$
n	order of unreduced system
OB	operation count in block elimination
OS	operation count in step elimination
$\{P\}$	force vector; elastic force response (RSS)
$\{P\}_i$	elastic force response for ith mode
$\{P\}_{ix}$	elastic force response for ith mode, lateral components
$\{P_o\}$	force vector at zero level
$\{\bar{P}\}$	reduced force vector
$\{\bar{P}_i\}$	$i^{\underline{th}}$ reduced force vector
P_i	element in $\{P\}$
$\bar{P}_i$	element in $\{\bar{P}\}$
q	order of reduced eigenvalue problem in Ritz analysis
$[R]$	used in block elimination $[\tilde{L}][R] = [K_{12}]$
RSS	root sum of squares of modal contributions
r	number of degrees of freedom to be eliminated
$[S]$	stress-displacement matrix
$[S_o]$	stress-displacement matrix at zero level
$[\bar{S}_i]$	$i^{\underline{th}}$ reduced stress-displacement matrix
S_a	acceleration response spectrum
S_d	displacement response spectrum
$[T]$	transformation matrix used for static condensation
$[T(\omega)]$	$[T]$ as function of ω
$[T']$	transformation matrix used for component mode synthesis

$[T_I]$	submatrix of $[T']$
$[T_i]$	transformation matrix derived from $[\bar{K}_i]$
T	natural period of vibration; indicates transpose of a matrix
T_M	natural period of vibration for monolithic shear wall
$\{u\}$	displacement vector; displacement response (RSS)
$\{u\}_i$	displacement vector for $i^{\underline{th}}$ mode
$\{v\}$	solution shapes in Ritz analysis
V	base shear (RSS)
V_M	base shear (RSS) for monolithic shear wall
V_i	base shear for $i^{\underline{th}}$ mode
$\{w\}$	subvector of $[S]$
$\{X\}$	displacement vector
$\{X_I\}$	subvector of $\{X\}$
$\{\bar{X}\}$	reduced displacement vector
$\{\bar{X}_i\}$	$i^{\underline{th}}$ reduced displacement vector
$[Y]$	used in block elimination $[\tilde{L}]^T[Y] = [R]$.
$\{y\}$	displacement vector for reduced equation of motion
z	used in operation count $z = r/n$
γ	modal participation factor
γ_M	modal participation factor for monolithic shear wall
γ_i	modal participation factor for $i^{\underline{th}}$ mode

δ	relative vertical joint displacement (RSS)
δ_s	relative joint displacement (RSS) for single walls
ε	measure for accuracy of frequencies and mode shapes
η_i	vertical coordinate for stress point i
μ_v	force reduction factor for horizontal storey shear and base shear
μ_c	force reduction factor for connector shear force
ν	Poisson's ratio
ξ_i	horizontal coordinate for stress point i
ρ	Rayleigh's quotient; mass density
$\{\sigma\}$	stress vector
$\{\sigma_i\}$	stress vector for $i^{\underline{th}}$ level
$\sigma_x, \sigma_y, \sigma_{xy}$	stresses in plane stress analysis
$\{\phi\}$	mode shape vector
$\{\phi_I\}$	mode shape vector associated with internal degrees of freedom
$\{\phi\}_i$	$i^{\underline{th}}$ mode shape vector
$\{\psi\}_i$	$i^{\underline{th}}$ assumed Ritz shape
ω	natural frequency
ω_i	$i^{\underline{th}}$ natural frequency

APPENDIX A

APPENDIX A

OPERATION COUNT AND STORAGE REQUIREMENTS FOR BLOCK AND STEP ELIMINATION

The conditions under which the operation count is performed are described in Section 3.2.3. Since symmetric matrices are involved, operations take place only in the upper triangle. Operation counts and storage requirements are presented separately for block and step elimination.

A1.1 BLOCK ELIMINATION

Block elimination consists of a series of matrix operations resulting in the following equations of Section 3.2.1:

$$[\bar{K}] = [K_{11}] - [R]^T[R] \qquad (3.4)$$

$$[\bar{M}] = [M_{11}] - [M_{12}][Y] -$$

$$- [Y]^T([M_{21}] - [M_{22}][Y]) \qquad (3.6)$$

The two equations, evaluated in Table A.1, on page 237 lead to a total number of operations given by

$$OB = \frac{3}{2} n^2 - nr^2 - \frac{1}{3} r^3 + \text{terms of lower order} \qquad (3.11)$$

and is obtained from summation of column 3. Corresponding storage requirements listed in Column 4 are $(n^2 + r(n-r))$.

A1.2 STEP ELIMINATION

The equations for one step elimination, derived in Section 3.2.2, are:

$$[\bar{K}] = [K_{11}] - \frac{1}{k_{nn}} \{g\}\{g\}^T \qquad (3.9)$$

and

$$[\bar{M}] = [M_{11}] - \frac{1}{k_{nn}} \{h\}\{g\}^T - \frac{1}{k_{nn}} \{g\}\{h\}^T + \frac{m_{nn}}{k_{nn}^2} \{g\}\{g\}^T \qquad (3.10)$$

An operation count for stiffness matrix [K] reduced during r steps is performed as follows:

Step	Operation Count
1^{st}	$\frac{(n-1)n}{2} \approx \frac{n^2}{2}$
2^{nd}	$\frac{(n-2)(n-1)}{2} \approx \frac{(n-1)^2}{2}$
$\vdots$	$\vdots$ $\quad$ $\vdots$
r^{th}	$\frac{(n-r)n-r+1)}{2} \approx \frac{(n-r+1)^2}{2}$
TOTAL	$N \approx \frac{1}{2} \sum_{i=n-r+1}^{n} i^2$

or

$$N = \frac{1}{2} \sum_{1}^{n} i^2 - \frac{1}{2} \sum_{1}^{n-r} i^2 \qquad (A.1)$$

An evaluation of the series leads to

$$N = \frac{1}{12} (n(n+1)(2n+1)) - \frac{1}{12}(s(s+1)(2s+1)) \qquad (A.2)$$

with

$$s = n-r$$

and

$$N = \frac{1}{2} n^2 r - \frac{1}{2} nr^2 + \frac{1}{6} r^3 + \text{terms of lower order} \qquad (A.3)$$

It can be seen from Eq. (3.10) that the same number of operations is required three more times for the reduction of the mass matrix giving a total

$$OS = 4N$$

or

$$OS = 2n^2 r - 2nr^2 + \frac{2}{3} r^3 + \text{terms of lower order} \qquad (3.12)$$

Considering storage requirements, it is obvious that only [K] and [M] need to be kept in core, leading to a total of approximately n^2 storage locations.

TABLE A.1 OPERATION COUNT AND STORAGE REQUIREMENT FOR BLOCK ELIMINATIONS

Matrix Operation	Remarks	Operation Count	Storage Requirement
$[K_{22}] = [\tilde{L}][\tilde{L}]^T$		$\frac{r^3}{6}$	$[K],[\tilde{L}]$
$[\tilde{L}][R] = [K_{21}]$	FS* for $[R]$	$\frac{r(r-1)(n-r)}{2}$	$[K],[\tilde{L}]$
$[R]^T[R]$	Symmetric	$\frac{r(r-n)^2}{2}$	$[K]$
$[\tilde{L}]^T[Y] = [R]$	BS for $[Y]$	$\frac{r(r-1)(n-r)}{2}$	$[K]$
$[Z_1] = [M_{22}][Y]$		$r^2(n-r)$	$[K],[M],[Z_1]$
$[Z_2] = [M_{21}]-[Z_1]$			$[K],[M],[Z_2]$
$[Y^T][Z_2]$	Symmetric	$\frac{r(r-n)^2}{2}$	$[K],[M],[Z_2]$
$[M_{12}][Y]$	Symmetric	$\frac{r(n-r)^2}{2}$	$[K],[M]$
	TOTAL	OB	$\underbrace{[K],[M]}_{n^2},\underbrace{[Z_2]}_{+\,r(n-r)}$

* FS Forward substitution
BS Backward substitution

APPENDIX B

APPENDIX B

FLOWCHART FOR REDUCTION ALGORITHM USING STEP ELIMINATION

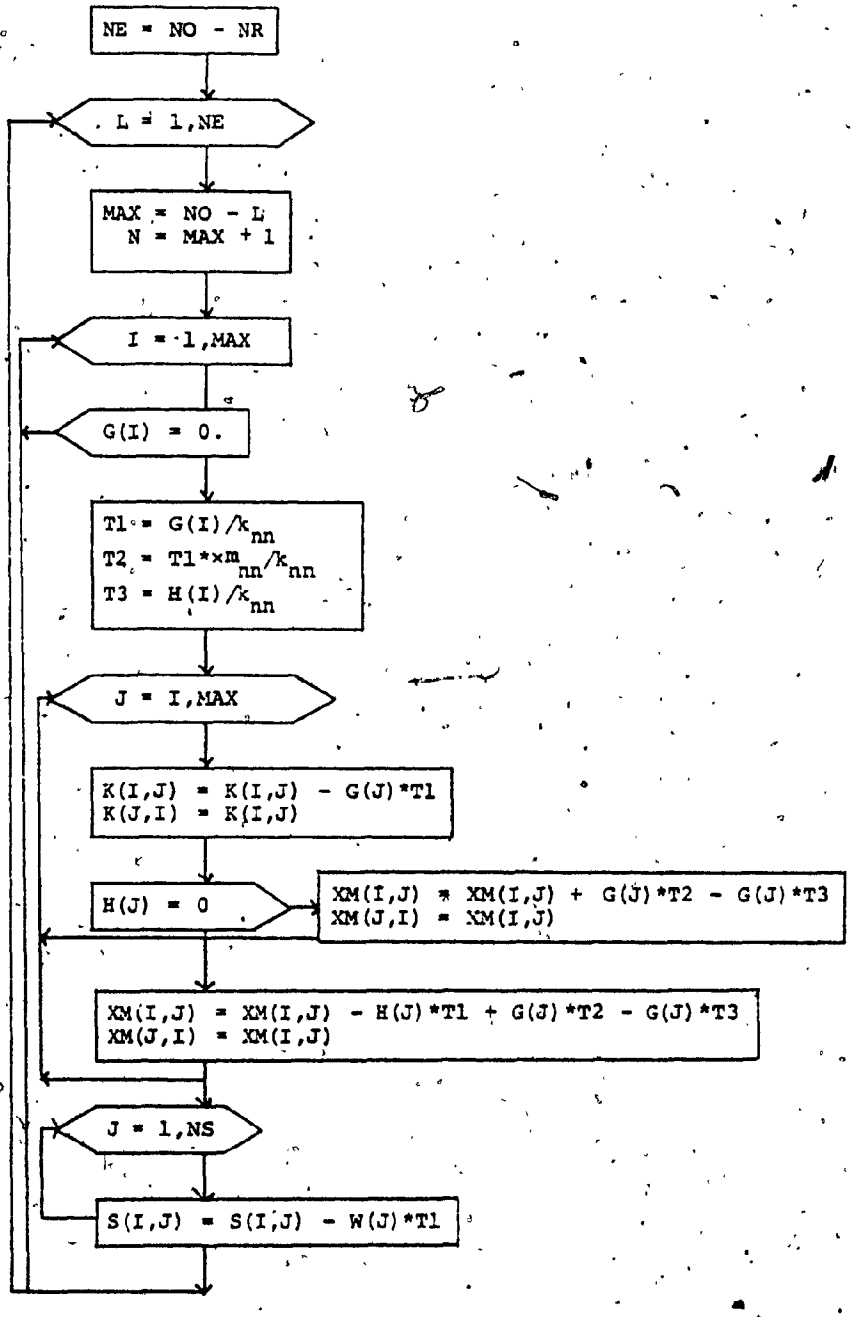

B1.1 SYMBOLS FOR VARIABLES AND MATRICES

NO	Order of original matrices
NR	Order of reduced matrices
K( )	Stiffness matrix
G( )	Subvector in stiffness matrix
k_{nn}	Last diagonal element in stiffness matrix
XM( )	Mass matrix
H( )	Subvector in mass matrix
xm_{nn}	Last diagonal element in mass matrix
S( )	Stress-displacement matrix
W( )	Sub-vector in stress-displacement matrix

B1.2 STORAGE SCHEME FOR MATRICES

The algorithm requires that degrees of freedom to be eliminated are labelled with the highest numbers in the numbering sequence.

APPENDIX C

APPENDIX C

INSTRUCTIONS FOR INPUT AND DESCRIPTION OF PROGRAM ARRANGEMENT TO CONFORM WITH SAP4

This Appendix contains a description as well as input instructions of additions to the structural analysis program SAP4 [24]. Some sections of this Appendix are to be inserted into the SAP4 manual at corresponding locations:

(1) Section C1.1, "Panel Element Description" corresponds to Section 4.9 in the SAP4 manual.

(2) Section C1.2, "Connector Element Description" corresponds to Section 4.10.

(3) Section C1.3, "Extension of Response Spectrum Analysis" is attached to Section 7.3.

(4) Section C2.1, "Input Instructions for Panel Element" is inserted as pages from IV.10.1 to IV.10.5.

(5) Section C2.2, "Input Instructions for Connector Element" is inserted as pages from IV.11.1 to IV.11.2.

(6) Section C2.3, "Additional Input Instructions for Response Spectrum Analysis" is to be inserted after item c. "spectrum data" on page VII.24.

Input examples as well as the overall program arrangement are presented in Sections C3.1 and C4.1, respectively.

C1.1 PANEL ELEMENT DESCRIPTION

A panel element is considered as a rectangular substructure with all interior nodes eliminated, leaving only boundary nodes.

The applied "four level" growth scheme demonstrated in Fig. 3.2 follows a single progression. Hence, the dimension in the horizontal direction (x-direction) remains constant, whereas expansion takes place in the vertical direction (in negative y-direction). The stepwise growth pattern can be visualized in three stages:

(1) Creation of the basic 4-node element (zero level).

(2) Creation of separate super element formations as shown in Fig. 3.2(a), namely end element, and level one and level two elements. These super elements can assume any of the formations demonstrated in Table 3.1 for single progression. Sequence of creation is indicated in Fig. 3.2(a) by the "growth direction".

(3) Coupling of the created super elements which leads to level three (Fig. 3.2(b)), or to level four (Fig. 3.2(c)) in an additional symmetric coupling.

A "consistent lumped" element mass matrix is derived from the full consistent mass matrix by distributing the total panel mass according to diagonal terms of the consistent mass matrix. A stress recovery throughout the panel element is pos-

sible by specifying stress point locations in the zero level element (see Fig. 3.9).

C1.2 CONNECTOR ELEMENT DESCRIPTION

The connector element model can be described as an idealized two-node spring element with 4 degrees of freedom and zero dimensions in space, as shown in Fig. 5.2. The connector element stiffness matrix is then formulated by specifying connector axial and shear stiffnesses.

Cl.3 EXTENSION OF RESPONSE SPECTRUM ANALYSIS

For an analysis of multistorey buildings, horizontal storey forces as well as base shears and base overturning moments, can be determined in an additional computation. Storey forces for the rth mode are herein expressed as

$$\{P\}_r = [M]\{\phi\}_r \gamma_r S_a$$

The mass assigned to an individual storey is summed from nodal masses of the corresponding nodal points prescribed during input phase. The modal base shear is computed from force vector $\{P\}_r$ as,

$$V_r = [1]\{P\}_{rx}$$

where [1] is a row vector of ones and $\{P\}_{rx}$ contains the lateral components of $\{P\}_r$. The modal base overturning moment is derived accordingly:

$$M_r = [x]\{P_r\}_x$$

where elements in row vector [x] specify the height of storey masses above ground.

It is noted that the present program version is limited to two-dimensional cases, where x- and y-directions are defined as horizontal and vertical, respectively.

C2.1 INPUT INSTRUCTIONS FOR PANEL ELEMENT

TYPE 10 - PANEL ELEMENT

A rectangular homogeneous panel element with interior nodes eliminated and optional boundary node arrangement is created. The element is developed in a one-dimensional growth fashion during a four-level elimination procedure (Fig. 3.2).

Additional instructions for input which has to precede that for panel elements are as follows:

(1) Coordinates of nodal points relating only to panel elements do not have to be specified (i.e., x = y = z = 0.0 for those points; see "NODAL POINT DATA" page III.1 in SAP4 manual). Boundary conditions of panel elements are defined in x-y plane.

(2) If zero level elements (basic 4-node elements) are created by SAP4, the following considerations are necessary: (a) Additional, fully constrained nodes (in y-z plane) have to be introduced in order to specify dimensions of those elements ("NODAL POINT DATA", page III.1); (b) Zero level element data have to precede directly panel element data. For element type and sequence of creation see NOTE (3), page 251.

1. Control Card (10 I5)

notes	columns	variable	entry
	5		Enter the number "9"
	6 - 10	NUME	Number of panel elements
	11 - 15	NUMAT	Number of different material property cards
(1)	16 - 20	IMAS	EQ. 2 for "consistent lumped" mass (EQ. 1 for consistent mass)
(2)	21 - 25	ND	Number of degrees of freedom per node
(3)	26 - 30	IS4	Number of different 4-node zero level elements created in SAP4

NOTES/

(1) Only a lumped mass model is accepted in SAP4 during assembly and solution. For IMAS = 1, Subroutine PANEL creates and prints a consistent panel element mass matrix; then exit follows.

(2) At present available for rectangular 4-node elements:

ND = 2	Plane stress elements are created by PANEL (IS4 = 0) or by SAP4 (IS4 ≠ 0).
ND = 3	Nonconforming plate bending elements are created by PANEL.

(3) At present, element "TYPE 4" for plane stress or plane strain can be created by SAP4 and retrieved by PANEL. The sequence of creation has to follow the sequence of created panel elements. Each group of identical panel elements require either one (with B1) or two (with B1 and B2) start elements. Hence, one or two zero level elements are to be defined according to the creation sequence of start elements (for definition of B1 and B2, see Section 3.b, Card 1, page 253). See also NOTE (2) on page 250.

2. Material Property Cards (I5,3F10.0,F15.0)

For each different set of properties one card is required; total = NUMAT.

notes	columns	variable	entry
	5	I	Number of property card
	6 - 15	E(I)	Young's modulus
	16 - 25	POI(I)	Poisson's ratio
	26 - 35	THI(I)	Panel thickness
	36 - 50	RO(I)	Mass density per unit volume

3. Panel Element Cards

a. nodal numbering (16I5,/,10I5,/,16I5,/,10I5)

notes	columns	variable	entry
	5	M	Number of panel element
	6 - 10	NNOD	Number of nodal points
	11 - 15	IE(1)	Nodal numbers, arranged
	16 - 20	IE(2)	counterclockwise (see
	⋮	⋮	Figs. 3.4 through 3.7)
		IE(NNOD)	
	cont'd		
(1)	in (15)	IGEN	Total number of identical panels; for nodal generation

NOTES/

(1) If IGEN ≠ 0, the next nodal numbering card is expected to give M,NNOD, with array IE(1), ... IE(NNOD) expressing the incremental differences of nodal points of two consecutive panel elements. The remaining (IGEN-2) nodal numbering cards need only M for input. For an identical panel element which is off sequence in the nodal generation, the nodal numbering has to be specified after which a new generation may follow, for which no further properties need be specified.

b. geometric properties

Card 1 (I2,I3,3I5,4F10.0,I5)

notes	columns	variable	entry
	2	IRPT	EQ.1; present panel element is identical to the previous one, no further input is necessary for this panel element EQ.2; same as above, in addition no stresses are computed EQ.0; default, normal continuation
	5	MATTYP	Material property card
	6 - 10	NON	Number of horizontal nodes
	11 - 15	NLV	Number of level one and level two elements
	16 - 20	NCOP4	Type of level four coupling (see Fig. 3.6); EQ.0. skips level four
	21 - 30	XL	Length of panel element in x-direction
	31 - 40	YL	Length of panel element in y-direction
	41 - 50	B1	Width of first start element
	51 - 60	B2	Width of second start element; if not required, B2 = 0
	61 - 65	NSPT	Number of stress points in basic 4-node element (at present only for static analysis)

Card 2 (16I5)

notes	columns	variable	entry
	5	LEV(1)	Type identifications for level one and level two elements, see Tables 3.2 and 3.3; total = NLV
	6 - 10	LEV(2)	
	:	:	
		LEV(NLV)	

Card 3 (16I5)

notes	columns	variable	entry
	5	NCOPL(1)	Types of coupling (level 3), see Figs. 3.4 and 3.5. If no coupling required, skip this card
	6 - 10	NCOPL(2)	
	:	:	
		NCOPL(NLV-1)	

c. location of stress points in basic 4-node element (I5,2F10.0)

One card is necessary for each stress point, total = NSPT. If NSPT = 0, skip this card.

notes	columns	variables	entry
	5	NPT	Number of stress point
	6 - 15	XSI(NPT)	Natural coordinates for stress points, see Fig. 3.9
	16 - 25	ETA(NPT)	

d. printing options

If not printing is required, leave one blank card.

notes	columns	variables	entry
	5	IPLOC	EQ.1; prints starting locations of dynamic arrays; otherwise EQ.0
	6 - 10	IPLSTOP	Same as IPLOC, but exit follows
	11 - 15	IPMAT	EQ.1; prints stiffness and mass matrix

C2.2 INPUT INSTRUCTIONS FOR CONNECTOR ELEMENT

TYPE 11 - CONNECTOR ELEMENT

A two-node connector or link element with two degrees of freedom per node - representing axial and shear deformations - is created.

1. Control Card (3I5)

notes	columns	variables	entry
	4 - 5		Enter number "10"
	6 - 10	NUME	Number of connector-elements
	11 - 15	NUMAT	Number of different material properties

2. Material Property Cards (I5,2F10.0)

For each different set of properties one card is required.

notes	columns	variables	entry
	5	MTY	Number of property card
	6 - 15	SA(MTY)	Axial stiffness
	16 - 25	SS(MTY)	Shear stiffness

3. Numbering and Orientation Card (7I5)

notes	columns	variables	entry
	5	MI	Number of element, not necessarily in numbering order
	6 - 10	NI	Node I
	11 - 15	NJ	Node J
	16 - 20	MTY	Number of property card
	21 - 25	IVH	Orientation IVH.EQ.1 for vertical joint IVH.EQ.2 for horizontal joint
	26 - 30	NS	Force components to be calculated NS.EQ.0 if no forces are to be calculated NS.EQ.2, axial and shear forces are calculated

(continued)

notes	columns	variables	entry
(1)	31 - 35	IGEN	Node generation IGEN.EQ.0, no generation, skip card number 4

4. Numbering Card for Node Generation (3I5)

notes	columns	variables	entry
	5	MI1	Last element in generation series
	6 - 10	NI1	Node NI of element MI1
	11 - 15	NJ1	Node NJ of element MI1

NOTES/

(1) If IGEN-NE.0 a numbering series for the next, elements (MI + IGEN), (MI + 2×IGEN) etc. is generated. Card No. 4 is necessary to indicate the last element of the series. The value (MI1-MI) has to be a multiple of IGEN. Nodal points NI and NJ are spaced at equal intervals.
For each new series to be created a new pair of cards 3 and 4 is necessary.

C2.3 ADDITIONAL INPUT INSTRUCTIONS FOR RESPONSE SPECTRUM ANALYSIS

These data which allow the computation of storey shears, base shear and overturning moment for multistorey structures are to be inserted after item c. "spectrum data." on page VII.24.

d. number of storeys and storey height (I5,F10.0)

notes	columns	variable	entry
	1 - 5	NSY	Total number of storeys
	6 - 15	SHT	Storey height

3. storey mass information (2I5)

For each storey one card is required (total = NSY), starting with the top storey.

notes	columns	variable	entry
(1)	1 - 5	ISY	Number of storey, in descending sequence from top (i.e., for top storey ISY = NSY)
	6 - 10	NJT	Number of nodal points assigned to the current storey. This includes nodes between floor levels. No nodes can be left out.

NOTES/

(1) The computational scheme of this Section requires that the global nodal numbering of the structure is in increasing order from bottom to top.

C3.1 INPUT EXAMPLES

```
INPUT EXAMPLE 1  - PANEL CANTILEVER (FIG.4.1A)
16    1    0    5    1
 1    1    1    1    1    1    1
 5    1    1    1    1    1    1    0    0    0    0    0    0    1
 6    1    1    0    0    0    1
16    1    1    0    0    0    1    0    0    0    0    0    0    1
 9    1    1    2    3
 1  30000.00        .30        .10 .000080733028
 1   16    1    2    3    4    5    6    7    8    9   10   11   12   13   14   15   16
 1    5    2    2  1.0000    2.0000      .2500
110  110
 2
 1    0    1
0
0
 0    1
INPUT EXAMPLE 2  - SHEAR WALL WITHOUT FLOOR MASSES (FIG.4.4D)
34    2    0   12    1    0
 1    1    1    1    1    1    1
 2    1    1    1    1    1    1    0    0    0    0    0    0    1
 5    1    1    1    1    1    1    0    0    0    0    0    0    1
 6    0    0    1    1    1    1
30    0    0    1    1    1    1    0    0    0    0    0    0    1
31    1    1    1    1    1    1         0.0       0.0       0.0
32    1    1    1    1    1    1         0.0       2.5       0.0
33    1    1    1    1    1    1         0.0       2.5       2.5
34    1    1    1    1    1    1         0.0       0.0       2.5
 4    1    1         2   00
 1                  .00481778
          576000.00 576000.00 576000.00        .20       .20       .20 240000.00
0
0
0
0
0
 1   31   32   33   34    1    0    0    0    0    0    0    .6667
 9    5    1    2    2    1
 1                      0.6667 .00481778
 1   10    1    2    3    4    5   10    9    8    7    6    5
 1    5    1    0   10.000    10.000      2.50
120
 0    0    0
 2   10    5    5    5    5    5    5    5    5    5    5
1
 3
1
 4
1
 5
1
10
0
 0    1
0
0
```

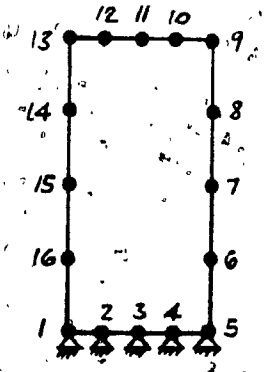

EXAMPLE 1

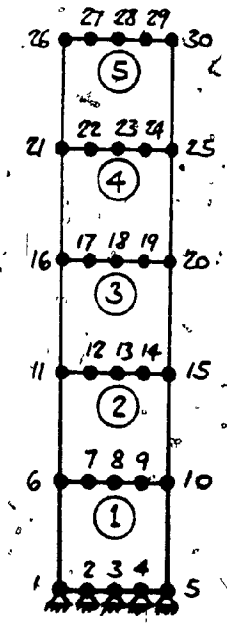

EXAMPLE 2

INPUT EXAMPLE 3 - 1-BAY 5-STOREY + MISSING PANEL + RIGID STOREY

```
 61    3    0    5    1
  1    1    1    1    1    1    1                                                  1
  9    1    1    1    1    1    1
 10    0    0    1    1    1    1
 54    0    0    1    1    1    1                                                  1
 55    1    1    1    1    1    1        0.        0.        0.
 56    1    1    1    1    1    1        0.        6.        0.
 57    1    1    1    1    1    1        0.        6.        3.
 58    1    1    1    1    1    1        0.        0.        3.
 59    1    1    1    1    1    1        0.       12.        0.
 60    1    1    1    1    1    1        0.       12.        4.
 61    1    1    1    1    1    1        0.        0.        4.
  4    4    1         2
  1                   0.004818
            576000.   576000.   576000.      0.17      0.17      0.17   246000.
```

```
  1   55   56   57   58    1                                                  1      0.6667
  2   55   56   57   58    1                                                  1      0.6667
  3   55   59   60   61    1                                                  1      0.6667
  4   55   56   57   58    1                                                  1      0.6667
  9    8    1    2    2    4
  1   576000.        0.17      0.6667   0.004818
  1    8    1    2    3    4    5    6    7    8
0 1    5    3    0         24.        12.         3.
  3  100  110
  1    1                   1
  1    0    1
  2    6   15   16   17   20   19   18
  1    5    2    1         24.        12.         3.
  3  100
  1
  1              1
  3    6   21   22   23   29   28   27
1
  5    6   43   44   45   51   50   49
1
  4    6   46   47   48   54   53   52
1
  7    6   24   25   26   32   31   30
1
  4   10   33   34   35   36   37   42   44   40   39   38
  1    5    2    0         24.        12.         4.
110  100
  1
  1              1
  8    7    5    6    7    8    9   14   13
  1    5    3    0         24.        12.         3.
  2  100  110
  1    1
  1              1
 10   23    2
  1     10000.    100000.          VERTICAL JOINTS
  2  10000000.  10000000.          HORIZONTAL JOINTS
  1   10   15    2    2    2    1
  3   12   17
  4   18   21    2    2    2    1
  6   20   23
  7   27   33    2    2    2    1
  9   29   35
 10   30   35    2    2    2    1
 12   32   37
 13   38   43    2    2    2    1
 15   40   45
 16   40   46    2    2    2    1
 18   42   48
 19   12   13    1    1    2
 20   23   24    1    1    2
 21   29   30    1    1    2
 22   45   44    1    1    2
 23   51   52    1    1    2
```

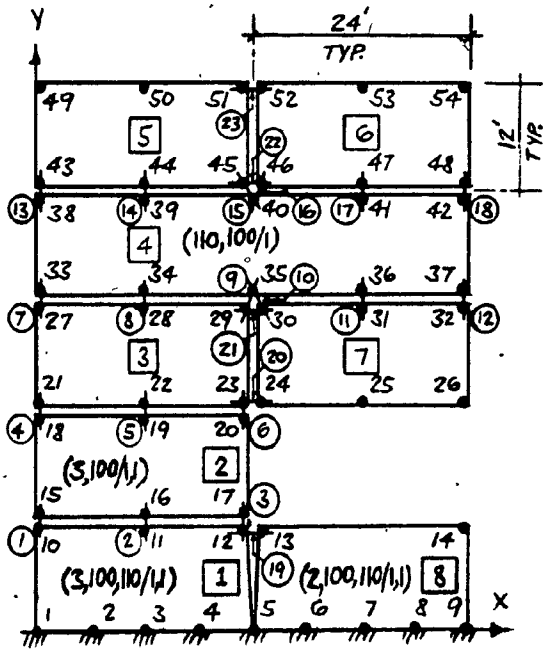

C4.1 OVERALL SCHEME OF CHANGES ON SAP4

Alterations to SAP4 which are described in this Appendix consist of (i) exchange of Subroutines, (ii) insertion of new Subroutines and (iii) modification on existing Subroutines. The following files were created for this purpose:

(1) ELM9, ELN9 and PANEL, relating to the panel element (where ELM9 and ELN9 replace ELMT9 and ELT9 in SAP4),

(2) ELM10, ELN10 and CONN, relating to the connector element (where ELM10 and ELN10 replace ELMT10 and ELT10 in SAP4),

(3) FORCES, relating to additions in response spectrum analysis, and

(4) MOS to perform modifications on existing SAP4 Subroutines.

The file manipulations necessary on SAP4 are indicated by the scheme on the two following pages. Listings of the files ELM9, ELN9 (containing the new files of ELMT9 and ELT9) as well as PANEL are given in Appendix D.

File Manipulations on SAP4

REC	NAME		
1	OVLZER		
2	SAPA	C	
3	INPUTJ		
4	ELTYPE		
5	TRUSS		
6	BEAM		
7	PLANE		
8	THREED		
9	SHELL		
10	BOUND		
11	SOL21		
12	ELMT9	ELM9 R	
13	ELMT10	ELM10 R	
14	ELMT11		
15	PIPE		
16	INL		
17	ERROR		
18	ADDSTF		
19	PRINTD		
20	STRESS		
21	CALBAN		
22	STRSC		
23	PRIST		
24	ST3D16		
25	OVL1		
26	ELT1		
27	RUSS		
28	OVL2		
29	ELT2		
30	TEAM		
31	NEWBM		
32	SLAVE		
33	OVL3		
34	ELT3A4		
35	PLNAX		
36	ELAW		
37	POSINV		
38	QUAD		
39	FORMB		
40	VECTOR		
41	CROSS		
42	DOT		
43	OVL4		
44	ELT5		
45	BRICKB		
46	DERIV		
47	LOAD		
48	LOSTR		
49	OVL5		
50	ELT6		
51	TPLATE		
52	STRETR		
53	CSTSTR		
54	LCT9ST		
55	GTSHEL		

REC	NAME			
56	QDCOS			
57	TDCOS			
58	TRFPRD			
59	SLST			
60	SLCCT			
61	LSTSTR			
62	LCTMOM			
63	OVL6			
64	ELT7			
65	CLAMP			
66	OVL7			
67	ELT8			
68	THOFE			
69	INP21			
70	CROSS2			
71	VECTR2			
72	SSLAW			
73	ST8R21			
74	FACEPR			
75	DER3DS			
76	FNCT			
77	OVL8			
78	ELT9	ELN9 R		
79	OVL9		PANEL & Assoc. SR's	A
80	ELT10	ELN10 R		
81	OVL10		CONN	A
82	ELT11			
83	OVL11			
84	ELT12			
85	PIPEK			
86	PIPES2			
87	PIPES3			
88	SELECT			
89	TANGBC			
90	BENDDC			
91	TANGKS			
92	PINVER			
93	BENDKS			
94	OVL12			
95	SOLEQ			
96	SESOL			
97	OVL13			
98	SOLEIG			
99	MODES			
100	SBLOCK			
101	SECNTD			
102	BANDET			
103	MULT			
104	SSPCEB			
105	DECOMP			
106	INVECT			
107	REDBAK			
108	EIGSOL			
109	JACOBI			
110	SCHECK			

File Manipulations on SAP4 (continued)

REC	NAME	
111	OVL14	
112	DYNRES	
113	HISTRY	
114	EMID	
115	LOAD1	
116	GMTN	
117	LOAD2	
118	RESPON	
119	DISPLR	
120	DISPLY	
121	ELOUTH	
122	PLOT	
123	STRSD1	
124	OVL15	
125	DYNSPE	
126	RESPEC	M
127	EMIDR	
128	SPECTR	M
129	SD	
130	STRESR	M
131	ELOUTR	FORCES A
132	OVL16	
133	SBSSOL	
134	STEP	
135	ADDMAS	
136	PLOAD	
137	EMIOS	
138	GROUND	
139	INDLY	
140	INTHIS	
141	LOADV	
142	INOUT	
143	SOLSTP	
144	TRIFAC	
145	REDVK	
146	SDSPLY	
147	SPLOT	
148	ELOUTS	
149	OPL	
150	* EOF *	

Symbols:

C ... Changes as indicated in Appendix D on page
R ... Replace indicated SAP4 Subroutines
A ... Insert indicated Subroutines
M ... Modifications as given in file MOS

APPENDIX D

FORTRAN LISTING OF SUBROUTINE PANEL

APPENDIX D

FORTRAN LISTING OF SUBROUTINE PANEL

The following Subroutine is an extension of the element library of the multipurpose program SAP4. A "panel element" is created applying the scheme as outlined in Chapter III.

Most of the important variables used are defined in Appendix C. For matrices and arrays the following symbols are employed:

S( )	stiffness matrices
B( )	mass matrices
F( )	stress-displacement matrices
LM( )	connectivity arrays

Subroutines to create element stiffness, mass and stress-displacement matrices on zero level are not included in this Listing (see SUBROUTINE ESTIF, ELMA and ESTRES).

The Overlay containing SUBROUTINE PANEL as well as SUBROUTINE ELM9 (on page 265) are to be inserted at indicated locations in SAP4. In addition, the following changes in the main program SAP4 are necessary:

(1) Addition of Tape 12 and Tape 13

(2) Extension of Common Block
/ELPAR/ by integer MTOTEM

(3) Specify, MTOTEM = 4045.

```
OVL8   1        OVERLAY (SSAP,10,0)


ELT9   1        PROGRAM ELT9
ELT9   2 C
ELT9   3 C   VARIABLE NODE SUPER FINITE ELEMENT OVERLAY
ELT9   4 C
ELT9   5        COMMON A(1)
ELT9   6        COMMON /CM/ AA(1)
ELT9   7        COMMON /ELPAR/ NPAR(14),NUMNP,MBAND,NELTYP,N1,N2,
ELT9   8       1               N3,N4,N5,MTOT,NEQ,MTOTEM
ELT9   9        COMMON /JUNK/ DUM(100),N6,N7,N8,N9,N10
ELT9  10 C
ELT9  11        CALL PANEL(AA(N1),AA(N2),AA(N3),AA(N4),AA(N5),AA(N6),
ELT9  12       1           AA(N7),AA(N8),AA(N9),NUMNP)
ELT9  13        RETURN
ELT9  14        END



PANE   1        SUBROUTINE PANEL(ID,X,Y,Z,T,E,POI,WT,THI,NUMNP)
PANE   2 C
PANE   3 C   SUBROUTINE TO CREATE A RECTANGULAR SUPER FINITE
PANE   4 C   ELEMENT WITH VARIABLE BOUNDARY NODE ARRANGEMENT
PANE   5 C   THIS SUBROUTINE IS COMPATIBLE WITH  " S A P 4 "
PANE   6 C
PANE   7 C                      PROGRAMMED BY H.P. HUTTELMAIER
PANE   8 C                      CONCORDIA UNIV   MONTREAL 1978
PANE   9 C
PANE  10        DIMENSION ID(NUMNP,1),X(1),Y(1),Z(1),T(1),E(1),POI(1)
PANE  11        DIMENSION WT(1),THI(1),LM(400),IE1(30),IE2(30)
PANE  12        DIMENSION XS(12,12),XP(12,4),XM(12),XSS(78)
PANE  13        COMMON A(1)
PANE  14        COMMON /ELPAR/ NPAR(14),NNNN,MBAND,NELTYP,N1,N2,N3,
PANE  15       1               N4,N5,MTOT,NEQ,MTOTEM
PANE  16        COMMON /JUNK/  LEV1(15),NCOPL(15),NLEV1(15),IE(30),
PANE  17       1               XSI(10),ETA(10)
PANE  18        COMMON /EXTRA/ MODEX
PANE  19        EQUIVALENCE(LM(13),XS(1,1)),(LM(159),XP(1,1))
PANE  20        EQUIVALENCE (LM(207),XM(1)),(LM(220),XSS(1))
PANE  21        NIAP=12
PANE  22        NUME=NPAR(2)
PANE  23        NUMAT=NPAR(3)
PANE  24        ND=NPAR(5)
PANE  25        IS4=NPAR(6)
PANE  26        NUMB=0
PANE  27        NCOUNT=10
PANE  28        WRITE(6,1006) NUME,NUMAT,NPAR(4),ND,IS4
PANE  29        IF(ND.EQ.3) GO TO 140
PANE  30        IF(MODEX.EQ.1) GO TO 140
PANE  31        IF(IS4.EQ.0) GO TO 140
PANE  32 C
PANE  33 C  GET BASIC ELEMENT FROM TAPE 7  (ELEMENT LIBRARY OF SAP4)
PANE  34 C  AND WRITE ON TAPE 13
PANE  35 C
PANE  36        REWIND 2
PANE  37        REWIND 13
PANE  38        DO 8 INX=1,IS4
PANE  39        READ(2) LRX,NDX,(LM(I),I=1,NDX),((XS(I,J),J=1,NDX),
PANE  40       1     I=1,NDX),((XP(I,J),I=1,NDX),J=1,4),(XM(I),I=1,NDX)
PANE  41 C
PANE  42 C   REARRANGE PLANE STRESS ELEMENT  (ELT4)
PANE  43 C
PANE  44        II=0
PANE  45        DO 3 I=1,7,2
PANE  46        II=II+1
PANE  47        LM(I)=II
PANE  48      3 LM(I+1)=II+6
PANE  49        DO 7 I=1,NDX
PANE  50        DO 7 J=I,NDX
PANE  51        II=LM(I)
PANE  52        JJ=LM(J)
PANE  53      5 IF(II.LE.JJ) GO TO 102
PANE  54        II=LM(J)
PANE  55        JJ=LM(I)
PANE  56    102 CONTINUE
PANE  57        IX=(J-1)*J/2+I
PANE  58      7 XSS(IX)=XS(II,JJ)
PANE  59        LRX=(NDX+1)*NDX/2
PANE  60        WRITE(13) LRX,(XSS(I),I=1,LRX)
PANE  61      8 CONTINUE
PANE  62        REWIND 13
PANE  63    140 CONTINUE
PANE  64        DO 10 I=1,NUMAT
PANE  65        READ(5,1001) NI,E(NI),POI(NI),THI(NI),WT(NI)
PANE  66        WRITE(6,1007)
PANE  67     10 WRITE(6,1011)NI,E(NI),POI(NI),THI(NI),WT(NI)
PANE  68    130 REWIND NTAP
PANE  69        IMAS=NPAR(4)
PANE  70        NUMB=NUMB+1
PANE  71        READ(5,1002) N,NNOD,(IF(I),I=1,NNOD),IGEN
PANE  72 C
PANE  73 C   CHECK IF NODE GENERATION REQUIRED
PANE  74 C
PANE  75        IF(IGEN.NE.0) GO TO 50
PANE  76        GO TO 52
PANE  77     50 NCOUNT=NUMB+IGEN-1
PANE  78        NNOD1=NNOD
PANE  79        NUMB1=NUMB+1
PANE  80        DO 31 I=1,NNOD1
PANE  81     31 IE1(I)=IE(I)
PANE  82        GO TO 70
PANE  83     52 CONTINUE
PANE  84        IF(NUMB.EQ.NUMB1) GO TO 55
PANE  85        IF(NUMB.LE.NCOUNT) GO TO 60
PANE  86        GO TO 70
PANE  87     55 CONTINUE
PANE  88        NNOD=NNOD1
PANE  89        DO 32 I=1,NNOD1
PANE  90        IE2(I)=IE(I)
PANE  91        IE(I)=IE1(I)+IE2(I)
PANE  92     32 IE1(I)=IE1(I)
PANE  93        GO TO 70
PANE  94     60 CONTINUE
PANE  95        NNOD=NNOD1
PANE  96        DO 34 I=1,NNOD1
PANE  97        IE1(I)=IE1(I)+IE2(I)
PANE  98     34 IE(I)=IE1(I)
PANE  99        CONTINUE
```

```
      IF(NUMB.EQ.NCOUNT) NCOUNT=0
   70 CONTINUE
      READ(5,1005) MATTYP,NHN,NLV1,NCOP4,XL,YL,BY1,BY2,NSPT
      IF(MATTYP.EQ.2030) NS=0
      IF(MATTYP.GE.1000) GO TO 125
      WRITE(6,1006)
      WRITE(6,1003) MATTYP,NHN,NLV1,NCOP4,XL,YL,BY1,BY2,NSPT
      NCOP=NLV1-1
      READ(5,1002) (LEV1(I),I=1,NLV1)
      WRITE(6,1009)
      WRITE(6,1002)(LEV1(I),I=1,NLV1)
      IF(NCOP.NE.0) READ(5,1002) (NCOPL(I),I=1,NCOP)
      WRITE(6,1010)
      IF(NCOP.NE.0)WRITE(6,1002) NCOP,(NCOPL(I),I=1,NCOP)
      IF(ND.EQ.2) NS=3*NSPT
      IF(ND.EQ.3) NS=0
      IF(NS.EQ.0) GO TO 85

C
C   NUMBER OF STRESS COMPONENTS AND STRESS POINT LOCATIONS
C
      WRITE(6,1012)
      DO 9 I=1,NSPT
      READ(5,1001) NPNT,XSI(NPNT),ETA(NPNT)
    9 WRITE(6,1011) NPNT,XSI(NPNT),ETA(NPNT)
   85 CONTINUE
C
C   INSTRUCTIONS FOR PRINTING
C
      READ(5,1002) IPLOC,IPLSTOP,IPMAT,NC,ISH
      WRITE(6,1013)
      WRITE(6,1002) IPLOC,IPLSTOP,IPMAT,NC,ISH
      WRITE(6,1014)
C
C   CALCULATE STORAGE ALLOCATIONS FOR DYNAMIC ARRAYS
C
      CALL ALLOC(IPLOC,IPLSTOP,ND,NHN,NLV1,
     1    LEV1,NLEV1,NCOP,NCOPL,NCOP4,
     1    L0,L1,L2,L3,L4,L5,L10,L20,L100,L200,
     2    K0,K1,K2,K3,K4,K5,K10,K20,K100,K200,
     3    M0,M1,M2,M3,M4,M5,M10,M20,M100,M200,NS,
     4     NEND,NHALF,NHALFS,MMM  )
C
C   CHECK STORAGE LENGTH OF  COMMON A(MTOT)  , AND OF
C   COMMON /EM/ QQQ(MTOTEM) IN ADDSTF
C
      NDF=NNOD*ND
      NWK=NDF*(NDF+1)/2
      LRQ1=2*6*NDF*NWK
      IF(MTOTEM.GE.LRQ1) GO TO 87
      MMX=LRQ1-MTOTEM
      WRITE(6,918) MMX,LRQ1
      STOP
   87 CONTINUE
      IF(MMM.GT.MTOT) GO TO 90
      GO TO 95
   90 CONTINUE
      MM1=MMM-MTOT
      WRITE(6,915) MM1
      STOP
   95 CONTINUE
      DO 11 I=1,MTOT
   11 A(I)=0.0
      DO 12 I=1,400
   12 LM(I)=0
      AX= XL/(NHN-1)
      IF(MODEX.EQ.1) GO TO 125
C
C   CREATE ELEMENT STIFFNESS MASS AND STRESS-DISPLACEMENT
C   MATRICES (ZERO LEVEL)
C
      MP=MATTYP
C
      CALL LVL0(ND,AX,BY1,BY2,A(L0),A(L1),A(K0),A(K1),
     1    A(M0),A(M1),XSI,ETA,NS,
     1     THI(MP),E(MP),POI(MP),WT(MP),IS4)
C
C   CREATE 1ST LEVEL ELEMENTS, I.E., START AND END ELEMENT
C   (END ELEMENT IS STORED ON TAPE NTAP)
C
      CALL LVL1(NTAP,ND,NS,NHN,LM(1),LM(101),LEV1,BY2,
     1    A(L0),A(L1),A(L2),A(L3),A(L5),
     1    A(K0),A(K1),A(K2),A(K3),A(K5),
     1    A(M0),A(M1),A(M2),A(M3),A(M5))
C
C   CHECK IF OTHER LEVELS ARE REQU'D
C
      IF(NLV1.GT.1) GO TO 96
      IF(LEV1(1).LT.100) GO TO 97
      NSTEP=LEV1(1)-100
      IF(NSTEP.EQ.0.AND.NCOP4.EQ.0) GO TO 98
      GO TO 96
   97 IF(NCOP4.EQ.0) GO TO 99
      GO TO 96
   98 N=2*NHN*ND
      LN=L2
      KN=K2
      GO TO 105
   99 N=(NEND*NHN)*ND
      LN=L5
      KN=K5
      GO TO 105
   96 CONTINUE
C
C   CREATE 2ND LEVEL ELEMENTS USING START ELEMENTS
C
      CALL LVL2(NTAP,ND,NS,NHN,NLV1,LEV1,NCOP,NEW2,NSD2,
     1 LM(1),LM(101),LM(201),A(L2),A(L3),A(L4),A(L5),
     2                       A(K2),A(K3),A(K4),A(K5),
     3                       A(M2),A(M3),A(M4),A(M5))
      N=NEW2
      NSD=NSD2
      LN=L5
      KN=K5
      MN=M5
      IF(NCOP.EQ.0) GO TO 100
C
C   CREATE 3RD LEVEL ELEMENT USING 1ST AND 2ND LEVEL ELMTS.
C
      CALL LVL3(NTAP,ND,NS,NHN,LEV1,NCOP,NCOPL,NSD3,LM(1),
     1LM(101),LM(201),A(L0),A(L10),A(K0),A(K10),A(M0),A(M10))
```

```
PANE 220        N=NHALF*ND
PANE 221        NSD=NSD3
PANE 222        MN=MD
PANE 223        LN=1
PANE 224        KN=KD
PANE 225    100 CONTINUE
PANE 226        IF(NCOP4.EQ.0) GO TO 105
PANE 227 C
PANE 228 C    LEVEL4 CREATES A SYMMETRIC SUPER ELEMENT
PANE 229 C    USING THE 3RD LEVEL ELEMENT
PANE 230 C
PANE 231        CALL LVL4(NTAP,ND,NS,NDN,NHALF,NHALFS,NEND,NCOP,NCOP4,
PANE 232       1    NEW4,NSD4,LM(1),LM(101),LM(201),A(LD),A(L100),
PANE 233       2    A(KD),A(K100),A(MD),A(M100))
PANE 234        N=NEW4
PANE 235        NSD=NSD4
PANE 236        MN=M100
PANE 237        LN=L100
PANE 238        KN=K100
PANE 239    105 CONTINUE
PANE 240 C
PANE 241 C    REARRANGE MATRICES (FROM MODE 1 TO MODE 2 )
PANE 242 C
PANE 243        CALL STORE12(NTAP,N,200,LM,A(LN))
PANE 244        IF(IPMAT.EQ.1) CALL WRITE20(NC,ISH,N,A(LN))
PANE 245 C
PANE 246 C    CHECK IF MASS MATRIX LUMPED OR CONSISTENT
PANE 247 C
PANE 248        IF(IMAS.NE. 1) GO TO 110
PANE 249        CALL STORE12(NTAP,N,200,LM,A(KN))
PANE 250        IF(IPMAT.EQ.1) CALL WRITE20(NC,ISH,N,A(KN))
PANE 251        RETURN
PANE 252    110 CALL LUMPDE(IMAS,ND,M,XL,YL,THI(MP),WT(MP),A(KN),LM)
PANE 253        KNN=KN+N-1
PANE 254        IF(IPMAT.EQ.1) WRITE(6,1004) (A(I),I=KN,KNN)
PANE 255        WRITE(6,1015)
PANE 256    120 CONTINUE
PANE 257    125 CONTINUE
PANE 258        WRITE(6,1002) M,NNOD,(IE(I),I=1,NNOD),IGEN
PANE 259        IF(ND.EQ.3) IIA=2
PANE 260        IF(ND.EQ.2) IIA=0
PANE 261        DO 30 I=1,NNOD
PANE 262        IEL=IE(I)
PANE 263        DO 30  L=1,ND
PANE 264        I1=(I-1)*ND+L
PANE 265        I2=I1A+L
PANE 266     30 LM(I1)=ID(IEL,I2)
PANE 267        NDN=ND*NNOD
PANE 268        IF(NDN.NE.N) WRITE(6,916) NDN,N
PANE 269        IF(NDN.NE.N.AND.MODEX.EQ.0) STOP
PANE 270        IF(MODEX.EQ.1) GO TO 136
PANE 271 C
PANE 272 C    CALCULATE BANDWIDTH AND WRITE STIFFNESS AND MASS
PANE 273 C    MATRIX ON TAPE 2
PANE 274 C
PANE 275        CALL CALPAN(MBAND,LM,A(KN),A(LN),NDN)
PANE 276        NSTO=NDN*NSD
PANE 277        WRITE(1) M,NDN,NS,NSD,NSTO
PANE 278        IF(NS.EQ.0) GO TO 136
PANE 279        MN1=MN

PANE 280        MN2=MN+NSTO-1
PANE 281 C
PANE 282 C    WRITE STRESS DISPLACEMENT MATRIX ON TAPE 1
PANE 283 C
PANE 284        WRITE(1) (LM(I),I=1,NDN),(A(I),I=MN1,MN2)
PANE 285        IF(IPMAT.NE.1) GO TO 136
PANE 286        IF(MATTYP.GE.1000) GO TO 136
PANE 287        WRITE(6,920)
PANE 288        WRITE(6,1002) NDN,NSD
PANE 289        DO 42 L=1,NDN
PANE 290        I1=MN+(L-1)*NSD
PANE 291        I2=MN+L*NSD-1
PANE 292        WRITE(6,1004) (A(I),I=I1,I2)
PANE 293        WRITE(6,922)
PANE 294     42 CONTINUE
PANE 295    136 CONTINUE
PANE 296        IF(NUMB.NE.NUME) GO TO 130
PANE 297 C
PANE 298   1001 FORMAT(I5,3F10.0,F15.0)
PANE 299   1005 FORMAT(4I5,4F10.0,4I5)
PANE 300   1006 FORMAT( 23H NUMBER OF ELEMENTS    =, I6 /
PANE 301       1         23H NUMBER OF MATERIALS  =, I6 /
PANE 302       2         23H MASS FORMULATION     =, I6 /
PANE 303       3         23H   EQ.1, CONSISTENT   ,  -      /
PANE 304       4         23H   EQ.2, LUMPED       , -    /
PANE 305       5         23H D.O.F. PER NODE      =, I6 /
PANE 306       6         23H NUMBER OF BASIC ELEMTS,         /
PANE 307       7         23H CREATED BY SAP4      =, I6 ///)
PANE 308   1007 FORMAT( 38H M A T E R I A L - P R O P E R T I E S,///
PANE 309       1          ,2X,3H NM,6X,6H E(NM),5X,
PANE 310       2          7H NU(NM),5X,6H THI(NM),4X,9H MASS(NM),/)
PANE 311   1008 FORMAT(/// 32H G E O M . - P R O P E R T I E S,//
PANE 312       1          ,6H  MTYP,5H  NDN,5H NLVL,6H NCOP4,2X,3H XL,
PANE 313       2          7X,3H YL,7X,4H BY1,6X,4H BY2,3X,5H NSPT,/)
PANE 314   1009 FORMAT(// 18H LEVL(I),I=1,NLVL /)
PANE 315   1010 FORMAT(// 26H  NCOP  NCOPL(I),I=1,NCOP /)
PANE 316   1011 FORMAT(I5,4E13.6)
PANE 317   1012 FORMAT(// 14H STRESSPOINTS,///,6H   NSP,
PANE 318       1          10H  XSI(NSP),4X,9H ETA(NSP),///)
PANE 319   1013 FORMAT(//// 37H P R I N T - I N S T R U C T I O N S ,//
PANE 320       1          6H IPLOC,6H ISTOP,6H IPMAT,/)
PANE 321   1014 FORMAT(1H1,/,28H CONTROL-INFORMATIONS  START,/)
PANE 322   1015 FORMAT(26H CONTROL-INFORMATIONS  END,/,1H1,/,
PANE 323       1        19H ELEMENT-NUMBERING,////,
PANE 324       2         5H    M,6H  NNOD,24H   (IE(I),I=1,NNOD),IGEN,//
PANE 325   1002 FORMAT(2615,/,2615)
PANE 326   1003 FORMAT(4I5,4F10.4,8I5)
PANE 327   1004 FORMAT(1X,12E11.4)
PANE 328    915 FORMAT(// 27H INCREASE STORAGE (MIOFF) BY   I6)
PANE 329    916 FORMAT(// 16H CHECK NUMBERING   215)
PANE 330    918 FORMAT( 20H INCREASE MIOFFM BY ,I6, 10H ...LEL= ,I6)
PANE 331    920 FORMAT(1H1)
PANE 332    922 FORMAT(/)
PANE 333        RETURN
PANE 334        END


ALLO   1        SUBROUTINE ALLOC(ILO,ILS,NL,NHN,NLVL,
ALLO   2       1  ILVL,NLEVL,NCOP,NCOPL,NCOP4,
```

```
ALLO    3       1  LT0,LT1,LT2,LT3,LT4,LT5,LT10,LT20,LT100,LT200,
ALLO    4       2  KT0,KT1,KT2,KT3,KT4,KT5,KT10,KT20,KT100,KT200,
ALLO    5       3  MT0,MT1,MT2,MT3,MT4,MT5,MT10,MT20,MT100,MT200,
ALLO    6       4  NS,NEND,NHALF,NHALFS,MMM)
ALLO    7 C
ALLO    8        DIMENSION LEV1(1),NCUPL(1),NLEV1(1)
ALLO    9        WRITE(6,910)
ALLO   10        LT0=1
ALLO   11        L1=L2=4
ALLO   12        L3=L4=2*NHN
ALLO   13        L5=L6=1
ALLO   14        LT1=LT2=LT3=LT4=LT5=LT6=LT10=LT20=LT100=LT200=1
ALLO   15        KT0=KT1=KT2=KT3=KT4=KT5=KT6=1
ALLO   16        NEND=NHALF=NHALFS=MMM=MMMS=0
ALLO   17        M1=M2=M3=M4=M5=M6=1
ALLO   18        M10=M20=M100=M200=0
ALLO   19        DO 10 I=1,NLV1
ALLO   20     10 NLEV1(I)=0
ALLO   21 C
ALLO   22 C    LT1,LT2   ARE STORAGE-END-LOCATIONS FOR ARRAYS
ALLO   23 C    S1(),S2() IN LEVEL0 AND LEVEL1
ALLO   24 C
ALLO   25 C    LT3,LT4,LT5     ARE STORAGE-END-LOCATIONS FOR ARRAYS
ALLO   26 C    SS(),SS1(),STEM() IN LEVEL1 AND LEVEL2
ALLO   27 C
ALLO   28        ICT=0
ALLO   29        DO 22 I=1,NLV1
ALLO   30        IF(LEV1(I).GE.100) GO TO 45
ALLO   31        IF(LEV1(I).EQ.1) NLEV1(I)=2*NHN
ALLO   32        IF(LEV1(I).EQ.2) NLEV1(I)=NHN+2
ALLO   33        IF(LEV1(I).EQ.3) NLEV1(I)=NHN+3
ALLO   34        IF(LEV1(I).EQ.4) NLEV1(I)=NHN+1
ALLO   35        IF(LEV1(I).EQ.5) NLEV1(I)=NHN
ALLO   36        IF(LEV1(I).EQ.6) NLEV1(I)=NHN+2
ALLO   37        NEND=NLEV1(I)-NHN
ALLO   38        L6=2*NHN
ALLO   39        GO TO 40
ALLO   40     45 CONTINUE
ALLO   41        IF(LEV1(I).GE.200) NSP=LEV1(I)-200
ALLO   42        IF(LEV1(I).GE.200) ICT=ICT+1
ALLO   43        IF(LEV1(I).GE.100.AND.LEV1(I).LT.200) NSP=LEV1(I)-100
ALLO   44        IF(NSP.LT.10) GO TO 50
ALLO   45        NLEV1(I)=2*NHN
ALLO   46        NEWL5=2*NHN
ALLO   47        NEWL6=3*NHN
ALLO   48        GO TO 60
ALLO   49     50 CONTINUE
ALLO   50        NLEV1(I)=(2**(NSP-1))*2+2*NHN
ALLO   51        NEWL6=NLEV1(I)+NHN-2
ALLO   52        NEWL5=(2**(NSP-1)-1)*2+2*NHN
ALLO   53        IF(NSP.EQ.0) NEWL6=NEWL5=2*NHN
ALLO   54     60 CONTINUE
ALLO   55        IF(I.EQ.1) NEND=NHN
ALLO   56        IF(NEWL5.GT.L5) L5=NEWL5
ALLO   57        IF(NEWL6.GT.L6) L6=NEWL6
ALLO   58     40 CONTINUE
ALLO   59        IF(NSP.GE.10) NSP=NSP/10
ALLO   60        NEWM5=2**(NSP-1)
ALLO   61        NEWM6=2**(NSP)
ALLO   62        IF(NSP.EQ.0) NEWM6=NEWM5=1
ALLO   63        IF(NEWM5.GT.M5) M5=NEWM5
ALLO   64        IF(NEWM6.GT.M6) M6=NEWM6
ALLO   65        IF(NCUP.EQ.0) GO TO 22
ALLO   66        M20=M20+NEWM6
ALLO   67        IF(I.EQ.(NLV1-1)) M10=M20
ALLO   68        MDIF=M20-M10
ALLO   69        IF(MDIF.GT.M10) M10=MDIF
ALLO   70     22 CONTINUE
ALLO   71 C
ALLO   72        IF(NCUP4.EQ.0) GO TO 65
ALLO   73        M100=M20
ALLO   74        IF(NCUP.EQ.0) M100=1
ALLO   75        IF(LEV1(I).GT.100) M100=M6
ALLO   76        M200=2*M100
ALLO   77     65 CONTINUE
ALLO   78 C
ALLO   79        L1=L1*ND
ALLO   80        L2=L2*ND
ALLO   81        L3=L3*ND
ALLO   82        L4=L4*ND
ALLO   83        L5=L5*ND
ALLO   84        L6=L6*ND
ALLO   85        LT1=LT0+(L1+1)*L1/2
ALLO   86        LT2=LT1+(L2+1)*L2/2
ALLO   87        IF(ICT.EQ.0) LT2=LT1+1
ALLO   88        LT3=LT2+(L3+1)*L3/2
ALLO   89        LT4=LT3+(L4+1)*L4/2
ALLO   90        IF(ICT.EQ.0) LT4=LT3+1
ALLO   91        LT5=LT4+(L5+1)*L5/2
ALLO   92        LT6=LT5+(L6+1)*L6/2
ALLO   93 C
ALLO   94 C    LT10,LT20   ARE STORAGELOCATIONS FOR ARRAYS
ALLO   95 C    S(),S3() IN LEVEL3
ALLO   96 C
ALLO   97        MMM=LT6
ALLO   98        IF(NCUP.EQ.0) GO TO 130
ALLO   99        L10=1
ALLO  100        L20=NLEV1(1)
ALLO  101        IF(NCUP.EQ.1) GO TO 100
ALLO  102        GO TO 110
ALLO  103    100 L10=NLEV1(1)
ALLO  104        L20=L10+NLEV1(2)-NHN
ALLO  105        NHALF=L20-NHN
ALLO  106        IF(NCUPL(1).EQ.2)NHALF=NHALF+2
ALLO  107        GO TO 120
ALLO  108    110 CONTINUE
ALLO  109        DO 25 I=1,NCUP
ALLO  110        II=I+1
ALLO  111        L20=L20+NLEV1(II)-2*NHN
ALLO  112        IF(NCUPL(1).EQ.2) L20=L20+2
ALLO  113        NHALF=L20
ALLO  114        IF(I.EQ.(NCUP-1))  L10=L20
ALLO  115     25 CONTINUE
ALLO  116        IF(NCUPL(NCUP).EQ.1) L20=L20+NHN
ALLO  117        IF(NCUPL(NCUP).EQ.2) L20=L20+NHN-2
ALLO  118    120 CONTINUE
ALLO  119        DO 27 I=1,NLV1
ALLO  120     27 IF(NLEV1(I).GT. L10) L10=NLEV1(I)
ALLO  121        L10=L10*ND
ALLO  122        L20=L20*ND
```

```
ALLO 123        LT10=(L10+1)*L10/2+1
ALLO 124        LT20=LT10+(L20+1)*L20/2
ALLO 125        NFIRST=NLEVI(1)
ALLO 126        NHALFS=M20*(NHN-1)*45
ALLO 127        IF(LT20.GT.MMM) MMM=LT20
ALLO 128    130 CONTINUE
ALLO 129        IF(NCOP4.EQ.0) GO TO 140
ALLO 130 C
ALLO 131 C    LT100,LT200  ARE STORAGELOCATIONS FOR ARRAYS
ALLO 132 C    S(),S4() IN LEVEL4
ALLO 133 C
ALLO 134        IF(NCOP.EQ.0) NHALF=NEND+NHN
ALLO 135        IF(NCOP.EQ.0) NHALFS=(NHN-1)*NS
ALLO 136        L100=NHALF*ND
ALLO 137        L200=2*L100-NHN*ND
ALLO 138        LT100=(L100+1)*L100/2+1
ALLO 139        LT200=LT100+(L200+1)*L200/2
ALLO 140        IF(LT200.GT.MMM) MMM=LT200
ALLO 141 C
ALLO 142 C    KT VALUES GIVE CORRESPONDING LOCATIONS FOR MASS MATRIX
ALLO 143 C
ALLO 144    140 CONTINUE
ALLO 145        KT0=MMM
ALLO 146        KT1=KT0+LT1
ALLO 147        KT2=KT0+LT2
ALLO 148        KT3=KT0+LT3
ALLO 149        KT4=KT0+LT4
ALLO 150        KT5=KT0+LT5
ALLO 151        KT6=KT0+LT6
ALLO 152        KT10=KT0+LT10
ALLO 153        KT20=KT0+LT20
ALLO 154        KT100=KT0+LT100
ALLO 155        KT200=KT0+LT200
ALLO 156        MMM=2*MMM
ALLO 157 C
ALLO 158 C    MT VALUES GIVE CORRESPONDING LOCATIONS FOR STRESS-
ALLO 159 C    DISPLACEMENT MATRICES
ALLO 160 C
ALLO 161        MT0=MT1=MT2=MT3=MT4=MT5=MT6=1
ALLO 162        MT10=MT20=MT100=MT200=1
ALLO 163        IF(NS.EQ.0) GO TO 145
ALLO 164        MT0=MMM
ALLO 165        MT1=MT0+NS*L1
ALLO 166        MT2=MT1+NS*L2
ALLO 167        IF(ICT.LQ.0) MT2=MT1+1
ALLO 168        MT3=MT2+NS*(NHN-1)*L3
ALLO 169        MT4=MT3+NS*(NHN-1)*L4
ALLO 170        IF(ICT.EQ.0) MT4=MT3+1
ALLO 171        MT5=MT4+N5*NS*(NHN-1)*L5
ALLO 172        MT6=MT5+N6*NS*(NHN-1)*L6
ALLO 173        MMMS=MT6
ALLO 174        IF(NCOP.EQ.0) GO TO 150
ALLO 175        MT10=MT0 +M10*NS*(NHN-1)*L10
ALLO 176        MT20=MT10+M20*NS*(NHN-1)*L20
ALLO 177        MMMS=MT20
ALLO 178    150 CONTINUE
ALLO 179        IF(NCOP4.EQ.0) GO TO 155
ALLO 180        MT100=MT0  +M100*NS*(NHN-1)*L100
ALLO 181        MT200=MT100+M200*NS*(NHN-1)*L200
ALLO 182        MMMS=MT200
ALLO 183    155 CONTINUE
ALLO 184    145 CONTINUE
ALLO 185        IF(ILO.EQ.1.OR.ILS.EQ.1) GO TO 165
ALLO 186        GO TO 160
ALLO 187    165 CONTINUE
ALLO 188 C
ALLO 189        WRITE(6,900) (NLEVI(I),I=1,4LV1)
ALLO 190        WRITE(6,900) L1,L2,L3,L4,L5,L6,L10,L20,L100,L200
ALLO 191        WRITE(6,900) LT0,LT1,LT2,LT3,LT4,LT5,LT6
ALLO 192        WRITE(6,900) LT10,LT20,LT100,LT200
ALLO 193        WRITE(6,900) KT0,KT1,KT2,KT3,KT4,KT5,KT6
ALLO 194        WRITE(6,900) KT10,KT20,KT100,KT200
ALLO 195        WRITE(6,900) NEND,NFIRST,NHALF
ALLO 196        WRITE(6,900) MMM
ALLO 197        WRITE(6,900) M1,M2,M3,M4,M5,M6,M10,M20,M100,M200
ALLO 198        WRITE(6,900) MT0,MT1,MT2,MT3,MT4,MT5,MT6
ALLO 199        WRITE(6,900) MT10,MT20,MT100,MT200
ALLO 200        WRITE(6,900) NHALFS
ALLO 201        WRITE(6,900) MMMS
ALLO 202 CC
ALLO 203    160 CONTINUE
ALLO 204        WRITE(6,915)
ALLO 205        IF(ILS.EQ.1) STOP
ALLO 206        IF(NS.NE.0) MMM=MMMS
ALLO 207    900 FORMAT(1216)
ALLO 208    910 FORMAT( 10H IN  ALLOC)
ALLO 209    915 FORMAT( 10H END ALLOC)
ALLO 210        RETURN
ALLO 211        END


CALP   1        SUBROUTINE CALPAN(MBAND,LM,XM,S,NDN)
CALP   2 C
CALP   3        DIMENSION LM(1),XM(1),S(1)
CALP   4        COMMON /EXTRA/ MODEX,MT8
CALP   5        MIN=100000
CALP   6        MAX=0
CALP   7        DO 800 L=1,NDN
CALP   8        IF(LM(L).EQ.0) GO TO 800
CALP   9        IF (LM(L).GT.MAX) MAX=LM(L)
CALP  10        IF (LM(L).LT.MIN) MIN=LM(L)
CALP  11    800 CONTINUE
CALP  12        NDIF=MAX-MIN+1
CALP  13        IF (NDIF.GT.MBAND) MBAND=NDIF
CALP  14        IF(MODEX.EQ.1) GO TO 810
CALP  15        NWK=NDN*(NDN+1)/2
CALP  16        LRD=1+6*NDN+NWK
CALP  17        NDN1=NDN+1
CALP  18        NDN5=NDN+5
CALP  19        DO 10 I=NDN1,NDN5
CALP  20     10 XM(I)=0.0
CALP  21 C
CALP  22        WRITE(2) LRD,NDN,(LM(I),I=1,NDN),(S(I),I=1,NWK),
CALP  23       1 (XM(I),I=NDN1,NDN5),(XM(I),I=1,NDN)
CALP  24        RETURN
CALP  25 C
CALP  26    810 WRITE (1) NDN,NS,(LM(I),I=1,NDN)
CALP  27        RETURN
CALP  28        END
```

```
ASSE   1        SUBROUTINE ASSEM(LM,N,S,SS,B,BB,LMS,NS,NSS,F,FF)
ASSE   2 C
ASSE   3 C   ASSEMBLY ROUTINE
ASSE   4 C
ASSE   5        DIMENSION LM(N),S(1),SS(1),B(1),BB(1)
ASSE   6        DIMENSION LMS(1),F(1),FF(1)
ASSE   7        IOLD=0
ASSE   8        DO 10 I=1,N
ASSE   9        DO 20 J=I,N
ASSE  10        Q=1.0
ASSE  11        IF(LM(I).LT.0) Q=-Q
ASSE  12        IF(LM(J).LT.0) Q=-Q
ASSE  13        IF(IABS(LM(I)).GT.IABS(LM(J))) GO TO 200
ASSE  14        IR = IABS(LM(I))
ASSE  15        IC = IABS(LM(J))
ASSE  16        GO TO 210
ASSE  17   200 IR = IABS(LM(J))
ASSE  18        IC = IABS(LM(I))
ASSE  19   210 INEW=(IC-1)*IC/2 + IR
ASSE  20        IOLD=(J-1)*J/2+I
ASSE  21        SS(INEW) = SS(INEW) + S(IOLD)*Q
ASSE  22        BB(INEW) = BB(INEW) + B(IOLD)*Q
ASSE  23     20 CONTINUE
ASSE  24        IF(NS.EQ.0) GO TO 10
ASSE  25        Q=1.0
ASSE  26        IF(LM(I).LT.0) Q=-1.0
ASSE  27        IR=IABS(LM(I))
ASSE  28        DO 25 J=1,NS
ASSE  29        IC=LMS(J)
ASSE  30        INEW=(IR-1)*NSS+IC
ASSE  31        IOLD=(I-1)*NS+J
ASSE  32        FF(INEW)=FF(INEW)+F(IOLD)*Q
ASSE  33     25 CONTINUE
ASSE  34     10 CONTINUE
ASSE  35        RETURN
ASSE  36        END
```

```
STAR   1        SUBROUTINE STAR(LO,NO,NR,S,B,NS,F)
STAR   2 C
STAR   3 C   REDUCTION ALGORITHM
STAR   4 C
STAR   5        DIMENSION S(1),B(1),F(1),LO(1)
STAR   6        DO 5 J=1,NO
STAR   7     5  LO(J)=(J+1)*J/2
STAR   8        NE=NO-NR
STAR   9        DO 10 M=1,NE
STAR  10        MAX=NO-M
STAR  11        N=MAX+1
STAR  12        MAXX=LO(MAX)
STAR  13        NN=LO(N)
STAR  14        DO 20 I=1,MAX
STAR  15        LOA=MAXX+I
STAR  16        LOB=NN
STAR  17        IF(S(LOA).EQ.0.0) GO TO 20
STAR  18        T1 = S(LOA)/S(LOB)
STAR  19        T2=T1*B(LOB)/S(LOB)
STAR  20        T3=B(LOA)/S(LOB)
STAR  21        DO 30 J=1,MAX
STAR  22        LOC=LO(J)-J+I
STAR  23        LOD=MAXX+J
STAR  24        S(LOC) =  S(LOC)-S(LOD)*T1
STAR  25        IF(B(LOD).EQ.0.0) GO TO 100
STAR  26        B(LOC)=B(LOC)-B(LOD)*T1+S(LOD)*T2-S(LOD)*T3
STAR  27        GO TO 30
STAR  28   100 CONTINUE
STAR  29        B(LOC)=B(LOC)+S(LOD)*T2-S(LOD)*T3
STAR  30    30 CONTINUE
STAR  31        IF(NS.EQ.0) GO TO 20
STAR  32        DO 35 J=1,NS
STAR  33        LOE=(I-1)*NS+J
STAR  34        LOF=(N-1)*NS+J
STAR  35        F(LOE)=F(LOE)-F(LOF)*T1
STAR  36    35 CONTINUE
STAR  37    20 CONTINUE
STAR  38    10 CONTINUE
STAR  39        RETURN
STAR  40        END
```

```
LVLO   1        SUBROUTINE LVLO(ND,A,BY1,BY2,S1,S2,B1,B2,
LVLO   2       1   F1,F2,XSI,ETA,NS,T,E,P,W,IS4)
LVLO   3 C
LVLO   4        DIMENSION S1(1),S2(1),B1(1),B2(1)
LVLO   5        DIMENSION F1(1),F2(1),XSI(1),ETA(1)
LVLO   6        DIMENSION STT(12,12),LOC(12)
LVLO   7        DATA LOC/1,2,3,10,11,12,7,8,9,4,5,6/
LVLO   8        WRITE(6,901)
LVLO   9        BY=BY1
LVLO  10        IC=0
LVLO  11        N4=4*ND
LVLO  12        NT=(N4+1)*N4/2
LVLO  13        NTS=N4*NS
LVLO  14   100 CONTINUE
LVLO  15        WRITE(6,904) T,E,P,W,A,BY
LVLO  16 C
LVLO  17 C   CREATION OF ELEMENT STIFFNESS MATRIX
LVLO  18 C
LVLO  19        IF(IS4.EQ.0) CALL ESTIF(ND,T,E,P,A,BY,S2)
LVLO  20        IF(IS4.NE.0) READ(13) NTX,(S2(I),I=1,IIX)
LVLO  21 C
LVLO  22 C   CREATION OF ELEMENT MASS MATRIX
LVLO  23 C
LVLO  24        CALL ELMA(ND,T,W,A,BY,B2)
LVLO  25 C
LVLO  26 C   CREATION OF ELEMENT STRESS-DISPLACEMENT MATRIX
LVLO  27 C
LVLO  28        CALL ESTRES(ND,N4,NS,E,P,A,BY,F2,XSI,ETA)
LVLO  29        IF(IC.EQ.1) GO TO 140
LVLO  30        IF(BY2.NE.0.0) GO TO 120
LVLO  31        DO 25 I=1,NT
LVLO  32        S1(I)=S2(I)
LVLO  33        S2(I)=0.0
LVLO  34        B1(I)=B2(I)
LVLO  35    25 B2(I)=0.0
```

```
LVLO   36        IF(NS.EQ.0) GO TO 60
LVLO   37        DO 30 I=1,NTS
LVLO   38        F1(I)=F2(I)
LVLO   39     30 F2(I)=0.0
LVLO   40     60 CONTINUE
LVLO   41        GO TO 140
LVLO   42    120 CONTINUE
LVLO   43        DO 35 I=1,NT
LVLO   44        S1(I)=S2(I)
LVLO   45        S2(I)=0.0
LVLO   46        B1(I)=B2(I)
LVLO   47     35 B2(I)=0.0
LVLO   48        BY=BY2
LVLO   49        IC=1
LVLO   50        IF(NS.EQ.0) GO TO 70
LVLO   51        DO 36 I=1,NTS
LVLO   52        F1(I)=F2(I)
LVLO   53     36 F2(I)=0.0
LVLO   54     70 CONTINUE
LVLO   55        GO TO 100
LVLO   56    140 CONTINUE
LVLO   57        WRITE(6,902)
LVLO   58    901 FORMAT( 11H IN  LEVELO )
LVLO   59    902 FORMAT( 11H END LEVELO)
LVLO   60    904 FORMAT(12E11.4)
LVLO   61    906 FORMAT(1215)
LVLO   62        RETURN
LVLO   63        END
```

```
LVL1    1        SUBROUTINE LVL1(NTAP,ND,NS,NHN,LM,LMS,LEV1,BY2,
LVL1    2       1    S1,S2,SS1,SS2,STEM,B1,B2,BB1,BB2,BTEM,
LVL1    3       2    F1,F2,FF1,FF2,FTEM)
LVL1    4 C
LVL1    5        DIMENSION S1(1),S2(1),SS1(1),SS2(1),STEM(1)
LVL1    6        DIMENSION B1(1),B2(1),BB1(1),BB2(1),BTEM(1)
LVL1    7        DIMENSION F1(1),F2(1),FF1(1),FF2(1),FTEM(1)
LVL1    8        DIMENSION LEV1(1),LM(1),LMS(1)
LVL1    9        WRITE(6,902)
LVL1   10 C
LVL1   11 C   CREATES START ELEMENT FOR BY1, OR FOR BY1 AND BY2
LVL1   12 C
LVL1   13        CALL STEL(ND,NS,NHN,LM,LMS,BY2,S1,S2,SS1,SS2,
LVL1   14       1  B1,B2,BB1,BB2,F1,F2,FF1,FF2)
LVL1   15 C
LVL1   16        IF(LEV1(1).GE.100) GO TO100
LVL1   17 C
LVL1   18 C   CREATES END ELEMENT AS SPECIFIED BY LEV1(1) USING BY1
LVL1   19 C
LVL1   20        CALL ENEL(NTAP,ND,NS,NHN,LM,LMS,LEV1(1),
LVL1   21       1  S1,SS1,STEM,B1,BB1,BTEM,F1,FF1,FTEM)
LVL1   22 C
LVL1   23    100 CONTINUE
LVL1   24        WRITE(6,904)
LVL1   25    902 FORMAT(  11H IN  LEVEL1)
LVL1   26    904 FORMAT( 11H END LEVEL1)
LVL1   27        RETURN
LVL1   28        END
```

```
STEL    1        SUBROUTINE STEL(ND,NS,NHN,LM,LMS,BY2,S1,S2,SS1,SS2,
STEL    2       1   B1,B2,BB1,BB2,F1,F2,FF1,FF2)
STEL    3 C
STEL    4        DIMENSION LM(1),S1(1),S2(1),SS1(1),SS2(1)
STEL    5        DIMENSION B1(1),B2(1),BB1(1),BB2(1)
STEL    6        DIMENSION LMS(1),F1(1),F2(1),FF1(1),FF2(1)
STEL    7        WRITE(6,950)
STEL    8        ND2 =2*ND
STEL    9        ND4 =4*ND
STEL   10        M   =NHN-1
STEL   11         NS =NS*M
STEL   12        DO 100 NEL =1,M
STEL   13 C
STEL   14 C   CONNECTIVITY ARRAY FOR MTYP=1
STEL   15 C
STEL   16        CALL END1(NEL,LM,M,ND,ND2)
STEL   17        IF(NS.EQ.0) GO TO 115
STEL   18        DO 10 I=1,NS
STEL   19        II=(NEL-1)*NS+I
STEL   20        LMS(I)=II
STEL   21     10 CONTINUE
STEL   22        WRITE(6,900) (LMS(I),I=1,NS)
STEL   23    115 CONTINUE
STEL   24        CALL ASSEM(LM,ND4,S1,SS1,B1,BB1,LMS,NS,NSS,F1,FF1)
STEL   25    100 CONTINUE
STEL   26        IF(BY2.EQ.0.0) GO TO 150
STEL   27        DO 120 NEL=1,M
STEL   28        CALL END1(NEL,LM,M,ND,ND2)
STEL   29        IF(NS.EQ.0) GO TO 120
STEL   30        DO 15 I=1,NS
STEL   31        II=(NEL-1)*NS+I
STEL   32        LMS(I)=II
STEL   33     15 CONTINUE
STEL   34    120 CONTINUE
STEL   35        CALL ASSEM(LM,ND4,S2,SS2,B2,BB2,LMS,NS,NSS,F2,FF2)
STEL   36    110 CONTINUE
STEL   37    150 CONTINUE
STEL   38        WRITE(6,952)
STEL   39    950 FORMAT( 12H IN  STARTEL)
STEL   40    952 FORMAT( 12H END STARTEL)
STEL   41        RETURN
STEL   42        END
```

```
ENEL    1        SUBROUTINE ENEL(NTAP,ND,NS,NHN,LM,LMS,MTYP,
ENEL    2       1  S1,SS1,SEND,B1,BB1,BEND,F1,FF1,FEND)
ENEL    3 C
ENEL    4        DIMENSION  S1(1),SS1(1),SEND(1)
ENEL    5        DIMENSION  B1(1),BB1(1),BEND(1)
ENEL    6        DIMENSION F1(1),FF1(1),FEND(1)
ENEL    7        DIMENSION LM(1),LMS(1)
ENEL    8        WRITE(6,950)
ENEL    9        ND2=ND*2
ENEL   10        ND3=ND*3
ENEL   11        ND4=ND*4
ENEL   12        M=NHN-1
ENEL   13        NS=NS*M
```

```
ENEL   14         N1=ND2*.NHN
ENEL   15         NT=(N1+1)*N1/2
ENEL   16         DO 5 I=1,NT
ENEL   17         SEND(I)=0.0
ENEL   18         BEND(I)=0.0
ENEL   19       5 CONTINUE
ENEL   20 C
ENEL   21 C    F O R M  E N D  E L E M E N T
ENEL   22 C
ENEL   23         GO TO (110,120,130,140,110,150) MTYP
ENEL   24 C
ENEL   25 C    T Y P E  1 OR  5
ENEL   26 C
ENEL   27     110 CONTINUE
ENEL   28         N1=2*ND*NHN
ENEL   29         NT=(N1+1)*N1/2
ENEL   30         NST=NS*M*N1
ENEL   31         DO 10 I=1,NT
ENEL   32         SEND(I)=SS1(I)
ENEL   33         BEND(I)=BB1(I)
ENEL   34      10 CONTINUE
ENEL   35         NODES=2*NHN
ENEL   36         IF(NS.EQ.0) GO TO 112
ENEL   37         DO 15 I=1,NST
ENEL   38      15 FEND(I)=FF1(I)
ENEL   39     112 CONTINUE
ENEL   40         IF(MTYP.EQ.1) GO TO 115
ENEL   41         NODES=NHN
ENEL   42         NRED =NHN*ND
ENEL   43         GO TO 225
ENEL   44 C
ENEL   45 C    T Y P E  2
ENEL   46 C
ENEL   47     120 DO 200 NEL=1,M
ENEL   48 C
ENEL   49         CALL END2(NEL,LM,M,ND,ND2,ND3,ND4,NODES)
ENEL   50         IF(NS.EQ.0) GO TO 135
ENEL   51         DO 20 I=1,NS
ENEL   52         II=(NEL-1)*NS+I
ENEL   53         LMS(I)=II
ENEL   54      20 CONTINUE
ENEL   55         WRITE(6,900) (LMS(I),I=1,NS)
ENEL   56     135 CONTINUE
ENEL   57         CALL ASSEM(LM,ND4,S1,SEND,B1,BEND,LMS,NS,NSS,F1,FEND)
ENEL   58 C
ENEL   59     200 CONTINUE
ENEL   60         NRED=(NHN+2)*ND
ENEL   61         GO TO 225
ENEL   62 C
ENEL   63 C    T Y P E  3
ENEL   64 C
ENEL   65     130 IF(NHN.GT.4) GO TO 102
ENEL   66         WRITE(6,960)
ENEL   67         STOP
ENEL   68     102 CONTINUE
ENEL   69         DO 220 NEL=1,M
ENEL   70 C
ENEL   71         CALL END3(NEL,LM,M,ND,ND2,ND3,ND4,NODES)
ENEL   72         IF(NS.EQ.0) GO TO 138
ENEL   73         DO 25 I=1,NS
ENEL   74         II=(NEL-1)*NS+I
ENEL   75         LMS(I)=II
ENEL   76      25 CONTINUE
ENEL   77         WRITE(6,900) (LMS(I),I=1,NS)
ENEL   78     138 CONTINUE
ENEL   79         CALL ASSEM(LM,ND4,S1,SEND,B1,BEND,LMS,NS,NSS,F1,FEND)
ENEL   80 C
ENEL   81     220 CONTINUE
ENEL   82         NRED=(NHN+3)*ND
ENEL   83         GO TO 225
ENEL   84 C
ENEL   85 C    T Y P E  4
ENEL   86 C
ENEL   87     140 DO 222 NEL=1,M
ENEL   88 C
ENEL   89         CALL END4(NEL,LM,M,ND,ND2,ND3,ND4,NODES)
ENEL   90         IF(NS.EQ.0) GO TO 142
ENEL   91         DO 30 I=1,NS
ENEL   92         II=(NEL-1)*NS+I
ENEL   93         LMS(I)=II
ENEL   94      30 CONTINUE
ENEL   95         WRITE(6,900) (LMS(I),I=1,NS)
ENEL   96     142 CONTINUE
ENEL   97         CALL ASSEM(LM,ND4,S1,SEND,B1,BEND,LMS,NS,NSS,F1,FEND)
ENEL   98 C
ENEL   99     222 CONTINUE
ENEL  100         NRED=NODES*ND
ENEL  101         GO TO 225
ENEL  102 C
ENEL  103 C    T Y P E  6
ENEL  104 C
ENEL  105     150 IF(NHN.GT.3) GO TO 103
ENEL  106         WRITE(6,970)
ENEL  107         STOP
ENEL  108     103 CONTINUE
ENEL  109         DO 223 NEL=1,M
ENEL  110         CALL END6(NEL,LM,M,ND,ND2,ND3,ND4,NODES)
ENEL  111         IF(NS.EQ.0) GO TO 144
ENEL  112         DO 35 I=1,NS
ENEL  113         II=(NEL-1)*NS+I
ENEL  114         LMS(I)=II
ENEL  115      35 CONTINUE
ENEL  116     144 CONTINUE
ENEL  117         WRITE(6,900) (LM(I),I=1,ND4)
ENEL  118         CALL ASSEM(LM,ND4,S1,SEND,B1,BEND,LMS,NS,NSS,F1,FEND)
ENEL  119     223 CONTINUE
ENEL  120         NRED=NODES*ND
ENEL  121     225 CONTINUE
ENEL  122         NDTOT=2*NHN*ND
ENEL  123 C
ENEL  124         CALL STAR(LM,NDTOT,NRED,SEND,BEND,NSS,FEND)
ENEL  125     115 CONTINUE
ENEL  126         NOD=NODES*ND
ENEL  127         NT =(NOD+1)*NOD/2
ENEL  128         NST=NS*M*NOD
ENEL  129 C
ENEL  130         WRITE(NTAP)NT,NOD
ENEL  131         WRITE(NTAP)(SEND(I),I=1,NT)
ENEL  132         WRITE(NTAP)(BEND(I),I=1,NT)
ENEL  133         IF(NS.EQ.0) GO TO 145
```

```
ENEL 134        WRITE(NTAP) NST,NSS
ENEL 135        WRITE(NTAP) (FEND(I),I=1,NST)
ENEL 136    145 CONTINUE
ENEL 137        WRITE(6,952)
ENEL 138    900 FORMAT(2015)
ENEL 139    950 FORMAT( 10H  IN ENDEL)
ENEL 140    952 FORMAT( 10H END ENDEL)
ENEL 141    960 FORMAT(// 21H FOR TYPE 3 NHN .GT.4//)
ENEL 142    970 FORMAT(// 21H FOR TYPE 6 NHN .GT.3//)
ENEL 143        RETURN
ENEL 144        END
```

```
LVL2   1        SUBROUTINE LVL2(NTAP,ND,NS,NHN,NLV1,LEV1,NCOP,NEW,NSO,
LVL2   2       1    LM1,LM2,LMS,SS1,SS2,SS,STEM,BB1,BB2,BB,BTEM,
LVL2   3       2    FF1,FF2,FF,FTEM)
LVL2   4 C
LVL2   5        DIMENSION SS1(1),SS2(1),SS(1),STEM(1)
LVL2   6        DIMENSION BB1(1),BB2(1),BB(1),BTEM(1)
LVL2   7        DIMENSION FF1(1),FF2(1),FF(1),FTEM(1)
LVL2   8        DIMENSION LM1(1),LM2(1),LMS(1),LEV1(1)
LVL2   9        WRITE(6,902)
LVL2  10        NEW=NSO=0
LVL2  11        N=2*ND*NHN
LVL2  12        NT=(N+1)*N/2
LVL2  13        NST=NS*(NHN-1)*N
LVL2  14        DO 35 I=1,NLV1
LVL2  15        IF(LEV1(I).LT.100) GO TO 35
LVL2  16        IF(LEV1(I).GE.200) GO TO 170
LVL2  17        IF(LEV1(I).GE.100.AND.LEV1(I).LT.200) GO TO 180
LVL2  18 C
LVL2  19 C   CREATES 2ND LEVEL ELEMENT USING START ELEMENT
LVL2  20 C   (WITH BY2),ACCORD. TO LEV1(I)
LVL2  21 C
LVL2  22    170 NSTEP=(LEV1(I)-200)
LVL2  23        DO 10 L=1,NT
LVL2  24        SS(L)=SS2(L)
LVL2  25     10 BB(L)=BB2(L)
LVL2  26        IF(NS.EQ.0) GO TO 190
LVL2  27        DO 15 L=1,NST
LVL2  28     15 FF(L)=FF2(L)
LVL2  29        GO TO 190
LVL2  30 C
LVL2  31 C   CREATES 2ND LEVEL ELEMENT USING START ELEMENT
LVL2  32 C   (WITH BY1),ACCORD. TO LEV1(I)
LVL2  33 C
LVL2  34    180 NSTEP=(LEV1(I)-100)
LVL2  35        DO 20 L=1,NT
LVL2  36        SS(L)=SS1(L)
LVL2  37     20 BB(L)=BB1(L)
LVL2  38        IF(NS.EQ.0) GO TO 190
LVL2  39        DO 25 L=1,NST
LVL2  40     25 FF(L)=FF1(L)
LVL2  41    190 CONTINUE
LVL2  42 C
LVL2  43        CALL LVL22(NTAP,ND,NS,NHN,NSTEP,NCOP,NEW,NSO,
LVL2  44       1  LM1,LM2,LMS,SS,STEM,BB,BTEM,FF,FTEM )
LVL2  45 C
LVL2  46     35 CONTINUE
LVL2  47        WRITE(6,904)
LVL2  48    902 FORMAT( 11H IN  LEVEL2)
LVL2  49    904 FORMAT( 11H END LEVEL2)
LVL2  50        RETURN
LVL2  51        END
```

```
LV22   1        SUBROUTINE LVL22(NTAP,ND,NS,NHN,NSTEP,NCOP,NEW,NSO,
LV22   2       1  LM1,LM2,LMS,S1,S2,B1,B2,F1,F2 )
LV22   3 C
LV22   4        DIMENSION S1(1),S2(1),B1(1),B2(1),F1(1),F2(1)
LV22   5        DIMENSION LM1(1),LM2(1),LMS(1)
LV22   6        WRITE(6,954)
LV22   7        NS1=NS2=NST2=NST3=0
LV22   8        IF(NSTEP.EQ.0) GO TO 95
LV22   9        GO TO 92
LV22  10     95 N2=2*NHN*ND
LV22  11        NT2=(N2+1)*N2/2
LV22  12        NS2=NS*(NHN-1)
LV22  13        NST2=NS2*N2
LV22  14        DO 5 I=1,NT2
LV22  15        S2(I)=S1(I)
LV22  16     5  B2(I)=B1(I)
LV22  17        IF(NS.EQ.0) GO TO 170
LV22  18        DO 7 I=1,NST2
LV22  19     7  F2(I)=F1(I)
LV22  20        GO TO 170
LV22  21     92 CONTINUE
LV22  22        IF(NSTEP.GE.10) GO TO 100
LV22  23        IC=0
LV22  24        GO TO 110
LV22  25    100 NSTEP =NSTEP/10
LV22  26        IC=1
LV22  27    110 CONTINUE
LV22  28        DO 10 II=1,NSTEP
LV22  29 C
LV22  30        CALL CONC2(IC,ND,NHN,II,LM1,LM2,N1,N2,N3)
LV22  31        IJ=0
LV22  32        DO 25 I=1,N3
LV22  33        DO 25 J=I,N3
LV22  34        IJ=IJ+1
LV22  35        S2(IJ)=0.0
LV22  36     25 B2(IJ)=0.0
LV22  37        IF(NS.EQ.0) GO TO 115
LV22  38        M1=2**(II-1)
LV22  39        M2=2*M1
LV22  40        NS1=M1*NS*(NHN-1)
LV22  41        NS2=M2*NS*(NHN-1)
LV22  42        NST2=NS2*N2
LV22  43        NST3=NS2*N3
LV22  44        DO 30 I=1,NST3
LV22  45     30 F2(I)=0.0
LV22  46        DO 35 I=1,NS1
LV22  47     35 LMS(I)=I
LV22  48    115 CONTINUE
LV22  49 C
LV22  50        CALL ASSEM(LM1,N1,S1,S2,B1,B2,LMS,NS1,NS2,F1,F2)
LV22  51        IF(NS.EQ.0) GO TO 120
LV22  52        DO 30 I=1,NST
```

```
      36 LMS(I)=I+NS1
     120 CONTINUE
C
      CALL ASSEM(LM2,N1,S1,S2,B1,B2,LMS,NS1,NS2,F1,F2)
      CALL STAR(LM1,N3,N2,S2,B2,NS2,F2)
      IF(II.EQ.NSTEP) GO TO 10
      IJ=0
      DO 40 I=1,N2
      DO 40 J=I,N2
      IJ=IJ+1
      S1(IJ)=S2(IJ)
   40 B1(IJ)=B2(IJ)
      IF(NS.EQ.0) GO TO 125
      DO 45 I=1,NST2
   45 F1(I)=F2(I)
  125 CONTINUE
   10 CONTINUE
      N12=(N2+1)*N2/2
  170 CONTINUE
C
      WRITE(NTAP) NT2,N2
      WRITE(NTAP) (S2(I),I=1,NT2)
      WRITE(NTAP) (B2(I),I=1,NT2)
      IF(NS.EQ.0) GO TO 174
      WRITE(NTAP) NST2,NS2
      WRITE(NTAP) (F2(I),I=1,NST2)
  174 CONTINUE
      IF(NCOP.EQ.0) GO TO 176
      DO 60 I=1,NT2
      S2(I)=0.0
   60 B2(I)=0.0
      IF(NS.EQ.0) GO TO 176
      DO 65 I=1,NST2
   65 F2(I)=0.0
  176 CONTINUE
      NEW=N2
      NSO=NS2
      WRITE(6,956)
  904 FORMAT(1X,12E11.4)
  906 FORMAT(/)
  920 FORMAT(1X,E11.4)
  900 FORMAT(12I5)
  902 FORMAT(36I3)
  954 FORMAT( 12H IN  LEVEL22)
  956 FORMAT( 12H END LEVEL22)
      RETURN
      END
```

```
      SUBROUTINE LVL3(NTAP,NO,NS,NHN,LEV1,NCOP,NCOPL,NDTOTS,
     1  LM1,LM2,LMS,S,S3,B,B3,F,F3)
C
      DIMENSION LEV1(1),NCOPL(1),LM1(1),LM2(1)
      DIMENSION S(1),S3(1),B(1),B3(1)
      DIMENSION LMS(1),F(1),F3(1)
      WRITE(6,900)
      NS1=NTS1=N2=NTS2=LASTS=NEXTS=0
      REWIND NTAP
      DO 50 II=1,NCOPL
C
C   CREATE CONNECTIVITY FOR THE 140 ELEMENTS
C   CREATE CONNECTIVITY ARRAY FOR THE TWO SUP. ELEM.
C   CONNECTED AT THE PRESENT COUPLING STEP
C
      IF(II.EQ.1) GO TO 110
      GO TO 120
  110 CONTINUE
C
C   READ END ELEMENT (OR FIRST ELEMENT FOR II=1) FROM TAPE
C
      READ(NTAP) NT1,N1
      READ(NTAP) (S(I),I=1,NT1)
      READ(NTAP) (B(I),I=1,NT1)
      LAST=N1/ND
      IF(NS.EQ.0) GO TO 115
      READ(NTAP) NTS1,NS1
      READ(NTAP) (F(I),I=1,NTS1)
      LASTS=NS1
  115 CONTINUE
  120 CONTINUE
C
      CALL CONC3(II,ND,NS,NHN,NDTOT,NEXT,LAST,NEAT,
     1   NDTOTS,LASTS,LEV1,NCOPL,LM1,LM2)
      IQ=0
      DO 10 I=1,NDTOT
      DO 10 J=1,NDTOT
      IQ=IQ+1
      S3(IQ)=0.0
   10 B3(IQ)=0.0
      IF(NS.EQ.0) GO TO 125
      DO 12 I=1,LASTS
   12 LMS(I)=I
      NTS=NDTOTS*NDTOT
      DO 13 I=1,NTS
   13 F3(I)=0.0
  125 CONTINUE
C
      CALL ASSEM(LM1,LAST,S,S3,B,B3,LMS,LASTS,NDTOTS,F,F3)
C
C   READ (II+1)ST SUP.ELEM. FROM TAPE NTAP (TO BE COUPLED
C   IN THE PRESENT LOOP.)
C
      READ(NTAP) NT2,N2
      READ(NTAP) (S(I),I=1,NT2)
      READ(NTAP) (B(I),I=1,NT2)
      IF(NS.EQ.0) GO TO 130
      READ(NTAP) NTS2,NS2
      READ(NTAP) (F(I),I=1,NTS2)
      NEXTS=NS2
      DO 14 I=1,NEXTS
   14 LMS(I)=I+LASTS
  130 CONTINUE
C
      CALL ASSEM(LM2,NEXT,S,S3,B,B3,LMS,NEXTS,NDTOTS,F,F3)
      NTSX=NDTOT*NDTOTS
C
      CALL STAR(LM1,NDTOT,NEXT,S3,B3,NDTOTS,F3)
      IQ=0
      DO 15 I=1,NEXT
```

```
LVL3   71        DO 15 J=I,NEXI
LVL3   72        IQ=IQ+1
LVL3   73        S(IQ)=S3(IQ)
LVL3   74     15 B(IQ)=B3(IQ)
LVL3   75        IF(NS.EQ.0) GO TO 135
LVL3   76        NTS=NEXI*NDTOTS
LVL3   77        DO 20 I=1,NTS
LVL3   78     20 F(I)=F3(I)
LVL3   79    135 CONTINUE
LVL3   80        LAST = NEXI/ND
LVL3   81        LASTS=NDTOTS
LVL3   82     50 CONTINUE
LVL3   83        WRITE(6,902)
LVL3   84    900 FORMAT( 11H IN  LEVEL3)
LVL3   85    902 FORMAT( 11H END LEVEL3)
LVL3   86        RETURN
LVL3   87        END
```

```
LVL4    1        SUBROUTINE LVL4(NTAP,ND,NS,NHN,NHALF,NHALFS,NEND,NCOP,
LVL4    2       1   NCUP4,NEW,NSS1,LM1,LM2,LMS,S,S4,B,B4,F,F4)
LVL4    3 C
LVL4    4        DIMENSION LM1(1),LM2(1),S(1),S4(1),B(1),B4(1)
LVL4    5        DIMENSION LMS(1),F(1),F4(1)
LVL4    6        WRITE(6,902)
LVL4    7        NS1=NSS1=0
LVL4    8 C
LVL4    9 C   IF ONLY TWO ENDELEMENTS ARE SYMMETRIC
LVL4   10 C   COUPLED READ FROM NTAP
LVL4   11 C
LVL4   12        IF(NCUP.NE.0) GO TO 100
LVL4   13        REWIND NTAP
LVL4   14        READ(NTAP) NET,NE
LVL4   15        READ(NTAP) (S(I),I=1,NET)
LVL4   16        READ(NTAP) (B(I),I=1,NET)
LVL4   17        NHALF=NE/ND
LVL4   18        IF(NS.EQ.0) GO TO 100
LVL4   19        READ(NTAP) NST,NS1
LVL4   20        READ(NTAP) (F(I),I=1,NST)
LVL4   21        NHALFS=NS1
LVL4   22    100 CONTINUE
LVL4   23 C
LVL4   24        CALL CONC4(ND,NHN,NHALF,NEND,NDTOT,NEW,NCUP4,LM1,LM2)
LVL4   25        NT=(NDTOT+1)*NDTOT/2
LVL4   26        DO 10 I=1,NT
LVL4   27        S4(I)=0.0
LVL4   28     10 B4(I)=0.0
LVL4   29        IF(NS.EQ.0) GO TO 110
LVL4   30        NS1=NHALFS
LVL4   31        NSS1=NS1*2
LVL4   32        NST=NDTOT*NSS1
LVL4   33        DO 15 I=1,NST
LVL4   34     15 F4(I)=0.0
LVL4   35        DO 20 I=1,NS1
LVL4   36     20 LMS(I)=I
LVL4   37    110 CONTINUE
LVL4   38 C
LVL4   39        CALL ASSEM(LM1,NHALF,S,S4,B,B4,LMS,NS1,NSS1,F,F4)
LVL4   40        IF(NS.EQ.0) GO TO 120
```

```
LVL4   41        NES=NS1/NS
LVL4   42        II=0
LVL4   43        DO 30 I=1,NES
LVL4   44        DO 30 L=1,NS
LVL4   45        II=II+1
LVL4   46     30 LMS(II)=NS1+(NES-I)*NS+L
LVL4   47    120 CONTINUE
LVL4   48 C
LVL4   49        CALL ASSEM(LM2,NHALF,S,S4,B,B4,LMS,NS1,NSS1,F,F4)
LVL4   50        CALL STAR(LM1,NDTOT,NEW,S4,B4,NSS1,F4)
LVL4   51        NST=NEW*NSS1
LVL4   52        WRITE(6,904)
LVL4   53    902 FORMAT( 11H IN  LEVEL4)
LVL4   54    904 FORMAT( 11H END LEVEL4)
LVL4   55        RETURN
LVL4   56        END
```

```
END1    1        SUBROUTINE END1(NEL,LM,M,ND,ND2)
END1    2 C
END1    3        DIMENSION LM(1)
END1    4        DO 15 I=1,ND2
END1    5        LM(I)     =(NEL-1)*ND+I
END1    6     15 LM(ND2+I)=(2*M-NEL+1)*ND+I
END1    7        RETURN
END1    8        END
```

```
END2    1        SUBROUTINE END2(NEL,LM,M,ND,ND2,ND3,ND4,NODES)
END2    2 C
END2    3        DIMENSION LM(ND4)
END2    4        IF(NEL.NE.1) GO TO 500
END2    5        DO 25 I=1,ND
END2    6        LM(I)     =I
END2    7        LM(ND+I)  =ND+I
END2    8        LM(ND2+I) =(2*M+1)*ND+I
END2    9     25 LM(ND3+I) =(M+2)*ND+I
END2   10        GO TO 590
END2   11 C
END2   12    500 IF(NEL.EQ.M) GO TO 510
END2   13        DO 30 I=1,ND2
END2   14        LM(I)     = (NEL-1)*ND+I
END2   15     30 LM(ND2+I) = (2*M-NEL+2)*ND+I
END2   16        GO TO 590
END2   17 C
END2   18    510 IF(NEL.NE.M) GO TO 590
END2   19        DO 32 I=1,ND
END2   20        LM(I)     =(NEL-1)*ND+I
END2   21        LM(ND+I)  = NEL*ND+I
END2   22        LM(ND2+I) =(NEL+1)*ND+I
END2   23     32 LM(ND3+I) =(M+3)*ND+I
END2   24    590 CONTINUE
END2   25        NODES=M+1+2
END2   26        WRITE(6,902)
END2   27    902 FORMAT( 7H TYPE 2)
END2   28        RETURN
END2   29        END
```

```
END3    1        SUBROUTINE END3(NEL,LM,M,ND,ND2,ND3,ND4,NODES)
END3    2 C
END3    3        DIMENSION LM(ND4)
END3    4        IF(NEL.NE.1) GO TO 600
END3    5        DO 34 I=1,ND
END3    6        LM(I)     = I
END3    7        LM(ND+I)  = ND+I
END3    8        LM(ND2+I)= (2*M+1)*ND+I
END3    9     34 LM(ND3+I)= (M+3)*ND+I
END3   10        GO TO 690
END3   11 C
END3   12    600 IF(NEL.GE.(M/2)) GO TO 610
END3   13        DO 36 I=1,ND2
END3   14        LM(I)     = (NEL-1)*ND+I
END3   15     36 LM(ND2+I)= (2*M-NEL+2)*ND+I
END3   16        GO TO 690
END3   17 C
END3   18    610 IF(NEL.NE.(M/2)) GO TO 620
END3   19        DO 38 I=1,ND
END3   20        LM(I)     = (NEL-1)*ND+I
END3   21        LM(ND +I)= (NEL  )*ND+I
END3   22        LM(ND2+I)= (M+2  )*ND+I
END3   23     38 LM(ND3+I)= (1.5*M+3)*ND+I
END3   24        GO TO 690
END3   25 C
END3   26    620 IF(NEL.NE.(M/2+1)) GO TO 630
END3   27        DO 40 I=1,ND
END3   28        LM(I)     = (NEL-1)*ND+I
END3   29        LM(ND+I) = (NEL  )*ND+I
END3   30        LM(ND2+I)= (1.5*M+2)*ND+I
END3   31     40 LM(ND3+I)= (M+2)*ND+I
END3   32        GO TO 690
END3   33 C
END3   34    630 IF(NEL.EQ.M) GO TO 640
END3   35        DO 42 I=1,ND2
END3   36        LM(I)     = (NEL-1)*ND+I
END3   37     42 LM(ND2+I)= (2*M-NEL+3)*ND+I
END3   38        GO TO 690
END3   39 C
END3   40    640 DO 44 I=1,ND
END3   41        LM(I)     = (NEL-1)*ND+I
END3   42        LM(ND+I) = (NEL*ND)+I
END3   43        LM(ND2+I)= (NEL+1)*ND+I
END3   44     44 LM(ND3+I)= (M+4)*ND+I
END3   45    690 CONTINUE
END3   46        NODES=M+1+3
END3   47        WRITE(6,903)
END3   48    903 FORMAT( 7H TYPE 3)
END3   49        RETURN
END3   50        END
```

```
END4    1        SUBROUTINE END4(NEL,LM,M,ND,ND2,ND3,ND4,NODES)
END4    2 C
END4    3        DIMENSION LM(ND4)
END4    4        RM=M+1.0
END4    5        R1=RM/2
END4    6        R2=(M/2)*1.0
END4    7        IF(R1.EQ.R2) GO TO 800
END4    8        WRITE(6,910)
END4    9        STOP
END4   10    800 CONTINUE
END4   11        IF(NEL.GE.(M/2)) GO TO 700
END4   12        DO 48 I=1,ND2
END4   13        LM(I)=(NEL-1)*ND+I
END4   14     46 LM(ND2+I)=(2*M-NEL+1)*ND+I
END4   15        GO TO 790
END4   16 C
END4   17    700 IF(NEL.NE.(M/2)) GO TO 710
END4   18        DO 52 I=1,ND
END4   19        LM(I)     =(NEL-1)*ND+I
END4   20        LM(ND+I) =NEL*ND    +I
END4   21        LM(ND2+I)=(M+1)*ND  +I
END4   22     52 LM(ND3+I)=(1.5*M+2)*ND+I
END4   23        GO TO 790
END4   24 C
END4   25    710 IF(NEL.NE.(M/2+1)) GO TO 720
END4   26        DO 56 I=1,ND
END4   27        LM(I)     =(NEL-1)*ND+I
END4   28        LM(ND+I) =NEL*ND    +I
END4   29        LM(ND2+I)=(1.5*M+1)*ND+I
END4   30     56 LM(ND3+I)=(M+1)*ND+I
END4   31        GO TO 790
END4   32 C
END4   33    720 DO 58 I=1,ND2
END4   34        LM(I)     =(NEL-1)*ND+I
END4   35     58 LM(ND2+I)=(2*M-NEL+2)*ND+I
END4   36    790 CONTINUE
END4   37        NODES=M+1+1
END4   38    910 FORMAT( 12H NHN NOT ODD )
END4   39        RETURN
END4   40        END
```

```
END6    1        SUBROUTINE END6(NEL,LM,M,ND,ND2,ND3,ND4,NODES)
END6    2 C
END6    3        DIMENSION LM(ND4)
END6    4        M1=1
END6    5        M2=2
END6    6        M3=M-1
END6    7        M4=M
END6    8        IF(NEL.EQ.M1) GO TO 10
END6    9        IF(NEL.EQ.M2) GO TO 20
END6   10        IF(NEL.EQ.M3) GO TO 30
END6   11        IF(NEL.EQ.M4) GO TO 40
END6   12        GO TO 50
END6   13     10 DO 12 I=1,ND
END6   14        LM(I)=I
END6   15        LM(ND+I)=ND+I
END6   16        LM(ND2+I)=(M+2)*ND+I
END6   17        LM(ND3+I)=(2*M+1)*ND+I
END6   18     12 CONTINUE
END6   19        GO TO 100
END6   20 C
END6   21     20 DO 22 I=1,ND
END6   22        LM(I)=ND+I
```

```
END6   23         LM(ND+I)=2*ND+I
END6   24         LM(ND2+I)=(2*M)*ND+I
END6   25         LM(ND3+I)=(M+2)*ND+I
END6   26      22 CONTINUE
END6   27         GO TO 100
END6   28 C
END6   29      30 DO 32 I=1,ND
END6   30         LM(I)=(M-2)*ND+I
END6   31         LM(ND+I)=(M-1)*ND+I
END6   32         LM(ND2+I)=(M+1)*ND+I
END6   33         LM(ND3+I)=(M+4)*ND+I
END6   34      32 CONTINUE
END6   35         GO TO 100
END6   36 C
END6   37      40 DO 42 I=1,ND
END6   38         LM(I)=(M-1)*ND+I
END6   39         LM(ND+I)=M*ND+I
END6   40         LM(ND2+I)=(M+3)*ND+I
END6   41         LM(ND3+I)=(M+1)*ND+I
END6   42      42 CONTINUE
END6   43         GO TO 100
END6   44 C
END6   45      50 DO 52 I=1,ND
END6   46         LM(I)=(NEL-1)*ND+I
END6   47         LM(ND+I)=NEL*ND+I
END6   48         LM(ND2+I)=(2*M-NEL+2)*ND+I
END6   49         LM(ND3+I)=(2*M-NEL+3)*ND+I
END6   50      52 CONTINUE
END6   51     100 CONTINUE
END6   52         NODES=M+3
END6   53         RETURN
END6   54         END
```

```
CON2    1         SUBROUTINE CONC2(IC,ND,NHN,II,LM1,LM2,N1,N2,N3)
CON2    2 C
CON2    3         DIMENSION  LM1(1),LM2(1)
CON2    4         IF(IC.EQ.1)GO TO 120
CON2    5 C
CON2    6 C    SIDENODES ARE NOT ELIMINATED
CON2    7 C
CON2    8         CALL SIN02(ND,NHN,II,LM1,LM2,N1,N2,N3)
CON2    9         GO TO 130
CON2   10     120 CONTINUE
CON2   11 C
CON2   12 C    SIDENODES ARE ELIMINATED
CON2   13 C
CON2   14         CALL NOSI2(ND,NHN,LM1,LM2,N1,N2,N3)
CON2   15     130 CONTINUE
CON2   16         RETURN
CON2   17         END
```

```
NOS2    1         SUBROUTINE NOSI2(ND,NHN,LM1,LM2,N1,N2,N3)
NOS2    2 C
NOS2    3         DIMENSION LM1(1),LM2(1)
NOS2    4         N=ND*NHN
NOS2    5         N1=2*ND+NHN
NOS2    6         N2=N1
NOS2    7         N3=3*ND+NHN
NOS2    8         DO 10 I=1,N
NOS2    9         LM1(I+N)=N+I
NOS2   10         LM2(I)=I
NOS2   11         LM2(N+I)=N2+I
NOS2   12      10 CONTINUE
NOS2   13         IC=0
NOS2   14         NN3=N3
NOS2   15         DO 20 ICOUNT=1,NHN
NOS2   16         DO 30 I=1,ND
NOS2   17         IC=IC+1
NOS2   18            LM1(IC)=NN3-ND+I
NOS2   19      30 CONTINUE
NOS2   20         NN3=NN3-ND
NOS2   21      20 CONTINUE
NOS2   22         WRITE(6,950)
NOS2   23     950 FORMAT (11H END NOSI02)
NOS2   24         RETURN
NOS2   25         END
```

```
SIN2    1         SUBROUTINE SIN02(ND,NHN,II,LM1,LM2,NT1,NT2,NT3)
SIN2    2 C
SIN2    3         DIMENSION LM1(1),LM2(1)
SIN2    4         N=ND*NHN
SIN2    5         N2=2*ND*NHN
SIN2    6         N3=3*ND*NHN
SIN2    7         NM=N-2*ND
SIN2    8         IS=(2**(II-1)-1)*ND
SIN2    9         NT1=N2+2*IS
SIN2   10         NT2=N2+4*IS+2*ND
SIN2   11         NT3=N3+4*IS
SIN2   12 C
SIN2   13 C    IS=DOF OF HALF THE SIDE NODES OF PREVIOUSLY
SIN2   14 C    ASSEMBLED ELEMENT (NOT INCL. CORNER NODES)
SIN2   15 C    NT1   NO OF DOF OF PREVIOUSY ASSEM. SUP ELEM.
SIN2   16 C    NT2   NO OF DOF OF SUP ELEM ASSEM. IN PRESENT LOOP
SIN2   17 C    NT3   SAME AS NT2, BUT INCL. INTERIOR DOF.
SIN2   18 C
SIN2   19         IF(II.EQ.1) GO TO 100
SIN2   20         DO 10 I=1,ND
SIN2   21         LM1(I)=LM2(N2+IS-ND+I)=N2 +3*IS+ND+I
SIN2   22         LM1(N-ND+I)=LM2(N+IS+I)=N+IS+I
SIN2   23      10 CONTINUE
SIN2   24         DO 20 I=1,N
SIN2   25         LM1(N+IS+I)=N+2*IS+ND+I
SIN2   26         LM2(I) = LM2(I)
SIN2   27      20 CONTINUE
SIN2   28         DO 30 I=1,NM
SIN2   29         LM2(N+IS+ND+I)=NT3-NM+I
SIN2   30      30 CONTINUE
SIN2   31         NIN=NHN-2
SIN2   32         IC=ND
SIN2   33         NN3=NT3
SIN2   34         DO 33 ICOUNT=1,NIN
SIN2   35         DO 36 I=1,ND
SIN2   36         IC=IC+1
SIN2   37         LM1(IC)=NN3-ND+I
```

```
SIN2   38      36 CONTINUE
SIN2   39         NN3=NN3-ND
SIN2   40      33 CONTINUE
SIN2   41         DO 40 I=1,IS
SIN2   42         LM1(N+I) = N+IS+ND+I
SIN2   43         LM1(2*N+IS+I) = 2*N + 2*IS +ND +I
SIN2   44         LM2(N+I) =N+I
SIN2   45         LM2(2*N+IS+I) =N2+3*IS+ 2*ND+I
SIN2   46      40 CONTINUE
SIN2   47         RETURN
SIN2   48 C
SIN2   49    100 CONTINUE
SIN2   50         DO 50 I=1,ND
SIN2   51         LM1(I)  =LM2(N2-ND+I)=N2+ND+I
SIN2   52         LM1(N-ND+I)=LM2(N+I) =N+I
SIN2   53      50 CONTINUE
SIN2   54         DO60  I=1,N
SIN2   55         LM1(N+I)=N+ND+I
SIN2   56         LM2(I)  =I
SIN2   57      60 CONTINUE
SIN2   58         DO 70 I=1,NN
SIN2   59         LM2(N+ND+I)=N2+2*ND+I
SIN2   60      70 CONTINUE
SIN2   61         NIN=NHN-2
SIN2   62         IC=ND
SIN2   63         NN3=N3
SIN2   64         DO 73 ICOUNT=1,NIN
SIN2   65         DO 76 I=1,ND
SIN2   66         IC=IC+1
SIN2   67         LM1(IC)=NN3-ND+I
SIN2   68      76 CONTINUE
SIN2   69         NN3=NN3-ND
SIN2   70      73 CONTINUE
SIN2   71         WRITE(6,952)
SIN2   72    952 FORMAT(' IN END SIDNO2')
SIN2   73         RETURN
SIN2   74         END
```

```
CON3    1         SUBROUTINE CONC3(IC,ND,NS,NHN,NDTOT,NEXT,LAST,NEXT,
CON3    2        1  NDTOTS,LASTS,LEV1,NCOPL,LM1,LM2)
CON3    3 C
CON3    4         DIMENSION LEV1(1),NCOPL(1),LM1(1),LM2(1)
CON3    5 C
CON3    6 C    FIND OUT OF SUPELEM FOR PRESENT COUPLING STEP IC
CON3    7 C
CON3    8         IF(LEV1(IC+1).GE.200) GO TO 110
CON3    9         ICHEK = LEV1(IC+1)-100
CON3   10         GO TO 120
CON3   11    110 ICHEK = LEV1(IC+1)-200
CON3   12    120 CONTINUE
CON3   13         IF(ICHEK.GE.10) GO TO 130
CON3   14 C
CON3   15 C    SIDENODES ARE NOT ELIMIN. DURING REDUCTION
CON3   16 C
CON3   17         NSTEP=ICHEK
CON3   18         IF(NSTEP.EQ.1)GO  TO  140
CON3   19         NEXT=(2*NHN+(2**NSTEP-1)*2)
CON3   20         GO TO 150
```

```
CON3   21 C
CON3   22 C    SIDENODES ARE ELIMIN. DURING REDUCTION
CON3   23 C
CON3   24    130 CONTINUE
CON3   25         NSTEP=ICHEK/10
CON3   26         NEXT =2*NHN
CON3   27         GO TO 150
CON3   28    140 CONTINUE
CON3   29         NEXT =(2*NHN+2)
CON3   30    150 CONTINUE
CON3   31         NDTOT=(LAST+NEXT-NHN)*ND
CON3   32         LAST=LAST*ND
CON3   33         NEXT=NEXT*ND
CON3   34         NEXTS=(2**NSTEP)*(NHN-1)*NS
CON3   35         NDTOTS=LASTS+NEXTS
CON3   36         IF(NCOPL(IC).EQ.1) CALL NOS13(ND,NHN,NDTOT,NEXT,
CON3   37        1  LAST,NEXT,LM1,LM2)
CON3   38         IF(NCOPL(IC).EQ.2) CALL SIND3(ND,NHN,NDTOT,NEXT,
CON3   39        1  LAST,NEXT,LM1,LM2)
CON3   40         RETURN
CON3   41         END
```

```
NOS3    1         SUBROUTINE NOS13(ND,NHN,NDTOT,NEXT,LAST,NEXT,LM1,LM2)
NOS3    2 C
NOS3    3         DIMENSION LM1(1),LM2(1)
NOS3    4 C
NOS3    5 C    COUPLING T Y P E 1
NOS3    6 C    CONNECTIVITY ARRAY FOR PREVIOUS ELEMENT
NOS3    7 C
NOS3    8         NINT=NHN*ND
NOS3    9         NEXT=NDTOT-NINT
NOS3   10         IQ=0
NOS3   11         NNTO=NDTOT
NOS3   12         DO 10 ICOUNT=1,NHN
NOS3   13         DO 15 I=1,ND
NOS3   14         IQ=IQ+1
NOS3   15         LM1(IQ)=NNTO-ND+1
NOS3   16      15 CONTINUE
NOS3   17         NNTO=NNTO-ND
NOS3   18      10 CONTINUE
NOS3   19         IR=LAST-NINT
NOS3   20         DO 20 I=1,IR
NOS3   21      20 LM1(NINT+I)=NEXT/2+I
NOS3   22 C
NOS3   23 C    CONNECTIVITY ARRAY FOR NEXT ELEMENT
NOS3   24 C
NOS3   25         IR=NEXT/2
NOS3   26         DO 30 I=1,IR
NOS3   27      30 LM2(I)=I
NOS3   28         DO 40 I=1,NINT
NOS3   29      40 LM2(IR+I)=NEXT+I
NOS3   30         IS=IR-NHN*ND
NOS3   31         IF(IS.EQ.0) RETURN
NOS3   32         DO 50 I=1,IS
NOS3   33         IRI=IR+NINT+I
NOS3   34      50 LM2(IRI)=NEXT-IS+I
NOS3   35         RETURN
NOS3   36         END
```

```
      SUBROUTINE SIND3(ND,NHN,NDTOT,NEXI,LAST,NEXT,LM1,LM2)
C
      DIMENSION LM1(1),LM2(1)
C
C   COUPLING  T Y P E  2
C   CONNECTIVITY ARRAY FOR PREVIOUS ELEMENT
C
      NINT=(NHN-2)*ND
      NEXI=NDTOT-NINT
      IS2 = NEXT/2 -NHN*ND
      DO 55 I=1,ND
   55 LM1(I) =NEXI-IS2-ND+I
      IQ=ND
      NNTO=NDTOT
      NHN2=NHN-2
      DO 60 ICOUNT=1,NHN2
      DO 62 I=1,ND
      IQ=IQ+1
      LM1(IQ)=NNTO-ND+I
   62 CONTINUE
      NNTO=NNTO-ND
   60 CONTINUE
      IR=LAST-NINT-ND
      DO 65 I=1,IR
      IN =NINT+ND+I
   65 LM1(IN)=NEXT/2+I
C
C  CONNECTIVITY ARRAY FOR NEXT SUP. ELEM.
C
      IR=NEXT/2 +ND
      DO 70 I=1,IR
   70 LM2(I)=I
      DO 75 I=1,NINT
   75 LM2(IR+I)=NEXI+I
      IS=IR-NHN*ND
      IF(IS.EQ.0) RETURN
      DO 80 I=1,IS
      IRI=IR+NINT+I
   80 LM2(IRI)=NEXI-IS+I
      RETURN
      END
```

```
      SUBROUTINE CONC4(ND,NHN,NHALF,NEND,NDTOT,
     1  NEW,NCOP4,LM1,LM2)
C
      DIMENSION LM1(1),LM2(1)
      IF(NCOP4.EQ.1) GO TO 100
      IF(NCOP4.EQ.2) GO TO 200
C
C   COUPLING TYPE 1
C
  100 CALL NOS14(ND,NHN,NHALF,NEND,NDTOT,NEW,LM1,LM2)
      GO TO 300
C
C   COUPLING TYPE 2
C
  200 CALL SIND4(ND,NHN,NHALF,NEND,NDTOT,NEW,LM1,LM2)
  300 CONTINUE
      NHALF=NHALF*ND
      DO 10 I=1,NHALF
   10 LM2(I)=-LM2(I)
      IF(ND.EQ.2) GO TO 400
      DO 20 I=1,NHALF,3
   20 LM2(I)=-LM2(I)
      IF(ND.EQ.3) GO TO 400
  400 CONTINUE
      NEND=NEND/ND
      RETURN
      END
```

```
      SUBROUTINE NOS14(ND,NHN,NHALF,NEND,NDTOT,NEW,LM1,LM2)
C
      DIMENSION LM1(1),LM2(1)
      NHD=NHN*ND
      NEW=(2*NHALF-2*NHN)*ND
      NDTOT=NEW+NHD
      NINT=NHN
      NIND=NHD
      NEND=NEND*ND
      NSID=(NHALF*ND-NEND-NHD)/2
      IQ=0
      NNTO=NDTOT
      DO 15 ICOUNT=1,NINT
      DO 20 I=1,ND
      IQ=IQ+1
   20 LM1(IQ)=NNTO-ND+I
      NNTO=NNTO-ND
   15 CONTINUE
      NM=(NHALF-NHN)*ND
      DO 30 I=1,NM
   30 LM1(NIND+I)=NEND+NSID+I
      DO 40 I=1,NIND
   40 LM2(I)=NEW+I
      DO 50 I=1,NSID
   50 LM2(NHD+I)=NEW-NSID+I
      NM=NEND+NSID
      DO 60 I=1,NM
   60 LM2(NHD+NSID+I)=I
      RETURN
      END
```

```
      SUBROUTINE SIND4(ND,NHN,NHALF,NEND,NDTOT,NEW,LM1,LM2)
C
      DIMENSION LM1(1),LM2(1)
      NHD=NHN*ND
      NEW   = (2*NHALF-2*NHN+2)*ND
      NDTOT=NEW+(NHN-2)*ND
      NINT=NHN-2
      NIND =(NHN-2)*ND
      NEND = NEND*ND
      NSID = (NHALF*ND -NEND -NHD)/2
```

```
SIN4    9        DO 10 I=1,ND
SIN4   12     10 LM1(I)= NEW-NSID-ND+I
SIN4   13        IO=ND
SIN4   14        NNIO=NDIGT
SIN4   15        DO 15 ICOUNT=1,NINT
SIN4   16        DO 20 I=1,ND
SIN4   17        IO=IO+1
SIN4   18     20 LM1(IO)=NNIO-ND+1
SIN4   19        NNIO=NNIO-ND
SIN4   20     15 CONTINUE
SIN4   21        NM=(NHALF-NHN+1)*ND
SIN4   22        DO 30 I=1,NM
SIN4   23     30 LM1(NHD-ND+I)=NEND*NSID+I
SIN4   24        DO 40 I=1,ND
SIN4   25     40 LM2(I)=NEND*NSID+I
SIN4   26        DO 50 I=1,NIND
SIN4   27     50 LM2(ND+I)=NEW+I
SIN4   28        NM=NSID*ND
SIN4   29        DO 60 I=1,NM
SIN4   30     60 LM2(NHD-ND+I)=NEW-NSID-ND+I
SIN4   31        NM=NEND*NSID
SIN4   32        DO 70 I=1,NM
SIN4   33     70 LM2(NHD*NSID+I)=I
SIN4   34        RETURN
SIN4   35        END
```

```
ESTI    1        SUBROUTINE ESTIF(T,E,P,A,B,S)
ESTI    2 C
ESTI    3        DIMENSION S(1)
ESTI    4 C
ESTI    5 C   ELEMENT STIFFNESS MATRIX IS CREATED
ESTI    6 C
ESTI    7 C      ND = NUMBER OF DEGREES OF FREEDOM PER NODE
ESTI    8 C      T  = ELEMENT THICKNESS
ESTI    9 C      E  = YOUNG'S MODULUS
ESTI   10 C      P  = POISSON'S RATIO
ESTI   11 C      A  = ELEMENT WIDTH
ESTI   12 C      B  = ELEMENT HEIGHT
ESTI   13 C      S()= STIFFNESS MATRIX STORED IN UPPER TRIANG.
ESTI   14 C           FORM , COL. BY COL. , FOR NUMBERING
ESTI   15 C           SEE FIG. 3.3
ESTI   16        RETURN
ESTI   17        END
```

```
ELMA    1        SUBROUTINE ELMA(ND,T,W,A,BY,B)
ELMA    2 C
ELMA    3        DIMENSION B(1)
ELMA    4 C
ELMA    5 C   ELEMENT MASS MATRIX IS CREATED
ELMA    6 C
ELMA    7 C      ND = NUMBER OF DEGREES OF FREEDOM PER NODE
ELMA    8 C      T  = ELEMENT THICKNESS
ELMA    9 C      RO = MASS DENSITY PER UNIT
ELMA   10 C      A  = ELEMENT WIDTH
ELMA   11 C      BY = ELEMENT HEIGHT
ELMA   12 C      B()= MASS MATRIX STORED IN UPPER TRIANG.
ELMA   13 C           FORM , COL. BY COL. , FOR NUMBERING
ELMA   14 C           SEE FIG. 3.3
ELMA   15        RETURN
ELMA   16        END
```

```
ESTR    1        SUBROUTINE ESTRES(ND,N4,NS,E,P,A,B,F,XSI,ETA)
ESTR    2 C
ESTR    3        DIMENSION F(NS,N4),XSI(1),ETA(1)
ESTR    4 C
ESTR    5 C   ELEMENT STRESS-DISPL. MATRIX IS CREATED
ESTR    6 C
ESTR    7 C      ND = NUMBER OF DEGREES OF FREEDOM PER NODE
ESTR    8 C      NS = NUMBER OF TOTAL STRESS COMPONENTS IN ELEMENT
ESTR    9 C      E  = YOUNG'S MODULUS
ESTR   10 C      P  = POISSON'S RATIO
ESTR   11 C      A  = ELEMENT WIDTH
ESTR   12 C      B  = ELEMENT HEIGHT
ESTR   13 C      F()= STRESS-DISPL. MATRIX STORED AS IN FIG. 3.8
ESTR   14 C      XSI()= COORDINATE IN Y-DIRECTION
ESTR   15 C      ETA()= COORDINATE IN X-DIRECTION
ESTR   16        RETURN
ESTR   17        END
```

```
LUMD    1        SUBROUTINE LUMPD(IMAS,ND,N,XL,YL,THI,WT,B,BT)
LUMD    2 C
LUMD    3        DIMENSION B(1),BT(1)
LUMD    4        GO TO (101,102),IMAS
LUMD    5    101 WRITE(6,1001)
LUMD    6        STOP
LUMD    7    102 CONTINUE
LUMD    8        RO=WT
LUMD    9        DO 10 I=1,N
LUMD   10        II=(I+1)*I/2
LUMD   11     10 BT(I)=B(II)
LUMD   12        TO=0.0
LUMD   13        IF(ND.NE.3) GO TO 100
LUMD   14 C
LUMD   15 C   CREATES CONSISTENT LUMPED MASS FROM CONSISTENT FULL
LUMD   16 C   MASS FOR PLATE BENDING (ROT. DOF ASSUMED AS ZERO)
LUMD   17 C
LUMD   18        DO 15 I=1,N,3
LUMD   19        TO=TO+BT(I)
LUMD   20     15 CONTINUE
LUMD   21        BA=RO*THI*XL*YL
LUMD   22        DO 20 I=1,N,3
LUMD   23        IX=I+1
LUMD   24        IY=I+2
LUMD   25        B(I)=BT(I)*BA/TO
LUMD   26        B(IX)=0.0
LUMD   27        B(IY)=0.0
LUMD   28     20 CONTINUE
LUMD   29    100 CONTINUE
LUMD   30 C
LUMD   31 C   CREATES CONSISTENT LUMPED MASS FOR PLANE STRESS
LUMD   32 C
LUMD   33        IF(ND.NE.2) GO TO 110
```

```
LUMD   34        DO 25 I=1,N,2
LUMD   35        IX=I
LUMD   36        IY=I+1
LUMD   37        TDX=TDX+BT(IX)
LUMD   38        TDY=TDY+BT(IY)
LUMD   39     25 CONTINUE
LUMD   40        BA=RO*TTT*XL*YL
LUMD   41        DO 30 I=1,N,2
LUMD   42        IX=I
LUMD   43        IY=I+1
LUMD   44        B(IX)=BT(IX)*BA/TDX
LUMD   45        B(IY)=BT(IY)*BA/TDY
LUMD   46     30 CONTINUE
LUMD   47    110 CONTINUE
LUMD   48   1001 FORMAT( 30H CONSISTENT M. M. NOT INCLUDED)
LUMD   49        RETURN
LUMD   50        END


STOR    1        SUBROUTINE STORE12(NA,N,LV,V,A)
STOR    2 C
STOR    3        DIMENSION V(LV),A(1)
STOR    4        REWIND NA
STOR    5        NT=(N+1)*N/2
STOR    6        IF(NT.LE.LV) LV=NT
STOR    7        NF=NT/LV
STOR    8        Q=1.0
STOR    9        QINF=Q*NF
STOR   10        QNT=Q*NT
STOR   11        QLV=Q*LV
STOR   12        QNF=QNT/QLV
STOR   13        LVLAST=NT-NF*LV
STOR   14        NF1=NF+1
STOR   15        IF(QNF.EQ.QINF)  NF1=NF
STOR   16        IF(QNF.EQ.QINF)  LVLAST=LV
STOR   17        N1=N2=0
STOR   18        DO 10 I=1,NF1
STOR   19        N1=(I-1)*LV+1
STOR   20        N2=I*LV
STOR   21        IF(I.EQ.NF1) N2=(I-1)*LV+LVLAST
STOR   22        WRITE(NA) (A(J),J=N1,N2)
STOR   23     10 CONTINUE
STOR   24        REWIND NA
STOR   25        IQ=0
STOR   26        IR=0
STOR   27        IX=0
STOR   28        DO 20 J=1,N
STOR   29        DO 20 I=1,J
STOR   30        II=I-1
STOR   31        LOC=(I+1)*I/2+(N-1)*II
STOR   32        IQ=IQ+1
STOR   33        IX=IX+1
STOR   34        IF(IQ.EQ.(LV+1).OR.J.EQ.I) GO TO 100
STOR   35        GO TO 110
STOR   36   100  IF(IR.EQ.NF) LV=LVLAST
STOR   37        READ (NA) (V(K),K=1,LV)
STOR   38        IQ=1
STOR   39        IR=IR+1
STOR   40   110  CONTINUE
STOR   41        A(LOC+J-I)=V(IQ)
STOR   42     20 CONTINUE
STOR   43        RETURN
STOR   44        END


WRIT    1        SUBROUTINE WRITE20(NN2,ISH,N,A)
WRIT    2 C
WRIT    3 C   NN2  ...NUMBER OF COLUMNS TO BE PRINTED
WRIT    4 C            ON ONE PAGE,BY DEFAULT = 12
WRIT    5 C   ISH  ...EQ.0 NO ZERO ROWS PRINTED BELOW (NN2,NN2)
WRIT    6 C   N    ...ORDER OF MATRIX
WRIT    7 C   V    ...WORKING VECTOR (MAX. 12 COLUMNS)
WRIT    8 C
WRIT    9        DIMENSION V(12),A(1)
WRIT   10        IF(NN2.EQ.0) NN2=12
WRIT   11        NT=(N+1)*N/2
WRIT   12        Q=1.0
WRIT   13        NB=N/NN2
WRIT   14        QNB=NB*Q
WRIT   15        QN=N*Q
WRIT   16        QNN2=NN2*Q
WRIT   17        QNB=QN/QNN2
WRIT   18        NB=NB+1
WRIT   19        IF(QNB.EQ.QNB) NB=NB-1
WRIT   20        WRITE(6,920)
WRIT   21        DO 10 K=1,NB
WRIT   22        J1=NN2*(K-1)+1
WRIT   23        J2=NN2*K
WRIT   24        N2=NN2
WRIT   25        NN=N
WRIT   26        IF(ISH.EQ.0) NN=J2
WRIT   27        IF(K.EQ.NB) NN=N
WRIT   28        IF(J2.GT.N) N2=N-J1+1
WRIT   29        DO 20 I=1,NN
WRIT   30        DO 30 J=1,N2
WRIT   31     30 V(J)=0.0
WRIT   32        II=I-1
WRIT   33        LOC=II*I/2+II*(N-II)
WRIT   34        IF(J2.LT.I)  GO TO 100
WRIT   35        IF(I.GT.J1.AND.I.LE.J2) GO TO110
WRIT   36        IF(J1.GE.I)  GO TO 120
WRIT   37        GO TO 100
WRIT   38    110 N1=I-J1+1
WRIT   39        DO 40 J=N1,N2
WRIT   40     40 V(J)=A(LOC-N1+1+J)
WRIT   41        GO TO 100
WRIT   42    120 CONTINUE
WRIT   43        DO 50 J=1,N2
WRIT   44     50 V(J)=A(LOC+J1-I+J)
WRIT   45    100 CONTINUE
WRIT   46        WRITE(6,900) (V(L),L=1,N2)
WRIT   47     20 CONTINUE
WRIT   48        WRITE(6,920)
WRIT   49     10 CONTINUE
WRIT   50    900 FORMAT(12E11.4)
WRIT   51    920 FORMAT(1H1)
WRIT   52        RETURN
WRIT   53        END
```

```
      SUBROUTINE ELM9
C
C  VARIABLE NODE PANEL ELEMENT
C
      COMMON A(1)
      COMMON /ELPAR/  NPAR(14),NUMNP,MBAND,NELTYP,N1,N2,N3,
     1                N4,N5,MTOT,NEQ,MTOTEM
      COMMON /JUNK/   LT,LH,DUM(98),N6,N7,N8,N9,N10,LM(100)
      COMMON /EXTRA/  MODEX,NTB
      COMMON /EM/ AA(1)
      WRITE(6,902)
      NTAP=12
      IF(NPAR(1).EQ.0) GO TO 500
      WRITE(6,910)
      WRITE(6,920)
      N6=N5*NUMNP
      N7=N6*NPAR(3)
      N8=N7*NPAR(3)
      N9=N8*NPAR(3)
      N10=N9*NPAR(3)
C
C  CHECK STORAGE LENGTH OF  COMMON /EM/ AA(MTOTEM)
C
      IF(MTOTEM.GE.N10) GO TO 110
      MMX=N10-MTOTEM
      WRITE(6,955)MMX,N10
      STOP
  110 CONTINUE
      DO 10 I=1,N10
   10 AA(I)=A(I)
C
      CALL OVERLAY(6HSSAP,8,0,6HRECALL)
      DO 20 I=1,N10
   20 A(I)=AA(I)
      GO TO 850
C
C   STRESS CALCULATION FOR STATIC LOADING
C
  500 CONTINUE
      REWIND NTAP
      IL=0
      DO 30 L=LT,LH
      IL=IL+1
      I1=N3+(IL-1)*NEQ
      I2=N3+IL*NEQ-1
      WRITE(NTAP) (A(I),I=I1,I2)
   30 CONTINUE
      NUME=NPAR(2)
      DO 800 MM=1,NUME
      REWIND NTAP
      READ(1) NUMB,NDN,NS,NSS,NST
      IF(NS.EQ.0) GO TO 800
      READ(1) (LM(I),I=1,NDN),(A(I),I=1,NST)
      WRITE(6,940) NDN,NS,NSS,NST
      WRITE(6,940) (LM(I),I=1,NDN)
C
C   AT I TO NST)  STORES NOW STRESS/DISPL. -MATRIX
C
      WRITE(6,910)
      WRITE(6,932) NUMB
      WRITE(6,934)
      DO 700 L=LT,LH
      READ(NTAP) (AA(I),I=1,NEQ)
      WRITE(6,935) (AA(I),I=1,NEQ)
C
C   AA( ) STORES NOW DISPLACEMENTS FOR LOADCASE L
C   A(LO1 TO LO2) STORES NEW CALCULATED STRESSES
C
      DO 32 I=1,NSS
      II=NST+I
   32 A(II)=0.0
      LO1=NST+1
      LO2=NST+NSS
      DO 720 K=1,NSS
      DO 720 I=1,NDN
      IS=LO1+K-1
      ISD=(I-1)*NSS+K
      ID=LM(I)
      IF(ID.EQ.0) GO TO 720
      A(IS)=A(IS)+A(ISD)*AA(ID)
  720 CONTINUE
      NEL=NSS/NS
      WRITE(6,912)
      DO 35 K=1,NEL
      I1=(K-1)*NS+LO1
      I2=K*NS+LO1-1
      WRITE(6,942) K,L,(A(I),I=I1,I2)
      WRITE(6,912)
   35 CONTINUE
      WRITE(6,913)
  700 CONTINUE
  800 CONTINUE
  850 CONTINUE
      WRITE(6,930)
  902 FORMAT( 10H IN  ELM9)
  910 FORMAT(1H1)
  912 FORMAT(/)
  913 FORMAT(///)
  935 FORMAT(12E11.4)
  940 FORMAT(2015)
  932 FORMAT(39H S T R E S S E S  F O R  PANELELEMENT ,I5/)
  934 FORMAT(18H ELEMENT      LOAD,/,
     1       18H NUMBER       CASE /)
  942 FORMAT(16,5X,16,5X,9E11.4,/,17X,9E11.4,/,17X,9E11.4)
  920 FORMAT( 36H E L E M E N T - T Y P E   E L M 9,
     1        23H    P A N E L E M E N T,/////)
  930 FORMAT( 10H END ELM9 )
  950 FORMAT(5I5,6E11.4)
  955 FORMAT( 20H INCRASE MTOTEM BY ,I6,9H ...N10= ,I5)
      RETURN
      END
```